UNIVERSITÉ DU QUÉBEC

MYTILICULTURE ET ÉCOSYSTÈME CÔTIER: MODÉLISATION INTÉGRÉE DE LEURS INTERACTIONS DANS LA LAGUNE DE GRANDE-ENTRÉE (ÎLES-DE-LA-MADELEINE, QUÉBEC)

THÈSE

PRÉSENTÉE À

L'UNIVERSITÉ DU QUÉBEC À RIMOUSKI

Comme exigence partielle du programme de

DOCTORAT CONJOINT EN OCÉANOGRAPHIE

PAR

Thomas GUYONDET

DÉCEMBRE 2009

"Lorsque la modélisation est inévitable,
Détends toi et jouis!"
Confucius (??)

"La Mer est un espace
de rigueur et de liberté."
Victor Hugo

REMERCIEMENTS

Mes premiers remerciements vont naturellement à mon directeur de recherche Vladimir Koutitonsky. Tout d'abord pour l'opportunité qu'il m'a offerte de participer à ce projet dont il est l'instigateur. En plus des connaissances et de l'expérience qu'il m'a transmises tout au long de ce doctorat, il a su me pousser quand il le fallait et m'encourager lorsque j'en avais besoin. Merci, Vlad, pour ta confiance et ta prévenance. Ce fut un honneur et un plaisir d'être ton dernier étudiant pendant près de neuf ans! Je te souhaite une belle retraite bien remplie.

Suzanne Roy et Jon Grant ont également suivi de près le déroulement de ce doctorat en tant que membre du comité de thèse et co-directeur de recherche, je les en remercie. Ils ont été des appuis importants pour des sujets qui m'étaient peu familiers a priori. Merci Suzanne de m'avoir initié à différentes techniques d'analyse d'échantillons et me permettre ainsi de mieux saisir l'ensemble du processus d'acquisition de données qui en bout de ligne détermine leur qualité.

Je tiens également à remercier Guglielmo Tita pour avoir accepté d'être le président de mon jury de thèse, pour avoir effectué le suivi de croissance des moules de Grande-Entrée et avoir partagé ces données et surtout pour son accueil ainsi que celui de l'ensemble du personnel de la station MAPAQ des Îles-de-la-Madeleine lors de nos différents séjours.

Les données relatives à l'environnement benthique ont été récoltées lors d'un projet mené en parallèle par l'équipe de l'Institut Maurice Lamontagne dirigée par Chris McKindsey et Philippe Archambault, un grand merci à eux et à leurs étudiantes Myriam Callier et Marion Richard pour la collecte, l'analyse et le partage de ces données. Au même titre Aurore Trottet a procédé à la collecte et à l'analyse des données sur la colonne d'eau et m'en a fait profiter au fur et à mesure de leur disponibilité, merci Aurore, également pour ton franc-parler rafraîchissant pendant les missions de terrain!

La collecte des données n'aurait pas été possible sans le support logistique de Sylvain Leblanc et Gilles Desmeules et leur dévouement proportionnel à la force du vent. Merci à vous. Olivier Pitre a également grandement contribué à ce projet par l'entretien des sondes immergées et l'analyse des séries temporelles qu'elles ont fournies et qui sont indispensables au fonctionnement du modèle numérique. Merci Olivier. Je remercie aussi Carlo Éloquin le producteur de moules de Grande-Entrée qui nous a permis de faire cette étude dans sa zone d'élevage et nous a fait profiter de sa connaissance du site, en plus de fournir son bateau à plusieurs reprises pour le travail dans la lagune.

Je voudrais adresser un merci tout particulier à Ian King, qui bien que nous ne nous soyons jamais rencontrés, s'est montré électroniquement disponible chaque fois que j'ai sollicité son aide au sujet du code FORTRAN des modèles RMA utilisés pour ce doctorat et qu'il a lui-même développés.

Pour le support financier qu'ils ont apporté au projet, je remercie le Fond Québécois de la Recherche sur la Nature et les Technologies (FQRNT) ainsi que la Société de Développement de l'Industrie Maricole du Québec (SODIM). Je remercie également le Réseau d'Aquaculture du Québec (RAQ) pour sa participation plus ciblée mais tout autant appréciée et l'UQAR-ISMER et Québec-Océan pour le soutien financier aux étudiants.

Je remercie Cédric Bacher pour avoir accepté de faire partie de mon jury de thèse et pour son accueil lors d'un stage de trois mois dans son laboratoire de l'IFREMER. Merci également à Stéphane Pouvreau, qui conjointement avec Cédric m'a initié aux joies du modèle DEB et a répondu patiemment à mes questions de néophyte.

Un énorme merci à Virginie et Sébastien pour tous les bons moments et pour l'hébergement à chacun de mes séjours à Rimouski.

Je terminerai en remerciant mes parents qui ont toujours appuyé inconditionnellement mes choix, quoiqu'il leur en coûte, quelques soient les océans à traverser.... et Karine et Mia qui m'ont supporté au quotidien et ont tout fait pour m'empêcher de devenir une moule virtuelle!

Merci à tous.

RÉSUMÉ

Dans le contexte de ressources marines surexploitées, l'aquaculture est appelée à fournir une part croissante des besoins nutritionnels de la population mondiale. De plus la culture de bivalves nécessite des techniques simples et des investissements restreints ce qui explique son essor actuel. Le développement de cette pratique majoritairement en zone côtière se heurte déjà à la question de la capacité de support des écosystèmes récepteurs. La complexité de ce type de problème, qui fait intervenir aussi bien l'hydrodynamique de la région concernée, les processus biogéochimiques régissant la production et la consommation de la nourriture des bivalves et l'écophysiologie de ces mollusques, nécessite le développement d'outils adaptés. La modélisation numérique fournit un cadre adéquat pour la réalisation de ce type d'études.

L'objectif de cette thèse est de développer un outil numérique permettant d'intégrer les trois aspects du problème de capacité de support et de considérer dans une même étude les différentes échelles spatiales mises en jeu, ce qui faisait défaut jusqu'alors. Le modèle ainsi développé sera mis à contribution pour étudier les interactions entre l'élevage mytilicole et l'écosystème de la lagune de Grande-Entrée, Îles-de-la-Madeleine, Golfe du Saint-Laurent.

Dans un premier temps, la modélisation numérique en éléments finis basée sur des données de terrain est utilisée pour étudier la dynamique des circulations tidale et résiduelle du système couplé de lagune "restreinte" et "coulante" des Îles-de-la-Madeleine. La lagune de Havre-aux-Maisons (HML) est considérée comme "restreinte" et présente une embouchure neutre en terme d'asymétrie tidale. La lagune de Grande-Entrée (GEL) est, elle, de nature "coulante" avec une dominance de jusant bien marquée au niveau de son embouchure, due aux interactions directes entre les principales composantes astronomiques de la marée. Le déséquilibre causé par les différentes caractéristiques d'absorption de l'onde de marée des deux embouchures se combine avec l'asymétrie morphologique interne du système pour produire un flux résiduel de HML vers GEL. La circulation résiduelle est aussi caractérisée par de plus fortes valeurs aux deux embouchures, de très faibles courants résiduels dans le bassin profond de HML et un dipôle de tourbillons résiduels couvrant les zones profondes de GEL.

Dans la deuxième partie de cette étude un modèle biogéochimique, couplé au moteur hydrodynamique mis au point précédemment, est développé pour étudier la dynamique de l'écosystème de la lagune Grande-Entrée, qui abrite un élevage commercial de moules. La calibration du modèle est basée sur la comparaison objective des résultats du modèle avec les observations récoltées lors d'une campagne d'échantillonnage sur le terrain, à la fois en terme de concentrations des variables d'état et de la magnitude des différents processus. Une analyse de sensibilité est ensuite réalisée pour tester les capacités prédictives du modèle. Les résultats du processus de calibration et de l'analyse de sensibilité établissent clairement la capacité du modèle à reproduire avec précision la dynamique de l'écosystème

lagunaire, y compris les effets de l'élevage mytilicole. Cette dynamique se caractérise en été par la dominance des processus de recyclage parmi les mécanismes d'apport en azote et également par le rôle dominant du réseau microbien, en particulier le microzooplancton, dans la détermination du niveau de productivité de ce système. L'activité mytilicole à son stade actuel de développement ne semble pas exercer d'influences majeures sur la dynamique du système à l'échelle globale.

Enfin, le modèle calibré physique-biogéochimique de la section précédente est amélioré par l'ajout d'un modèle écophysiologique de type budget d'énergie dynamique (DEB) et est utilisé pour étudier les interactions entre la ferme mytilicole de GEL et l'écosystème côtier qui l'abrite, aussi bien à l'échelle locale qu'à celle du système au complet. En utilisant un jeu de paramètres de la littérature pour le DEB, le modèle couplé reproduit assez précisément la croissance locale des moules ainsi que sa répartition spatiale sur toute la ferme. Les flux métaboliques des moules sont également bien reproduits, ce qui autorise l'étude des relations moules/environnement.

Les résultats montrent l'importance des moules dans le cycle de l'azote à l'échelle locale dans la zone d'élevage. Malgré l'influence réduite qu'exerce la ferme mytilicole à l'échelle du système complet, elle possède toutefois la capacité de modifier la structure de l'écosystème de la lagune de Grande-Entrée.

Selon les résultats du modèle couplé, le stock de moules en élevage pourrait être considérablement augmenté avant d'atteindre la capacité de production maximale de la GEL. Toutefois, si l'aspect écologique est pris en compte les résultats obtenus utilisés conjointement avec des critères objectifs tels que les empreintes de déplétion, montrent que la capacité de support de la GEL est beaucoup plus restreinte. Cette estimation peut néanmoins être qualifiée de conservatrice puisqu'elle s'appuie uniquement sur la période estivale où l'influence des moules est maximale.

L'outil numérique développé lors de ce doctorat offre la possibilité d'estimer la capacité de support écologique d'une région côtière pour l'aquaculture de bivalves en incluant à la fois les processus à l'échelle locale et de toute la lagune.

ABSTRACT

In the context of over-exploited marine resources, aquaculture should provide an increasing part of the food demand worldwide. Thanks to the simple technical level and the low investments it requires, shellfish culture is developing rapidly. This development takes place mainly in coastal areas where it already raises the question of the carrying capacity of the receiving ecosystems. The complexity of such a problem, mixing aspects of the hydrodynamics of the system, the biogeochemical processes influencing the production and consumption of bivalve food and the ecophysiology of these molluscs, requires the set up of adequate tools. Numerical modelling provides the ideal framework for this kind of study.

The main goal of the present thesis is to develop a numerical tool integrating the three aspects of the carrying capacity problem and to consider the diverse spatial scales involved, which is lacking from previous studies. The model will then be used to investigate the interactions between the mussel farm and the ecosystem of Grande-Entrée lagoon, Magdalen Islands, Gulf of Saint-Lawrence.

In the first part of the work, finite element numerical modelling based on field data is used to study the tidal and tidally induced residual circulation dynamics of the coupled "restricted" and "leaky" coastal lagoon system of the Magdalen Islands. Havre-aux-Maisons Lagoon (HML) is of a "restricted" nature with a neutral inlet in terms of tidal asymmetry. Grande-Entrée Lagoon (GEL) is of a "leaky" nature with a marked ebb dominance at the inlet due to direct interactions between the main astronomical tidal constituents. The imbalance caused by the different tidal filtering characteristics of both inlets combines with the internal morphological asymmetries of the system to produce a residual throughflow from HML to GEL. The residual circulation is also characterized by strongest values at both inlets, very weak residual currents in HML deep basin and a dipole of residual eddies over the deeper areas of GEL.

In the second step of the study, a biogeochemical model coupled to the hydrodynamic model of the previous section is developed to study the dynamics of GEL's ecosystem sheltering a commercial mussel aquaculture farm. The model calibration is based on the objective comparison of model results and observations from a field sampling program both in terms of state variable concentrations and process rate magnitudes. A sensitivity analysis is then carried out to test the predictive ability of the model. The results of both the calibration process and the sensitivity analysis strongly establish the capacity of the model to accurately reproduce the lagoon's ecosystem dynamics, including the effects of cultured mussels. These dynamics are characterized in summer by the dominance of recycling processes among inorganic nitrogen input mechanisms and the dominant role of the microbial food web, especially the microzooplankton, in setting the productivity level of the system. The mussel culture activity in its present state does not seem to exert any major influence on the system dynamics at the global scale.

Finally, the calibrated fine resolution physical-biogeochemical model is improved with the addition of a dynamic energy budget (DEB) and used to investigate the local and system scale interactions between the mussel farm and the receiving coastal ecosystem. Using a set of published parameters for the DEB, the coupled model reproduces both the local mussel growth and its spatial repartition over the farm area quite accurately. Mussel related process rates are also well reproduced, allowing the study of mussel/environment interactions.

Results show the local importance of cultured mussels in the cycling of nitrogen within the cultivation area. Despite the strongly reduced influence exerted by the mussel farm at the scale of the entire system, the culture activity still has the ability to alter the structure of Grande-Entrée lagoon's ecosystem.

The coupled model results show that the mussel stock could be greatly increased before reaching the maximum production capacity of GEL. However, when the ecological aspect is accounted for, using model results along with objective criteria such as the depletion footprint curve, the overall carrying capacity of GEL must be significantly reduced.

The coupled fine scale numerical model developed for this study gives the opportunity to assess the ecological carrying capacity of a coastal region for shellfish culture accounting for both local and system scale processes.

TABLE DES MATIÈRES

LISTE DES TABLEAUX

LISTE DES FIGURES

CHAPITRE PREMIER
INTRODUCTION GÉNÉRALE

1.1 SYSTÈMES LAGUNAIRES

1.1.1 Définition - Particularités

Une lagune peut être définie d'une manière générale comme une masse d'eauplus ou moins isolée de l'océan ouvert par une barrière naturelle, un cordon de dunes ou un récif corallien. Nombres de lagunes entrent donc dans la définition plus globale d'estuaire donnée par Cameron & Pritchard (1963). Ce sont souvent des systèmes de faible profondeur ayant une ou plusieurs connexions plus ou moins restreintes avec l'océan. Une classification des lagunes a d'ailleurs été établie selon l'intensité de leurs échanges avec la zone côtière adjacente (Kjerfve, 1986). Les lagunes représentent environ 13% des zones côtières mondiales (Kjerfve, 1994), ce qui fait d'elles une importante interface entre les milieux terrestres et océaniques. Comme la plupart des régions côtières, qui fournissent plus de 24% de la production primaire marine nette globale et entre 60 et 65% de la production mondiale de poissons et de mollusques (Schot, 1999), les lagunes sont des zones très productives. Elles constituent également des nourriceries pour de nombreuses espèces d'oiseaux, de poissons et de crustacés.

Les lagunes jouent donc un rôle écologique majeur à cette interface Terre-Mer. Par ailleurs, leur position géographique et leur forte productivité ont toujours exercé une attraction importante sur les populations humaines. Dans le dernier siècle,

l'industrialisation et la croissance exponentielle de la population ont fortement augmenté les pressions anthropiques subies par les régions côtières (aujourd'hui près de 50% de la population mondiale est établie à moins de 50 kilomètres de la côte). L'augmentation des superficies allouées à l'agriculture dans chaque bassin versant, ainsi que l'industrialisation et l'urbanisation du littoral ont souvent pour conséquence l'augmentation des apports en sels nutritifs, en matières en suspension (organiques et inorganiques) et en polluants d'origine chimique ou bactérienne. Les lagunes avec leurs échanges restreints avec l'océan constituent des milieux d'autant plus sensibles. À ces pressions s'ajoutent celles dues à l'exploitation de certaines ressources par la pêche et l'aquaculture. Ces systèmes ont donc subi dans les dernières décennies des impacts néfastes de plus en plus soutenus (Sherman, 1994).

1.1.2 Écosystème et gestion durable

Depuis la fin des années 80, l'Écologie a pris une nouvelle orientation qui s'appuie sur le concept d'organisation hiérarchique des environnements naturels faisant intervenir leurs composantes physiques, chimiques et biologiques (Vadineanu, 2006). La notion d'écosystème se trouve ainsi à la base de cette science dont les objectifs sont l'identification de ces systèmes et l'étude de leur dynamique de production et leur capacité de support. Ce changement d'orientation s'est fait conjointement avec l'émergence de la notion de développement ou gestion durable «consacrée» lors de la Conférence de Rio en 1992. Le développement durable fait également appel au concept d'écosystème en s'opposant à la vision antérieure qui scindait l'environnement en différents compartiments.

Cette évolution parait logique tant il semble important d'éviter toute situation où la solution retenue pour résoudre un problème s'avèrerait, a posteriori, néfaste pour une autre composante du système. Dans le contexte des régions côtières soumises à l'aquaculture, cela se traduit par une approche écosystémique récemment définie par Soto et al. (2008) comme "une stratégie pour l'intégration de la pratique aquacole au sein de l'écosystème, qui vise au développement durable, à l'équité et à la résilience des systèmes social et écologique interconnectés". Aboutir à cette perception globale nécessite l'emploi d'outils puissants et intégrateurs. À l'heure actuelle, la modélisation numérique ou l'analyse systémique, basées essentiellement sur les aspects biogéochimiques de l'écosystème doivent être accompagnées d'une analyse des coûts et bénéfices induits par une pratique telle que l'aquaculture sur l'ensemble des biens et services fournis par les écosystèmes côtiers (Zheng et al., 2009).

1.1.3 Structure trophique typique

Dans le cas des zones côtières et des lagunes en particulier, il est possible d'extraire une structure générale de l'écosystème comprenant les premiers maillons du réseau trophique, communs à ces régions (Figure I-1). Les sels nutritifs, nitrate (NO_3^-), ammonium (NH_4^+), phosphate (PO_4^{3-}) et silicate ($Si(OH)_4$) et l'énergie lumineuse fournissent la base de la production primaire (la structure représentée à la Figure I-1 ne prend en compte que les sels nutritifs azotés car ce constituant est souvent considéré comme l'élément limitant en zone côtière (Ryther & Dunstan, 1971)). Les producteurs autotrophes peuvent être scindés en deux grands groupes, les microalgues (planctoniques et benthiques) et les macrophytes

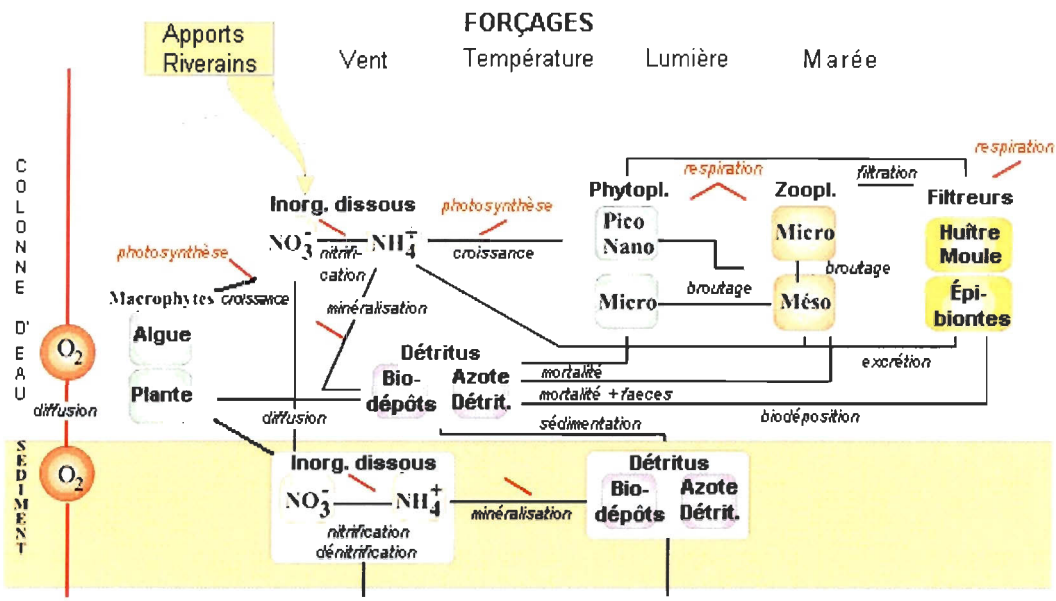

Figure I-1 Cycle de l'azote dans la structure typique de la base d'un écosystème lagunaire (tiré de www.ifremer.fr).

benthiques (macroalgues et plantes aquatiques). Cette production primaire est consommée soit fraîche, soit sous forme détritique par les herbivores planctoniques (zooplancton) et benthiques (zooplancton, bivalves filtreurs…) et par les détritivores benthiques. La Figure I-1 se limite à ces premiers maillons formant la base commune des écosystèmes côtiers, les échelons supérieurs font intervenir nombres d'espèces de poissons, d'oiseaux marins et d'autres prédateurs.

Ces premiers maillons recèlent déjà des particularités propres aux régions côtières. La caractéristique géomorphologique la plus marquante de ces systèmes est leur faible profondeur, qui conditionne la structure même de l'écosystème. Dans ces zones peu profondes, qui sont souvent bien mélangées verticalement, les interactions entre le sédiment

et la colonne d'eau revêtent une importance à l'échelle du système entier, si bien qu'elles ont été regroupées sous le terme de couplage benthique-pélagique (Nixon et al., 1976; Callender & Hammond, 1982). Les principaux processus qui s'y rattachent, sont la reminéralisation de la matière organique en sels nutritifs dans les couches superficielles du sédiment et la diffusion de ces sels vers la colonne d'eau, la sédimentation et la remise en suspension de la matière organique... La présence même de microphytobenthos et de macrophytes benthiques découle directement de la faible profondeur de ces systèmes qui permet la pénétration d'une quantité suffisante de lumière jusqu'au fond. La composante benthique joue donc un rôle prépondérant dans les cycles biochimiques (Webster & Harris, 2004) et peut conditionner le fonctionnement de l'écosystème au complet. Une étude menée dans les régions côtières du Danemark (Blackburn & Henriksen, 1983) a en effet montré que l'azote fourni par la reminéralisation dans les sédiments pouvait représenter de 30 à 100 % de l'azote nécessaire pour supporter la production primaire de ces zones.

Enfin une autre particularité de ces écosystèmes qui découle directement de l'importance de la reminéralisation dans les cycles des nutriments est la présence simultanée ou successive de deux types de production primaire. La production primaire nouvelle qui utilise des sels nutritifs nouvellement introduits dans le système par les apports riverains, le ruissellement, les précipitations et les échanges avec l'océan est principalement générée par des espèces phytoplanctoniques de grande taille et à croissance rapide comme les diatomées. Dans les régions tempérées, ce type de production est souvent limité dans le temps aux périodes des blooms printanier et automnal et aux périodes suivant de fortes précipitations. À l'inverse, la production primaire régénérée s'appuie sur les sels nutritifs

provenant du recyclage de la matière organique, soit directement dans la colonne d'eau ou depuis le sédiment. Ce type de production est dû à des cellules de plus petite taille et est présent tout au long de l'année, il constitue la base du réseau microbien formé par les plus petites cellules phytoplanctoniques (nano et picoplancton), les bactéries, les protozoaires et le microzooplancton, qui peut à son tour être brouté par le mésozooplancton rejoignant ainsi le réseau trophique classique (Azam et al., 1983). En s'appuyant sur l'important recyclage des sels nutritifs rencontré dans les systèmes lagunaires, le réseau microbien peut s'avérer la voie privilégiée des flux de matière dans ces premiers échelons de l'écosystème, en dehors des périodes de bloom où le réseau classique sera dominant.

1.1.4 Circulation des eaux

Afin que toute analyse d'écosystème soit complète, il convient d'en étudier, en plus de la structure trophique, les structures temporelles et spatiales (Levin, 1992). Or l'hydrodynamisme d'un système en fixe plusieurs degrés de variabilité aussi bien temporelle que spatiale. De plus, la structure trophique de la Figure I-1 montre que nombre des variables sont en suspension ou dissoutes dans la colonne d'eau et subissent donc les effets des mouvements des masses d'eau. L'étude de la circulation des eaux à l'intérieur du système et de ses échanges avec les régions adjacentes semble donc être le point de départ de toute étude d'écosystème. L'hydrodynamisme d'un système répond aux forçages atmosphériques, dont la période de variabilité s'étend de quelques jours (vent, pression atmosphérique) à plusieurs mois (précipitations, débits d'eau douce) et aux forçages

astronomiques (marée), dont l'échelle de variabilité temporelle est assez vaste, mais qui comprend principalement une période de quelques heures (cycle de marée diurne ou semi-diurne) et une période de quelques jours (cycle morte-eau, vive-eau). L'autre importante échelle temporelle d'un écosystème est celle contenue dans la structure trophique présentée au point précédent et qui repose sur le rythme des échanges entre les compartiments (intensité des flux) et sur le rythme de croissance propre à chacune des variables. Tout comme pour le transport à long terme des matières dissoutes et en suspension (Zimmerman, 1979), c'est la circulation résiduelle des eaux qui correspond le mieux à cette échelle «biologique» (Taboada et al., 1998). Il s'agit donc d'estimer la circulation moyenne des eaux due à la fois au forçage atmosphérique et au forçage tidal sur une période adéquate. En effet, la circulation résiduelle peut être à la fois causée par (Robinson, 1981):

- la friction du vent s'exerçant localement à la surface de l'eau;
- des gradients horizontaux de densité;
- un gradient dans le niveau d'eau moyen dû à des processus dynamiques s'exerçant dans les régions environnantes de la zone d'étude;
- des non-linéarités dans la dynamique de la circulation tidale.

Il convient donc d'étudier l'importance relative et le rôle joué par chacun de ces mécanismes dans la circulation résiduelle du système afin de comprendre le transport des masses d'eau et des substances qu'elles contiennent.

Du fait de son importance dans le transport des polluants et des variables des écosystèmes pélagiques, la circulation résiduelle a fait l'objet de nombreuses études théoriques et appliquées (Imasato, 1983; Feng et al., 1986b; Ridderinkhof & Zimmerman,

1990a). Le dernier mécanisme mentionné ci-dessus est de loin le plus complexe et il a été le sujet privilégié de plusieurs de ces études. Il s'agit en effet de comprendre comment la marée, phénomène oscillatoire, peut engendrer dans les zones côtières peu profondes, des courants résiduels non oscillatoires. Les principaux processus mis en jeu sont:

- les interactions des courants de marée avec la topographie, au passage d'une embouchure étroite par exemple, où de forts gradients dans les courants de marée peuvent s'établir (Zimmerman, 1978; Imasato, 1983; Ridderinkhof & Zimmerman, 1990a);
- les interactions des courants de marée avec la bathymétrie, par exemple lorsque celle-ci présente une pente dans la direction perpendiculaire à l'écoulement, ce qui crée un gradient dans les forces de friction selon cette direction (Robinson, 1981);
- les interactions des courants de marée avec les gradients de densité, par exemple en présence d'une circulation estuarienne typique (une couche d'eau douce sur une couche d'eau plus dense circulant en directions opposées), la marée impose une asymétrie flot/jusant, le jusant renforçant la circulation estuarienne alors que le flot la combat (Jay, 1990).

Ces phénomènes ont généralement pour effet de créer deux grands types de flots résiduels, des tourbillons mais également des flots unidirectionnels, qui peuvent s'avérer d'une importance capitale dans le transport des matières dissoutes et en suspension (Ridderinkhof & Zimmerman, 1990a).

Étant donné la complexité de ces mécanismes et les particularités propres à chaque système, il est difficile d'extraire des informations suffisantes sur la circulation résiduelle d'une région côtière par de simples mesures *in situ,* d'autant plus qu'elle possède une importante variabilité spatiale. La plupart des études a donc également recours à la modélisation numérique (Ridderinkhof & Zimmerman, 1990b; Tee & Lefaivre, 1990; Taboada et al., 1998).

1.2 SITE D'ÉTUDE

Les Îles-de-la-Madeleine sont situées sur le plateau Madelinien, région peu profonde au centre du Golfe du Saint-Laurent (Figure I-2). L'archipel est constitué de six îles reliées entre elles par des îles barrières, délimitant ainsi trois importantes lagunes. La lagune de Havre-aux-Basques se trouve à l'extrémité sud-ouest de l'archipel. Au centre se situe la lagune de Havre-aux-Maisons (HML) qui communique par une passe très étroite avec la lagune de Grande-Entrée (GEL) au nord-est (Figure I-2). La présente étude porte principalement sur la lagune de Grande-Entrée et incorpore des éléments concernant la HML dans les cas où ces deux systèmes ne peuvent être dissociés.

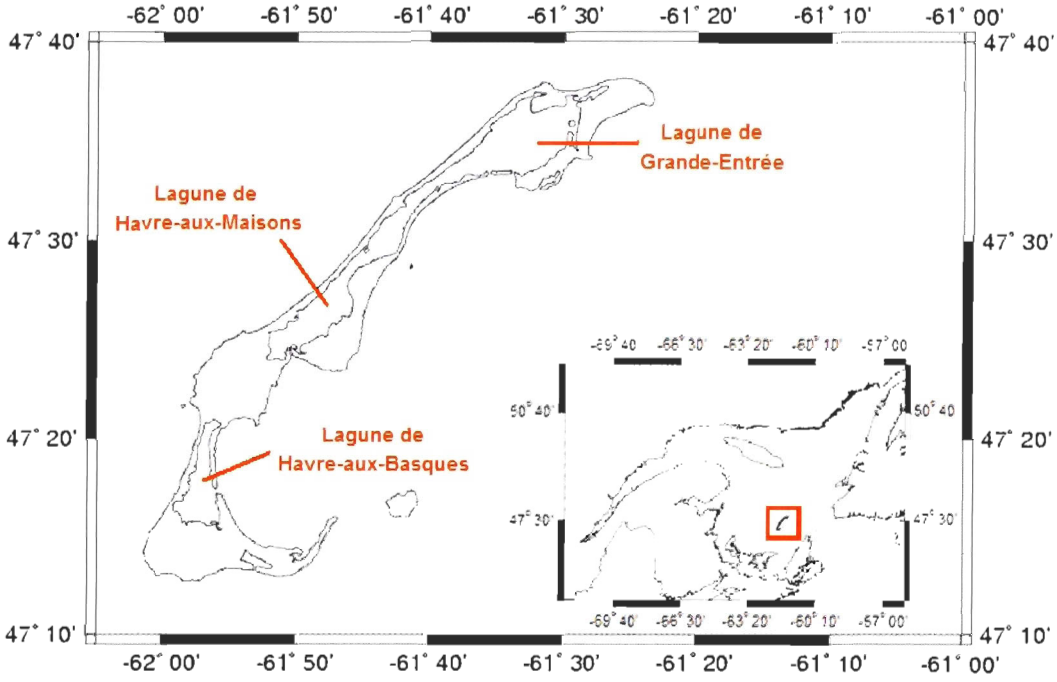

Figure I-2 Carte de la zone d'étude, l'archipel des Îles-de-la-Madeleine, Québec, Canada.

1.2.1 Morphologie

La GEL est la plus grande des lagunes des Îles-de-la-Madeleine (IdM) avec une longueur maximale d'environ 25 km et une superficie de 58 km² (Mayzaud et al., 1992). La lagune est peu profonde, en moyenne 3 m, et présente deux zones distinctes (Figure I-3). Ces deux zones sont séparées par un chenal de navigation de 100 m de largeur, de 6 à 8 m de profondeur et 10.5 km de long dont 8 km à l'intérieur de la lagune, menant de l'embouchure au sud, au quai de chargement d'une mine de sel située sur la côte nord de la lagune (Drapeau, 1988). À l'ouest du chenal se trouvent des hauts fonds sablonneux et la profondeur dépasse rarement 3 m. La région à l'est par contre est constituée d'un bassin

plus profond (5-6.5 m) au fond vaseux (Koutitonsky et al., 2002). La GEL possède deux frontières ouvertes, l'embouchure principale sur le Golfe Saint-Laurent (GSL), d'une section d'environ 3000 m² et également une étroite ouverture vers la HML au sud-ouest d'une section de seulement 300 m² (Drapeau, 1988; Koutitonsky, 2005).

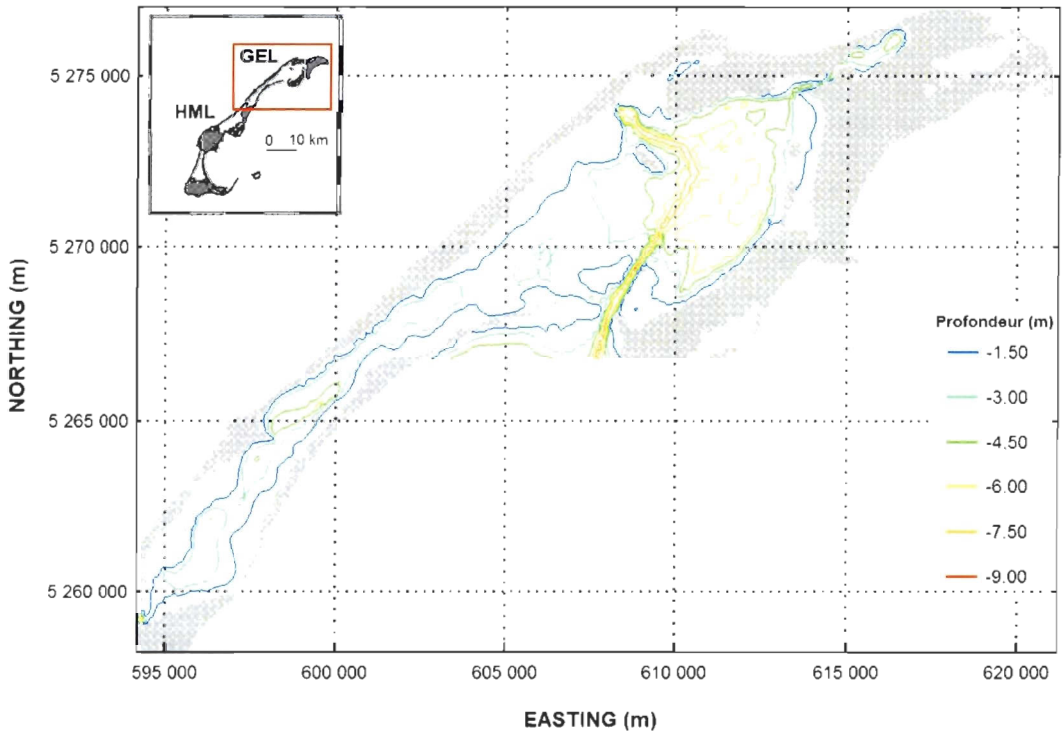

Figure I-3 Carte bathymétrique de la lagune de Grande-Entrée (GEL).

1.2.2 Forçages

Dans la région de la GEL, les vents dominants sont du secteur ouest et ils présentent très peu de périodes de calme (Drapeau, 1988). La période de variabilité privilégiée pour le forçage météorologique sur les Îles-de-la-Madeleine varie entre 3 et 10 jours (Koutitonsky & Bugden, 1991). De plus, la plus grande dimension de la GEL étant orientée selon un axe sud-ouest, nord-est, elle se trouve dans une des directions privilégiées des vents qui peuvent donc avoir une influence non négligeable sur la circulation des eaux dans la lagune (Koutitonsky et al., 2002, Koutitonsky, 2006).

La Figure I-4 représente les fluctuations du niveau d'eau à l'embouchure de la GEL durant le mois de juin 2001. L'amplitude du signal de marée varie de 0.2 m en période de morte-eau à 0.6 m en vive-eau. L'analyse harmonique de ces signaux à l'embouchure et à l'intérieur de la GEL montre que le forçage tidal est de nature mixte avec une dominance semi-diurne et que l'amplitude du signal n'est pas significativement réduite par les forces de friction au passage de l'embouchure de la lagune (Koutitonsky et al., 2002).

L'étude de la circulation des eaux dans la GEL montre que les deux régions distinctes de la lagune, à l'ouest et à l'est du chenal de navigation, se différencient également par le temps de renouvellement de leurs eaux par les eaux du GSL (Fig. I-5). Le renouvellement du bassin profond à l'est s'avère plus lent que celui des zones situées proches de l'embouchure et à l'ouest du chenal de navigation (Koutitonsky & Tita, 2006). Cette étude montre également l'importance du forçage météorologique sur la circulation des eaux dans la GEL puisqu'il est capable de réduire de moitié le temps de renouvellement des eaux du bassin profond (Fig. I-5). L'hydrodynamique impose donc des contraintes différentes aux

deux principales régions de la GEL, les courants de marée étant également nettement plus forts dans la région ouest, de l'ordre de 0.2 à 0.5 $m.s^{-1}$, qu'à l'est du chenal où ils dépassent rarement 0.05 $m.s^{-1}$ (Koutitonsky et al., 2002).

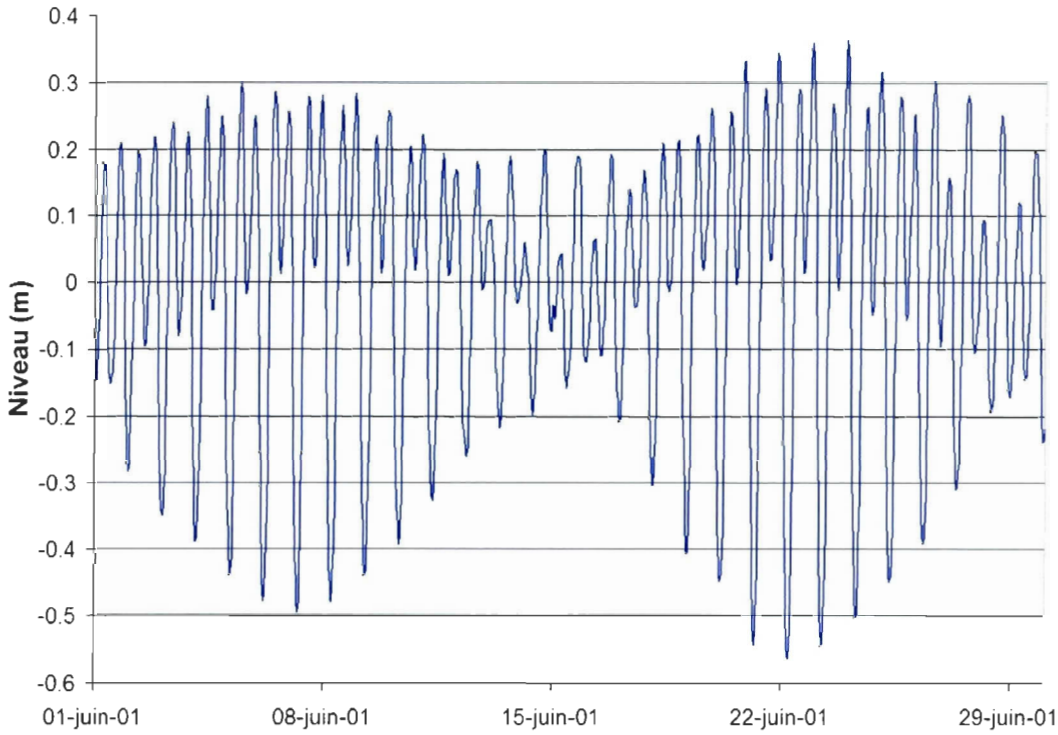

Figure I-4 Fluctuations du niveau d'eau à l'embouchure de la GEL en juin 2001.

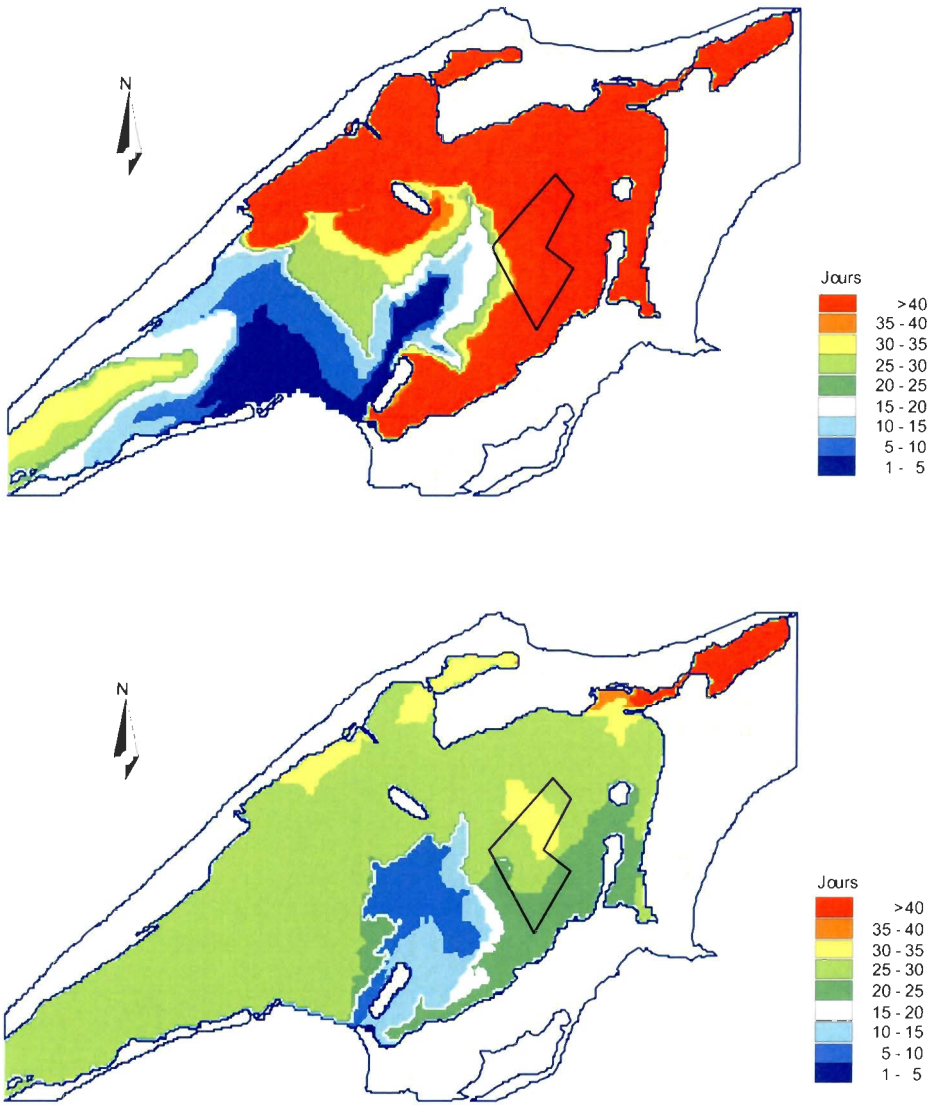

Figure I-5 Distribution spatiale du temps de renouvellement local des eaux dans la couche de surface (0 - 1.5 m) de la lagune de Grande-Entrée pour la période du 24 mai 2001 au 9 juillet 2001, sous l'effet de : (1) les marées observées (haut) et (2) les marées et les vents observés (bas). Tiré de Koutitonsky & Tita (2006).

1.2.3 Caractéristiques de l'écosystème

En 1988-1989, une étude multidisciplinaire a dégagé les grandes caractéristiques de l'écosystème pélagique de la GEL (Roy et al., 1991; Souchu et al., 1991; Mayzaud et al., 1992). Cette étude a montré en particulier que vis-à-vis de ses principaux paramètres (température, salinité, concentrations en sels nutritifs...), le système était généralement homogène suivant la verticale, conséquence des faibles profondeurs rencontrées dans la lagune, de l'absence d'apports d'eau douce et du mélange par les vents rarement calmes. La Figure I-6 présente quelques unes des données obtenues lors de cette étude en 1989 pour les stations A, à l'intérieur de la lagune et P située dans le GSL, à proximité des Îles-de-la-Madeleine. La courbe de température montre une évolution saisonnière caractéristique avec un maximum supérieur à 20°C atteint à la mi-août. Les salinités dans la lagune sont assez stables à l'exception d'une baisse marquée de 31 à moins de 30 PSU au mois d'août, cette caractéristique se reproduit d'une année sur l'autre et est attribuée à l'arrivée dans la région des eaux provenant de la crue printanière du fleuve Saint-Laurent. Concernant les sels nutritifs (NH_4^+, PO_4^{3-} et $Si(OH)_4$), les concentrations sont généralement faibles et très légèrement supérieures à l'extérieur de la lagune ($[NH_4^+]$ = 0-0.7 µM, $[PO_4^{3-}]$ = 0.25-0.7 µM, $[Si(OH)_4]$ = 0.3-1.6 µM ; Souchu et al., 1991; Mayzaud et al., 1992). Les concentrations en phosphate (PO_4^{3-}) présentent une moins grande variabilité temporelle que celles d'ammonium (NH_4^+) et de silicate ($Si(OH)_4$). Aucune donnée concernant les concentrations en nitrate (NO_3^-) n'apparaît dans cette étude car les concentrations sont restées inférieures au seuil de détection de la méthode utilisée, confirmant là aussi des concentrations faibles tout au long de la période estivale et au début de l'automne. Une des particularités des

lagunes des Îles-de-la-Madeleine est qu'elles ne reçoivent aucun apport d'eau douce et de sels nutritifs provenant de rivières, la superficie et l'altitude des reliefs des îles étant trop faibles pour qu'un cours d'eau important ne se développe. Les sources de sels nutritifs se limitent donc aux apports depuis le GSL, aux précipitations et à la reminéralisation de la matière organique dans la colonne d'eau et dans les couches superficielles des sédiments.

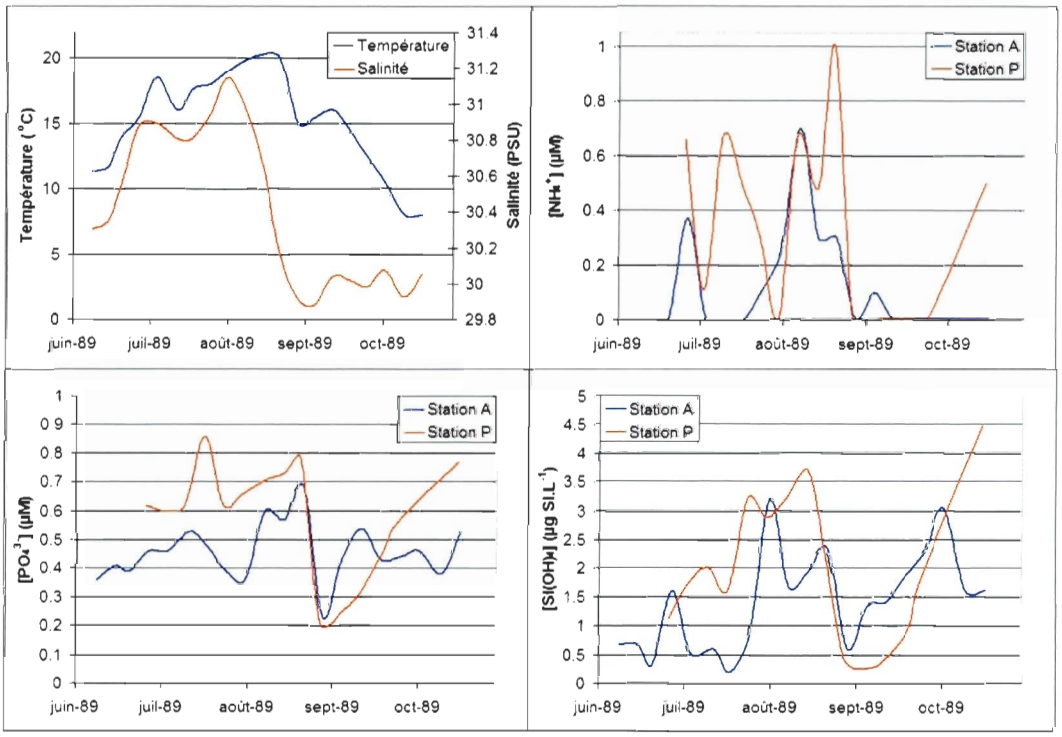

Figure I-6 Séries temporelles de différents paramètres de la colonne d'eau mesurés à l'intérieur (Station A) et à l'extérieur de la GEL (Station P) en 1989. Les courbes de température et salinité correspondent à la Station A (tiré de Mayzaud et al., 1992).

La Figure I-7 présente la répartition des apports suivant les différentes sources d'azote et de phosphore (Souchu & Mayzaud, 1991 et résultats non publiés), s'appuyant sur les données récoltées en 1989, à l'intérieur de la GEL. L'excrétion par la biomasse de

moules en élevage à cette époque représente des flux d'azote et de phosphore non négligeables dans la dynamique de ces sels. Mais il apparaît surtout que la reminéralisation de la matière organique et la diffusion depuis les sédiments jouent un rôle majeur dans les cycles de ces composés, qui représentent la base de la chaîne de production de l'écosystème lagunaire.

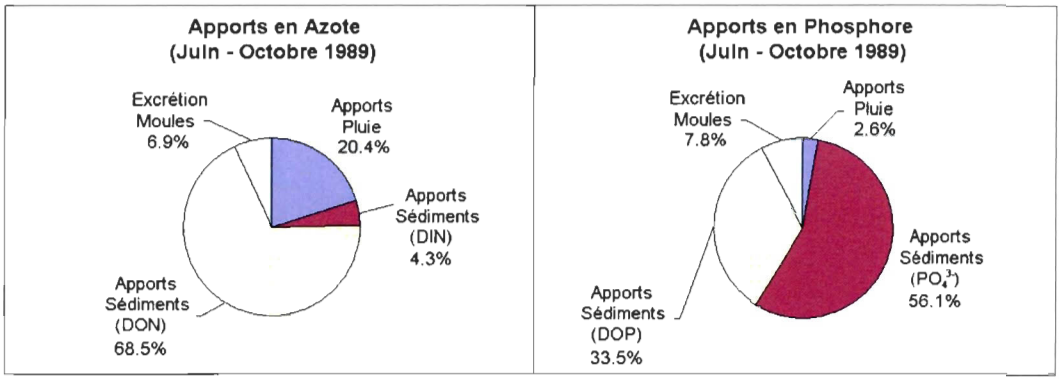

Figure I-7 Répartition des différents apports d'azote et de phosphore dans la GEL (Souchu & Mayzaud, 1991 et résultats non publiés).

La concentration en chlorophylle *a*, indice de la biomasse phytoplanctonique, est généralement assez faible, variant de 0.5 $\mu g.L^{-1}$ au printemps à 2 $\mu g.L^{-1}$ à l'automne et est sensiblement la même à l'intérieur et à l'extérieur de la GEL (Roy et al., 1991; Mayzaud et al., 1992). Quant à la composition de la communauté phytoplanctonique, elle semble dominée tout au long de la période d'échantillonnage de cette étude et également lors de l'été 2003 (Trottet et al., 2008a) par des espèces de petites tailles tels les microflagellés. Enfin, les biomasses zooplanctoniques sont également assez faibles, exprimées en poids sec elles diminuent de 10 $mg.m^{-3}$ au printemps à moins de 4 $mg.m^{-3}$ au début de l'automne (tendance également observée en 2003 par Trottet et al., 2007).

Il ressort que les mécanismes de couplage des milieux benthique et pélagique semblent jouer un rôle important dans le fonctionnement de l'écosystème lagunaire, en particulier en ce qui concerne les cycles des sels nutritifs. De plus, on note la présence dans les zones peu profondes de la lagune de bancs de zostères (*Zostera marina*), qui sont réputés comme des zones très productives et peuvent donc contribuer de façon non négligeable aux flux de matière dans la GEL. L'abondance de cellules phytoplanctoniques de petites tailles et les faibles apports de sels nutritifs laissent présager de l'importance du recyclage de ces sels et de la production primaire régénérée initiant un réseau microbien servant de principale base à l'écosystème lagunaire durant la période estivale. Enfin, il est à noter qu'une importante contrainte est exercée sur le fonctionnement de l'écosystème de la GEL par la présence d'un couvert de glace fixe du mois de janvier à la mi-avril (Drapeau, 1988). Ce couvert de glace interrompt aussi pratiquement complètement les activités récréo-touristiques, de pêche et d'aquaculture qui cohabitent dans la GEL pendant le reste de l'année.

La présente étude s'appuie sur une campagne d'échantillonnage multidisciplinaire (hydrodynamique, chimique et biologique) réalisée en 2003-2004 et dont les résultats seront décrits au fur et à mesure de leur utilisation dans les chapitres suivants.

1.3 LA MYTILICULTURE

1.3.1 Des origines à nos jours

L'aquaculture de moules est une des formes d'aquaculture les plus anciennes puisqu'on retrouve des traces de récolte de moules en Espagne datant d'au moins 400 av.

J.C. (Caceres-Martinez & Figueras, 1997). L'aquaculture en général et de moules en particulier s'est répandue pratiquement partout dans le monde et représente une voie de production de nourriture de plus en plus importante pour subvenir aux besoins de la population mondiale (Smaal, 2002). Aujourd'hui, les principaux producteurs sont la Chine, l'Espagne, les Pays-Bas, la France, la Nouvelle-Zélande… (FAO, 2009). D'une façon générale l'aquaculture a connu un fort développement dans les dernières décennies (Fig. I-8) et en particulier la mytiliculture car elle demande souvent des investissements inférieurs à d'autres types d'élevage (Cranford et al., 2003).

Au Canada Atlantique et au Québec en particulier, la mytiliculture est une pratique relativement récente, le début de l'exploitation commerciale des élevages datant seulement du milieu des années 80. Toutefois la production de moules a connu un essor rapide notamment dans les dix dernières années où la production annuelle au Québec est passée de 98 t en 1998 à 500 t en 2001 (MAPAQ, 2001).

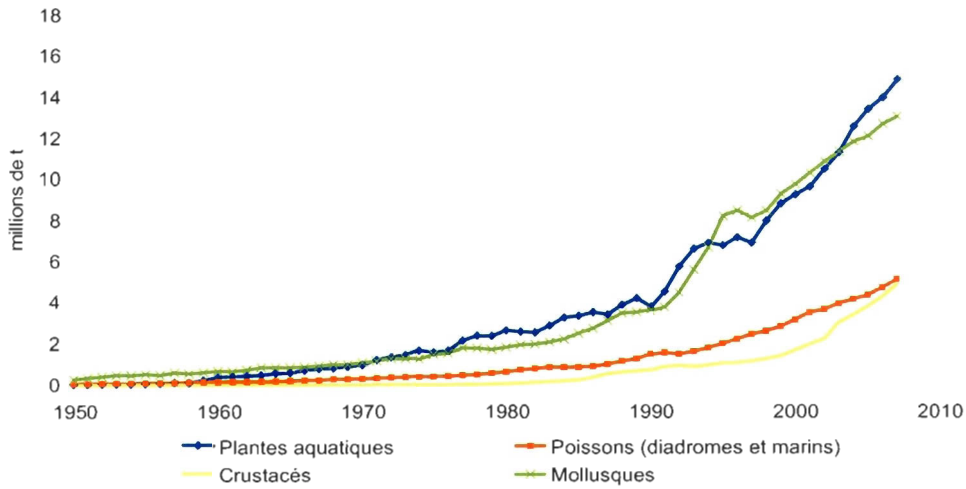

Figure I-8 Production annuelle mondiale d'aquaculture par principaux groupes d'espèces (FAO, 2009).

1.3.2 Techniques de culture

La culture de moules se fait selon trois grandes méthodes d'élevage. La méthode traditionnelle est la culture sur le fond, encore beaucoup utilisée aux Pays-Bas ainsi qu'au Danemark. Les moules colonisant naturellement les fonds des zones inter et subtidales, la méthode consiste simplement à ensemencer les surfaces de culture situées dans ces zones avec de jeunes moules et à les récolter lorsqu'elles ont atteint la taille souhaitée, généralement par une technique de dragage. Une deuxième méthode un peu moins répandue consiste à utiliser des pieux, appelés bouchots, enfoncés dans le sédiment, également en zone sub ou intertidale, pour servir de support aux moules qui y restent fixées durant toute la période de grossissement (Figure I-9a). Ces bouchots peuvent également servir de collecteur pour le naissain de jeunes moules, auquel cas aucune manipulation n'est nécessaire en dehors de la phase de récolte. Enfin la troisième technique, de plus en plus employée, est la culture en suspension dans la colonne d'eau. Les moules se fixent ou sont ensemencées sur des morceaux de corde qui sont attachés à une structure flottante, raft, ou à une longue ligne ou filière soutenue par des bouées (Figure I-9b). Cette méthode est employée en zone subtidale et récemment des essais de culture au large ont également été réalisés. Bien que cette méthode nécessite un plus grand nombre de manipulations, elle permet généralement une croissance des moules plus rapide en les plaçant dans des conditions plus propices d'accès à la nourriture (phytoplancton et matière organique particulaire (MOP)) et de température des eaux (Garen et al., 2004).

Un point commun à ces techniques est que la culture de moules, comme d'autres bivalves filtreurs ne nécessite aucun ajout de nourriture. Ces organismes puisent leurs ressources dans les particules naturellement présentes en suspension dans l'eau.

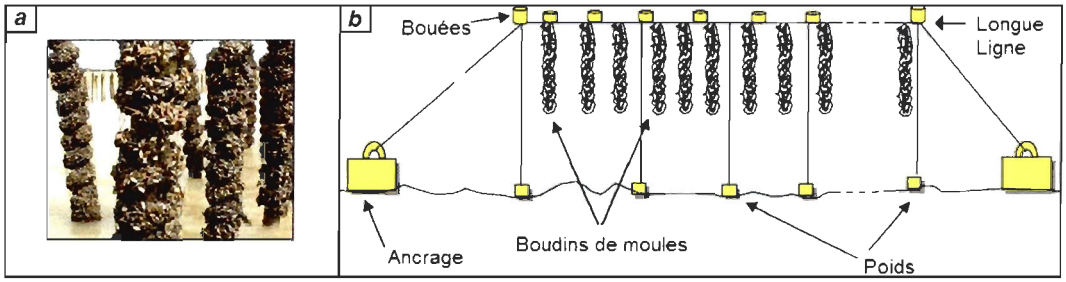

Figure I-9 Deux techniques de mytiliculture : (a) sur bouchots et (b) en suspension sur filières.

1.3.3 La mytiliculture aux Îles-de-la-Madeleine

La culture de moules aux Îles-de-la-Madeleine remonte au milieu des années 80. Elle représente la plus grosse production aquacole des îles avec 161 t de moule bleue (*Mytilus edulis*) en 2001 (SODIM, 2002), devant le pétoncle géant (*Placopecten magellanicus*. Les moules sont cultivées à l'intérieur des lagunes et en mer (depuis 2008 seulement) selon la méthode en suspension sur des filières. La production commerciale est réalisée, dans les lagunes, par deux entreprises. Chacune d'elles exploite une zone d'élevage différente, une est située dans la HML et l'autre dans la partie est de la GEL (Fig. I-10). Depuis quelques années, les boudins traditionnels (Fig. I-9b) qui pendent librement dans la colonne d'eau sont peu à peu remplacés par des boudins continus, qui sont ininterrompus d'un bout à l'autre de la filière mais sont rattachés à la ligne maîtresse à intervalles réguliers (Fig. I-11).

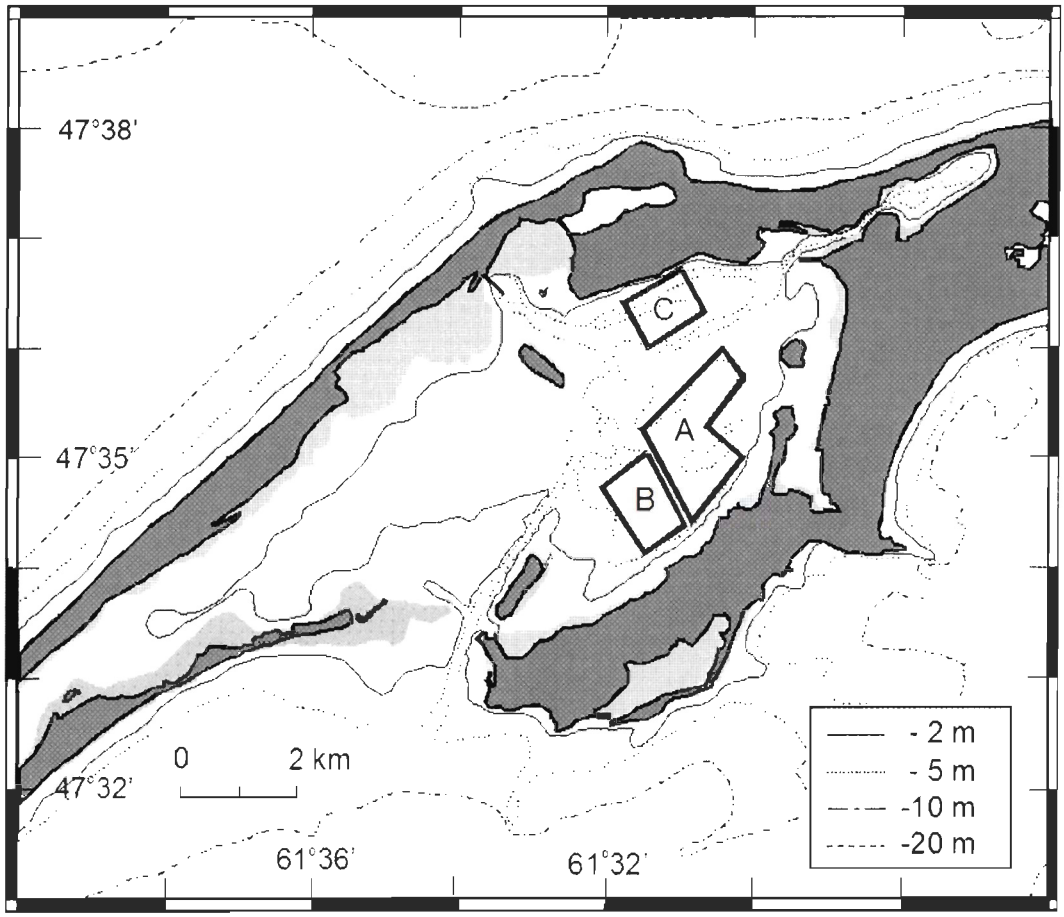

Figure I-10 Zones d'élevages aquacoles dans la Lagune de Grande-Entrée (A et B: culture de moules; C: culture de pétoncles). Seule la zone A était en exploitation lors de la campagne d'échantillonnage de 2003-2004.

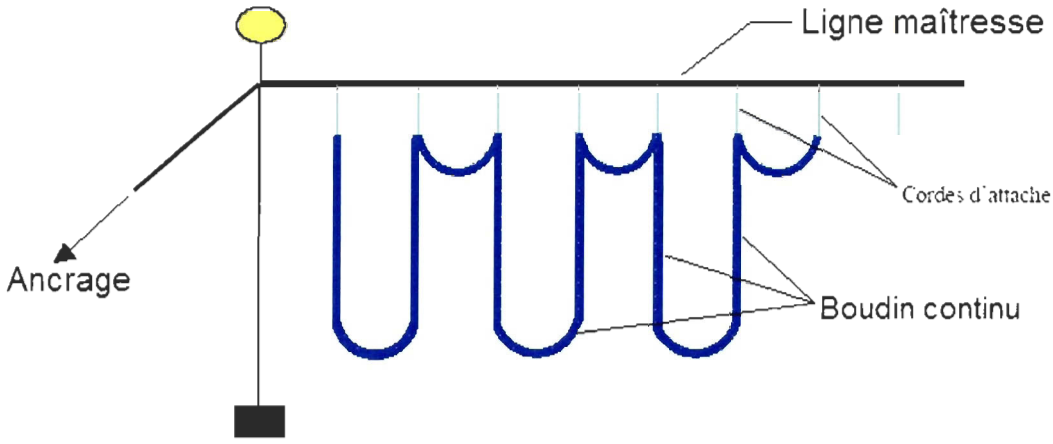

Figure I-11 Configuration d'une filière supportant un boudin en continu.

Cette technique originaire de Nouvelle-Zélande permet de réduire les manipulations, de mécaniser les opérations de mise en boudin des jeunes moules et également de faciliter la récolte (Darnell, 2000). La zone de culture de la GEL accueille 318 filières (données MAPAQ 2002-2003), dont 75% sont équipées de boudins continus, ce qui représente environ 50 millions de moules en élevage réparties sur deux cohortes. Pendant la majeure partie de la période de grossissement (juin à octobre, Fig. I-12), une seule cohorte est présente dans la ferme, après la fin de la récolte de la cohorte précédente (début de l'été) et avant l'ensemencement de la cohorte suivante en octobre (Fig. I-12). Cet élevage ainsi que ses interactions avec l'écosystème de la GEL constituera le point central de la présente étude.

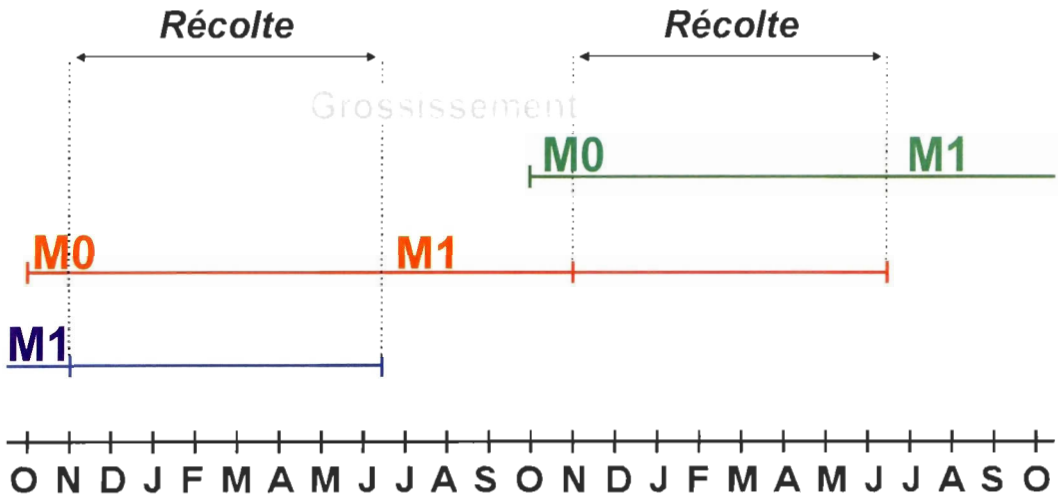

Figure I-12 Calendrier des principales phases de l'élevage mytilicole dans la lagune de Grande-Entrée, montrant trois cohortes successives (bleue, rouge et verte) avec la seule cohorte intermédiaire (rouge) pendant la majeure partie de la période de grossissement (mai à novembre).

1.4 CAPACITÉ DE SUPPORT POUR L'ÉLEVAGE DE BIVALVES FILTREURS

1.4.1 Historique et définitions

La mytiliculture, malgré les récents essais en pleine mer, se pratique presque exclusivement en zone côtière et même souvent à l'intérieur de systèmes semi-fermés tels des estuaires ou des lagunes (Gibbs, 2004), qui offrent des régions abritées propices à l'installation des élevages (Bompais, 1991). L'absence d'ajout de nourriture dans l'élevage des moules a fait en sorte de susciter moins de méfiance de la part des autres usagers des régions côtières que dans le cas d'élevage de poissons par exemple (Dahlbäck & Gunnarsson, 1981; Folke & Kautsky, 1992). L'introduction d'une importante biomasse de bivalves filtreurs peut même s'avérer bénéfique pour un système côtier. Grâce à leur

capacité à filtrer d'importants volumes d'eau et à retenir notamment les cellules phytoplanctoniques, ces organismes peuvent constituer un moyen efficace de contrôle de l'eutrophisation (Cloern, 1982; Officer et al., 1982; Meeuwig et al., 1998). De plus, les moules étant destinées à la consommation humaine, les activités mytilicoles nécessitent des critères environnementaux, en particulier en terme de qualité des eaux, tout à fait compatibles avec d'autres activités récréatives ou de conservation (Smaal, 2002).

Néanmoins, les superficies allouées à la pratique mytilicole sont souvent importantes, ce qui peut entraîner des conflits avec d'autres usages de la zone côtière (Grant et al., 1993; Deslous-Paoli et al., 1998). En outre, il s'est avéré que l'introduction de telles biomasses de filtreurs sans aucun suivi des conditions environnementales pouvait conduire à des situations où le reste de l'écosystème et les bivalves eux-mêmes pouvaient en pâtir. Dans la Baie de Marennes-Oléron, France, la biomasse d'huîtres en élevage était devenue telle que la période de grossissement avait plus que doublée (Bacher, 1989; Héral, 1991). Un autre exemple est l'estuaire Oosterschelde, Pays-Bas, où les études montrent que les bivalves exploitent déjà à pleine capacité les ressources phytoplanctoniques (van Stralen & Dijkema, 1994; Smaal et al., 2001). Dès le début des années 80 la notion de capacité de support des systèmes accueillant les élevages est apparue. Elle consistait alors à dimensionner les élevages pour que leurs effets sur les concentrations en nourriture (phytoplancton et MOP) restent raisonnables (Incze et al., 1981). Par la suite, les problèmes avec les élevages existant et la spécificité de chacun des sites ont forcé la multiplication des études de capacité de support et l'évolution des méthodes employées pour résoudre ces problèmes

(Bacher, 1989; Carver & Mallet, 1990; Grant et al., 1993; Raillard & Ménesguen, 1994; Dowd, 1997; Bacher et al., 1998; Ferreira et al., 1998).

Il a résulté de ces nombreux travaux plusieurs définitions de la notion même de capacité de support. Récemment, Inglis et al. (2000) puis McKindsey et al. (2006) ont regroupé ces définitions selon quatre catégories correspondant à des capacités de support physique, de production, écologique ou sociale. La capacité physique est souvent la plus facile à déterminer puisqu'elle réfère strictement à l'espace disponible dans le système considéré et pour la technique d'élevage envisagée. D'un point de vue de la production aquacole, la capacité de support peut être définie comme le stock de bivalves pour lequel la production annuelle de la cohorte commercialisable est maximisée (Bacher et al., 1998). Par contre d'un point de vue purement écologique, la capacité de support est définie par la taille d'une population supportée pendant une période donnée, par un système donné (Smaal et al., 2001) ou dans un contexte d'aquaculture, par le stock maximal pouvant être cultivé sans causer d'impact significatif sur l'écosystème récepteur (Inglis et al., 2000). Quant à la composante sociale, sa subjectivité, sa dépendance vis-à-vis des trois autres composantes et le fait qu'elle implique l'ensemble des utilisateurs de la région côtière visée, font en sorte qu'elle peut difficilement être étudiée par un seul travail de modélisation.

L'évolution de la dernière décennie vers une gestion et un développement durable des zones côtières oblige à formuler une définition combinant les perspectives écologique et d'exploitation. La définition pourrait alors être formulée ainsi: biomasse en culture pouvant

être supportée de façon durable par l'écosystème récepteur, sans mettre en péril l'élevage ou d'autres espèces. Une définition plus large s'appuyant sur une notion d'écosystème composé de différentes fonctions, a même été établie. Suite à l'apparition, en Asie particulièrement, de nouvelles pratiques aquacoles utilisant plusieurs fonctions des écosystèmes côtiers en combinant l'élevage de producteurs (algues) et de consommateurs (bivalves), les chercheurs ont dû généraliser la définition. La capacité de support devenait donc le niveau jusqu'auquel un processus ou une variable peut être modifié dans un écosystème donné, sans conduire la structure ou le fonctionnement de cet écosystème au-delà de limites acceptables (Duarte et al., 2003). Bien que la notion de «limites acceptables» soit difficile à définir, si des normes précises sont établies concernant la qualité des eaux ou d'autres critères alors cette capacité de support s'intègre parfaitement dans une gestion durable des régions côtières.

Quelle que soit la définition choisie, les méthodes pour adresser ces problèmes ont évolué dans une direction commune. Les implications de l'introduction des élevages de bivalves dans les écosystèmes côtiers sont si nombreuses et complexes que les chercheurs en sont venus à une méthodologie intégrée cherchant à décrire le fonctionnement de l'écosystème au complet et permettant d'observer les effets des bivalves en particulier. Cette méthodologie s'appuie sur la combinaison de mesures *in situ* et de modélisation numérique de l'évolution spatiale et temporelle des principales composantes des écosystèmes récepteurs et de leurs interactions (Héral, 1993; Bacher et al., 1998; Ferreira et al., 1998; Bacher et al., 2003; Duarte et al., 2003).

1.4.2 Relations entre les bivalves filtreurs et leur environnement

Afin d'évaluer la capacité de support d'un système pour la culture de moules, il est nécessaire de comprendre l'ensemble des interactions entre ces organismes et leur environnement. Cette relation doit être envisagée dans ses deux sens, celui pour lequel les bivalves agissent sur leur environnement et celui où c'est l'environnement qui agit sur eux. Une étude de capacité de support doit donc faire intervenir des processus ayant trait à l'écophysiologie des bivalves, à l'approvisionnement de ces bivalves en nourriture et à la production et consommation de cette nourriture à l'échelle de l'écosystème (Prins et al., 1998). Les principales relations ainsi que leurs effets sont répertoriés au Tableau I-1. La plupart de ces relations ont déjà été étudiées indépendamment les unes des autres. Il en ressort d'une part que les effets importants de l'environnement sur le métabolisme des bivalves contraignent à prendre en compte plusieurs paramètres tels que la température de l'eau, la vitesse du courant, la biomasse phytoplanctonique ou encore les concentrations en MOP et MIP. D'autre part, les effets des bivalves sur le milieu sont multiples et peuvent atteindre un degré tel qu'ils modifient le fonctionnement même de l'écosystème. De plus il existe de nombreux couplages entre ces différentes relations. En effet, par leur broutage ou leur biodéposition les bivalves sont capables de stimuler la production primaire, c'est-à-dire que par leur activité de nutrition ils influencent la dynamique de leur propre nourriture en faisant intervenir d'autres compartiments et processus de l'écosystème tels que les sédiments et le recyclage des sels nutritifs.

L'ensemble de ces relations et leur couplage rend le fonctionnement du système fortement non-linéaire. Il s'avère alors quasiment impossible de prévoir l'effet d'un paramètre sans prendre en compte l'ensemble du système. Ceci explique l'évolution des études de capacité de support pour l'aquaculture vers des méthodes multidisciplinaires, intégrées, faisant appel à la modélisation numérique pour analyser ce fonctionnement non-linéaire. Toutefois, la plupart de ces études, même récentes, ne font pas intervenir le système complet. Elles découplent souvent les parties biologiques et physiques du problème en utilisant des modèles en boîtes spatiales pour lesquels la description de l'hydrodynamique du système est restreinte à un jeu de paramètres décrivant les échanges entre les boîtes (Raillard & Ménesguen, 1994; Dowd, 1997; Bacher et al., 1998; Ferreira et al., 1998; Dowd, 2000). Les premières études faisant intervenir le couplage complet des parties biologiques et physiques sont apparues ces dernières années (Bacher et al., 2003; Duarte et al., 2003), mais l'intégration de la partie hydrodynamique s'est parfois faite au détriment d'une représentation détaillée de l'écosystème.

Afin d'évaluer la capacité de support d'une région côtière pour l'aquaculture de bivalves, il convient donc avant tout d'étudier le fonctionnement de l'écosystème, les forces qui le structurent et déterminent le niveau de base et l'évolution temporelle et spatiale de ses principaux paramètres.

Tableau I-1 Principales relations bivalves/environnement et leurs effets.

Relation	Facteur/Processus	Effets
Environnement/Bivalves (Écophysiologie)	Température	Détermination de la répartition géographique selon l'espèce
		Régulation du métabolisme (filtration, respiration), de la reproduction (Widdows & Bayne, 1971; Bayne & Widdows, 1978; Widdows et al., 1979; Bayne & Newell, 1983; Bayne et al., 1987; Bayne et al., 1993)
	Salinité	Détermination de la répartition géographique selon l'espèce
	Vitesse du courant	Diminution du taux de filtration pour vitesse trop élevée (Wildish & Miyares, 1990)
	Ratio [MOP]/[MIP]	MIP peut nuire à la nutrition (Cranford & Hill, 1999)
		MOP nécessaire à la survie, à la croissance, souvent le facteur limitant (Bayne et al., 1989; Smaal & van Stralen, 1990; Navarro et al., 1991)
Bivalves/Nourriture	Broutage	Déplétion ou non suivant la densité de bivalves et l'hydrodynamique (Dame, 1993; Dame, 1996; Jørgenson, 1996; Smaal et al., 1997)
		Stimulation de la production primaire (Asmus & Asmus, 1991; Dame, 1993; Prins et al., 1998; Nakamura & Kerciku, 2000; Cranford et al., 2003) par:
		• Augmentation de la lumière disponible par diminution de la turbidité
		• Augmentation du taux de croissance du phytoplancton car vieilles cellules sont broutées rapidement
		• Augmentation de la disponibilité des nutriments par diminution de la biomasse phytoplanctonique
		• Augmentation du recyclage des nutriments
		Petites cellules phytoplanctoniques favorisées car non broutées (Prins et al., 1998; Cranford et al., 2003)
		Cellules phytoplanctoniques à croissance rapide favorisées par pression de broutage et utilisation privilégiée des nutriments recyclés (Prins et al., 1998; Cranford et al., 2003)
		Influence sur les flux d'énergie à l'échelle du système si densité de bivalves importante (Cloern, 1982; Officer et al., 1982; Nichols, 1985; Hily, 1991; Smaal & Prins, 1993; Dame, 1996; Dame & Prins, 1998; Prins et al., 1998)
Bivalves/Zooplancton	Broutage	Diminution de la biomasse zooplanctonique par ingestion, surtout du microzooplancton (Cranford et al., 2003 ; Trottet et al., 2008b)
		Diminution de la biomasse zooplanctonique par compétition car capacité de filtration plus élevée et métabolisme plus faible permettant une meilleure survie lors des périodes de faible abondance en nourriture (Prins et al., 1998)

Tableau I-1 (suite)

Bivalves/Nutriments	Excrétion	Excrétion directement dans la colonne d'eau de NH_4^+ peut stimuler la production primaire (Maestrini et al., 1986; Dame, 1996) et peut même contrôler la dynamique de l'azote dans certains systèmes (Dame et al., 1991; Strain, 2002)
	Récolte	Représente un puits net pour d'importantes quantités de nutriments incorporés dans la biomasse des bivalves (Tenore et al., 1982)
	Broutage	Augmentation de la disponibilité des nutriments par diminution de la biomasse phytoplanctonique
	Biodéposition	Augmentation du taux de sédimentation (Grant et al., 1995) provoque un enrichissement en matière organique (MO) des sédiments superficiels (Folke & Kautsky, 1989) qui conduit à une augmentation de la reminéralisation et donc du recyclage des nutriments (Dahlbäck & Gunnarsson, 1981; Kaspar et al., 1985; Feuillet-Girard et al., 1988; Barranguet et al., 1994; Grant et al., 1995; Christensen et al., 2003) Pour élevage en suspension, reminéralisation au niveau des boudins, donc dans la colonne d'eau Dépendamment de l'enrichissement en MO: • Augmentation ou diminution de la dénitrification entraînant ou pas une limitation en azote (Chapelle, 1995; Chapelle et al., 2000; Cranford et al., 2003) • Relargage de PO_4^{3-} libéré des hydroxydes de fer (Nixon et al., 1980; Mesnage, 1994) • Augmentation de la réduction dissimilatrice de NO_3^- en NH_4^+ (Gilbert et al., 1997) • Diminution du taux de nitrification (Gilbert et al., 1997)
Bivalves/Oxygène	Respiration	Consommation directe d'oxygène
	Biodéposition	Enrichissement en MO des sédiments conduit à l'augmentation de la demande en O_2 (x 2 sous des lignes de moules (Christensen et al., 2003)) si la demande est trop forte des conditions anoxiques se développent, créant un milieu néfaste pour la flore et la faune benthiques et en particulier les bivalves si élevés sur le fond
Bivalves/Communautés benthiques	Biodéposition	Enrichissement en MO des sédiments entraîne l'augmentation de l'abondance des bactéries et de la méiofaune benthique (Dahlbäck & Gunnarsson, 1981; Mirto et al., 2000) Enrichissement en MO des sédiments entraîne la diminution de la biomasse et/ou de la diversité du macrobenthos (Tenore et al., 1982; Mattson & Linden, 1983; Kaspar et al., 1985; Stenton-Dozey et al., 1999; Chamberlain et al., 2001)
	Structures d'élevage	Effet d'attraction sur certaines espèces macrobenthiques: homards, crabes...(Dumbauld et al., 2009)

MO: Matière Organique, MOP (MIP): Matière Organique (Inorganique) Particulaire

1.4.3 Échelles spatiales et temporelles impliquées

La complexité des problèmes de capacité de support se traduit également dans la gamme des échelles spatiales et temporelles qu'il est nécessaire d'inclure afin d'en réaliser une étude exhaustive.

Échelles spatiales

L'introduction d'un important stock de bivalves se fait avant tout sentir au niveau local, dans la zone d'élevage. Les principaux effets sont répertoriés au Tableau I-1, allant de la déplétion de la biomasse phytoplanctonique et de la MOP à l'augmentation du recyclage des nutriments. Ces effets peuvent donc aussi bien représenter des bénéfices, contrôle de l'eutrophisation, que des coûts, amplification de l'eutrophisation par stimulation de la production primaire. Il devient alors délicat de connaître l'effet net ou global sur le fonctionnement de l'écosystème. Ce passage de l'échelle locale à l'échelle globale représente une des difficultés majeures de ce type d'études (Asmus & Asmus, 1991; Cranford et al., 2003). Certains travaux ont formulé l'hypothèse que pour une biomasse élevée, les bivalves pouvaient exercer des contraintes sur un système entier (Cloern, 1982; Officer et al., 1982; Dame, 1993; Smaal et al., 2001). Les exemples de la Baie de Marennes-Oléron (France) ou de l'Estuaire Oosterschelde (Pays-Bas) semblent confirmer cette hypothèse (Bacher, 1989; Smaal et al., 2001). Toutefois jusqu'à présent il n'a pas été montré comment, ni à partir de quelle biomasse de bivalves pour un système donné, ces effets locaux pouvaient se répercuter sur le fonctionnement global du système.

Ceci est dû en partie aux méthodes utilisées qui abordent le problème soit à l'échelle locale, soit à l'échelle globale, ou encore à une échelle intermédiaire comme c'est le cas des modèles en boîtes. La structure de ces modèles est figée dans des boîtes qui par définition doivent être homogènes pour chacun des paramètres et ne peut donc détailler les processus à une échelle plus restreinte; un bilan à l'échelle globale est tout de même possible. Une méthode prenant en compte cette échelle locale semble donc nécessaire pour que les bilans effectués à l'échelle globale ne soient pas biaisés.

Échelles temporelles

Comme dans tout système physique, les échelles de variabilité spatiales et temporelles d'un écosystème côtier sont liées. Ainsi l'utilisation de modèles en boîtes ou de budgets globaux (Carver & Mallet, 1990) pour l'étude de la capacité de support tient au fait que l'échelle de variabilité temporelle prépondérante considérée par ces études est l'échelle saisonnière. Cette échelle est dictée par le forçage météorologique, qui crée un cycle pour des paramètres tels que la température de l'eau ou l'intensité lumineuse qui se répercutent sur les sources de nourriture et le métabolisme des bivalves et donc sur la croissance de ces organismes. Toutefois le forçage tidal, contrainte importante agissant sur les régions côtières, impose une échelle de variabilité temporelle beaucoup plus courte. Certains systèmes côtiers peuvent donc subir des changements, en particulier dans la quantité et la qualité du seston, au moins aussi importants à l'échelle tidale qu'à l'échelle saisonnière (Prins et al., 1998). Or les bivalves filtreurs sont capables de s'adapter rapidement aux

changements dans leur environnement, spécialement lorsqu'il est question de la quantité de leur nourriture ou de sa qualité exprimée par le rapport entre les concentrations en MOP et MIP (Cranford et al., 1998). Il semble donc nécessaire d'inclure également cette variabilité à court terme dans toute étude visant à comprendre de façon détaillée le fonctionnement d'un écosystème côtier.

La compréhension complète du fonctionnement d'un écosystème passe par l'étude de trois échelles de variabilité, les échelles spatiale, temporelle et d'organisation écologique (Levin, 1992). Le présent travail dans la Lagune de Grande-Entrée vise donc l'étude des forçages déterminant les conditions d'évolution spatiales et temporelles dans cette région. Dans ces conditions, l'étude du fonctionnement du système biogéochimique devra aboutir à la compréhension des interactions entre ses différentes variables pour déduire en particulier l'organisation des flux de matière et de sels nutritifs. Alors il devrait être possible de comprendre quels rôles jouent les bivalves en culture dans ce système et quels peuvent être les effets d'une modification de leur biomasse.

1.5 OBJECTIFS

1.5.1 Objectif principal

Les objectifs principaux du projet dans lequel s'insère cette étude visent à estimer la capacité de support et à évaluer les impacts de l'activité mytilicole sur l'écosystème

lagunaire de la Grande-Entrée. Le présent travail tentera d'apporter une contribution à chacun de ces volets et se fixe donc pour principal objectif de comprendre:

Ce qui contrôle et structure la productivité d'un écosystème lagunaire et dans quelle mesure l'introduction d'une mytiliculture dans cette lagune peut modifier cette productivité.

Il s'agira donc de comprendre l'importance relative des facteurs contrôlant la productivité de l'écosystème de la lagune de Grande-Entrée et l'impact de la mytiliculture sur cette productivité en utilisant une méthode «intégrée», permettant de tenir compte des interactions entre ces facteurs. Comme mentionné précédemment, il convient d'étudier tout d'abord les facteurs et forçages physiques qui seront par la suite imposés à la structure biologique, voire trophique, pour obtenir une description complète du fonctionnement de l'écosystème. Enfin, les conséquences de la présence des moules en élevage sur ce fonctionnement pourront être évaluées. Ces étapes constituent les objectifs spécifiques de cette étude.

1.5.2 Objectifs spécifiques

Objectif 1: Comment la circulation des eaux dans le système lagunaire des Îles-de-la-Madeleine s'organise-t-elle en réponse aux forçages atmosphérique et tidal? Quel rôle joue l'hydrodynamique dans la détermination du niveau de productivité de la lagune de Grande-Entrée?

Il est nécessaire dans un premier temps de comprendre le fonctionnement hydrodynamique du système lagunaire, c'est-à-dire les variabilités spatiale et temporelle des niveaux d'eau et des courants, imposées par les forces atmosphériques et astronomiques agissant sur ce système.

La productivité d'un système côtier repose sur sa productivité primaire. La seconde partie de cet objectif sera donc de comprendre le rôle joué par l'hydrodynamique dans l'établissement du niveau de production phytoplanctonique. Cette production est essentiellement contrainte par les concentrations en sels nutritifs et l'intensité lumineuse disponible. Il s'agira donc d'étudier premièrement comment le fonctionnement hydrodynamique structure d'une part le transport des matières en suspension et dissoutes à l'intérieur de la Lagune de Grande-Entrée et d'autre part les échanges entre la lagune et les régions adjacentes qui servent de puits ou de source pour ces mêmes substances. Deuxièmement, la dynamique des matières en suspension, y compris les processus de sédimentation et remise en suspension, devra être détaillée pour comprendre son rôle dans l'établissement des niveaux d'intensité lumineuse dans les eaux de la lagune.

Objectif 2: Quels sont les processus des cycles des sels nutritifs susceptibles de contrôler, de limiter la productivité de l'écosystème?

Il s'agit ici d'observer le fonctionnement dynamique de l'écosystème lagunaire (nutriments, phytoplancton, détritus organiques et zooplancton) pour évaluer l'ensemble des processus de ces cycles et leurs interactions. Un modèle biogéochimique (NPZD) devra donc être couplé au moteur hydrodynamique et calibré à l'aide de données de terrain pour reproduire la dynamique de ce système. La structure de ce modèle devra être adaptée aux

spécificités de la lagune de Grande-Entrée révélées par les précédentes études (Roy et al., 1991; Souchu & Mayzaud, 1991; Souchu et al., 1991; Mayzaud et al., 1992) et les campagnes de mesures effectuées dans le cadre de ce projet. Une attention particulière devra être portée sur les mécanismes de couplage benthique-pélagique et leur importance dans la répartition des flux de matière et de sels nutritifs. Pour cela le modèle devra incorporer des variables distinctes pour les différentes formes de l'azote inorganique, nitrate et ammonium, ainsi qu'une variable représentant la concentration en oxygène dissout.

Objectif 3: L'activité mytilicole peut-elle influencer, dans quelque sens que ce soit, la productivité de l'écosystème lagunaire?

Dans le cadre du fonctionnement global de l'écosystème établit par l'objectif 2, les interactions entre les bivalves et leur milieu récepteur devront être quantifiées. La réalisation de cet objectif passera donc par le couplage avec le modèle hydrodynamique-biogéochimique, d'un module représentant les moules en élevage. Ce module devra reproduire les différents processus de l'écophysiologie des moules cultivées à Grande-Entrée. Il faudra alors évaluer les conséquences de la mytiliculture tant au niveau local que pour l'ensemble de l'écosystème lagunaire. Il s'agira également de comprendre si ces conséquences peuvent être modifiées, ou limitées par une gestion adéquate de l'élevage. Un objectif connexe est d'évaluer la capacité de support de cette lagune pour la mytiliculture.

Chacun de ces trois objectifs fait l'objet d'un chapitre de cette thèse rédigé sous forme d'article scientifique.

CHAPITRE 2

TIDAL AND RESIDUAL CIRCULATIONS IN COUPLED RESTRICTED AND LEAKY LAGOONS

Thomas GUYONDET and Vladimir G. KOUTITONSKY

Article publié en 2008 dans

Estuarine, Coastal and Shelf Science, Vol. 77, p. 396-408

RÉSUMÉ: La modélisation numérique en éléments finis basée sur des données de terrain est utilisée pour étudier la dynamique des circulations tidale et résiduelle d'un système couplé de lagune "restreinte" et "coulante" situé aux Îles-de-la-Madeleine, Golfe du Saint-Laurent. La lagune de Havre-aux-Maisons (HML) est considérée comme "restreinte" et présente une embouchure neutre en terme d'asymétrie tidale. La lagune de Grande-Entrée est, elle, de nature "coulante" avec une dominance de jusant bien marquée au niveau de son embouchure, due aux interactions directes entre les principales composantes astronomiques de la marée. Le déséquilibre causé par les différentes caractéristiques d'absorption de l'onde de marée des deux embouchures se combine avec l'asymétrie morphologique interne du système pour produire un flux résiduel de HML vers GEL. La circulation résiduelle est aussi caractérisée par de plus fortes valeurs aux deux embouchures, de très faibles courants résiduels dans le bassin profond de HML et un dipôle de tourbillons résiduels couvrant les zones profondes de GEL. De nouvelles investigations, notamment des expériences numériques de transport de traceur seront nécessaires pour comprendre de manière plus approfondie la circulation à long terme de ce système lagunaire.

ABSTRACT: Finite element numerical modelling based on field data is used to study the tidal and tidally induced residual circulation dynamics of a coupled "restricted" and "leaky" coastal lagoon system located in the Magdalen Islands, Gulf of Saint-Lawrence. Havre-aux-Maisons Lagoon (HML) is of a "restricted" nature with a neutral inlet in terms of tidal asymmetry. Grande-Entrée Lagoon (GEL) is of a "leaky" nature with a marked ebb dominance at the inlet due to direct interactions between the main astronomical tidal constituents. The imbalance caused by the different tidal filtering characteristics of both inlets combines with the internal morphological asymmetries of the system to produce a residual throughflow from HML to GEL. The residual circulation is also characterized by strongest values at both inlets, very weak residual currents in HML deep basin and a dipole of residual eddies over the deeper areas of GEL. Further investigations including numerical tracer experiments will be necessary to achieve a full understanding of the long term circulation of this lagoonal system.

2.1 INTRODUCTION

Lagoons are highly attractive places owing to their abundant natural and recreational resources, sheltered areas and/or beautiful landscapes. However, due to their narrow connection to the open ocean, they are, among other coastal systems, the most sensitive to human disturbances. Their restricted connections to the open sea often reduce their ability to flush exogenous substances leading to poor water renewal, eutrophication and other water quality problems. Hence, understanding water circulation within lagoons and their exchanges with the open sea becomes a prerequisite for sustainable management of these systems.

Several studies have addressed the exchange and transport processes between lagoons and oceans (Longuet-Higgins, 1969; van de Kreeke, 1976; Dronkers and Zimmerman, 1982). The methods used are either based on tidal asymmetry (Aubrey and Speer, 1985; Fry and Aubrey, 1990; van Maren et al., 2004) or on residual flow determination (Longuet-Higgins, 1969; Feng et al., 1986a,b; Tee and Lefaivre, 1990; Ridderinkhof and Loder, 1994; Loder et al., 1997; Janzen and Wong, 1998; Wei et al., 2004), with the latter giving a detailed spatial representation of transport processes. Residual circulation in coastal areas may be generated either by non-linear interactions between tidal constituents and topography and bathymetry (tide-induced), wind stress, density gradients, fresh water inflows or external water level gradients for multiple inlet systems (Uncles, 1982; Feng et al., 1986b; Smith, 1990; LeBlond, 1991; Prandle, 1991; Aubrey et al. 1993). Given the

number of processes involved, recent studies have ultimately relied on numerical models. A particular attention must be given to forcing functions in the coastal area as they set the spatial and temporal variability of the system. In the absence of fresh water input, tides and meteorological conditions are usually the most influencing forcings. Even though meteorological forcing is important at times (Smith, 1990), tides will remain the dominant periodic forcing in most cases. Finally, inlet morphology, topography and bathymetry play a major role in the dynamics of coastal lagoons and other semi-enclosed coastal systems (Keulegan, 1967; Zimmerman, 1981; DiLorenzo, 1988; van de Kreeke, 1988; Shetye and Gouveia, 1992; Aubrey et al., 1993; Fortunato and Oliveira, 2005). Therefore, the knowledge of external forcing alone is not sufficient as the response of each coastal lagoon depends on its tidal inlet geomorphology and, as such , is unique. In fact, coastal lagoons have been subdivided according to their tidal and morphological charateristics into "choked", "restricted" and "leaky" systems (Kjerfve, 1986). This classification confirms the tight link between the inlet characteristics and the ability of the lagoon to exchange water with the open sea (Kjerfve and Knoppers, 1991).

The objective of the present work is to investigate the tidal dynamics and the tide-induced residual circulation of a coupled two-lagoon system and reach a better understanding of how their inlet characteristics affect the transport and exchange processes between them and the open sea. A numerical model is set up to accurately represent the dynamics of this system under the influence of natural forcings. The finite element method was chosen for its ability to accurately represent complex coastlines (Legrand et al. 2006).

The tidal residuals are known to be highly influenced by the topography of the system. Hence, an unstructured grid that allows an additional refinement close to the shore helps to avoid unrealistic residuals in coastal areas (Jones and Davies, 2007). This numerical study of residual circulation and the development of the 3D hydrodynamic model is a first step towards a more comprehensive study of the long term circulation of this lagoonal system and the three-dimensional ecosystem dynamics of one of the lagoons.

2.2 MATERIAL AND METHODS

2.2.1 Study area

The two-lagoon system is part of the Magdalen Island Archipelago located in the southern Gulf of Saint-Lawrence (Fig. II-1). The system includes Havre-aux-Maisons lagoon (HML) to the southwest and Grande-Entrée lagoon (GEL) to the northeast. Both lagoons are connected to the Gulf of Saint-Lawrence (GSL) through tidal inlets, with GEL inlet cross section of 2960 m^2 (Drapeau, 1988) being much wider than HML's section of 620 m^2 (Koutitonsky, 2005). The two lagoons are linked through a narrow inlet, 300 m^2 in cross section (Koutitonsky, 2005). This coupled lagoons system has a surface area of approximately 108 km^2 and is rather shallow with a mean depth of about 3 m. Both lagoons present a deeper basin on their eastern side where depths vary between 5 and 6 m. A characteristic for GEL is the presence of a dredged 8 m deep navigation channel going from the entrance up to the northern shore (Fig. II-1).

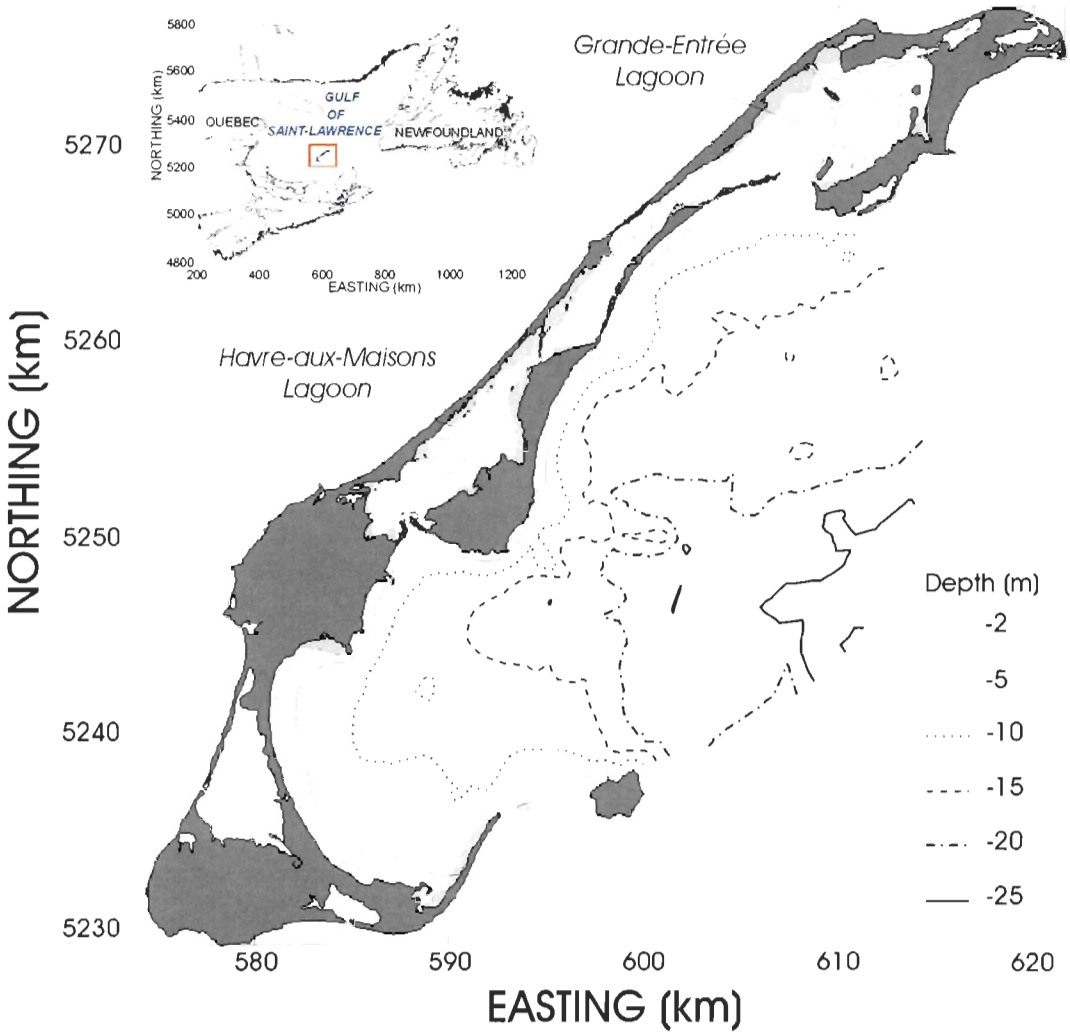

Figure II-1 Location and bathymetry of the Magdalen Islands study area.

This coupled system is mainly forced by tides and meteorological processes as there is no river discharge into the lagoons. Tides on the shallow (ca. 50 m) Magdalenian bank surrounding the islands are of small amplitude (0.5 m during spring tides) and of mixed but mainly semi-diurnal type (Koutitonsky et al., 2002). Stations shown in Fig. II-2 were used in summer 2001 (May-July) to monitor water levels and/or currents at different points of interest in the system (tide gauges and current meters moored at 1m above the bottom). Hourly time series of wind speed and direction and atmospheric pressure were recorded at station M (Fig. II-2) and were considered to be constant over the whole model domain. Water levels recorded at external stations L10 and L11 served as boundary conditions for the model simulations while stations inside the lagoons were used for model calibrations (see next section).

Regional atmospheric forcings are known to affect low frequency water level fluctuations through an inverse barometer effect of the atmospheric pressure and a non-local wind set up/down effect at the scale of the GSL (Koutitonsky et al., 2002). Local winds are predominantly blowing from the western sector and calm conditions are scarce (Drapeau, 1988). Moreover a predominant orientation of the wind along the longitudinal axis of the lagoonal system has been noticed (Koutitonsky et al., 2002). Another characteristic of this system is the presence of an ice cover from January to mid-April in average conditions (Drapeau, 1988). The present work focusses only on the deterministic effects of tidal forcing alone during the ice-free season.

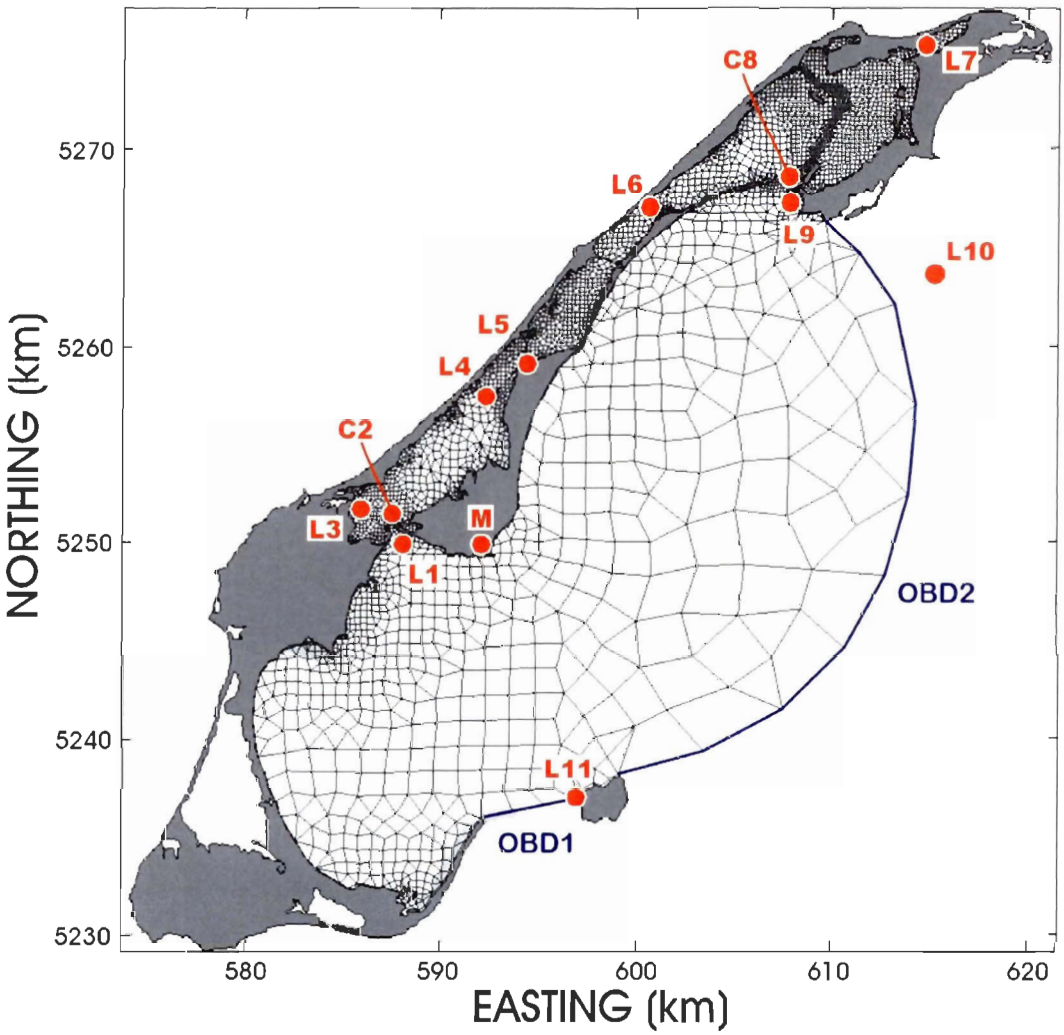

Figure II-2 Location of the summer 2001 sampling stations (L : tidal gauge, C : current meter, M : meteorological station) and calculation grid of the numerical model RMA-10 with its two open boundaries (OBD1 and OBD2).

In this context, both lagoon-inlet systems set the way external forcings are transmitted to the inner parts of the system (DiLorenzo, 1988). GEL and HML inlets may be broadly characterized using the repletion coefficient (K) defined as (Keulegan, 1967; van de Kreeke, 1988; Kjerfve and Knoppers, 1991):

$$K = \frac{T}{2\pi a_0}\frac{A_C}{A_B}\sqrt{\frac{2gRa_0}{(\alpha+\beta+\gamma)R+2FL_C}} \qquad (1)$$

with the semi-diurnal tidal period T = 12.42h, the semi-diurnal tidal amplitude a_0 = 0.2 m, the inlet cross-sections A_C mentionned above, the lagoon surface areas A_B = 34 and 74 km^2 for HML and GEL respectively, the hydraulic radii at the entrance R = 4.1 and 3.8 m, respectively, and the acceleration due to gravity g. As the friction factors F (0.002 to 0.006) were not known a priori for HML and GEL inlets and as the repletion coefficient only varies by 0.3 (HML) and 0.5 (GEL) over the whole range of F values, the median value of 0.004 was used for both inlets. The length of the inlets L_C was set to 700 and 2000 m for HML and GEL respectively. The parameter α accounting for the velocity distribution over the inlet cross-section was set to 0.3 for GEL where the flow is concentrated by the navigation channel over a small part of the cross-section and to 0.2 for HML which exhibits a narrower inlet with uniform depths. The coefficient β corresponds to the fraction of kinetic energy dissipated in the transition between the entrance and the inlet channel. Both inlets present relatively smooth transitions due to the slowly convergent coastlines for HML and due to the navigation channel extending offshore for GEL. Hence, the same value

$\beta = 0.3$ was used for both. Finally, γ represents the fraction of remaining kinetic energy lost at the lagoon side of the inlet. In the absence of any major channel and due to the rapidly divergent coastlines HML's inlet presents a much more abrupt transition than GEL's leading to a larger dissipation of kinetic energy. To reflect this γ was given a value of 0.7 for HML and 0.3 for GEL (van de Kreeke, 1988). According to the classification introduced by Kjerfve (1986) and values of $K = 1.2$ and $K = 0.7$ for GEL and HML respectively, this system is a coupled "leaky" (GEL) and "restricted" (HML) lagoonal system.

It is now possible to assess the conditions set inside both lagoons by these dynamically different inlets and examine how these conditions interact through the tight connexion between HML and GEL to have a complete picture of the system circulation behaviour.

2.2.2 Model description

General characteristics

The model used for the present work is RMA-10 (King, 1982). It is a three dimensional (3D) finite element hydrodynamic model developped for coastal and estuarine systems. It uses the Newton-Raphson iterative approach with the Galerkin weighted residuals to solve a 3D set of non linear equations. These basic equations are the Reynolds form of the Navier-Stokes equations for motion, the continuity equation, a convection-

diffusion equation for transport of heat and/or salinity and the equation of state for density (see Appendix). The momentum equation in the vertical direction is simplified using the hydrostatic assumption. In the vertical, the model uses a modified sigma transformation that preserves the original bottom profile or a Z-level coordinate (King, 1985). Another feature of RMA-10 is the possibility to mix different levels of spatial representation in the same application. For instance, the model domain may be represented by areas where 3D equations are solved, next to shallower areas where the depth-averaged 2D equations are solved. This improves the calculation cost as compared to a full 3D application (King, 1985). RMA-10 also offers different options for turbulence closure methods. In this study, the Smagorinsky closure scheme (Smagorinsky, 1963) was used in the horizontal. In the vertical, the original RMA-10 scheme was used. In this scheme, the vertical eddy viscosity coefficients are only varying with depth and are given a quadratic distribution over the water column with a mid-depth maximum value determined during the calibration process. A constant vertical eddy viscosity which is a too rough parametrization is improved here by this parabolic profile. As shown by Lee and Davies (1999), a vertical eddy viscosity may be sufficient to represent the overall tidal dynamics of a coastal system, but a critical point in assessing the quality of model results lies in the comparison of observed and simulated near-bed currents. Despite the scarcity of near-bed current data, this comparison is presented in the calibration section (3.1) for two critical areas of the system, namely HML's and GEL's inlets. Finally, RMA-10 uses a modified semi-implicit Crank-Nicolson time stepping scheme for unsteady flows which allows the use of rather long time steps, reducing the calculation time (King, 1993).

Application to the Magdalen Islands system

The RMA-10 model was employed for the HML-GEL lagoonal system based on data collected in summer 2001. The horizontal finite element grid structure used for this study is shown on Fig. II-2. Considering subsequent ecosystem modelling requirements and CTD profiles showing only slight thermal stratification during calm summer conditions (Booth, 1994), the vertical structure of the 3D model consisted of two vertical layers (3 nodes) of equal thickness. Most of the elements are of a quadrangular shape and a few triangles complete the grid in less regular regions. A poor representation of the coastline may lead to the generation of unrealistic tidal residuals (Jones and Davies, 2007). The refinement strategy hence consisted in maximizing the grid resolution in shallow nearshore areas. The grid was also refined along the navigation channel inside GEL to better represent this deep and narrow feature expected to play an important role in the lagoon hydrodynamics. The elements have typical side lengths varying between 80 m in the most refined areas inside the lagoons to 2000 m for the coarser part in the GSL. The 3D grid is composed of 6587 quadratic elements for a total of 19333 nodes. The model domain has two open boundaries (OBD1 and OBD2) where water levels have been specified. The positions of OBD1 and OBD2 were set as far as possible from the actual entrances of the lagoonal system in order not to bias the dynamics of the inlet areas. Water levels at station 11 were imposed along OBD1, while a linear interpolation between water levels at station 11 and 10 was imposed along OBD2. Finally, atmospheric pressure and wind friction were imposed on the free surface during the calbration process. Given the lack of river discharge and the observed small density gradients either in horizontal or vertical direction during the summer period,

all simulations were done with a constant density distribution (barotropic conditions). A time step Δt = 360s was used for all simulations leading to a maximum CFL number of approximately 4.5 in the most refined areas of the grid. All data needed for initial conditions, boundary conditions and forcings were collected simultaneously during the 2001 field sampling mentionned above.

Two types of simulations, both covering the same 31 day long period (from 25 May to 25 June 2001), were carried out. These simulations differ by the set of forcings used:

a. "REAL" simulation: the model is forced by observed water level fluctuations at the open boundaries and meteorological forcing at the surface. This represents conditions closest to reality and this simulation was used for calibration purposes only;
b. "TIDAL" simulation: the model is forced by pure tidal oscillations at the open boundaries (obtained from the harmonic analysis of observed water level fluctuations (Foreman, 1977)). This simulation was used for the study of the tidally induced residual circulation described in the next sections.

2.2.3 Residual flows and water levels

Model results from the "Tidal" simulation were analyzed for residuals using the harmonic analysis of water levels (Z_0) and currents (U_0, V_0) at each node of the grid. This

simulation being forced by tidal oscillations only the residuals obtained are internally generated by the dynamical behaviour of the lagoonal system.

A two day spin up period was allowed for the model to stabilize, then the residual flows and water levels in HML and GEL were evaluated over the period corresponding to the last 29 diurnal cycles of the simulation.

2.3 RESULTS

2.3.1 Model calibration

Results of the "Real" simulation were used for tuning the model. The calibration was based on two parameters, the bottom friction scaled by a unique Manning coefficient (n) over the whole area and the maximum value of the vertical eddy coefficient (ε_Z). The process relied on the comparison of observed and simulated water levels (stations 1, 3, 4, 5, 6, 7 and 9) and bottom currents (stations 2 and 8). The best results were obtained for n = 0.031 and ε_Z = 1 Pa.s. Figure II-3a,b shows the comparison between observed and simulated water levels inside each lagoon at stations 4 and 6 respectively. Both phase and amplitude of the water level fluctuations are well reproduced by the model. Harmonic analysis of observed and simulated water levels was also made for all sampling stations located inside the model domain. Results for the main tidal components O1, K1, M2 and S2 are presented in Table II-1. Except for station 5 located at the junction of HML and GEL where the phase of the semi-diurnal constituants is slightly off, model results are in close agreement with observations. This indicates that the tidal part of the water level fluctuations is well described by the model in most of the system. The MO3 constituent is

also included in Table II-1 to represent shallow water waves generated by non-linear processes inside the system. Model results are in fairly good agreement with observed values of amplitude and phase of this compound tide. This indicates a rather good representation of non-linear processes by the model. Stations 5 and 7 present the greatest deviation as for the main tidal components. Moreover, more than 92% of the total variance of the water level fluctuations is reproduced by the model (Table II-1) at all stations except station 5 and 7 where the poorer representation of the tidal signal already impairs the model behaviour. Comparison between observed and simulated bottom currents along their principal axis at both entrances (stations 2 and 8) were also made and are presented in Fig. II-3c,d. It appears that flows through these inlets are generally well reproduced by the model. Phase and amplitude of the currents are correctly simulated at GEL's mouth. The discrepancy between the observed and simulated orientation of the current's principal axis (Table II-2) may be due to local bathymetric features not resolved by the model. At HML's entrance the phase and orientation are correctly represented but the amplitude of the current is slightly underestimated. More detailed and recent bathymetric data in this energetic area would probably lead to a better representation of the flow. Rapid spatial variation in current speed in such an area may also lead to the discrepancy between single point observations and model outputs. Nevertheless, at both entrances more than 91% of the variance contained in the current signal is reproduced by the model (Table II-2).

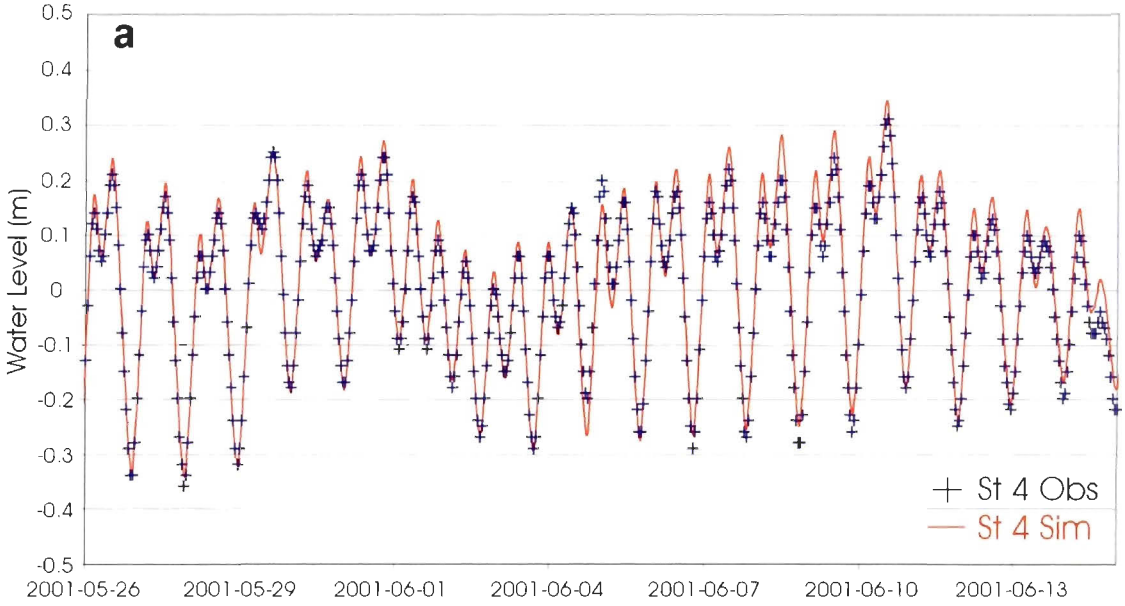
a
Water Level (m)
0.5
0.4
0.3
0.2
0.1
0
-0.1
-0.2
-0.3
-0.4
-0.5
2001-05-26
2001-05-29
2001-06-01
2001-06-04
2001-06-07
2001-06-10
2001-06-13
St 4 Obs
St 4 Sim

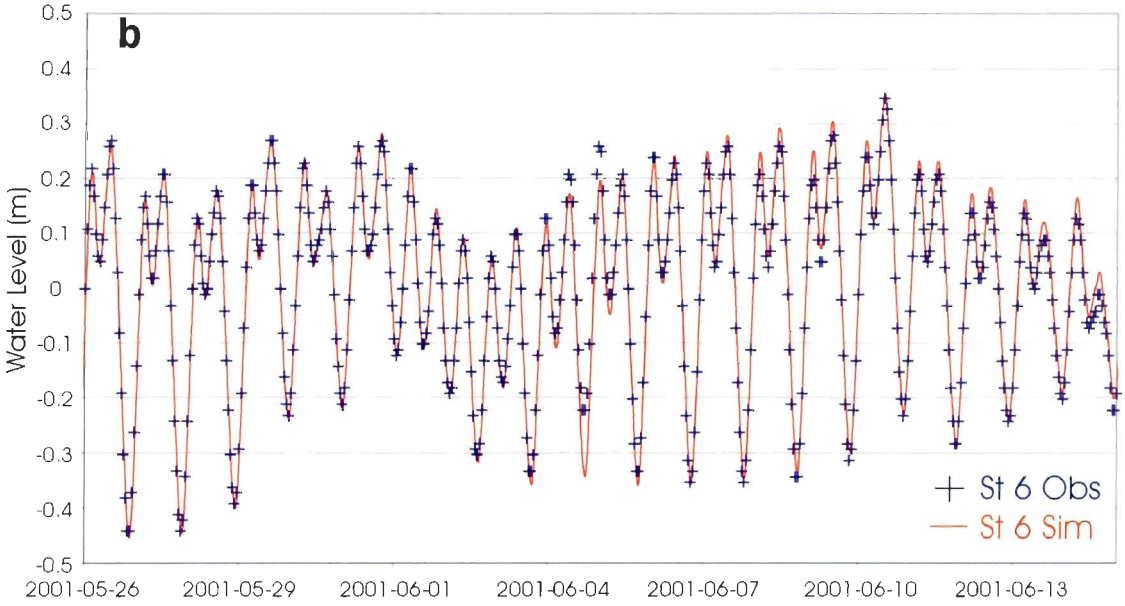
b
Water Level (m)
0.5
0.4
0.3
0.2
0.1
0
-0.1
-0.2
-0.3
-0.4
-0.5
2001-05-26
2001-05-29
2001-06-01
2001-06-04
2001-06-07
2001-06-10
2001-06-13
St 6 Obs
St 6 Sim

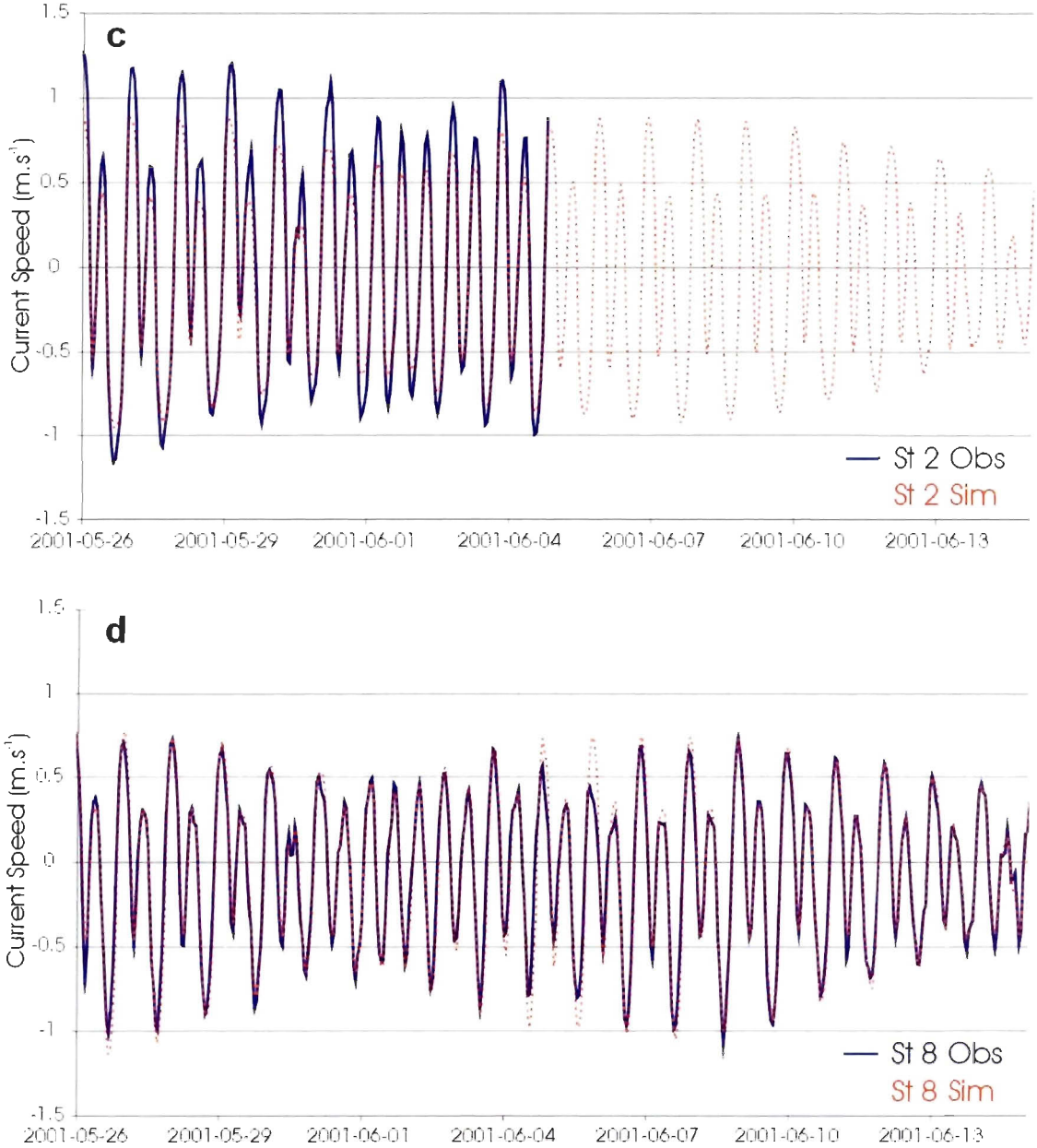

Figure II-3 Comparison of observed (Obs) and simulated (Sim) water levels (a and b) and currents (c and d) at four different stations in HML and GEL.

Table II-1 Harmonic analysis (amplitude in m and phase in degrees) of observed (Obs) and simulated (Sim) water levels with 95% confidence intervals at all sampled stations inside the model domain. Total variance of the observed water level time series explained by the model simulation.

	O1				K1			
	Amplitude		Phase		Amplitude		Phase	
	Obs	Sim	Obs	Sim	Obs	Sim	Obs	Sim
St1	0.12±0.01	0.12±0.01	220.1±5	226.1±4	0.12±0.01	0.11±0.01	247.0±4	248.3±4
St3	0.08±0.01	0.09±0.01	263.8±7	267.5±7	0.09±0.01	0.09±0.01	291.3±6	294.6±6
St4	0.08±0.01	0.09±0.01	266.4±6	267.7±6	0.09±0.01	0.09±0.01	295.7±6	294.7±6
St5	0.09±0.01	0.10±0.01	274.8±7	264.7±6	0.10±0.01	0.10±0.01	301.9±7	290.5±5
St6	0.09±0.01	0.11±0.01	254.0±7	254.8±5	0.10±0.01	0.11±0.01	280.0±6	279.4±6
St7	0.10±0.01	0.10±0.01	254.2±6	254.8±5	0.10±0.01	0.10±0.01	280.4±6	280.2±5
St9	0.12±0.01	0.12±0.01	224.3±5	227.1±4	0.12±0.01	0.11±0.01	247.7±4	249.3±4
	M2				S2			
	Amplitude		Phase		Amplitude		Phase	
	Obs	Sim	Obs	Sim	Obs	Sim	Obs	Sim
St1	0.19±0.003	0.19±0.01	285.9±1	286.0±2	0.06±0.003	0.06±0.01	329.4±3	331.0±6
St3	0.10±0.004	0.11±0.01	349.6±2	348.4±4	0.02±0.004	0.02±0.01	36.4±11	39.6±20
St4	0.10±0.004	0.11±0.01	351.8±2	348.4±4	0.02±0.003	0.02±0.01	46.2±10	39.9±21
St5	0.12±0.01	0.13±0.01	5.9±2	343.6±4	0.03±0.005	0.03±0.01	65.4±12	39.6±18
St6	0.14±0.003	0.15±0.01	328.9±1	326.96±3	0.03±0.003	0.04±0.01	25.7±4	21.3±13
St7	0.13±0.004	0.13±0.01	321.9±2	324.2±3	0.03±0.004	0.03±0.01	11.3±7	14.9±15
St9	0.19±0.004	0.18±0.005	282.7±1	281.6±2	0.06±0.004	0.06±0.005	329.2±4	327.5±4
	MO3				Total variance explained			
	Amplitude		Phase					
	Obs	Sim	Obs	Sim	%			
St1	0.009±0.003	0.007±0.002	55.1±14	45.7±21	97.7			
St3	0.009±0.002	0.013±0.004	184.9±10	198.7±15	92.3			
St4	0.010±0.003	0.014±0.004	188.8±13	197.1±16	96.7			
St5	0.019±0.004	0.018±0.004	209.4±14	180.1±14	73.6			
St6	0.013±0.003	0.016±0.004	153.7±12	155.3±13	97.4			
St7	0.010±0.003	0.014±0.003	165.1±18	162.7±14	77.6			
St9	0.007±0.002	0.006±0.002	70.8±17	51.1±19	98.9			

Table II-2 Comparison of observed and simulated orientation of current principal axis at HML's (St.2) and GEL's inlet (St.8) and total variance of the observed current time series explained by the model simulation at these same stations.

	Principal axis direction		Total variance explained
	Obs	Sim	%
St 2	94.4	93.0	94.1
St 8	69.5	77.5	91.6

2.3.2 Tidal dynamics

Figure II-4 gives an overview of the current velocity field during spring tides at maximum flood (Fig.II-4a,b) and maximum ebb (Fig.II-4c,d), as computed from the"Tidal" simulation. It can be seen that both inlets are the most dynamic areas with currents reaching about 0.8 $m.s^{-1}$. The maximum tidal fluxes hence reach values of 2500 $m^3.s^{-1}$ and 500 $m^3.s^{-1}$ at GEL and HML's entrance respectively. In HML, the current speed quickly decreases to about 5 $cm.s^{-1}$ in the deeper area. GEL is marked by the presence of the navigation channel which concentrates the flow both at flood and ebb. In the deeper basin, east of the channel, current speeds drop fairly quickly to typical values of 5 $cm.s^{-1}$ whereas the western part of the lagoon is more dynamic with currents of 20 $cm.s^{-1}$. This situation may be explained by the shallower depths and the convergent coastlines that make the western part of the lagoon significantly narrower and by phase differences beween the tide in both lagoons.

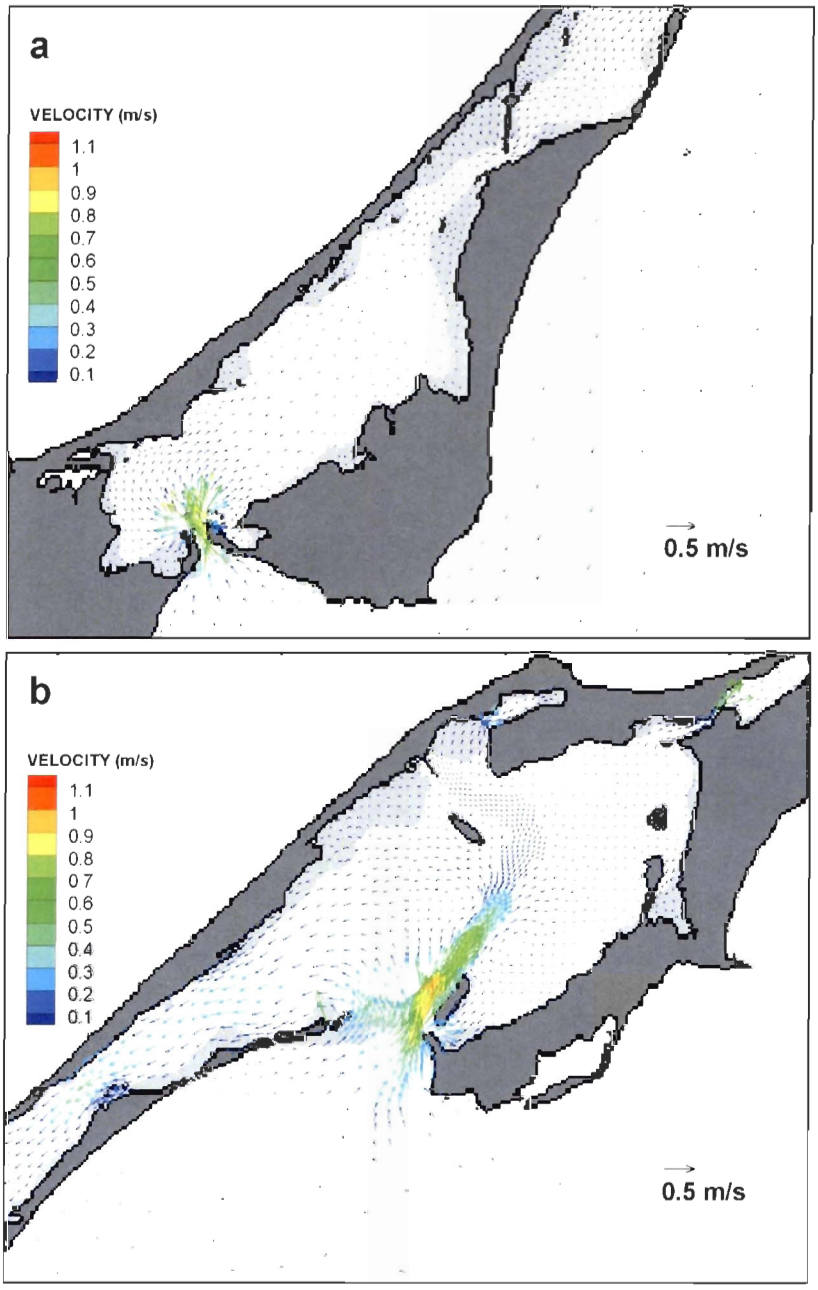
a
VELOCITY (m/s)
1.1
1
0.9
0.8
0.7
0.6
0.5
0.4
0.3
0.2
0.1
0.5 m/s
b
VELOCITY (m/s)
1.1
1
0.9
0.8
0.7
0.6
0.5
0.4
0.3
0.2
0.1
0.5 m/s

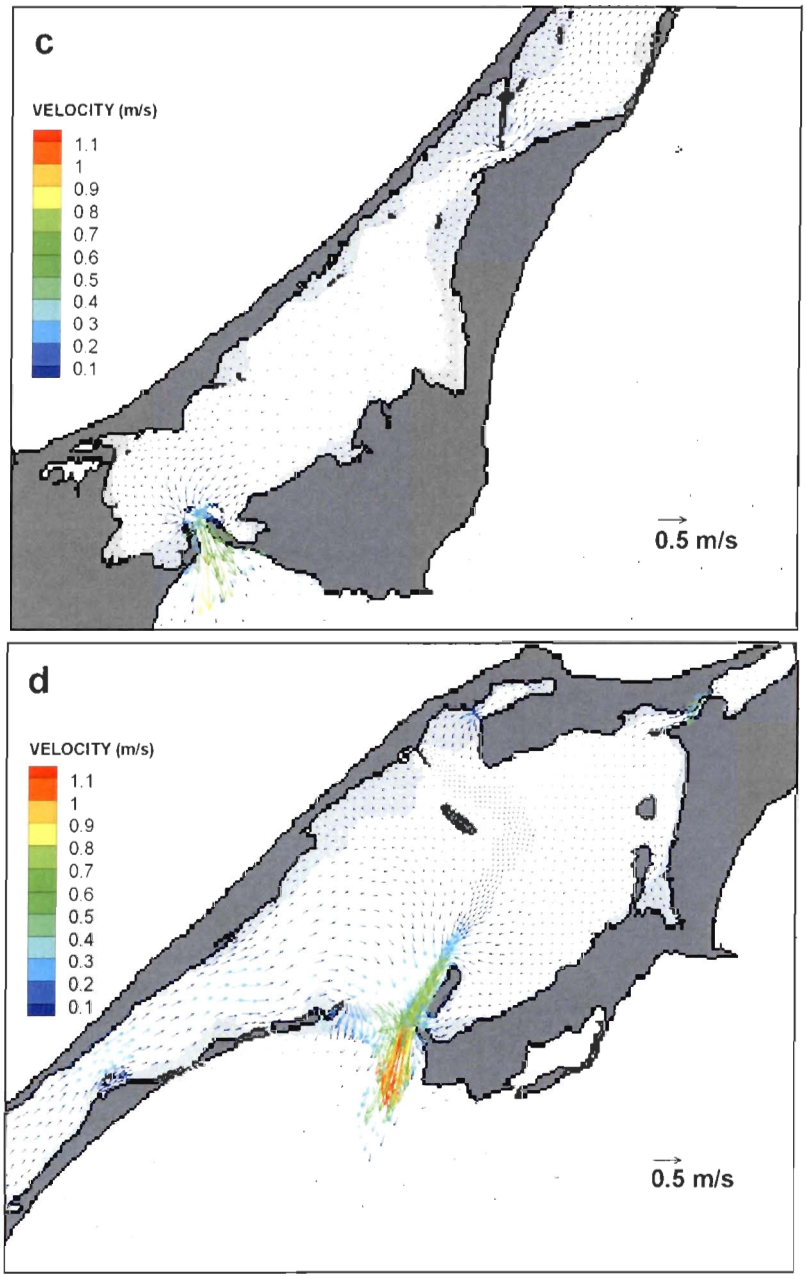

Figure II-4 Model results for the surface layer tidal currents in maximum flood (panels a and b) and ebb conditions (panels c and d). The vector color represents the velocity magnitude following the color scale shown.

Harmonic analysis of levels at each surface node of the numerical grid gives a spatially detailed description of tidal amplitude and phase (Fig. II-5). The constituents S2 and K1 having similar propagation patterns as M2 and O1 respectively, they are not included in Fig. II-5. These results show that all major tidal constituents (O1, K1, M2 and S2) are attenuated at both entrances and as the tide travels further inside the lagoons. Together with this amplitude attenuation there is an increase in phase lag. This indicates a system dominated by friction as a mechanism for energy dissipation and tidal signal modulation (Aubrey and Speer, 1985; Salles et al., 2005). This result is confirmed by the harmonic analysis of observed water level time series at inner stations (Table II-1). Fig. II-5 also explicitly shows the difference between HML and GEL inlets foreseen by the discrepancy of their repletion coefficients (section 2.1). HML is more of a restricted nature than GEL where a greater part of the incoming energy reaches the lagoon interior and the phase lag introduced at the entrance is much smaller, despite similar tidal signals just outside both entrances (Table II-1, stations 1 and 9). Moreover, once inside HML the tidal wave is almost not damped nor delayed anymore due to the rather large and deep basin forming its eastern side. Conversely, GEL's internal morphology, especially the throat section leading to HML, further acts to damp and slow the tidal wave down. These results are of major importance for the dynamics of the system as a whole. Whereas tidal forcings are of similar amplitude and almost in phase just off HML and GEL entrances, the characteristics just mentioned introduce an asymmetry in the system. Using stations 4 and 6 as representative of HML and GEL respectively, it can be seen that the tide in GEL is of stronger amplitude and leading that in HML (Table II-1). This leads to a pressure gradient

being established from GEL to HML during the flood and in the opposite direction during the ebb causing the flow to reverse from ebb to flood at the junction between the two lagoons (Fig. II-4a and c).

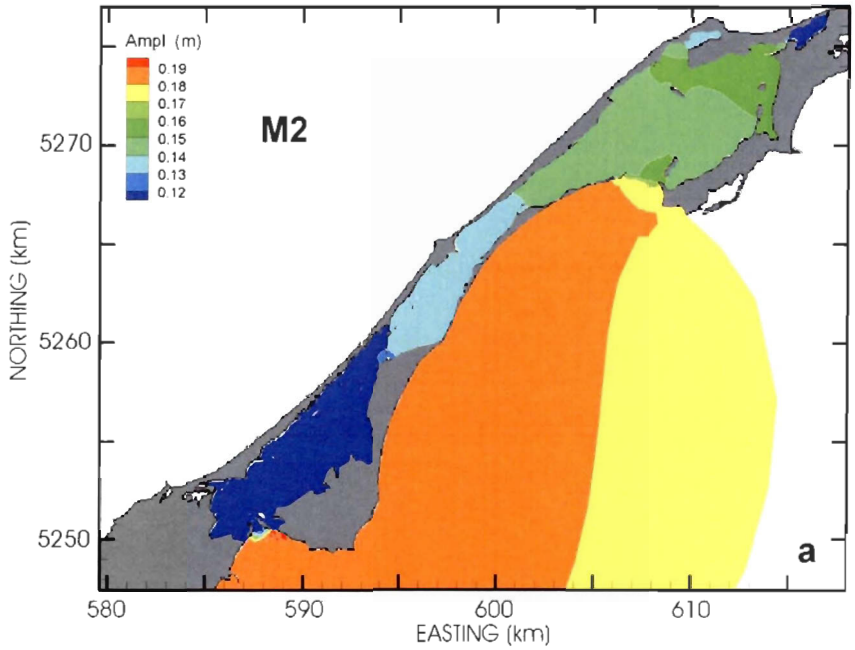
Ampl (m)
0.19
0.18
0.17
0.16
0.15
0.14
0.13
0.12
M2
a
5270
5260
5250
NORTHING (km)
580
590
600
610
EASTING (km)

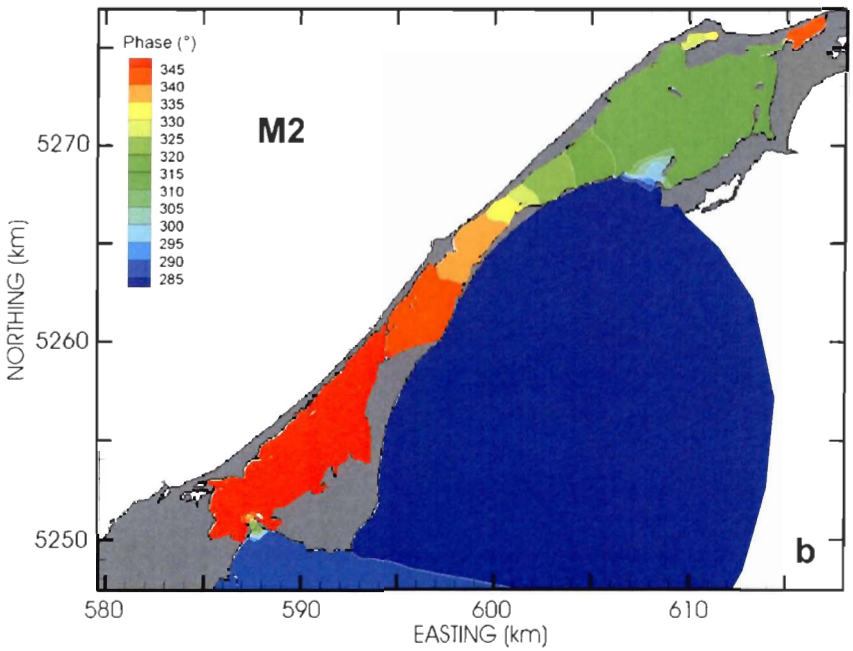
Phase (°)
345
340
335
330
325
320
315
310
305
300
295
290
285
M2
b
5270
5260
5250
NORTHING (km)
580
590
600
610
EASTING (km)

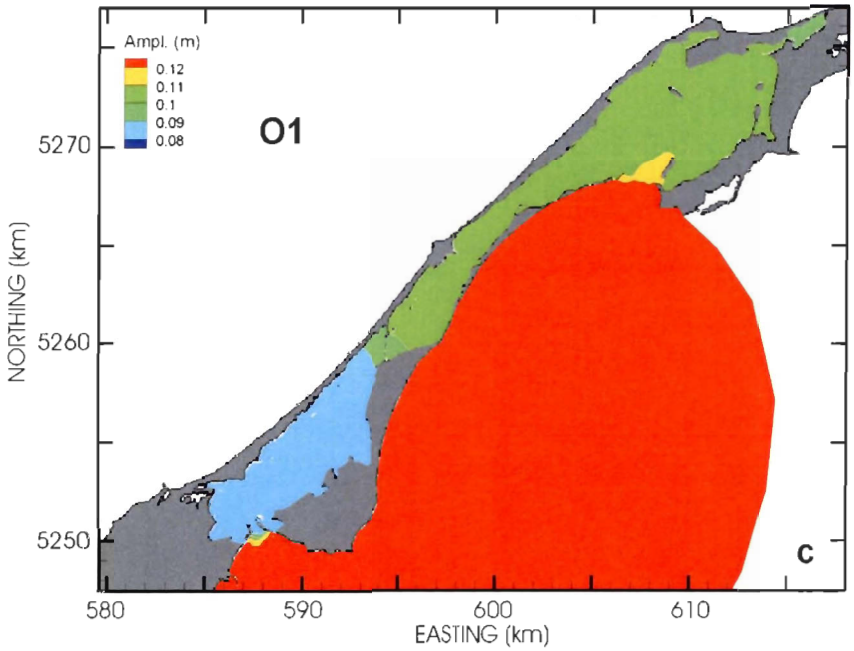
Ampl. (m)
0.12
0.11
0.1
0.09
0.08
O1
5270
5260
5250
NORTHING (km)
580
590
600
610
EASTING (km)
c

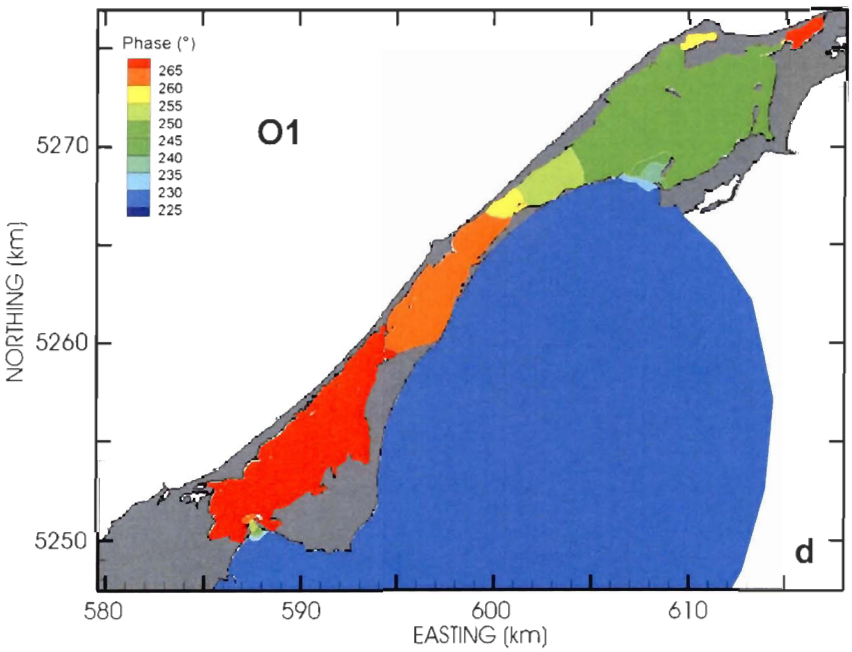
Phase (°)
265
260
255
250
245
240
235
230
225
O1
5270
5260
5250
NORTHING (km)
580
590
600
610
EASTING (km)
d

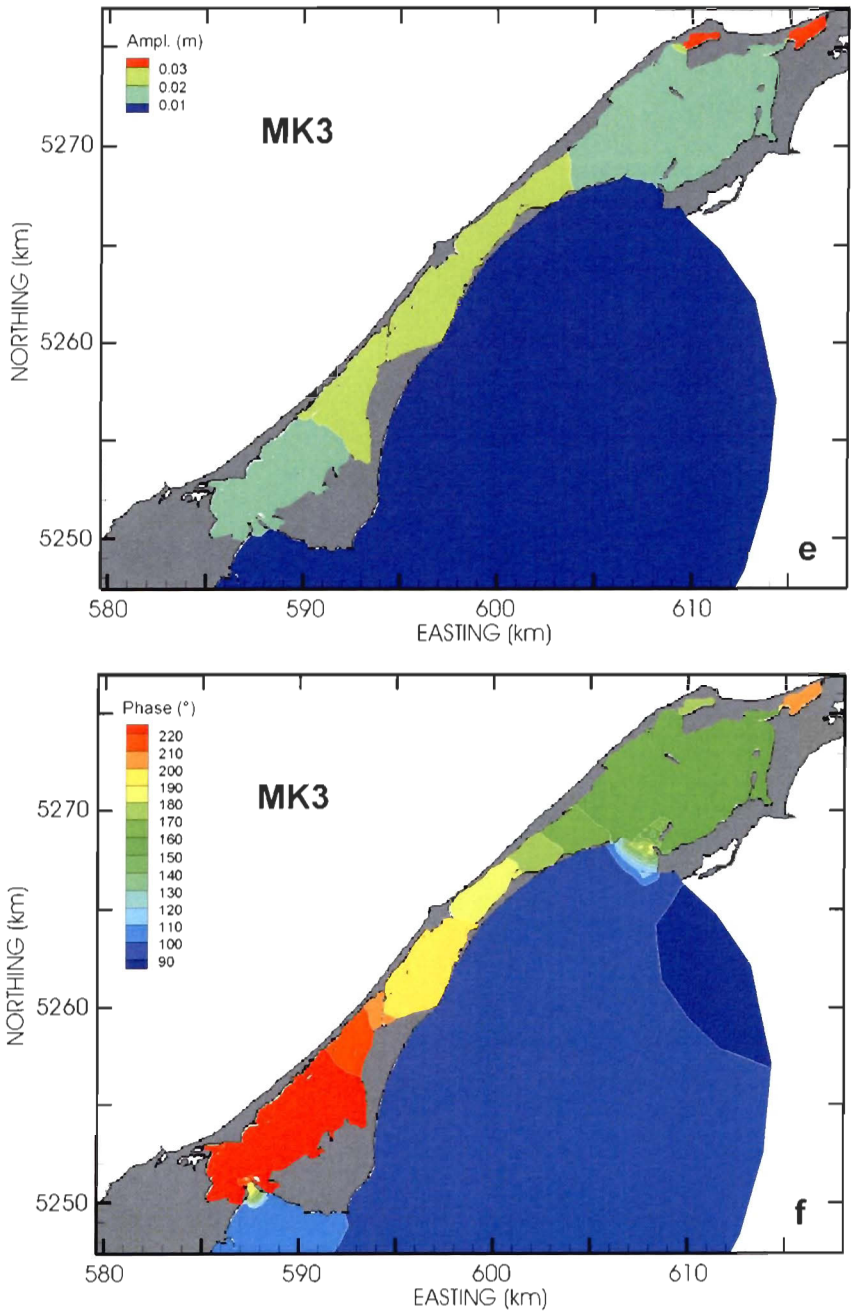

Figure II-5 Results of the harmonic analysis of water level time series over the whole domain area for the main constituents M2, O1 and the compound tide MK3.

In addition to the first order effect of friction just mentioned, several non-linear mechanisms come to play in the propagation of tidal waves in shallow water regions. A common feature of these non-linear mechanisms is to allow the tidal consitutents to interact either with themselves to create residuals and/or overtides or with each other to generate compound tides (Parker, 1991). Residuals will be addressed in later sections. Concerning over- and compound tides, in such a system dominated by M2 the first harmonic expected is the overtide M4 (Aubrey and Speer, 1985). But here surprisingly the amplitude ratio M4/M2 never exceeds 4%. However as mentioned above, O1 and K1 being important constituents as well, their interactions with M2 lead to the generation of the compound tides MO3 and MK3, the only harmonics reaching a noticeable magnitude (Fig. II-5e,f; MO3 not shown as very similar to MK3). Here a small fraction of the energy of the major constituents seems to be transferred to compound tides (MO3 and MK3). These components see a slight increase in amplitude as the tide propagates inside both lagoons (Fig II-5e). This transfer of energy induced by non-linear processes such as bed friction and/or tide/bathymetry interactions is slightly stronger in GEL as the tidal wave travels over the shallow internal throat section. Comparison of power spectral density (PSD) of water level fluctuations (Percival and Walden, 1993) between entrances and inner stations (Fig. II-6) confirms the overall energy decrease of the signal due to friction and also shows explicitly the transfer of part of the energy lost by diurnal and semi-diurnal constituents to ter-diurnal species. This transfer is maximum at the junction between both lagoons (as seen in harmonic analysis results, Table II-1) where the signal is the most affected by non-linear shallow water processes and tidal constituent interactions.

The model seems to reproduce this non-linear generation quite accurately as amplitude and phase of MK_3 observed at station 5 (0.026 m and 233°) compare reasonably well with the ones obtained with the model in this area (0.02-0.03 m and 210-220°). Other interactions between O1 and K1, M2 and O1 and M2 and K1 may generate compound tides of the same frequency as M2, K1 and O1 respectively. Each of these compound tides would then be masked by the astronomical constituent of same frequency which possesses a much larger amplitude.

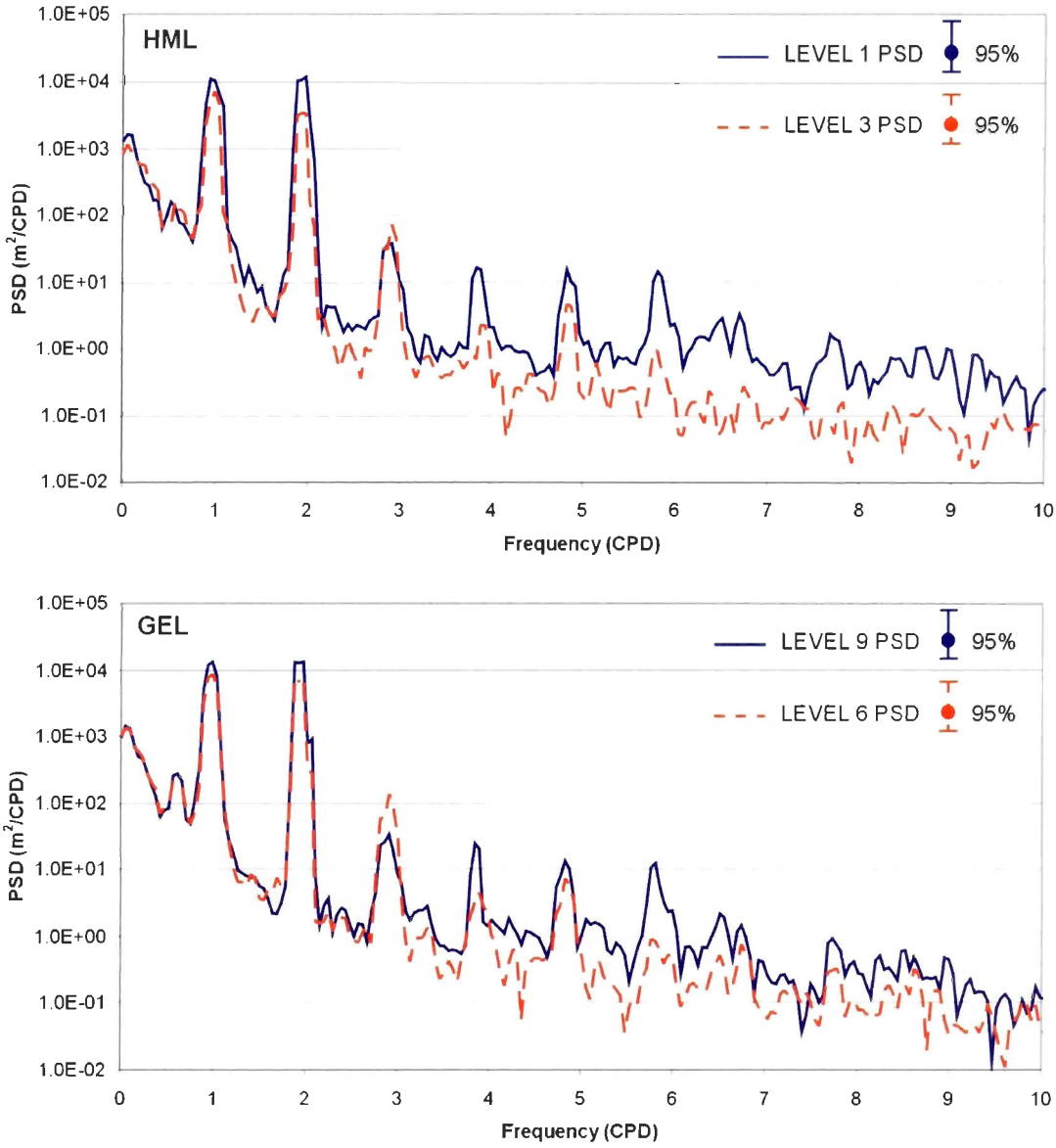

Figure II-6 Power spectral densities (PSD) of water level time series at the inlet and inside HML (top) and GEL (bottom), with 95% confidence interval. Frequency expressed in cycles per day (CPD).

To complete this overview of the system's tidal dynamics it can be noticed from the time series of Fig. II-3c,d that HML's entrance exhibits maximum ebb and flood currents of approximately the same strength whereas GEL's mouth encounters an asymmetrical pattern, with maximum currents being consistently stronger at ebb. This tidal asymmetry and the absence of the M4 constituent noticed above could seem paradoxal. But as mentionned in previous studies (Ranasinghe and Pattiaratchi, 2000; Hoitink et al., 2003; van Maren et al., 2004) in systems where semi-diurnal and diurnal signals are of the same order of magnitude a tidal asymmetry may arise from the direct interaction between M2, O1 and K1 rather than from overtides generated by shallow water processes and friction, a more common mechanism in systems dominated by semi-diurnal species (Aubrey and Speer, 1985; Speer and Aubrey, 1985; Fry and Aubrey, 1990).

2.3.3 Residual flows and water levels

Residual flows are of greater interest than tidal currents for the transport of dissolved or suspended matter as they inform about long term circulation patterns and fate of the transported matter. Residual flows in coastal systems are mainly generated by non-linear interactions between tidal constituents and coastal topography and bathymetry (tide-induced), wind stress, density gradients, fresh water inflows and external water level gradients for multiple inlet systems (Feng et al., 1986b; Smith, 1990; Uncles, 1982 and others). As mentionned earlier, fresh water inflows are not an issue here and the assumption was made that density gradients do not play a major role in the water circulation of HML-

GEL system at least during summer. In the following we will be looking at tide-induced residuals only. This is done by extracting the mean from the harmonic analysis of water levels and currents obtained with the "Tidal" simulation over several (29) diurnal tidal periods. The boundary conditions used did not contain any residual such that the residual circulation obtained is only due to the tide propagation inside the system.

First, a drop in residual water level which is a typical feature of tidal inlets (Ridderinkhof, 1988a) can be observed at both entrances (Fig. II-7). It is more obvious for GEL where it covers a far greater area but this trough is of comparable depth (1-2 cm) at both inlets. This trough is caused by the rapid reduction of the flow section and may be assimilated to a Bernoulli effect (Ridderinkhof, 1988b). Its depth may then be assessed using the following equation:

$$\varsigma = -\frac{\overline{u^2}}{2g} \qquad (3)$$

where ζ is the residual water level, u the tidal current, g the acceleration due to gravity and the overbar represents the mean over a tidal period. For a tidal flow amplitude of 0.8 $m.s^{-1}$ as observed in HML and GEL inlets, the resulting trough in residual water level is about 1.6 cm deep, which confirms the values obtained with the numerical model.

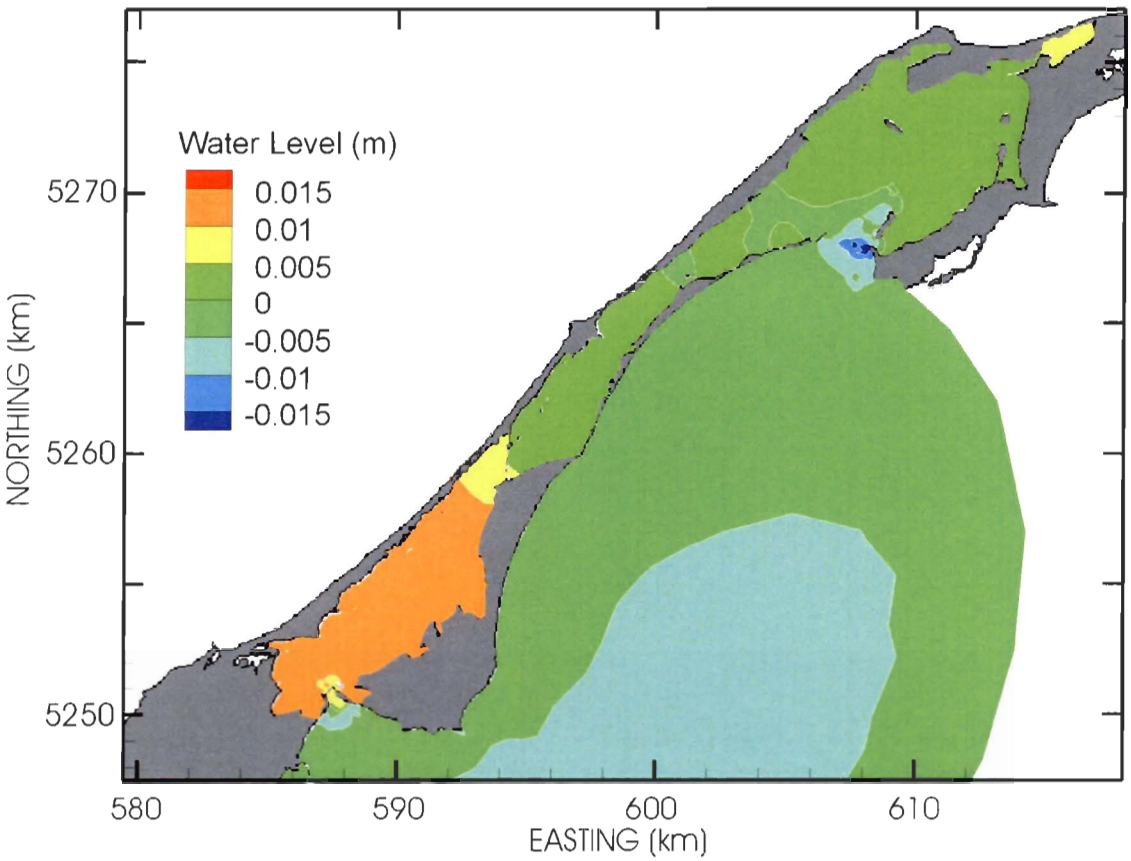

Figure II-7 Tide-induced residual water levels obtained from the harmonic analysis of model results over a period of 29 diurnal tidal cycles.

Residual flows in HML surface layer do not present a very clear pattern except at the inlet where the flow is separated in an incoming part spreading just inside the lagoon and an outgoing flow that concentrate on the western side just off the inlet (Fig. II-8a). Residual currents are strongest at the inlet reaching 7-8 $cm.s^{-1}$ and vanish rapidly further inside the lagoon with typical values of 1 $cm.s^{-1}$ or less in the deeper basin.

The inlet is also the area of GEL where the strongest residual currents occur reaching up to 10 $cm.s^{-1}$ in the surface layer. Station 8 provides the only current time series long enough to compare observed and simulated residual currents. Residual flow intensity and direction (0.07 $m.s^{-1}$ and -82.4°/East) simulated by the model are in rather good agreement with the observed values (0.06 $m.s^{-1}$ and -90.9°/East) at GEL's entrance. Further inside the lagoon, a pattern typical of tidal inlets (Imasato, 1983; Robinson, 1983) can be observed with the formation of two residual eddies (Fig. II-8c). The residual flow that otherwise concentrates in the navigation channel splits in two branches approximately halfway to the northern coast of the lagoon creating a clockwise rotating eddy to the east of the channel and an anticlockwise to the west. These cells are closing in a convergence point just north of the small island located on the eastern side of the entrance. In addition to friction, these residual eddies are known to be mainly generated by the inertial effect whose importance is enhanced in places with strong gradients in velocity (LeBlond, 1991). The eastern eddy that occupies the deeper basin seems to cover a greater area than the western one. The latter is more damped by bottom friction in this shallower area and may also be constrained by the presence of the small island to the north. Whereas the formation of residual eddies by the

non linear interactions of tidal currents and variable bathymetry/topography of headlands is a common feature, the position of these eddies in GEL is rather unusual. In previous studies (Imasato, 1983; Ridderinkhof and Zimmerman, 1990a) the residual eddies were observed right behind the two capes forming the inlet. Here in GEL both eddies are pushed further inside the lagoon. One explanation for this may be the particular topography/bathymetry of the entrance area. The combined presence of the navigation channel that concentrates the flow, a shallow sand bank on the western side and the small island on the eastern side of the entrance creates the equivalent of an extended inlet (Fig. II-1) that only ends at the northern tip of the small island where both eddies converge. This hypothesis is strengthened by the work of Drapeau (1988) who was testing different inlet lengths in an empirical estimate of the inlet stability. Another confirming observation is the presence of another eddy corresponding to the ebbing situation and located just off the inlet on the western side in a more usual position (Fig. II-8c).

This last point raises the question of the absence of a second eddy for the ebbing situation to complete the usually observed residual quadrupole (Imasato, 1983; Ridderinkhof and Zimmerman, 1990a). Here again the topography of this area with the channel on the eastern side along the coast that stretches straight to the south may explain the absence of the fourth eddy. However the proximity of the open boundary may lead to a slightly altered representation of this area of the domain which may conceal the last residual eddy.

As mentioned in section (2.3.2) tidal propagation in HML and GEL leads to a water level gradient between these two lagoons which reverses from ebb to flood. Averaging the water level over several tidal periods reveals a residual situation where HML level is above GEL's (Fig. II-7), corresponding to the ebb pattern. This gradient creates a residual throughflow from HML to GEL that can be seen at the junction between the two lagoons (Fig. II-8b) and represents a constant flux of about 2 $m^3.s^{-1}$. According to previous studies of connected tidal basins some sort of asymmetry must exist for a constant flow between the basins to develop (van de Kreeke, 1976; Ridderinkhof, 1988b). This asymmetry may either be external (difference in tidal forcings) or internal (discrepancies in morphology and/or bathymetry). For the present system the tidal analysis of section 3.2 showed that just outside both inlets the tidal conditions do not present any significant differences. However, the particular nature of each inlet introduces a first asymmetry in the tidal conditions right at the entrances with a tidal wave in advance and of greater amplitude for GEL. It has also been noticed that going from the entrances to the junction between the lagoons GEL is narrower, shallower and longer than HML, adding internal asymmetries to the system. Using a 1D analytical model of two connected tidal basins Ridderinkhof (1988b) showed that in terms of asymmetrical tidal forcings the residual flow is oriented from the basin where the tidal wave first enters and/or where it has the largest amplitude. Considering the asymmetry in tidal forcing only the residual flow should then be directed from GEL to HML. According to Ridderinkhof's model in the absence of any external asymmetries the residual flow is directed to the deeper and/or longer and/or narrower basin. Except for the depth difference between GEL and HML which is rather small ($H_{GEL}/H_{HML} \approx 0.9$) the

length ($L_{GEL}/L_{HML} \approx 1.7$) and width ($B_{GEL}/B_{HML} \approx 0.6$) ratios would lead to a residual flow from HML to GEL. The residual flow predicted by the 3D numerical model being directed from HML to GEL it seems that the internal asymmetries of the system overcome the imbalance in tidal forcings. In particular the opposition of the long and narrow throat section of GEL's western part to the wide and deep basin of HML's eastern side counterbalances the external asymmetry sets by the leaky and restricted nature of their respective inlets.

Results for deeper layers are not presented here as they show very similar patterns, revealing that in these barotropic tidal conditions, residual flows are homogenous in the vertical direction. In particular, the residual eddies observed over the deeper parts of GEL extend over the entire water column.

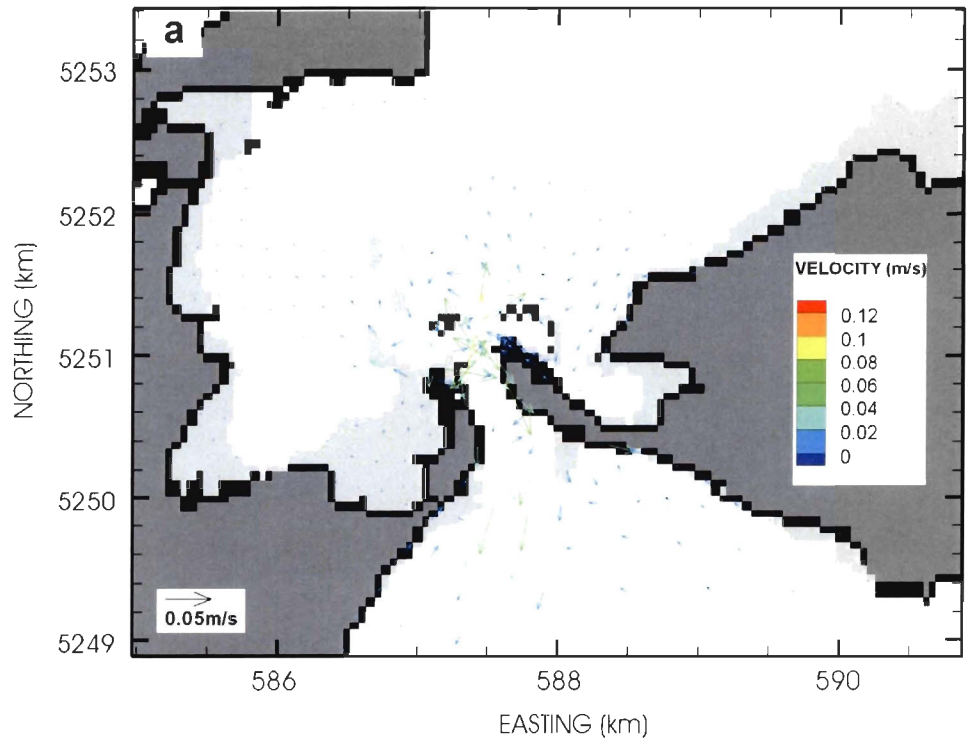
a
5253
5252
5251
5250
5249
NORTHING (km)
586
588
590
EASTING (km)
VELOCITY (m/s)
0.12
0.1
0.08
0.06
0.04
0.02
0
0.05m/s

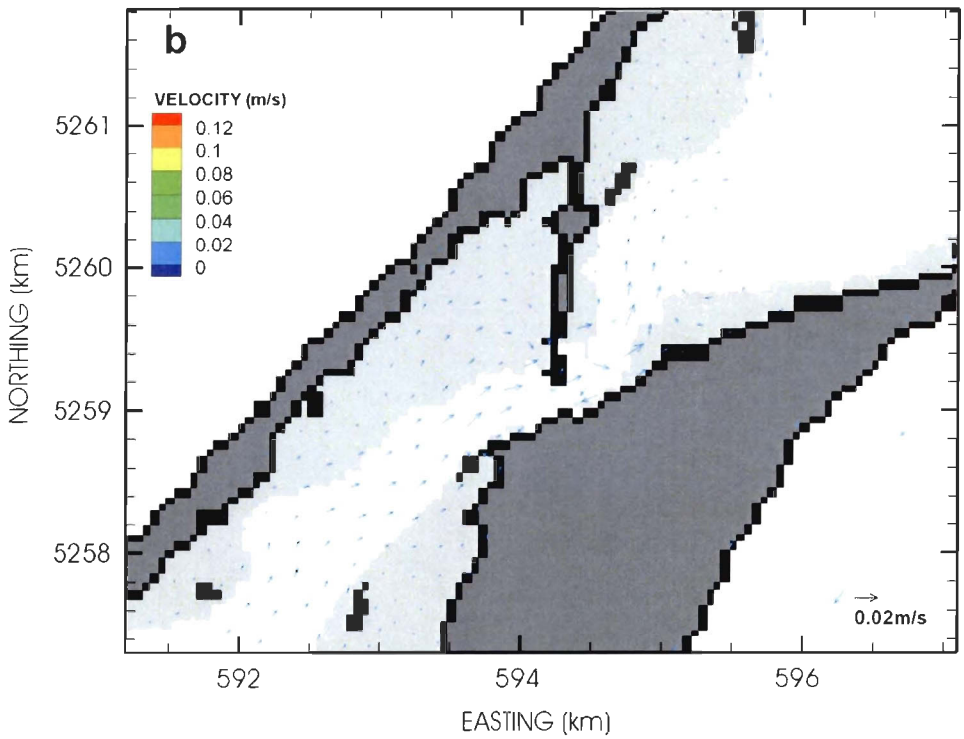
b
5261
5260
5259
5258
NORTHING (km)
592
594
596
EASTING (km)
VELOCITY (m/s)
0.12
0.1
0.08
0.06
0.04
0.02
0
0.02m/s

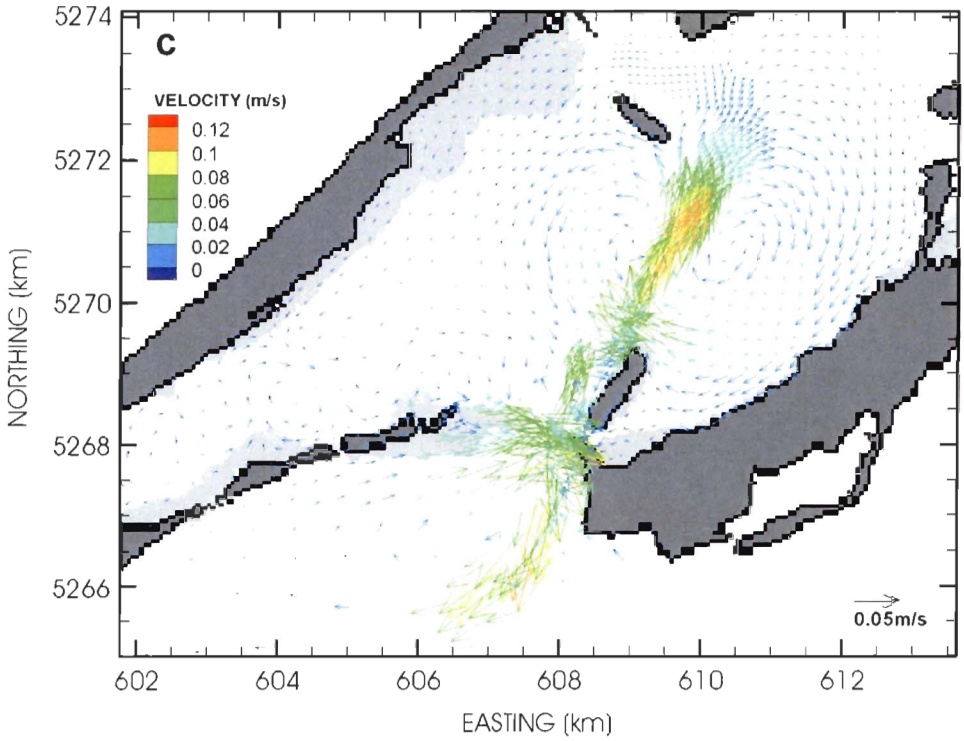

Figure II-8 Surface layer tide-induced residual currents in a) HML's inlet area, b) HML-GEL junction area and c) GEL's inlet area.

2.4 SUMMARY AND CONCLUDING REMARKS

The combined use of field data and numerical modelling allowed us to investigate the deterministic behaviour of a coupled "restricted" and "leaky" coastal lagoon system submitted to the influence of tidal forcing. Data analysis alone showed that tidal currents in GEL inlet present a marked ebb dominance that is explained by direct interactions between the main astronomical tidal constituents rather than non-linear overtide generation. This ebb dominance is usually considered as a sign of geomorphological stability (Aubrey and Speer, 1985) as the lagoon has the ability to flush incoming sediments. This stability is confirmed by the study carried out by Drapeau (1988) in the years following the first dredging of the navigation channel. This asymmetry also reveals the ability of the inlet to flush other suspended or dissolved substances leading to a rather short flushing time of lagoon areas directly surrounding the inlet (Koutitonsky and Tita, 2006). Conversely, current data revealed a more neutral character for HML's inlet in terms of tidal asymmetry and consequently for sediment fluxes. This is also confirmed by the results of a detailed study of sediment transport in this area showing no significant net transport through HML's inlet (Koutitonsky, 2005). Finally, harmonic analysis of observed water levels proved distinct responses of each lagoon to similar tidal forcings leading to an imbalance creating favourable conditions for the generation of a tide-induced residual throughflow from one lagoon to the other.

Finite element numerical modelling was then used to reproduce the hydrodynamics of the system and study in more details the residual circulation. The calculation of residual currents confirmed the presence of a tide-induced throughflow going from HML to GEL. It was shown that this constant flow results from the opposing effect of the asymmetry in tidal forcing caused by the different nature of both inlets and the internal morphological dissimilarities. This constant flow represents a not inconsiderable flushing mechanism for inner regions far from the direct influence of inlets as shown by van de Kreeke (1976) referring to this process as tide-induced mass transport. Although inlet areas present the strongest residual currents for both lagoons, the rest of the lagoons experience quite different residual circulations. HML is characterized by a rapid decrease in residual current away from the inlet with residual flows almost vanishing in the deeper basin, sign of a slow turnover in this part of the lagoon. GEL residual circulation is more characteristic of tidal inlets with the generation of residual eddies, one on the ebbing side of the inlet and two inside the lagoon. Inner eddies are unusually pushed away from the inlet because of GEL's entrance morphology and the presence of the navigation channel that stretch the inlet further inside the lagoon. The eastern circulation cell sits over the deeper basin of GEL leading to the isolation of this part of the lagoon.

In summary this coupled-lagoons system presents three morphological particularities that deeply affect its dynamical behaviour. First, the two lagoons are connected which allows an exchange between them and induces a linked response to external forcings. In each lagoon this response is different than what it would be for two separated lagoons

whose circulations would only be driven by their respective inlets and inner morphologies/bathymetries. The second particularity of this system is the distinct dynamical behaviour of each inlet which combined with the third characteristic, the internal morphological asymmetry, induces a tidally-driven exchange between the two lagoons. Meteorological influence was only included for model calibration purposes. Blackford (1978) studied wind-driven currents over the Magdalen shallows and observed that they follow the 2-3 day burst pattern of the wind stress. Such wind events would probably alter the residual circulation described here but their influence would be limited to a few tidal cycles as suggested by the work of Koutitonsky (2006). A more detailed study would be necessary to determine the actual effect of this local forcing and also address the non local meteorological forcings and their influence on the residual circulation in the lagoonal system.

Finally, a more complete understanding of the long term circulation of this lagoonal system will be achieved by the use of more sophisticated tools as numerical tracer experiments. Nevertheless, the present work represents a useful basis to analyze the results of these future experiments.

APPENDIX

RMA-10 numerical model equations:

- Momentum:

$$\rho\left\{\frac{\partial u}{\partial t}+u\frac{\partial u}{\partial x}+v\frac{\partial u}{\partial y}+w\frac{\partial u}{\partial z}\right\}-\frac{\partial}{\partial x}\left(\varepsilon_{xx}\frac{\partial u}{\partial x}\right)-\frac{\partial}{\partial y}\left(\varepsilon_{xy}\frac{\partial u}{\partial y}\right)-\frac{\partial}{\partial z}\left(\varepsilon_{xz}\frac{\partial u}{\partial z}\right)+\frac{\partial p}{\partial x}-\Gamma_x=0$$

$$\rho\left\{\frac{\partial v}{\partial t}+u\frac{\partial v}{\partial x}+v\frac{\partial v}{\partial y}+w\frac{\partial v}{\partial z}\right\}-\frac{\partial}{\partial x}\left(\varepsilon_{yx}\frac{\partial v}{\partial x}\right)-\frac{\partial}{\partial y}\left(\varepsilon_{yy}\frac{\partial v}{\partial y}\right)-\frac{\partial}{\partial z}\left(\varepsilon_{yz}\frac{\partial v}{\partial z}\right)+\frac{\partial p}{\partial y}-\Gamma_y=0$$

$$\rho\left\{\frac{\partial w}{\partial t}+u\frac{\partial w}{\partial x}+v\frac{\partial w}{\partial y}+w\frac{\partial w}{\partial z}\right\}-\frac{\partial}{\partial x}\left(\varepsilon_{zx}\frac{\partial w}{\partial x}\right)-\frac{\partial}{\partial y}\left(\varepsilon_{zy}\frac{\partial w}{\partial y}\right)-\frac{\partial}{\partial z}\left(\varepsilon_{zz}\frac{\partial w}{\partial z}\right)+\frac{\partial p}{\partial z}+\rho g-\Gamma_z=0$$

using the hydrostatic approximation the momentum equation in the vertical direction is reduced to: $\frac{\partial p}{\partial z}+\rho g=0$

- Continuity:

$$\frac{\partial u}{\partial x}+\frac{\partial v}{\partial y}+\frac{\partial w}{\partial z}=0$$

- Transport of heat and/or salinity (salinity used as an example)

$$\frac{\partial s}{\partial t}+u\frac{\partial s}{\partial x}+v\frac{\partial s}{\partial y}+w\frac{\partial s}{\partial z}-\frac{\partial}{\partial x}\left(D_x\frac{\partial s}{\partial x}\right)-\frac{\partial}{\partial y}\left(D_y\frac{\partial s}{\partial y}\right)-\frac{\partial}{\partial z}\left(D_z\frac{\partial s}{\partial z}\right)-\theta_s=0$$

- Equation of state:

$$\rho=F(S)$$

with:

x, y, z: cartesian coordinates, z being the ascendant vertical
u, v, w: velocities in the cartesian directions
ρ: water density
g: acceleration due to density
p: water pressure
$\varepsilon_{xx...}$: turbulent eddy coefficients
Γ: external tractions that operate on the boundaries or on the interior
S: salinity
$D_{x...}$: eddy diffusion coefficients
θ_s: source/sink for the transported variable

CHAPITRE 3

A COASTAL BIOGEOCHEMICAL MODEL TO STUDY THE INTERACTIONS BETWEEN CULTURED BIVALVES AND THEIR ENVIRONMENT – MODEL SET UP AND SENSITIVITY ANALYSIS

T. GUYONDET, J. GRANT,
S. ROY, V. G. KOUTITONSKY and G. TITA

Article soumis à
Ecological Modelling

RÉSUMÉ: Un modèle couplé physique-biogéochimique à fine résolution est développé pour étudier la dynamique de l'écosystème d'une lagune abritant un élevage commercial de moules. La calibration du modèle est basée sur la comparaison objective des résultats du modèle avec les observations récoltées lors d'une campagne d'échantillonnage sur le terrain, à la fois en terme de concentrations des variables d'état et de la magnitude des différents processus. Une analyse de sensibilité est ensuite réalisée pour tester les capacités prédictives du modèle. Les résultats du processus de calibration et de l'analyse de sensibilité établissent clairement la capacité du modèle à reproduire avec précision la dynamique de l'écosystème lagunaire, y compris les effets de l'élevage mytilicole. Cette dynamique se caractérise en été par la dominance des processus de recyclage parmi les mécanismes d'apport en azote et également par le rôle dominant du réseau microbien, en particulier le microzooplancton, dans la détermination du niveau de productivité de ce système. L'activité mytilicole à son stade actuel de développement ne semble pas exercer d'influences majeures sur la dynamique du système à l'échelle globale. Toutefois, certaines améliorations devront être apportées au modèle pour évaluer plus précisément ces influences.

ABSTRACT: A fine resolution coupled physical-biogeochemical model is developed to study the dynamics of a coastal lagoon ecosystem sheltering a commercial mussel aquaculture farm. The model calibration is based on the objective comparison of model results and observations from a field sampling program both in terms of state variable concentrations and process rate magnitudes. A sensitivity analysis is then carried out to test the predictive ability of the model. The results of both the calibration process and the sensitivity analysis strongly establish the capacity of the model to accurately reproduce the lagoon ecosystem dynamics, including the effects of cultured mussels. These dynamics are characterized in summer by the dominance of recycling processes among inorganic nitrogen input mechanisms and the dominant role of the microbial food web, especially microzooplankton, in setting the productivity level of the system. The mussel culture activity in its present state does not seem to exert any major influence on the system dynamics at the global scale. However, model refinements are required to estimate theses effects more accurately.

3.1 INTRODUCTION

The interactions between marine bivalve filter feeders and the surrounding ecosystem have been the subject of several studies for both natural (Officer et al., 1982; Dame, 1993, Dame et al., 2002) and cultivated (Grenz et al., 1990; Gilbert et al., 1997; Gibbs, 2004) populations. Most of the recent studies in this field (Chapelle et al., 2000; Pastres et al., 2001; Duarte et al., 2003; Grant et al., 2008; Marinov et al., 2008) are based on numerical models due to the diversity of these interactions and the difficulty in explaining the behaviour of systems dominated by bivalves using linear dynamics only (Dame et al., 2002).

Like other biogeochemical problems, the models used to study bivalve–ecosystem interactions have to be carefully designed in order to provide the best possible framework for answering the questions at hand. In this particular case, several characteristics of the problem restrict the range of suitable models.

First of all, bivalve populations, either natural or cultured (the latter of which will be the main focus here) are commonly found in small, sheltered coastal systems like bays, estuaries or lagoons with irregular topography and bathymetry. In such regions, hydrodynamics are known to represent a major forcing. These physical aspects plus the need to distinguish between areas with and without shellfish require a model with a rather fine resolution. Carrying-capacity studies have also pointed out the need to include processes both at the local (farm) and global (system) scales (Grant et al., 1993).

Moreover, bivalve filter feeders are known to act directly or indirectly on several ecosystem processes (Prins et al., 1998). Large populations of these animals may control nutrient fluxes through the excretion of ammonia and biodeposition that may stimulate benthic metabolism, increasing the recycling of inorganic nutrients (Officer et al., 1982; Kaspar et al., 1985; Stenton-Dozey et al., 2001; Christensen et al., 2003; Richard et al., 2007). Their excretion may enhance local primary production (Trottet et al., 2008a), but their grazing activity can lower the phytoplankton biomass (Fréchette & Bourget, 1985; Navarro et al., 1991; Grant et al., 2008). This grazing activity, being selective in terms of the size of the particles retained, may influence the size structure of the suspended matter as well as induce shifts in the composition of planktonic communities (Trottet et al., 2008a). The relationship between bivalves and planktonic heterotrophs is more clearly negative, since bivalves can feed on the smaller species and also represent fierce competitors for all grazers (Lehane & Davenport, 2006; Trottet et al., 2008a). A comprehensive study on the role of bivalves in the functioning of coastal ecosystems requires the integration of all the interactions mentioned above. In terms of modelling, this translates into a very detailed biogeochemical structure including several forms of inorganic nutrients, several size classes of phytoplankton and zooplankton, and the bivalves themselves in the pelagic domain as well as a benthic subsystem to account for the effects of biodeposition and the potentially important role of pelagic–benthic coupling in these coastal areas.

Combining a fine spatial resolution with a detailed biogeochemical structure has long been a modeller's nightmare. In the first modelling studies, both spatial resolution and ecosystem detail description were limited (Incze et al., 1981; Bacher, 1989). Subsequent

studies of bivalve–environment interactions managed to develop either the biogeochemical representation in box models (Raillard & Ménesguen, 1994; Dowd, 1997; Ferreira et al., 1998; Chapelle et al., 2000; Nakamura & Kerciku, 2000; Grant et al., 2007) or the spatial representation coupling detailed transport models with very simple pelagic food webs (Bacher et al., 1997; Dowd, 2003). With the rapid increase in computer performance and the rising concerns about the effects of shellfish culture on coastal ecosystems, most recent studies have started to incorporate both aspects in their detailed form using two- or three-dimensional coupled hydrodynamic–biogeochemical models (Duarte et al. 2003; Grant et al., 2008; Marinov et al., 2008; Spillman et al., 2008; Maar et al., 2009).

The present contribution is part of a multidisciplinary project aimed at the estimation of the carrying capacity of a shallow lagoon for mussel (*Mytilus edulis*) culture. This study embodies two aspects of the carrying-capacity question: mussel production optimization and the ecological consequences of this practice. The purpose of this paper is to present the numerical framework developed to address the problem. Thus, the Material and Methods section presents both the study area with its main characteristics, as revealed by field studies and which conditioned the choice of the model structure, and a detailed description of the coupled hydrodynamic–biogeochemical model itself. In the Results section, the calibration process and results are reported as well as the sensitivity analysis and the information it reveals about the ecosystem functioning. In the last section, a description of nitrogen cycling through the lagoonal ecosystem based on model results precedes our conclusions about further possible developments.

3.2 MATERIAL AND METHODS

3.2.1 Study area

Grande-Entrée lagoon (GEL) is the northernmost water body of the Îles-de-la-Madeleine, Gulf of St. Lawrence (GSL), Canada (Fig. III-1). GEL covers an area of approximately 58 km^2 and has two openings, one wide inlet from the GSL and one narrow pass at its southwestern end connecting it with Havre-aux-Maisons lagoon (HML). An 8 m deep navigation channel runs from a few kilometres offshore in the GSL through the main inlet and up to the north coast of the lagoon. The mean depth of 3 m is unevenly distributed, with a shallow sandy area on the western side of the channel and a deeper (6–7 m) muddy basin on the eastern side, where the mussel farm is located (Fig. III-1).

Hydrodynamics

The hydrodynamics of this system have been studied in the past (Koutitonsky et al., 2002; Koutitonsky & Tita, 2006; Guyondet & Koutitonsky, 2008). Here, we will only give an overview of the main characteristics reported in these previous works. Tides and meteorology represent the main forcing for GEL in the absence of any river discharge. Due to the proximity of an amphidromic point for the M2 tide in the GSL, tidal forcing is of rather small amplitude (0.5 m during spring tides) and of a mixed but mainly semi-diurnal type. Winds are seldom calm in this area (Drapeau, 1988), leading to generally well mixed waters in the vertical. GEL has been described as a "leaky" lagoon, with the tide almost

freely entering the lagoon because of the wide inlet and the presence of the navigation channel. This channel actually concentrates the flow during both the ebb and flood tides, with the strongest tidal currents in excess of 0.5 $m.s^{-1}$ in the inlet area. The remainder of the lagoon is divided into a shallow western area where tidal currents reach up to 0.2 $m.s^{-1}$ and a deep eastern basin with weak tidal currents (0.05 $m.s^{-1}$). Water renewal times by tides for GEL were shown to lie in the range of 1 to more than 40 days, going from the inlet area to inner parts of the lagoon. Meteorological forcing may enhance water renewal, especially in inner regions, leading to renewal times between 15 and 30 days in the mussel farm area in the deep eastern basin depending on the conditions. During the main mussel growth period, from June to October, water temperatures range from 10 to 21 °C with a maximum in late July or early August. Over this same period, salinity does not vary much, with values between 30 and 31 and a decreasing trend due to the arrival in the Îles-de-la-Madeleine area of the spring freshet waters from the St. Lawrence River.

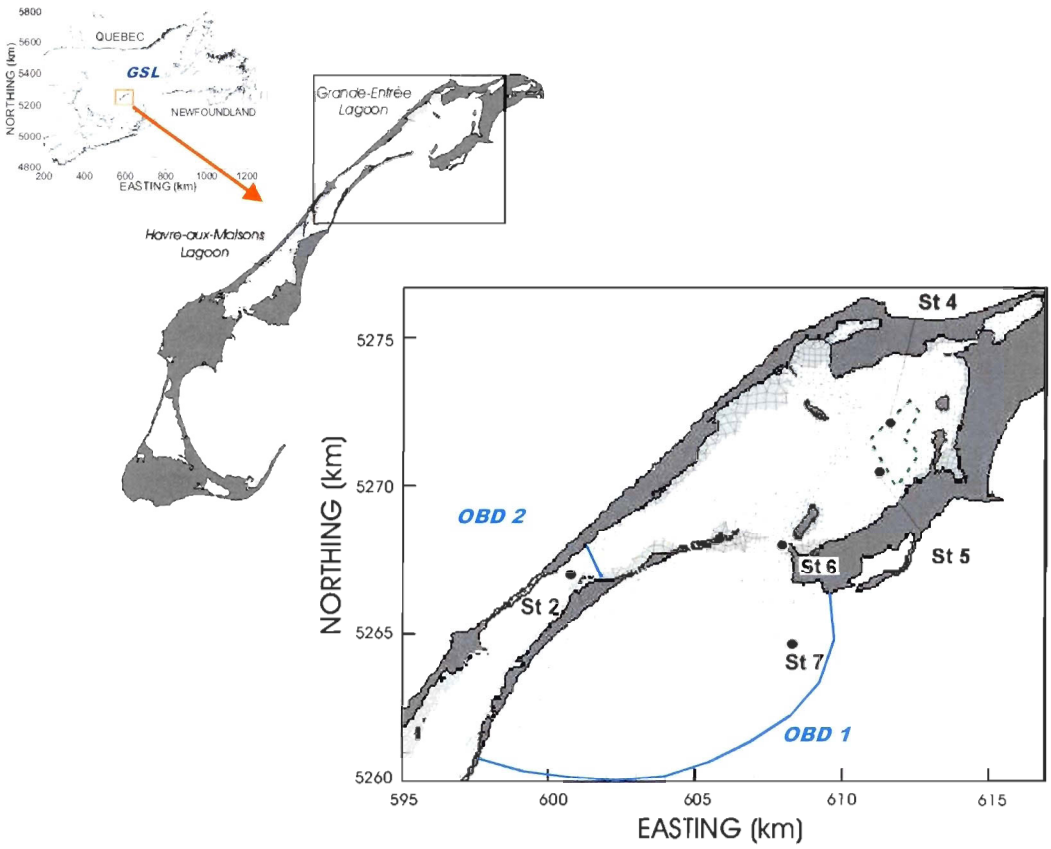

Figure III-1 Map of the study area showing the model grid with its two open boundaries (OBD), the mussel farm (dashed polygon) and the summer 2003 sampling stations (St).

Biogeochemistry

In the last twenty years, two multidisciplinary field sampling campaigns took place in GEL to address carrying-capacity issues. The first one was carried out in 1988–1989, only a few years after the mussel farm started production. It focused mainly on water column processes and led to the publication of several papers describing the pelagic environment and estimating the role of mussels in nitrogen and phosphorus cycling (Roy et al., 1991; Souchu & Mayzaud, 1991; Souchu et al., 1991). The second sampling program, on which the present modelling work is based, gathered information on water, sediment, and mussel physiology parameters during the summer of 2003 (June–October) and was completed with a shorter sampling period in 2004 for rates of primary production and microzooplankton grazing. The major results are reported in various publications. In the present paper, only the main features that constrained the model set-up will be reviewed.

During summer, the pelagic environment is characterized by low nutrient concentrations (nitrate: $[NO_3^-] = 0.3 \pm 0.02$ µM, phosphate: $[PO4_3^-] = 0.3 \pm 0.17$ µM, silicic acid: $[Si(OH)_4^-] = 0.9 \pm 0.55$ µM; Trottet et al., 2008a). Nitrogen is thought to be the limiting component for the productivity of this system. Concentrations of chlorophyll *a*, a proxy for the total phytoplankton biomass, are also low, ranging from 0.8 to 3.11 $\mu g.L^{-1}$ (Trottet et al., 2007). Considering these two first aspects, the primary production, with a mean of 335 $mgC.m^{-2}.d^{-1}$ is relatively high (Trottet et al., 2008a). This indicates that nutrient recycling probably plays a major role in setting the level of productivity of this system. The pelagic food web is dominated by small species of phytoplankton

(prymnesiophyceae, prasinophyceae, cryptophyceae…) and micro-zooplankton (heterotrophic protists: ciliates and tintinnids). In terms of biomass heterotrophs are dominant most of the time except during short diatom blooms. These last two features suggest that the microbial food web is an important pathway for matter and energy in this shallow lagoon.

In GEL, mussels are grown in suspension using long lines that hold continuous mussel socks at 2–4 m below the surface. Two cohorts of mussels may coexist in the farm area, but most of the older mussels have been harvested by the beginning of summer. The younger cohort then grows rapidly and usually reaches commercial size in fall, when the next cohort is seeded. Mussels have been shown to feed both on phytoplankton and zooplankton in this coastal environment (Trottet et al., 2008b). Mussel biodeposition leads to an increase in the sedimentation rate of up to twice the rates observed outside the mussel farm (Callier et al., 2006). Rapid sinking of mussel biodeposits and low current speeds in the deep basin of GEL cause the biodeposits not to disperse broadly but to accumulate on the bottom near the farm (Callier et al., 2006; Weise et al., 2009).

Data on the benthic environment are only available in the deep basin. At the sediment–water interface, high consumption of dissolved oxygen was recorded using benthic chambers, with fluxes between -70 and -440 $mg.m^{-2}.h^{-1}$ (Richard et al., 2007). A persistent flux of ammonium (NH_4^+) from the sediments was observed, with values between 0.23 and 1.2 $mgN.m^{-2}.h^{-1}$ over the summer period. Nitrate (NO_3^-) fluxes were the smallest recorded and were either coming out or entering into the sediment on the different sampling dates (-1.94×10^{-2} to 1.19×10^{-2} $mgN.m^{-2}.h^{-1}$). The negative redox potential and the

short oxygen penetration depth suggest that the sediment is in a reduced state (Callier et al., 2007). A major fraction of the large oxygen flux mentioned above could then be attributed to the oxidation of reduced compounds such as sulphides that are produced during the anaerobic degradation of organic matter.

3.2.2 Data collection

The modelling work reported here is based on a multidisciplinary field sampling program undertaken during summer 2003 (June to October). Various components of the GEL ecosystem were observed, providing the data necessary to force and calibrate the coupled hydrodynamic–biogeochemical model. The following sections briefly present the different types of data and the method of sampling and analysis used. The references for the publications describing the field and laboratory work in detail are also given.

Water column parameters

All meteorological data (air temperature, atmospheric pressure, wind speed and direction, solar radiation and cloudiness) were obtained as hourly values from the Environment Canada meteorological station located 30 km southwest of the study area. Daily precipitation data (in mm) from the same station were used and mean concentrations in ammonium and nitrate in rainwater were calculated from values obtained during the 1988–1989 study (Souchu & Mayzaud, 1991) because inorganic nutrient concentrations in

precipitation has not varied much over North America since that time (Skjelkvaale et al., 2001).

Tide gauges were moored at all stations shown on Fig. III-1 to record time series of water level fluctuations. Current meters were deployed at stations 5 and 6 at 1m above the bottom to record currents in the deep basin and at the lagoon's entrance, respectively.

Stations 2, 4, 5 and 7 were visited weekly during summer 2003 from 28 June to 9 September and on 18 October. Water samples taken from 1m below the surface and 1m above the bottom were analyzed for phytoplankton pigments (HPLC analysis that discriminated two size classes: cells smaller [model variable SP] and larger [model variable LP] than 3 μm), nutrients (nitrate [model variable NO3]), organic carbon and nitrogen content of the suspended particulate matter (SPM), and taxonomic identification (discriminating between autotrophs [SP and LP] and heterotrophs [microzooplankton: model variable SZ]) (Trottet et al., 2007). The concentration of organic detritus (model variable D) was obtained by subtracting the total phytoplankton biomass and the microzooplankton biomass from the organic content of the SPM. Mesozooplankton biomass (model variable LZ) was estimated on three occasions (16 July, 22 August and 11 September) using a plankton net (ϕ = 50 cm, 200 μm mesh) towed horizontally below the water surface around each station.

In addition to this sampling program, instruments were moored at each station 1m above the bottom to continuously record several parameters. YSI (SonTek/YSI, San Diego, USA) environmental probes were used to measure water levels, water temperature (model variable T), salinity, dissolved oxygen concentrations (model variable O2) and total

chlorophyll *a* concentrations (from fluorescence) at 20 min intervals. The calibration of the probes and the detailed analysis of the various time series are reported in Pitre (2007). Table III-1 summarizes the available data for each pelagic model variable at each station. When data for a particular variable were not available at one of the boundary stations (2 or 7), data from the closest station were used. Ammonium (model variable NH4) was not measured in summer 2003, so a constant value corresponding to the average concentration observed in summer 2004 (Trottet et al., 2007) was imposed at both boundaries.

Data collected at the peripheral stations 2 and 7 were used to force the coupled hydrodynamic–biogeochemical model at its open boundaries while the inner stations 4, 5 and 6 were used for calibration purposes.

Table III-1 Data availability for each variable and at each station during the summer 2003 field sampling program (LZ data only includes three sampling dates over the study period).

	Station				
	S2	**S4**	**S5**	**S6**	**S7**
Level	X	X	X	X	X
Current			X	X	
Dissolved oxygen (O2)	X	X	X		
Water temperature (T)	X	X	X		X
Large phytoplankton (LP)	X	X	X		X
Small phytoplankton (SP)	X	X	X		X
Organic detritus (D)	X	X	X		X
Ammonium (NH4)					
Nitrite-Nitrate (NO3)	X	X	X		X
Mesozooplankton (LZ)		(X)	(X)		(X)
Microzooplankton (SZ)		X	X		

Mussel parameters

In summer 2003, one-year-old mussels occupied only the northwestern side of the mussel culture lease area (Fig. III-2). They were grown on 159 long lines that were 100 m in length and separated by 20 m. During summer 2003, an average of 31.8×10^6 one-year-old mussels were hanging from these lines, giving a mussel density of 100 mussels.m^{-2} in the cultivation area (G. Tita, unpublished). An in situ mussel growth experiment conducted from July to December 2003 provided monthly time series of mussel shell lengths and dry meat weights (Grant et al., 2007). Sedimentation rates and biodeposit production by mussels were also observed in situ using sediment traps. The sinking velocity of mussel faecal material was also measured in a cylindrical glass sinking column (see Callier et al., 2006 for more details).

Benthic parameters

Benthic chambers were used by Richard et al. (2007) to measure the fluxes of dissolved oxygen, ammonium and nitrate at the sediment–water interface on a monthly basis from July to September 2003 both inside and outside the mussel cultivation area. These fluxes will be compared to the sediment–water diffusive fluxes obtained with the model.

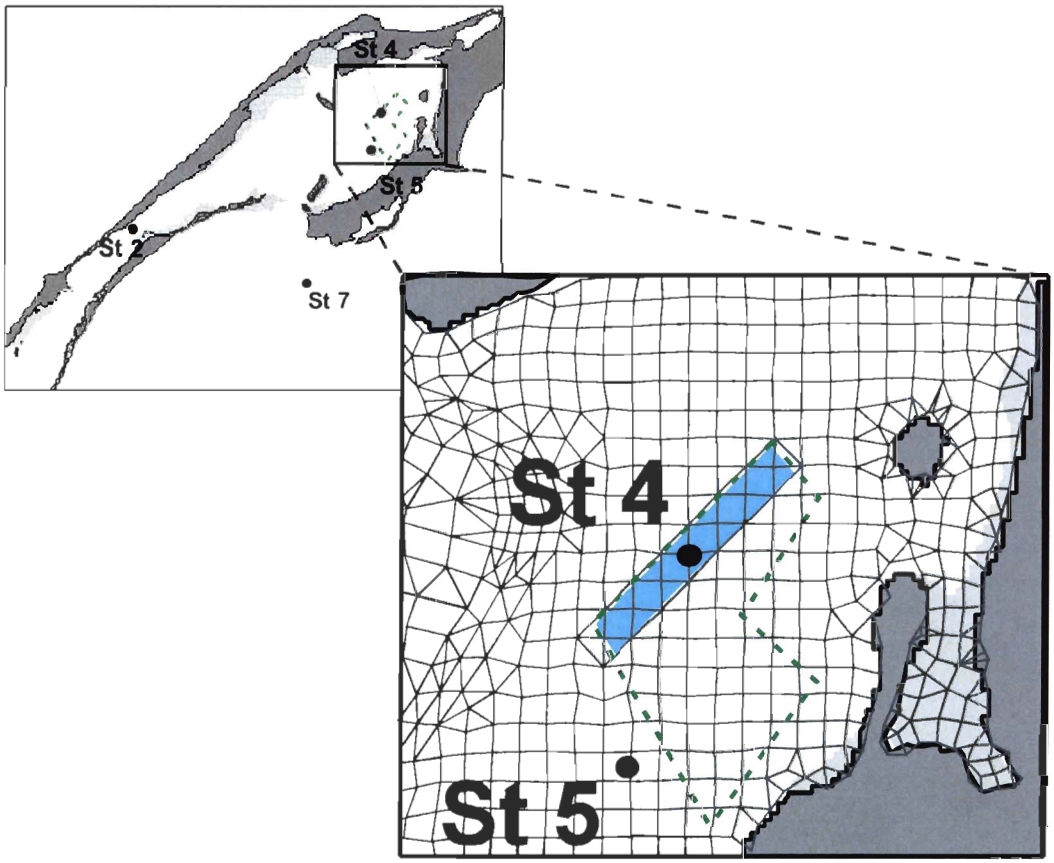

Figure III-2 Grande-Entrée Lagoon mussel farm (dashed polygon) with the summer 2003 sampling stations and the location of the one-year-old cohort (blue shaded area).

3.2.3 Model description

Hydrodynamics

A previous study (Guyondet and Koutitonsky, 2008) focused on water circulation in the lagoonal system of the Îles-de-la-Madeleine using a 3D finite element model (RMA-10; King, 1982, 1985, 1988) of both HML and GEL. Only GEL is considered in the present work. This restricted domain area was then extracted from the previous model grid. Hence, the GEL grid has two open boundaries, one off the mouth in the Gulf of St. Lawrence (Fig. III-1, OBD1) and another located between the two lagoons in the southwestern part of GEL (OBD2). The original grid was slightly refined along the navigation channel running from the mouth up to the north shore and also east of the channel in the deeper basin to better represent the mussel farm area (Fig. III-2). Due to tidal and wind mixing and the absence of freshwater discharge, no major vertical stratification was ever observed in this shallow lagoon during the summer period (Souchu et al., 1991; Booth, 1994; Guyondet & Koutitonsky, 2008). The present model was thus run in a 2D depth-averaged configuration.

Hourly water level data recorded at stations 7 and 2 (Fig. III-1) were used as open boundary conditions 1 and 2, respectively. The model also included precipitation, atmospheric pressure and wind fluctuations at the water surface.

Results of this restricted model agree well (not shown) with the full model results for the summer 2001 (Guyondet & Koutitonsky, 2008). Hence, only a brief validation of the hydrodynamic simulation will be presented here for the summer 2003.

Biogeochemical structure

Since nitrogen is thought to be the limiting nutrient in this system (Souchu et al., 1991), it was used here as the model currency. The biogeochemical structure of the model represents the cycling of nitrogen through different states in the pelagic and benthic subsystems. It was adapted from the finite element water quality model RMA-11 (King, 2003). The pelagic compartment comprises 10 state variables (Fig. III-3). Two forms of dissolved inorganic nitrogen (DIN) are considered: ammonium (NH4) and nitrite–nitrate (NO3). These two nutrients fuel a microbial food web: small phytoplankton (SP<3 μm) and microzooplankton (SZ), and a herbivorous food web: large phytoplankton (LP>3 μm) and mesozooplankton (LZ). Both of these pathways are completed by a single detritic variable (D) receiving all forms of non-living particulate organic matter coming from faeces production and mortality in these low trophic levels. Dissolved oxygen (O2) is also included for its role in respiratory and oxidation processes. Ultimately, the results of this model will be used (in a subsequent paper) to study the interactions between cultured bivalves in suspension in the water column and their environment. Hence, two additional variables representing the individual mass of mussels (M) and their biodeposits (BDP) are included in the pelagic structure of the model. Water temperature and light are the only parameters forcing the different processes describing the dynamic behaviour of the system. Water temperature is obtained through a complete heat budget calculation (King, 2003) forced by the observed meteorological data and observations of temperature at the open boundaries.

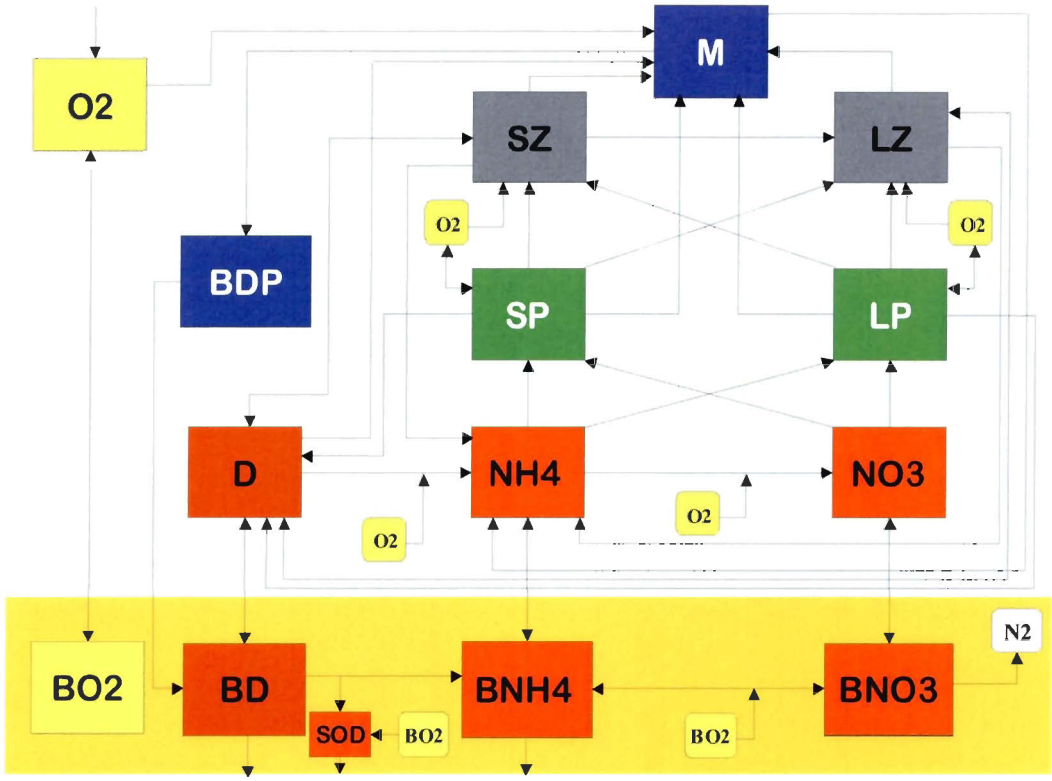

Figure III-3 Structure of the biogeochemical model based on the nitrogen cycle through the pelagic (O2: dissolved oxygen, NH4: ammonium, NO3: nitrite-nitrate, D: organic detritus, LP: phytoplankton>3µm, SP: phytoplankton<3µm, LZ: mesozooplankton, SZ: microzooplankton, M: mussel individual weight, BDP: mussel biodeposits) and benthic subsystems (BO2: dissolved oxygen in interstitial water, SOD: sediment oxygen demand, BD: organic detritus in sediment, BNH4: ammonium in interstitial water, BNO3: nitrite-nitrate in interstitial water, N2: nitrogen gas).

At the bottom of the water column, a 0.1 m thick sediment layer is represented. In this benthic module, the particulate organic matter (BD) reaching the bottom through natural sedimentation and biodeposition is either resuspended into the water column, buried in deep inactive sediment, or remineralized, increasing the sediment oxygen demand (SOD) and producing dissolved inorganic forms (ammonium: BNH4 and nitrite–nitrate: BNO3). The oxic mineralization (decreasing the SOD) and nitrification–denitrification processes are controlled by the concentration of dissolved oxygen (BO2) in interstitial water. The remainder of the SOD represents all the different reduced species (Mn^{2+}, Fe^{2+}, H_2S and CH_4) formed during the anoxic degradation of BD. Finally, all benthic dissolved variables are allowed to dynamically exchange with their pelagic counterpart through diffusive fluxes at the sediment–water interface.

All dissolved and particulate pelagic variables are transported by water movements. This transport is represented using the following 2D depth-averaged advection–dispersion equation:

$$h\left(\frac{\partial C}{\partial t}+u\frac{\partial C}{\partial x}+v\frac{\partial C}{\partial y}\right)-\frac{\partial}{\partial x}\left(D_x h\frac{\partial C}{\partial x}+D_{xy}h\frac{\partial C}{\partial y}\right)-\frac{\partial}{\partial y}\left(D_{xy}h\frac{\partial C}{\partial x}+D_y h\frac{\partial C}{\partial y}\right)-h\theta_C=0$$

where t represents the time; (x, y) the cartesian coordinates; (u, v) the velocities in the cartesian directions obtained from the hydrodynamic model simulation; h the water depth from the hydrodynamic model; C the concentration of any transported constituent; D_x, D_y, D_{xy} the eddy diffusion coefficients; and θ_C the source/sink for the transported constituent. These source/sink terms as well as the equations for the mussel and benthic variables are

detailed in Table III-2. The meaning and value of the parameters forming these equations are given in Table III-3 along with the range of values found in the literature.

Table III-2 Biogeochemical model equations.

VARIABLE	EQUATIONS – SOURCE/SINK TERMS
LARGE PHYTOPLANKTON (LP, mgC.m^{-3})	$\theta_{LP} = \mu_0^{LP}.e^{k_\rho^{LP}T}.Limit_N^{LP}.Limit_L^{LP}.LP - \beta_0^{LP}.e^{k_r^{LP}.T}.LP - \lambda^{LP}.e^{k_r^{LP}.T}.LP - n^M.\frac{\varepsilon_{LP}^M.LP}{\varepsilon_D^M.D+\varepsilon_{LP}^M.LP+\varepsilon_{SP}^M.SP+\varepsilon_{SZ}^M.SZ+\varepsilon_{LZ}^M.LZ}.c_I^M.Limit_F^M.I^M.e^{k_\rho^M.T}.M^{1+b_I^M}$ $-\frac{\varepsilon_{LP}^{LZ}.LP}{\varepsilon_D^{LZ}.D+\varepsilon_{LP}^{LZ}.LP+\varepsilon_{SP}^{LZ}.SP+\varepsilon_{SZ}^{LZ}.SZ}.c_I^{LZ}.Limit_F^{LZ}.I^{LZ}.e^{k_\rho^{LZ}.T}.LZ - \frac{\varepsilon_{LP}^{SZ}.LP}{\varepsilon_D^{SZ}.D+\varepsilon_{LP}^{SZ}.LP+\varepsilon_{SP}^{SZ}.SP}.c_I^{SZ}.Limit_F^{SZ}.I^{SZ}.e^{k_\rho^{SZ}.T}.SZ$ with: $Limit_N^{LP} = X_{NH4}^{LP} + X_{NO3}^{LP}$ where $X_{NH4}^{LP} = \frac{NH4}{NH4+K_{NH4}^{LP}}$; $X_{NO3}^{LP} = \frac{NO3}{NO3+K_{NO3}^{LP}}.\frac{K_{NH4}^{LP}}{NH4+K_{NH4}^{LP}}$ $Limit_L^{LP} = \frac{1}{h}\int_0^h \frac{I(z)}{I_o^{LP}}\exp\left(1-\frac{I(z)}{I_o^{LP}}\right)dz$ for $I<I_o^{LP}$ (Steele, 1962) and $Limit_L^{LP}=1$ for $I\geq I_o^{LP}$ where: $I(z)=I_S.e^{-\lambda.z}$ with I_S: water surface light intensity and λ: light attenuation coefficient, $\lambda=\lambda_0+\lambda_1.(\text{Chl a/C}^{LP}.LP+\text{Chl a/C}^{SP}.SP)+\lambda_2.(\text{Chl a/C}^{LP}.LP+\text{Chl a/C}^{SP}.SP)^{2/3}$ $Limit_F^{LZ} = \frac{(\varepsilon_D^{LZ}.D+\varepsilon_{LP}^{LZ}.LP+\varepsilon_{SP}^{LZ}.SP+\varepsilon_{SZ}^{LZ}.SZ)}{(\varepsilon_D^{LZ}.D+\varepsilon_{LP}^{LZ}.LP+\varepsilon_{SP}^{LZ}.SP+\varepsilon_{SZ}^{LZ}.SZ)+K_F^{LZ}}$; $Limit_F^{SZ} = \frac{(\varepsilon_D^{SZ}.D+\varepsilon_{LP}^{SZ}.LP+\varepsilon_{SP}^{SZ}.SP)}{(\varepsilon_D^{SZ}.D+\varepsilon_{LP}^{SZ}.LP+\varepsilon_{SP}^{SZ}.SP)+K_F^{SZ}}$ $Limit_F^M = \frac{(\varepsilon_D^M.D+\varepsilon_{LP}^M.LP+\varepsilon_{SP}^M.SP+\varepsilon_{SZ}^M.SZ+\varepsilon_{LZ}^M.LZ)^2}{(\varepsilon_D^M.D+\varepsilon_{LP}^M.LP+\varepsilon_{SP}^M.SP+\varepsilon_{SZ}^M.SZ+\varepsilon_{LZ}^M.LZ)^2+K_F^{M^2}}$
SMALL PHYTOPLANKTON (SP, mgC.m^{-3})	$\theta_{SP} = \mu_0^{SP}.e^{k_\rho^{SP}T}.Limit_N^{SP}.Limit_L^{SP}.SP - \beta_0^{SP}.e^{k_r^{SP}.T}.SP - \lambda^{SP}.e^{k_r^{SP}.T}.SP - n^M.\frac{\varepsilon_{SP}^M.SP}{\varepsilon_D^M.D+\varepsilon_{LP}^M.LP+\varepsilon_{SP}^M.SP+\varepsilon_{SZ}^M.SZ+\varepsilon_{LZ}^M.LZ}.c_I^M.Limit_F^M.I^M.e^{k_\rho^M.T}.M^{1+b_I^M}$ $-\frac{\varepsilon_{SP}^{LZ}.SP}{\varepsilon_D^{LZ}.D+\varepsilon_{LP}^{LZ}.LP+\varepsilon_{SP}^{LZ}.SP+\varepsilon_{SZ}^{LZ}.SZ}.c_I^{LZ}.Limit_F^{LZ}.I^{LZ}.e^{k_\rho^{LZ}.T}.LZ - \frac{\varepsilon_{SP}^{SZ}.SP}{\varepsilon_D^{SZ}.D+\varepsilon_{LP}^{SZ}.LP+\varepsilon_{SP}^{SZ}.SP}.c_I^{SZ}.Limit_F^{SZ}.I^{SZ}.e^{k_\rho^{SZ}.T}.SZ$ with: $Limit_N^{SP} = X_{NH4}^{SP} + X_{NO3}^{SP}$ where $X_{NH4}^{SP} = \frac{NH4}{NH4+K_{NH4}^{SP}}$; $X_{NO3}^{SP} = \frac{NO3}{NO3+K_{NO3}^{SP}}.\frac{K_{NH4}^{SP}}{NH4+K_{NH4}^{SP}}$ $Limit_L^{SP} = \frac{1}{h}\int_0^h \frac{I(z)}{I_o^{SP}}\exp\left(1-\frac{I(z)}{I_o^{SP}}\right)dz$ for $I<I_o^{SP}$ (Steele, 1962) and $Limit_L^{SP}=1$ for $I\geq I_o^{SP}$

Table III-2 (continued)

LARGE ZOOPLANKTON (LZ, mgC.m^{-3})	$\theta_{LZ} = c_1^{LZ}.AE^{LZ}.Limit_F^{LZ}.I^{LZ}.e^{k_P^{LZ}.T}.LZ - c_R^{LZ}\beta_R^{LZ}.e^{k_r^{LZ}.T}.LZ - \lambda^{LZ}.e^{k_r^{LZ}.T}.LZ - n^M.\frac{\varepsilon_{LZ}^M.LZ}{\varepsilon_D^M.D+\varepsilon_{LP}^M.LP+\varepsilon_{SP}^M.SP+\varepsilon_{SZ}^M.SZ+\varepsilon_{LZ}^M.LZ}c_1^M.Limit_F^M.I^M.e^{k_P^M.T}.M^{1+b_1^M}$ with : $AE^{LZ} = \frac{AE_D^{LZ}\varepsilon_D^{LZ}.D + AE_P^{LZ}\left(\varepsilon_{LP}^{LZ}.LP + \varepsilon_{SP}^{LZ}.SP\right) + AE_{SZ}^{LZ}\varepsilon_{SZ}^{LZ}.SZ}{\varepsilon_D^{LZ}.D+\varepsilon_{LP}^{LZ}.LP+\varepsilon_{SP}^{LZ}.SP+\varepsilon_{SZ}^{LZ}.SZ}$
SMALL ZOOPLANKTON (SZ, mgC.m^{-3})	$\theta_{SZ} = c_1^{SZ}.AE^{SZ}.Limit_F^{SZ}.I^{SZ}.e^{k_P^{SZ}.T}.SZ - c_R^{SZ}\beta_R^{SZ}.e^{k_r^{SZ}.T}.SZ - \lambda^{SZ}.e^{k_r^{SZ}.T}.SZ - n^M.\frac{\varepsilon_{SZ}^M.SZ}{\varepsilon_D^M.D+\varepsilon_{LP}^M.LP+\varepsilon_{SP}^M.SP+\varepsilon_{SZ}^M.SZ+\varepsilon_{LZ}^M.LZ}c_1^M.Limit_F^M.I^M.e^{k_P^M.T}.M^{1+b_1^M}$ with : $AE^{SZ} = \frac{AE_D^{SZ}\varepsilon_D^{SZ}.D + AE_P^{SZ}\left(\varepsilon_{LP}^{SZ}.LP + \varepsilon_{SP}^{SZ}.SP\right)}{\varepsilon_D^{SZ}.D+\varepsilon_{LP}^{SZ}.LP+\varepsilon_{SP}^{SZ}.SP}$
ORGANIC DETRITUS (D, mgN.m^{-3})	$\theta_D = N/C^{LP}\left(\beta_0^{LP}+\lambda^{LP}\right)e^{k_r^{LP}.T}.LP + N/C^{SP}\left(\beta_0^{SP}+\lambda^{SP}\right)e^{k_r^{SP}.T}.SP + N/C^{LZ}\lambda^{LZ}.e^{k_r^{LZ}.T}.LZ + N/C^{SZ}\lambda^{SZ}.e^{k_r^{SZ}.T}.SZ$ $+ N/C^{LZ}\frac{(1-AE_{LP}^{LZ})\varepsilon_{LP}^{LZ}.LP + (1-AE_{SP}^{LZ})\varepsilon_{SP}^{LZ}.SP + (1-AE_{SZ}^{LZ})\varepsilon_{SZ}^{LZ}.SZ - AE_D^{LZ}\varepsilon_D^{LZ}.D}{\varepsilon_D^{LZ}.D+\varepsilon_{LP}^{LZ}.LP+\varepsilon_{SP}^{LZ}.SP+\varepsilon_{SZ}^{LZ}.SZ}c_1^{LZ}.Limit_F^{LZ}.I^{LZ}.e^{k_P^{LZ}.T}.LZ$ $+ N/C^{SZ}\frac{(1-AE_{LP}^{SZ})\varepsilon_{LP}^{SZ}.LP + (1-AE_{SP}^{SZ})\varepsilon_{SP}^{SZ}.SP - AE_D^{SZ}\varepsilon_D^{SZ}.D}{\varepsilon_D^{SZ}.D+\varepsilon_{LP}^{SZ}.LP+\varepsilon_{SP}^{SZ}.SP}c_1^{SZ}.Limit_F^{SZ}.I^{SZ}.e^{k_P^{SZ}.T}.SZ$ $- n^M.N/C^M\frac{\varepsilon_D^M.D}{\varepsilon_D^M.D+\varepsilon_{LP}^M.LP+\varepsilon_{SP}^M.SP+\varepsilon_{SZ}^M.SZ+\varepsilon_{LZ}^M.LZ}c_1^M.Limit_F^M.I^M.e^{k_P^M.T}.M^{1+b_1^M} - \min_0^D.Limit_{O2}^D.e^{k_{min}^D.T}.D - \frac{w_S^D}{h}.D$ with: $Limit_{O2}^D = \frac{O2}{O2+K_{O2}^D}$

Table III-2 (continued)

AMMONIUM (NH4, mgN.m^{-3})	$\theta_{NH4} = \min_0^D.Limit_{O2}^D.e^{k_{min}^D.T}.D + N/C^{LZ}c_R^{LZ}\beta_R^{LZ}.e^{k_r^{LZ}.T}.LZ + N/C^{SZ}c_R^{SZ}\beta_R^{SZ}.e^{k_r^{SZ}.T}.SZ$ $+ n^M.N/C^M\left(\sigma_\gamma^M.c_I^M.AE^M.Limit_F^M.I^M.e^{k_p^M.T}.M^{1+b_I^M} + c_R^M\beta_R^M.e^{k_r^M.T}.M^{1+b_R^M}\right)$ $-nitr_0^{NH4}.Limit_{O2}^{NH4}.e^{k_{nitr}^{NH4}.T}.NH4 - N/C^{LP}\mu_0^{LP}.e^{k_p^{LP}T}.X_{NH4}^{LP}.Limit_L^{LP}.LP - N/C^{SP}\mu_0^{SP}.e^{k_p^{SP}T}.X_{NH4}^{SP}.Limit_L^{SP}.SP + Diff_0^{NH4}.\left(1+\frac{T}{20}\right).\frac{\alpha}{\frac{(BLT+h)}{2}}.\frac{(BNH4-NH4)}{h}$ with: $Limit_{O2}^{NH4} = \frac{O2}{O2+K_{O2}^{NH4}}$
NITRATE (NO3, mgN.m^{-3})	$\theta_{NO3} = nitr_0^{NH4}.Limit_{O2}^{NH4}.e^{k_{nitr}^{NH4}.T}.NH4 - N/C^{LP}\mu_0^{LP}.e^{k_p^{LP}T}.X_{NO3}^{LP}.Limit_L^{LP}.LP - N/C^{SP}\mu_0^{SP}.e^{k_p^{SP}T}.X_{NO3}^{SP}.Limit_L^{SP}.SP + Diff_0^{NO3}.\left(1+\frac{T}{20}\right).\frac{\alpha}{\frac{(BLT+h)}{2}}.\frac{(BNO3-NO3)}{h}$
DISSOLVED OXYGEN (O2, mgO$_2$.L^{-1})	$\theta_{O2} = K_a^{O2}(O2_{Sat}-O2) + \frac{1}{1000}\Big[p_{O2}^{LP}.\mu_0^{LP}.e^{k_p^{LP}T}.Limit_N^{LP}.Limit_L^{LP}.LP - r_{O2}^{LP}.\beta_0^{LP}.e^{k_r^{LP}.T}.LP + p_{O2}^{SP}.\mu_0^{SP}.e^{k_p^{SP}T}.Limit_N^{SP}.Limit_L^{SP}.SP - r_{O2}^{SP}.\beta_0^{SP}.e^{k_r^{SP}.T}.SP$ $- r_{O2}^{LZ}.c_R^{LZ}\beta_R^{LZ}.e^{k_r^{LZ}.T}.LZ - r_{O2}^{SZ}.c_R^{SZ}\beta_R^{SZ}.e^{k_r^{SZ}.T}.SZ - n^M.r_{O2}^M\left(\sigma_\gamma^M.c_I^M.AE^M.Limit_F^M.I^M.e^{k_p^M.T}.M^{1+b_I^M} + c_R^M\beta_R^M.e^{k_r^M.T}.M^{1+b_R^M}\right)$ $- r_{O2}^D.\min_0^D.Limit_{O2}^D.e^{k_{min}^D.T}.D - r_{O2}^{NH4}.nitr_0^{NH4}.Limit_{O2}^{NH4}.e^{k_{nitr}^{NH4}.T}.NH4 - \frac{wfract}{h}rel^{SOD}.SOD + Diff_0^{O2}.\left(1+\frac{T}{20}\right).\frac{\alpha}{\frac{(BLT+h)}{2}}.\frac{(BO2-O2*1000)}{h}\Big]$ with $wfract = \alpha.BLT$ and K_a^{O2}, atmospheric reaeration rate (d^{-1}) based on wind speed (u_w in m.s^{-1}) and given by: $K_a^{O2}=0.048.u_w$ for $u_w < 3.6$m.s^{-1}; $K_a^{O2}=0.773.u_w-2.61$ for $3.6 < u_w < 13$m.s^{-1}; $K_a^{O2}=1.6.u_w-13.3$ for $u_w > 13$m.s^{-1} (Liss and Merlivat, 1986)
BIODEPOSITS (BDP, mgN.m^{-3})	$\theta_{BDP} = n^M.N/C^M\frac{(1-AE_{LP}^M).\varepsilon_{LP}^M.LP + (1-AE_{SP}^M).\varepsilon_{SP}^M.SP + (1-AE_{SZ}^M).\varepsilon_{SZ}^M.SZ + (1-AE_D^M).\varepsilon_D^M.D}{\varepsilon_D^M.D + \varepsilon_{LP}^M.LP + \varepsilon_{SP}^M.SP + \varepsilon_{SZ}^M.SZ + \varepsilon_{LZ}^M.LZ}.c_I^M.Limit_F^M.I^M.e^{k_p^M.T}.M^{1+b_I^M}$ $- \min_0^D.Limit_{O2}^D.e^{k_{min}^D.T}.BDP - \frac{w_S^{BDP}}{h}.BDP$
MUSSEL INDIVIDUAL MASS (M, mgC)	$\frac{dM}{dt} = (1-\sigma_\gamma^M).c_I^M.AE^M.Limit_F^M.I^M.e^{k_p^M.T}.M^{1+b_I^M} - c_R^M\beta_R^M.e^{k_r^M.T}.M^{1+b_R^M}$ with: $AE^M = \frac{AE_D^M\varepsilon_D^M.D + AE_P^M(\varepsilon_{LP}^M.LP + \varepsilon_{SP}^M.SP) + AE_Z^M(\varepsilon_{SZ}^M.SZ + \varepsilon_{LZ}^M.LZ)}{\varepsilon_D^M.D + \varepsilon_{LP}^M.LP + \varepsilon_{SP}^M.SP + \varepsilon_{SZ}^M.SZ + \varepsilon_{LZ}^M.LZ}$

Table III-2 (end)

SEDIMENT OXYGEN DEMAND (SOD, $mgO_2.m^{-3}$)	$\frac{dSOD}{dt} = r_{O2}^{BD}.\min_0^{BD}.e^{k_{min}^{BD}.T}.BD.\frac{pfract}{wfract} - oxi_0^{SOD}.e^{k_T^{SOD}.T}.Limit_{BO2}^{SOD}.SOD - burial^{SOD}.SOD - rel^{SOD}.SOD - \frac{r_{O2}^{BD}}{r_{BD}^{BNO3}}.denit_0^{BNO3}.Limit_{BO2}^{BNO3}.e^{k_T^{BNO3}.T}.BNO3$ with: $Limit_{BO2}^{SOD} = \frac{BO2}{BO2 + K_{BO2}^{SOD}}$; $Limit_{BO2}^{BNO3} = 1 - \frac{BO2}{BO2 + K_{BO2}^{BNO3}}$; $pfract = (1-\alpha).BLT$
BED DETRITUS (BD, $mgN.m^{-3}$)	$\frac{dBD}{dt} = -\min_0^{BD}.e^{k_{min}^{BD}.T}.BD - burial^{BD}.BD - M^{BD}.\delta_r^{BD}.BD + \frac{1}{pfract}\left(w_S^{D}.D + w_S^{BDP}.BDP\right)$ with $\delta_r^{BD} = 0$ if $\tau_b \le \tau_{crit}^{BD}$ and $\delta_r^{BD} = \frac{\tau_b - \tau_{crit}^{BD}}{\tau_{crit}^{BD}}$ if $\tau_b \ge \tau_{crit}^{BD}$
BED AMMONIUM (BNH4, $mgN.m^{-3}$)	$\frac{dBNH4}{dt} = \min_0^{BD}.e^{k_{min}^{BD}.T}.BD.\frac{pfract}{wfract} - burial^{BNH4}.BNH4 - nitr_0^{BNH4}.Limit_{BO2}^{BNH4}.e^{k_{nitr}^{BNH4}.T}.BNH4$ $+ \%red^{BNO3}.denitr_0^{BNO3}.Limit_{BO2}^{BNO3}.e^{k_{denitr}^{BNO3}.T}.BNO3 + Diff_0^{NH4}.\left(1+\frac{T}{20}\right).\frac{\alpha}{\frac{(BLT+h)}{2}}.\frac{(NH4 - BNH4)}{wfract}$ with: $Limit_{BO2}^{BNH4} = \frac{BO2}{BO2 + K_{BO2}^{BNH4}}$
BED NITRATE (BNO3, $mgN.m^{-3}$)	$\frac{dBNO3}{dt} = nitr_0^{BNH4}.Limit_{BO2}^{BNH4}.e^{k_{nitr}^{BNH4}.T}.BNH4 - denitr_0^{BNO3}.Limit_{BO2}^{BNO3}.e^{k_{denitr}^{BNO3}.T}.BNO3 + Diff_0^{NO3}.\left(1+\frac{T}{20}\right).\frac{\alpha}{\frac{(BLT+h)}{2}}.\frac{(NO3 - BNO3)}{wfract}$
BED DISSOLVED OXYGEN (BO2, $mgO_2.m^{-3}$)	$\frac{dBO2}{dt} = -r_{O2}^{BNH4}.nitr_0^{BNH4}.Limit_{BO2}^{BNH4}.e^{k_{nitr}^{BNH4}.T}.BNH4 - oxi_0^{SOD}.e^{k_T^{SOD}.T}.Limit_{BO2}^{SOD}.SOD + Diff_0^{O2}.\left(1+\frac{T}{20}\right).\frac{\alpha}{\frac{(BLT+h)}{2}}.\frac{(O2*1000 - BO2)}{wfract}$

Table III-3 List of parameters forming the biogeochemical model equations, including the value used in the present study, the units, a range of values found in the literature for calibrated parameters and the corresponding references. Column "S" indicates the parameters included in the sensitivity analysis.

	Parameter	S	Value	Units	Comments	Range	References
Large Phyto (LP)	$Chl\ a/C^{LP}$		1/30	$mgChl\ a.mgC^{-1}$			Claustre et al., 1994
	N/C^{LP}		0.176	$mgN.mgC^{-1}$	corresponding to a molar ratio of 1/7		
	$p_{O2}{}^{LP}$		3.119	$mgO2.mgC^{-1}$	O2 produced per unit of LP photosynthesis		
	$r_{O2}{}^{LP}$		2.667	$mgO2.mgC^{-1}$	O2 consumed per unit of LP respiration		
	$k_P{}^{LP}$		0.05	$°C^{-1}$	LP growth temperature factor	0.017–0.07	Dowd, 1997; Duarte et al., 2003; Grégoire & Lacroix, 2001
	$k_r{}^{LP}$		0.07	$°C^{-1}$	LP respiration temperature factor		Chapelle et al., 2000
	$I_o{}^{LP}$	*	100	$J.m^{-2}.s^{-1}$	Optimum light intensity for LP	50–300	Chapelle et al., 2000; Nunes et al., 2003; Cugier et al., 2005
	$K_{NO3}{}^{LP}$	*	9	$mgN.m^{-3}$	Nitrate (NO3) half saturation coefficient for LP	4.2–21	Pinazo et al., 1996; Grégoire et al., 1998; Tian et al., 2000
	$K_{NH4}{}^{LP}$	*	14	$mgN.m^{-3}$	Ammonium (NH4) half saturation coefficient for LP	14–28	Chapelle et al., 1994; Grégoire et al., 1998; Li et al., 2000
	λ_0		0.69	m^{-1}	non-algal light extinction coefficient		calculated from SPM (Lohrenz et al., 1999)
	λ_1		0.0088	$m^{-1}.(\mu gChla.L^{-1})^{-1}$	Linear self-shading coefficient		default value RMA-11; King, 2003
	λ_2		0.054	$m^{-1}.(\mu gChla.L^{-1})^{-2/3}$	Non-linear self-shading coefficient		default value RMA-11; King, 2003
	$\mu_0{}^{LP}$	*	1	d^{-1}	LP maximum growth rate at 0°C	0.45–1.2	Chapelle et al., 1994; Duarte et al., 2003
	$\beta_0{}^{LP}$	*	0.02	d^{-1}	LP respiration rate at 0°C	0.01–0.1	Chapelle et al., 1994; Grégoire et al., 2008
	λ^{LP}	*	0.02	d^{-1}	LP mortality rate	0.005–0.05	Chapelle et al. 1994; Tian et al, 2000; Dzierzbicka-Glowacka, 2005
Small Phyto (SP)	$Chl\ a/C^{SP}$		1/80	$mgChl\ a.mgC^{-1}$			Claustre et al., 1994
	N/C^{SP}		0.176	$mgN.mgC^{-1}$	corresponding to a molar ratio of 1/7		
	$p_{O2}{}^{SP}$		3.119	$mgO2.mgC^{-1}$	O2 produced per unit of SP photosynthesis		
	$r_{O2}{}^{SP}$		2.667	$mgO2.mgC^{-1}$	O2 consumed per unit of SP respiration		
	$k_P{}^{SP}$		0.05	$°C^{-1}$	SP growth temperature factor	0.017–0.07	Eppley, 1972; Duarte et al., 2003; Grégoire & Lacroix 2001
	$k_r{}^{SP}$		0.07	$°C^{-1}$	SP respiration temperature factor		
	$I_o{}^{SP}$	*	200	$J.m^{-2}.s^{-1}$	Optimum light intensity for SP	50–300	Chapelle et al., 2000; Nunes et al., 2003; Cugier et al., 2005
	$K_{NO3}{}^{SP}$	*	7	$mgN.m^{-3}$	Nitrate (NO3) half saturation coefficient for SP	0.7–21	Grégoire et al., 1998; Tian et al., 2000, Grégoire et al., 2008
	$K_{NH4}{}^{SP}$	*	2.8	$mgN.m^{-3}$	Ammonium (NH4) half saturation coefficient for SP	0.7–7	Grégoire et al., 1998; Tian et al., 2000, Grégoire et al., 2008
	$\mu_0{}^{SP}$	*	0.88	d^{-1}	SP maximum growth rate at 0°C	0.8–1.2	Chapelle et al., 2000; Duarte et al., 2003
	$\beta_0{}^{SP}$	*	0.04	d^{-1}	SP respiration rate at 0°C	0.01–0.05	Chapelle et al., 2000; Grégoire et al., 2008
	λ^{SP}	*	0.02	d^{-1}	SP mortality rate	0.02–0.06	Grégoire et al., 1998; Guillaud et al., 2000; Cugier et al., 2005

Table III-3 (continued)

	Parameter	S	Value	Units	Comments	Range	References
Large Zoo (LZ)	N/C^{LZ}		0.194	$mgN.mgC^{-1}$	corresponding to a molar ratio of 1/6		
	$r_{O2}{}^{LZ}$		2.667	$mgO2.mgC^{-1}$	O2 consumed per unit of LZ respiration		
	$k_P{}^{LZ}$		0.11	$°C^{-1}$	LZ ingestion temperature factor		Deason, 1980
	$k_r{}^{LZ}$		0.07	$°C^{-1}$	LZ respiration temperature factor		Bougis, 1976
	$K_F{}^{LZ}$	*	80	$mgC.m^{-3}$	Food half saturation coefficient for LZ	60–160	Li et al., 2000 ; Grégoire et al., 2008
	$\varepsilon_D{}^{LZ}$	*	0.10	-	LZ preference for D	0.1–0.5	Tian et al., 2000 ; Grégoire & Lacroix, 2001
	$\varepsilon_{LP}{}^{LZ}$	*	0.70	-	LZ preference for LP	0.25–0.9	Grégoire et al., 1998 ; Griffin et al., 2001
	$\varepsilon_{SP}{}^{LZ}$	*	0.22	-	LZ preference for SP	0.2–0.5	Grégoire et al., 1998 ; Griffin et al., 2001 ; Oguz et al., 1999
	$\varepsilon_{SZ}{}^{LZ}$	*	0.30	-	LZ preference for SZ	0.23–0.75	Grégoire et al., 1998 ; Griffin et al., 2001 ; Oguz et al., 1999
	I^{LZ}	*	0.5	d^{-1}	LZ ingestion rate	0.15–0.8	Oguz et al., 1999 ; Ji et al., 2008
	$\beta_R{}^{LZ}$	*	0.05	d^{-1}	LZ respiration rate	0.01–0.1	Chapelle et al., 1994 ; Grégoire & Lacroix, 2001 ; Cugier et al., 2005
	λ^{LZ}	*	0.02	d^{-1}	LZ mortality rate	0.0065–0.2	Li et al., 2000 ; Grant et al., 2007
	$c_I{}^{LZ}$		0.19205	-	LZ ingestion scaling factor		
	$c_R{}^{LZ}$		0.246597	-	LZ respiration scaling factor		
	$AE_P{}^{LZ}$	*	0.4	-	LZ assimilation efficiency for phytoplankton (LP, SP)	0.18–0.9	Conover, 1966 ; Tian et al., 2000 ; Griffin et al., 2001 ; Ji et al., 2008
	$AE_D{}^{LZ}$	*	0.3	-	LZ assimilation efficiency for D		
	$AE_{SZ}{}^{LZ}$	*	0.35	-	LZ assimilation efficiency for SZ		
Small Zoo (SZ)	N/C^{SZ}		0.194	$mgN.mgC^{-1}$	corresponding to a molar ratio of 1/6		
	$r_{O2}{}^{SZ}$		2.667	$mgO2.mgC^{-1}$	O2 consumed per unit of SZ respiration		
	$k_P{}^{SZ}$		0.11	$°C^{-1}$	SZ ingestion temperature factor		
	$k_r{}^{SZ}$		0.07	$°C^{-1}$	SZ respiration temperature factor		
	$K_F{}^{SZ}$	*	120	$mgC.m^{-3}$	Food half saturation coefficient for SZ	14–120	Grégoire et al., 1998 ; Tian et al., 2000
	$\varepsilon_D{}^{SZ}$	*	0.3	-	SZ preference for D	0.05–0.7	Oguz et al., 1999 ; Tian et al., 2000
	$\varepsilon_{LP}{}^{SZ}$	*	0.25	-	SZ preference for LP	0.2–0.33	Oguz et al., 1999 ; Griffin et al., 2001
	$\varepsilon_{SP}{}^{SZ}$	*	0.32	-	SZ preference for SP	0.1–0.8	Grégoire et al., 1998 ; Griffin et al., 2001
	I^{SZ}	*	1	d^{-1}	SZ ingestion rate	1–1.7	Grégoire et al., 1998 ; Tian et al., 2000
	$\beta_R{}^{SZ}$	*	0.1	d^{-1}	SZ respiration rate	0.02–0.2	Baretta-Bekker et al., 1995 ; Griffin et al., 2001
	λ^{SZ}	*	0.04	d^{-1}	SZ mortality rate	0.005–0.04	Oguz et al., 1999 ; Chapelle et al., 2000
	$c_I{}^{SZ}$		0.19205	-	SZ ingestion scaling factor		
	$c_R{}^{SZ}$		0.246597	-	SZ respiration scaling factor		
	$AE_P{}^{SZ}$	*	0.4	-	SZ assimilation efficiency for phytoplankton (LP, SP)	0.28–0.64	Griffin et al., 2001 ; Grégoire et al., 2008
	$AE_D{}^{SZ}$	*	0.3	-	SZ assimilation efficiency for D		

Table III-3 (continued)

	Parameter	S	Value	Units	Comments	Range	References
Detritus (D)	r_{O2}^{D}		15.143	$mgO2.mgN^{-1}$	O2 consumed per unit of D remineralization		stoechiometry
	k_{min}^{D}		0.07	$℃^{-1}$	D remineralization temperature factor		
	K_{O2}^{D}	*	2.5	$mgO2.L^{-1}$	O2 half saturation coeff. For D remineralization	0.5–4.45	Chapelle et al., 2000 ; Giusti & Marsili-Libelli, 2006
	min_0^{D}	*	0.02	d^{-1}	D remineralization rate at 0℃	0.01–0.2	Chapelle, 1995 ; Bergamasco & Zago, 1999 ; Romero et al., 2004 ; Okunishi et al., 2005 ; Haag, 2006
	w_S^{D}	*	0.5	$m.d^{-1}$	D settling velocity	0.1–1	Chapelle et al., 1994 ; Robson & Hamilton, 2004
Ammonium (NH4)	r_{O2}^{NH4}		4.5714	$mgO2.mgN^{-1}$	O2 consumed per unit of NH4 oxidation		stoechiometry
	k_{nitr}^{NH4}		0.07	$℃^{-1}$	NH4 oxidation temperature factor		
	K_{O2}^{NH4}	*	2	$mgO2.L^{-1}$	O2 half saturation coefficient for NH4 oxidation	0.32–2	Chapelle et al., 2000 ; Grégoire & Lacroix, 2001
	$nitr_0^{NH4}$	*	0.06	d^{-1}	NH4 oxidation rate at 0℃	0.01–0.1	Baretta-Bekker et al., 1995 ; Chapelle et al., 2000
Bed Detritus (BD)	r_{O2}^{BD}		15.143	$mgO2.mgN^{-1}$	BO2 consumed per unit of BD remineralization		stoechiometry
	k_{min}^{BD}		0.07	$℃^{-1}$	BD remineralization temperature factor		
	K_{O2}^{BD}	*	0.5	$mgO2.L^{-1}$	BO2 half saturation coeff. For BD remineralization	0.256–0.5	Chapelle, 1995; Boudreau, 1996
	min_0^{BD}	*	0.005	d^{-1}	BD remineralization rate at 0℃	3.0e-6–0.03	Wainright & Hopkinson, 1997 ; Grégoire & Lacroix, 2001
	$burial^{BD}$	*	1.00E-04	d^{-1}	BD burial rate	6.85^{e}-5–1.34^{e}-4	Pett, 1989 ; Cerco & Cole, 1994
	M^{BD}	*	0.1	d^{-1}	BD maximum erosion rate		
	τ_{cnt}^{BD}	*	0.025	$N.m^{-2}$	Critical shear stress for BD erosion	0.02–0.16	Ariathurai & Krone, 1976 ; Maa et al., 1998 ; Beaulieu, 2003 ; Walker & Grant, 2009
Bed Ammonium (BNH4)	d^{BNH4}	*	0.01728	$m^2.d^{-1}$	BNH4 diffusion coefficient in sediments	5.42^{e}-5–0.01728	Li & Gregory, 1974 ; DiToro et al., 1990 ; Chapelle, 1995 ; Jimenez-Montealegre et al., 2002
	r_{O2}^{BNH4}		4.5714	$mgO2.mgN^{-1}$	BO2 consumed per unit of BNH4 oxidation		stoechiometry
	k_{nitr}^{BNH4}		0.07	$℃^{-1}$	BNH4 oxidation temperature factor		
	K_{O2}^{BNH4}	*	4	$mgO2.L^{-1}$	BO2 half saturation coefficient for BNH4 oxidation		Chapelle, 1995 ; Robson & Hamilton, 2004
	$nitr_0^{BNH4}$	*	0.2	d^{-1}	BNH4 oxidation rate at 0℃	0.1–0.75	Chapelle, 1995 ; Ruardij & van Raaphorst, 1995
	$burial^{BNH4}$	*	0.01	d^{-1}	BNH4 burial rate		
Bed Nitrate (BNO3)	d^{BNO3}	*	0.001728	$m^2.d^{-1}$	BNO3 diffusion coefficient in sediments	5.41^{e}-5–0.01728	Li & Gregory, 1974 ; DiToro et al., 1990 ; Chapelle, 1995 ; Jimenez-Montealegre et al., 2002
	r_{BD}^{BNO3}		5.3	-	BNO3 consumed per unit of BD (denitrification)		stoechiometry
	k_{denitr}^{BNO3}		0.07	$℃^{-1}$	BNO3 denitrification temperature factor		
	K_{O2}^{BNO3}	*	2	$mgO2.L^{-1}$	BO2 half saturation coeff. For BNO3 denitrification	0.3–2	Chapelle, 1995; Robson & Hamilton, 2004
	$denitr_0^{BNO3}$	*	0.3	d^{-1}	BNO3 denitrification rate at 0℃	0.05–10	Jahnke et al., 1982; Goloway & Bender, 1982
	$\%red^{BNO3}$	*	0.189	-	fraction of BNO3 reduced to BNH4		stoechiometry
Bed Dissolved Oxygen (BO2)	d^{BO2}	*	0.0864	$m^2.d^{-1}$	BO2 diffusion coefficient in sediments	1.27^{e}-4–0.0864	DiToro et al., 1990 ; Hoffman et al., 1991 ; Chapelle, 1995

Table III-3 (end)

	Parameter	S	Value	Units	Comments	Range	References
Sediment Oxygen Demand (SOD)	K_{O2}^{SOD}	*	0.5	$mgO2.L^{-1}$	BO2 half saturation coefficient for SOD oxidation	0.256–0.5	Chapelle, 1995; Boudreau, 1996
	k_{oxi}^{SOD}		0.07	$°C^{-1}$	SOD oxidation temperature factor		
	$oxid_0^{SOD}$	*	0.005	d^{-1}	SOD oxidation rate at 0°C	3.0e-6–0.03	Wainright & Hopkinson, 1997; Grégoire & Lacroix, 2001
	$burial^{SOD}$	*	1.00E-04	d^{-1}	SOD burial rate		
	rel^{SOD}	*	1.00E-04	d^{-1}	SOD release rate to the water column		
Sediments	α	*	0.8	-	Sediment porosity		
Mussel (M)	N/C^M		0.176	$mgN.mgC^{-1}$	corresponding to a molar ratio of 1/7		
	r_{O2}^M		2.667	$mgO2.mgC^{-1}$	O2 consumed per unit of M respiration		
	k_P^M		0.07	$°C^{-1}$	M ingestion/respiration temperature factor		
	σ_γ^M	*	0.2	-	M cost of growth coeffiicent		see references in Grant et al., 2007
	n^M		16.667	$ind.m^{-3}$	Mussel density		
	ε_D^M	*	0.5	-	M preference for D		
	ε_{LP}^M	*	1	-	M preference for LP		
	ε_{SP}^M	*	0.2	-	M preference for SP		
	ε_{SZ}^M	*	1	-	M preference for SZ		
	ε_{LZ}^M	*	0.3	-	M preference for LZ		
	K_F^M	*	100	$mgC.m^{-3}$	Food half saturation coefficient for M		see references in Grant et al., 2007
	I^M	*	0.2	d^{-1}	M ingestion rate		see references in Grant et al., 2007
	β_R^M	*	0.01	d^{-1}	M respiration rate		see references in Grant et al., 2007
	c_I^M		0.247717	-	M ingestion scaling factor		
	c_R^M		0.375311	-	M respiration scaling factor		
	b_I^M	*	-0.32	-	M allometric coefficient of ingestion		see references in Grant et al., 2007
	b_R^M	*	-0.3	-	M allometric coefficient of respiration		see references in Grant et al., 2007
	AE_P^M	*	0.52	-	M assimilation efficiency for phytoplankton (LP, SP)		
	AE_D^M	*	0.47	-	M assimilation efficiency for D	0.15–0.55	Tremblay et al., 1998
	AE_Z^M	*	0.52	-	M assimilation efficiency for zooplankton (LZ, SZ)		
Biodeposits (BDP)	w_S^{BD}	*	846	$m.d^{-1}$	BDP settling velocity	233–1564	Callier et al., 2006

Basically, LP and SP are limited in their growth either by inorganic nutrient availability following a Michaelis-Menten law with an inhibition of NO3 uptake by NH4 or by light according to Steele's formula (Steele, 1962). Food limitation of LZ and SZ growth also follows a Michaelis-Menten dynamic. LZ and SZ can feed on both types of phytoplankton and D. Small zooplankton also represents a source of food for LZ. Each class of zooplankton has a specific preference and assimilation efficiency for each type of prey. Mussels can feed on all types of particulate organic matter (LP, SP, LZ, SZ and D) with different preferences and assimilation efficiencies for each kind. A Holling Type III law is used to represent the limitation of mussel growth by food availability. Detritus that are not grazed are either mineralized to produce NH4 or sink to the bottom. Ammonium is also produced by the excretion of all heterotrophs and may be oxidized to NO3. In the water column, O2 is consumed by the respiration of phytoplankton (LP and SP), zooplankton (LZ and SZ) and mussels and by the mineralization of D and SOD released to the water and by the nitrification of NH4. Finally, except for the settling (D and BDP) and resuspension (BD) mechanisms in the water column and the burial (BD, SOD and NH4) and release (SOD) mechanisms in the sediment, all processes are scaled by the water temperature. An exponential law, $\exp(k_T.T)$, is used for all the processes except the diffusion of dissolved variables at the sediment–water interface, which follows a linear scaling: (1+T/20) (Li & Gregory, 1974).

Contrary to the other pelagic variables, the mussel variable is not transported by the water and only occurs in the cultivation area (shaded section on Fig. III-2). It represents the soft tissue mass of a representative individual. The variations of this mass are determined

by a scope for growth equation (Table III-2) that describes the balance between gains through ingestion and losses through respiration. This ecophysiological model was successfully used within an ecosystem box model to reproduce the growth of mussels cultured in GEL (Grant et al., 2007).

3.2.4 Model application

A major advantage of the RMA models is the decoupling of the hydrodynamic and biogeochemical simulations. This enables one to run the hydrodynamic part first; the biogeochemical part then uses a conservative scheme to calculate the transport of pelagic variables from the results of the hydrodynamic simulation. Therefore, the computational cost of the biogeochemical simulations is lowered by not recalculating the hydrodynamics each time and by using a different time step for the biogeochemical part, which does not need a time step as short as the hydrodynamic part. This becomes of particular interest during the time consuming calibration and sensitivity analysis stages. RMA models also include a semi-implicit time stepping scheme that enables the use of rather long time steps. For the present study, a 360 s time step was used for the hydrodynamic simulation while a longer 1800 s time step was used for the biogeochemical calculations.

The biogeochemical structure described above was used to reproduce the GEL ecosystem during summer 2003 from 27 June to 17 October. Before starting with the main simulation period, the model was allowed to stabilize over a 20 day spin-up period, roughly corresponding to the water renewal time of the lagoon (Koutitonsky & Tita, 2006). During

this spin-up, the model was forced with real hydrodynamic and meteorological conditions. However, the biochemical boundary conditions were held constant to the value at the start of the main period except for water temperature, which followed natural conditions in order to ensure a good agreement between the simulated and observed temperature on 27 June.

The open boundary conditions 1 and 2 obtained from stations 7 and 2, respectively, of the sampling program are shown on Figure III-4. Figure III-5 shows the main meteorological forcings, i.e., the wind speed, which is known to affect the dynamics of shallow coastal systems, and the precipitation recorded in summer 2003, since it represents the major source of dissolved inorganic nitrogen (DIN) in the system (Souchu & Mayzaud, 1991).

The initial concentrations of pelagic variables were set to the mean of boundary values at the start of the period of interest. An iterative process was used to adjust the initial concentrations of the benthic variables and make sure these concentrations were stabilized before the end of the spin-up period.

Because no mussel weight data were available at the start of the simulation, the initial value of the variable M was included in the calibration process. As mentioned earlier, only one-year-old mussels are present in the farm during most of summer, so the model only includes this cohort. Moreover, no population processes are included in the model and the density of cultured mussels is held constant at 100 mussels.m^{-2} or 16.667 mussels.m^{-3} for a mean depth of 6 m in the cultivation area.

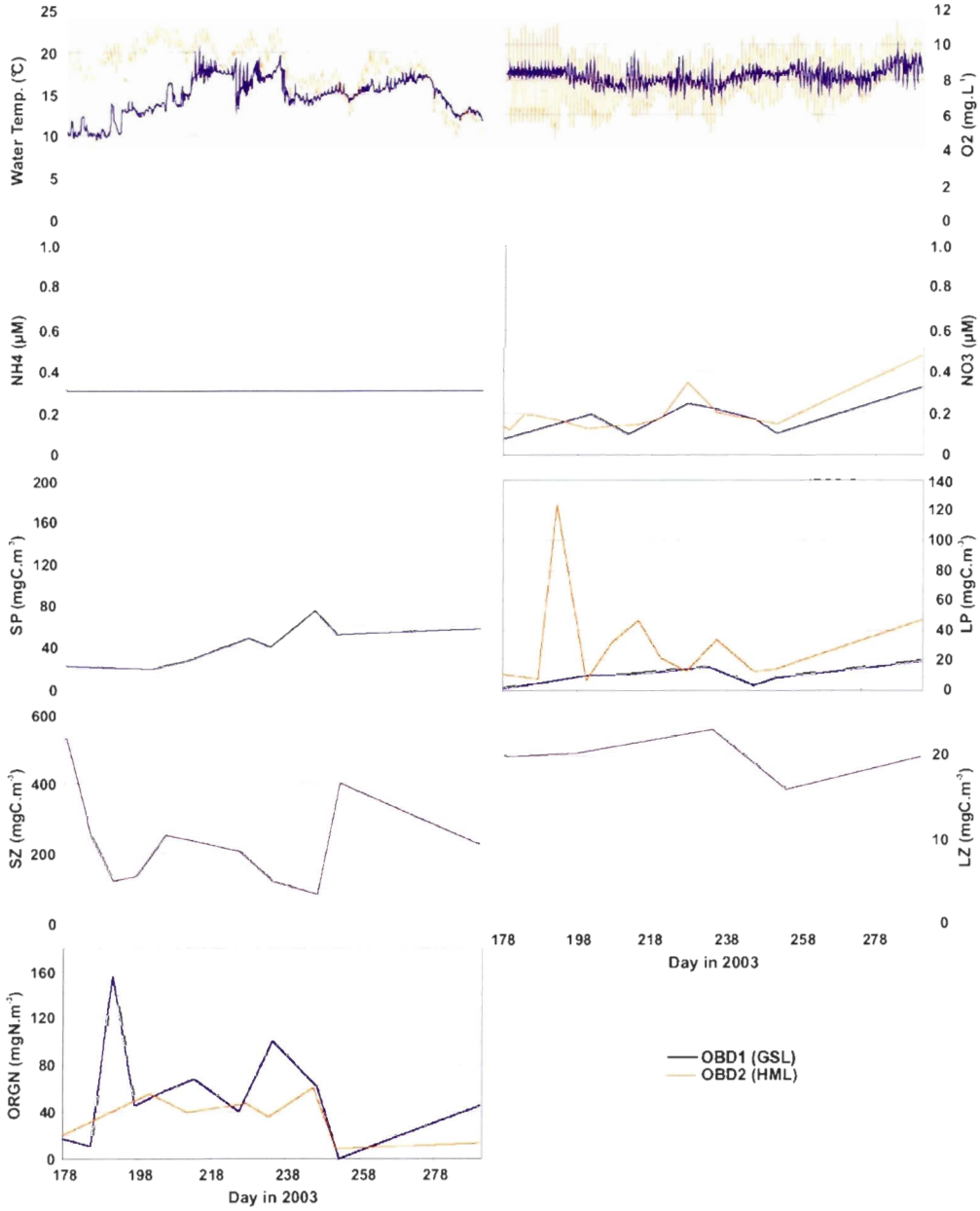

Figure III-4: Open boundary conditions (OBD1: connexion with the Gulf of St. Lawrence, OBD2: connexion with Havre-aux-Maisons lagoon) recorded during summer 2003 and imposed on the model to reproduce the GEL biogeochemical dynamics (see Fig. III-3 for variable definitions).

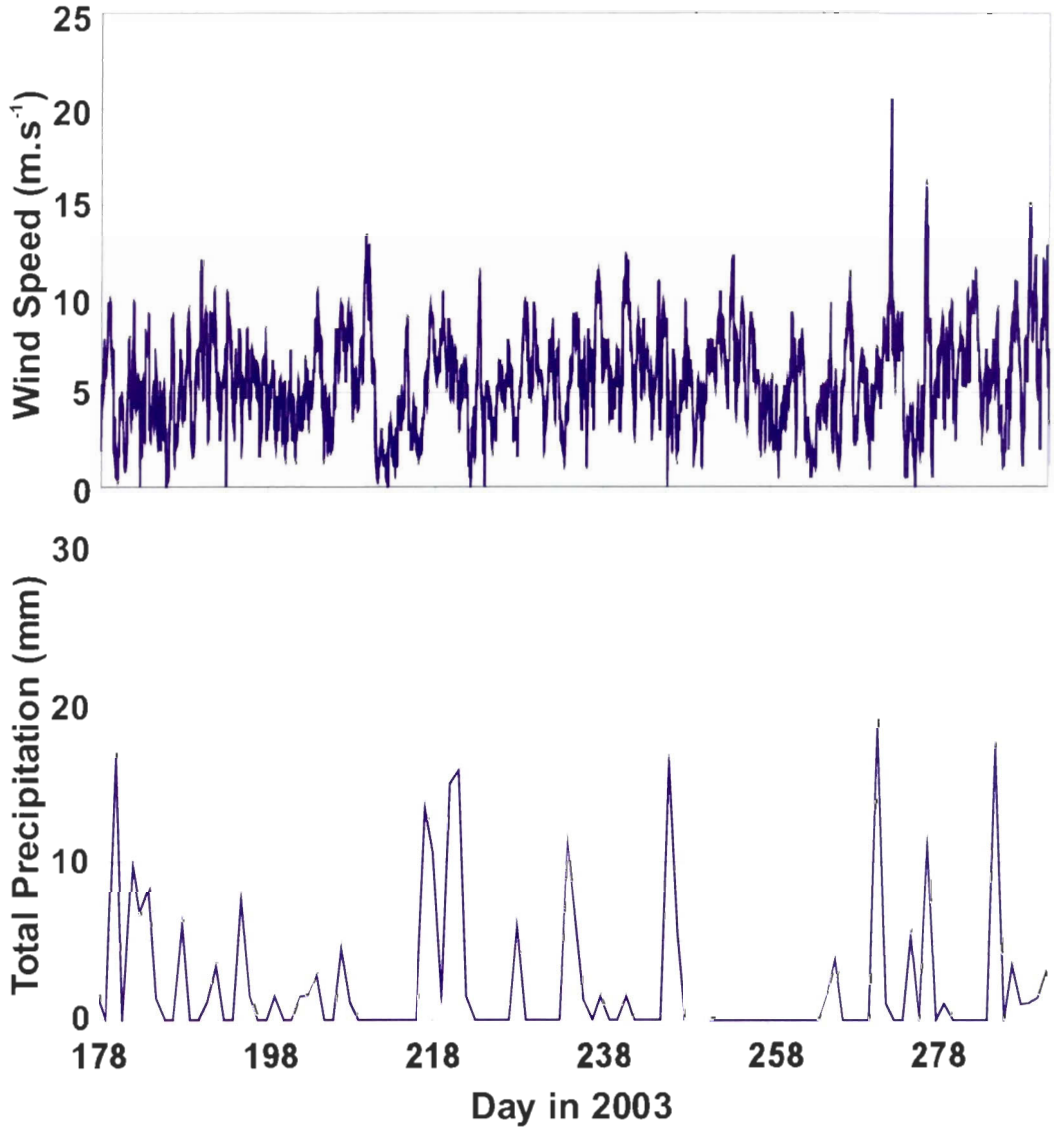

Figure III-5 Meteorological conditions (top panel: wind speed; bottom panel: precipitation amount) observed during summer 2003 over the Magdalen Island area.

3.2.5 Model calibration and sensitivity analysis

Calibration

The model calibration was based both on the visual and objective comparisons of observations and model results. The normalized root mean square error (RMSn) was used as an objective measure of model result quality for hydrodynamic parameters. RMSn expresses the mean error in terms of percentage of the observed data range and is calculated as follows:

$$RMSn = 100 * \left[\frac{\sqrt{\frac{1}{n}\sum_{i=1}^{n}\left(M_{x,i} - D_{x,i}\right)^2}}{D_x^{\max} - D_x^{\min}} \right]$$

where $M_{x,i}$ and $D_{x,i}$ are the predicted and observed variable values at station x and date i, respectively, n is the number of comparison dates, and $D_x^{\max}$ and $D_x^{\min}$ are respectively the maximum and minimum values of variable x observed during the comparison period.

Radach & Moll (2006) proposed the cost function approach as a standard method of biogeochemical model validation. Hence, for biochemical variables, the cost function (C_x) at the regional scale (specific stations and time resolving) defined by OSPAR et al. (1998) was used as the objective index of the goodness of fit between observed and predicted data and was calculated as follows:

$$C_x = \frac{1}{2} \cdot \frac{\frac{1}{n}\sum_{i=1}^{n}\left|M_{x,i} - D_{x,i}\right|}{sd_x} + \frac{1}{2} \cdot \left(1 - r_x\right)$$

where $M_{x,i}$ and $D_{x,i}$ are the predicted and observed variable values at station x and date i, respectively, n is the number of comparison dates, sd_x is the standard deviation of observed data at station x over the entire comparison period, and r_x is the correlation coefficient between the predicted and observed time series over the entire comparison period. C_x is expressed in standard deviation units. For $C_x<1$, $1\leq C_x<2$, $2\leq C_x<3$ and $C_x>3$, model results are respectively considered very good, good, reasonable and poor (Radach & Moll, 2006). This cost function was estimated for each pelagic variable for which observed data were available and at both stations 4 and 5.

To start the calibration process, an initial parameter set was taken from Tian et al. (2000), whose model had a similar biogeochemical structure and was applied in the GSL close to the Îles-de-la-Madeleine. Some of the parameters (see Table III-3) were then varied inside the range found in the literature to improve the model predictions (i.e., lower the cost functions).

Sensitivity Analysis

To address the model sensitivity, each parameter marked in Table III-3 as well as the boundary conditions for each state variable and the meteorological forcing (air temperature T_{air}, wind speed W_{sp}, incoming solar radiation SolRad, and NH4 and NO3 concentrations in precipitation) were varied by ±10% and the results of these two simulations were compared with the standard run by calculating the percentage of the model result change for a 1% variation in the parameter, as expressed by the sensitivity index (S):

$$S = \left(\frac{100}{p}\right) \cdot \frac{1}{n} \cdot \sum_{i=1}^{n} \frac{\left|M_i - M_i^*\right|}{M_i^*}$$

where p is the percentage of the parameter variation (i.e., 10), n is the number of comparison dates, M_i is the new variable value at the comparison date i and M_i^* is the variable value from the standard run on the same date i. The mean of S(+10%) and S(-10%) was taken and this value was averaged over the whole model domain.

3.3 RESULTS

3.3.1 Model calibration

Hydrodynamics

The inter-comparison (not shown) of the present model with the 3D model of the HML–GEL system (Guyondet & Koutitonsky, 2008) over the summer 2001 period gives a first indication of the GEL 2D model's capacity to reproduce the hydrodynamics of this lagoon. In order to confirm this for the summer 2003 period, model results and observed data were compared in terms of water level fluctuations (stations 4, 5 and 6) and currents (stations 5 and 6). This comparison results (RMSn) show an overall good agreement between observed and predicted time series of hydrodynamic parameters. Water level fluctuations are well reproduced by the model throughout the lagoon, with RMSn values not exceeding 10% at any of the stations (S4: 9.0%; S5: 8.4% and S6: 2.2%). Currents at the entrance of GEL are also well reproduced by the model, with an RMSn error <15% at station 6. Currents are not as well reproduced in the deep basin, as shown by the RMSn

slightly over 20% at station 5. Currents in this part of the lagoon are quite slow, with observed values seldom exceeding 5 $cm.s^{-1}$, so even a small error becomes large compared to the current magnitude. Moreover, it is likely that the deeper basin is one of the areas of the lagoon where the 2D approximation is less suitable to represent the natural 3D water circulation. Nevertheless, even at station 5, model results are of reasonable quality and the model captures the order of magnitude of the currents in this area, with observed and predicted currents in the range 1.6×10^{-2} – 5.1 $cm.s^{-1}$ and 6.10^{-2} – 5.3 $cm.s^{-1}$, respectively.

Biogeochemistry

The calibration process led to the set of biogeochemical parameters reported in Table III-3. Several parameters stayed at the initial value extracted from the model developed by Tian et al. (2000); otherwise they were kept within the range found in the literature. The values of mussel ecophysiological parameters were kept identical to those used in the previous box model study (Grant et al., 2007), except that assimilation efficiency was taken in the range of values observed for GEL mussels (Tremblay et al., 1998). For particles large enough to be filtered, mussels do not seem to exert any active food selection in GEL, with the fraction of each type of prey retained being similar to the fraction of each prey in the surrounding waters (Trottet et al., 2008b). Therefore, mussel preferences for the different types of food not included in the box model were chosen mostly according to the range of particle sizes that mussels can feed on. Hence, SP (<3 μm) is mainly too small and was given a low preference (ε_{SP}^{M} = 0.2) as was LZ (ε_{LZ}^{M} = 0.3), since only larger mussels are

able to feed efficiently on mesozooplankton (Lehane & Davenport, 2002) and even larval stages of this type of prey have the ability to avoid the capture (Green et al., 2003). Mussels can efficiently filter both LP and SZ ($\varepsilon_{LP}^{M} = \varepsilon_{SZ}^{M} = 1$). Finally, D was given a lower preference ($\varepsilon_{D}^{M} = 0.5$) to account for its potentially lower energetic content due to degradation and mussel preference for living material (Newell et al., 1989).

Benthic state variables were not included in this analysis because no data on the concentration of these variables in interstitial water were available. The accuracy of benthic processes was only tested using observations of sediment–water exchange fluxes.

State variables

According to the cost function values shown in Table III-4, all model results for pelagic variables at both stations 4 and 5 are in the "very good" or "good" range. Some discrepancies are apparent when the graphical comparisons of observed data and model predictions are examined (Fig. III-6 and 7).

Water temperature, the main forcing function of most of the biochemical processes, is one of the most accurately predicted variables (Table III-4). This indicates that the physical processes of water transport and air–sea exchange are well reproduced by the model. The model captures both the timing and range of the seasonal trend, showing a slow increase in temperature from the start of the period until a maximum at the end of July – beginning of August. The temperature then begins to decrease at the end of August by a succession of drops followed by more stable periods. Starting from the second drop at the beginning of October (day 275) at station 4 (Fig. III-6a) or two weeks earlier at station 5 (Fig. III-7a), the

model tends to underestimate the water temperature and the discrepancy with observed values then reaches a maximum of 1.5 °C. This period corresponds to the beginning of the windy autumn period (Fig. III-5). The intense cooling in the model prediction may then result from a slight overestimation of the wind effect in air–sea heat transfer.

Table III-4 Results of the model calibration for pelagic biogeochemical variables expressed as the cost function (C_x in standard deviation units) comparing observed data and model predictions. ND: no data. See Table III-1 for variable definitions.

	S4	S5
T	0.22	0.25
O2	0.50	0.44
LP	0.64	0.74
SP	1.10	1.06
D	1.16	0.96
NH4	ND	ND
NO3	1.27	1.34
LZ	0.23	0.22
SZ	0.39	0.40

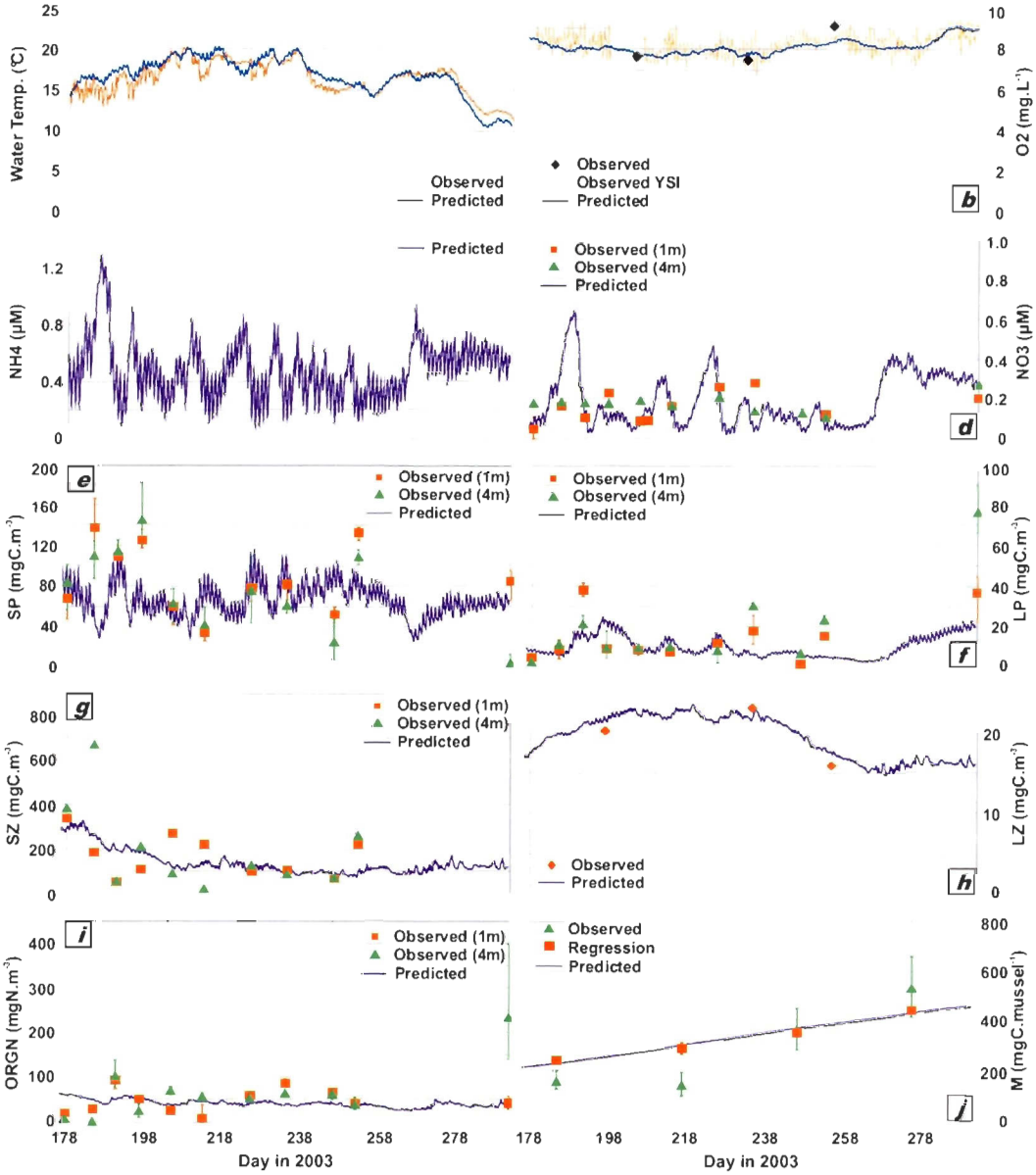

Figure III-6 Comparison of observed and predicted time series of pelagic variables at station 4 inside the mussel cultivation area (see Fig. III-3 for variable definitions).

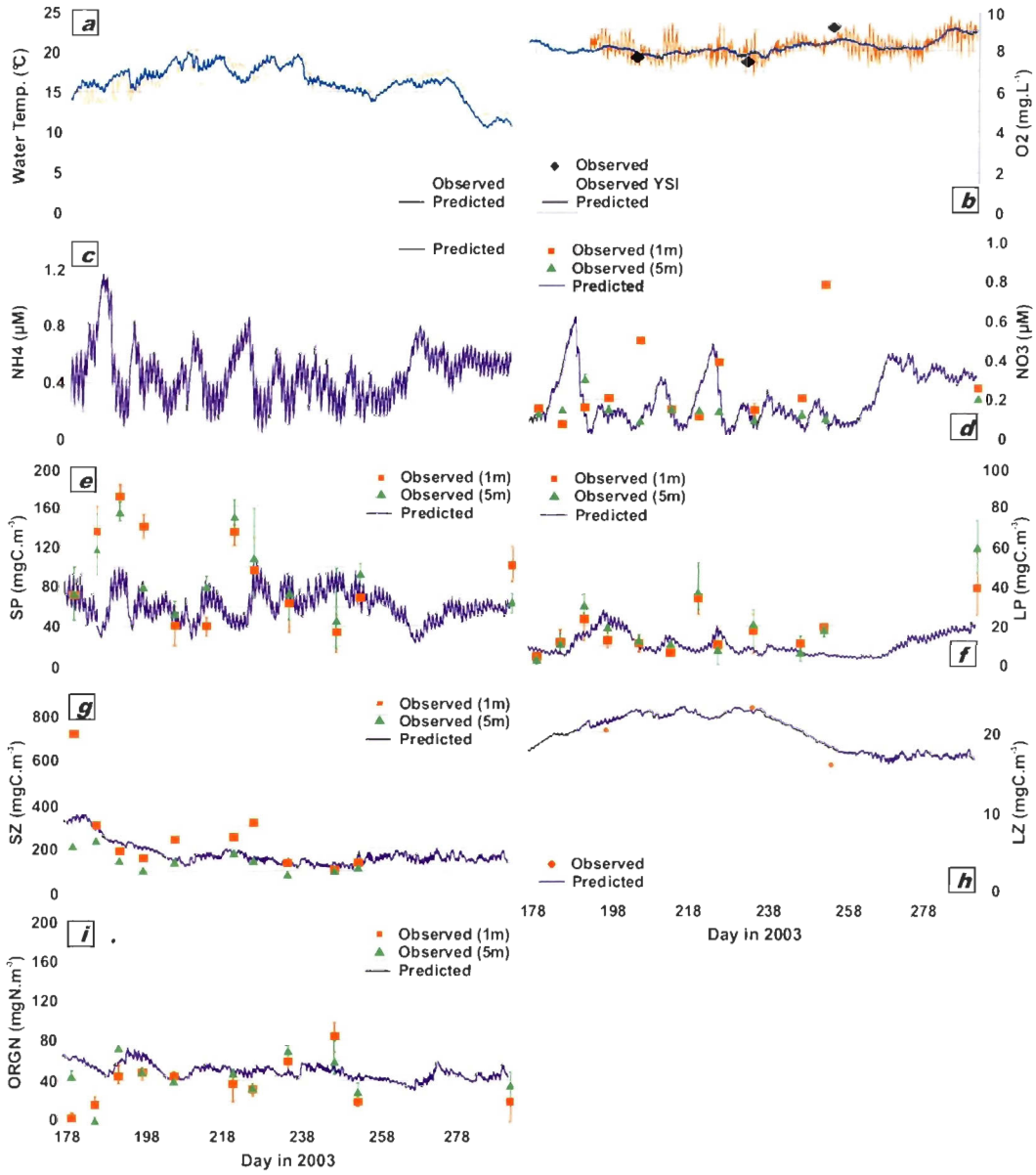

Figure III-7 Comparison of observed and predicted time series of pelagic variables at station 5 outside the mussel cultivation area (see Fig. III-3 for variable definitions).

Low frequency fluctuations in dissolved oxygen, mainly due to the negative correlation with water temperature (Pitre, 2007), are well reproduced by the model (Fig. III-6b and III-7b). The phase of the diurnal oscillations of this variable is accurately predicted but their range is underestimated. This discrepancy may be attributed, at least in part, to the effects of the benthic flora and fauna on the dissolved oxygen concentrations near the bottom where the probe was moored; benthic organisms were not included in the model.

No ammonium data were collected during summer 2003. However, according to observations made in summer 2004, the model reproduces the correct order of magnitude for this variable, with a simulated mean concentration of 0.46 μM (Fig. III-6c and III-7c) compared to 0.3 μM measured in 2004 (Trottet et al., 2007).

Summer concentrations of nitrate are very low in GEL (Fig. III-6d and III-7d) and do not vary much, especially at station 4, where they ranged between 0.05 and 0.28 μM. Moreover, this variable does not show any particular trend during summer. Overall, the model prediction agrees well with the observations. The predicted time series presents two major peaks (day 188 and 223) and an increase in October (starting from day 260), all of which correspond to the most rainy periods (Fig. III-5). This pattern is not as clearly present in the observed nitrate concentrations, which may be due to the sampling frequency not allowing the capture of these short bursts and/or to the high variability of nitrate concentrations in precipitation (Souchu & Mayzaud, 1991) not being included in the model.

Summer biomass of large phytoplankton did not vary much: most of the observations (St. 4 and 5) lie in the range of 5–20 $mgC.m^{-3}$, corresponding to 0.17–0.67 µg Chl *a*.L^{-1} (Fig. III-6f and III-7f). The observed time series at both stations show three peaks above this range. The first and last occurred at the same time at both stations (days 191 and 291). The first peak is rather well reproduced by the model, with only a slight delay compared to the observations. The last peak is underestimated by the model at both stations, and the intermediate peak, which occurred two weeks earlier at station 5 (day 220) compared to station 4 (day 234), is not represented by the model. Observations show that LP biomass was higher close to the bottom than in the surface waters during both the intermediate and the last peak. Moreover, all these maxima occurred during or just after strong wind and rain events (Fig. III-5) and benthic pennate diatoms were observed in the water column samples (Trottet et al., 2007). In the absence of any major discrepancy between predicted and observed nitrate concentrations, a reasonable explanation of the underestimation of LP biomass by the model at these particular dates would then be the resuspension of benthic microalgae not reproduced by the model since it does not include any benthic microalgae. By increasing the LP biomass in the water column, this resuspension mechanism may have allowed the development of a short bloom fuelled by the additional nitrate brought in by the precipitation.

Observed time series show that small phytoplankton biomass is quite stable through summer as well and twice as high as LP (Fig. III-6e and III-7e), with most of the data between 30 and 90 $mgC.m^{-3}$ (0.37 – 1.12 µg Chl *a*.L^{-1}). The SP biomass presents the same

peak as LP biomass at the beginning of the period (days 185–197). The model reproduces this peak at both stations, but with both an underestimated amplitude and duration. Part of this discrepancy may be explained by the overestimation by the model of the microzooplankton biomass during the second half of this peak, leading to an overestimated grazing pressure on SP. Other model variable uncertainties may also explain the poorer quality of the results during this short period, for example, ammonium is the main substrate for SP growth, but there are no data available. SP biomass is rather well reproduced by the model for the remainder of the period except for a second peak observed only at station 5 (days 220–225) and slightly underestimated and delayed by the model. The model predictions of both LP and SP biomass reach a local minimum while observed values are at a local maximum (day 220). The model behaviour may be explained by a combination of factors. The rainy and windy conditions at this time (Fig. III-5) suggest that a dense cloud cover was present over the system. This is confirmed by low values of incoming solar radiations for several days (not shown) and by a local minimum in predicted water temperature that slightly underestimates the observed temperature (Fig. III-7a). Both the reduced water temperature and reduced light availability induce a decrease in phytoplankton production in the model, leading to the low in LP and SP biomass. Five days later, when the light intensity is back to "normal" summer values and water temperature starts to increase again, model SP has already used the excess ammonium to grow back to observed values (Fig. III-7e). Although resuspension may have increased the discrepancy between observations and model predictions, it seems that the natural phytoplankton was not greatly affected by the slight decrease in water temperature and the large reduction of

light intensity during this particular event and was able to positively respond to the nutrient input from the rain. Finally, the diurnal fluctuations of both LP and SP biomass were compared with observed chlorophyll *a* time series presented by Pitre (2007). Model results agree well with observations both in terms of diurnal amplitude (the daily maximum concentration reaches up to twice the minimum) and daily maximum timing (observed between 8 p.m. and midnight and simulated between 6 and 11 p.m.). Hence, the model seems to reproduce the diurnal primary production cycle quite accurately.

Mesozooplankton biomass observations are too few to make a detailed comparison with the model prediction. However, the general trend showing a slight increase during the summer to reach a maximum in mid-August (day 230) and then a decrease in late August – early September seems to be well reproduced by the model both in timing and amplitude (Fig. III-6h and III-7h).

The observed time series of microzooplankton biomass start with a steep decrease from an overall maximum at the beginning of the period to a local minimum two weeks later (day 191) at station 4 and three weeks later (day 197) at station 5 (Fig. III-6g and III-7g). The model also predicts a rapid decrease at this time but not as steep as and slightly longer than observed. This initial drop is followed by a long period of stable or slightly decreasing SZ biomass, well reproduced by the model. Finally, a sharp increase occurred between the last two observation dates at station 4 that is only marginally captured by the model. The higher the trophic level, the more the uncertainties for lower trophic levels can

affect the quality of the model results. Here, the sharp increase at the end of the period coincides with an increase in SP biomass that is poorly reproduced by the model (Fig. III-6e), leading to a discrepancy in SZ biomass as well.

Detritic organic matter concentrations follow the same temporal pattern at both stations except for a sharp increase in bottom concentration at station 4 on the last observation date (Fig. III-6i and III-7i). Very low concentrations were observed at the beginning of the period followed by a local maximum in early July (day 191), a slow decrease over the next 20 days and a second maximum at the end of August (days 234–246). The model fails to reproduce the initial low concentrations and the second peak, but it does predict the first peak followed by the gently decreasing concentrations. There are no obvious explanations for these discrepancies from other model variables. Two potential explanations may be found in the representation of the organic detritus dynamics used by the model. First, the model does not account for all detritus sources, for example, detritus from terrestrial origin and from macroalgae and aquatic macrophytes are not included in the model, which may explain part of the second peak's underestimation. The second source of uncertainty is related to the resuspension of organic detritus, which is based on a bed shear stress intensity that does not explicitly account for waves in the model. However, winds from different directions may create very different wave conditions in the lagoon, leading to different potentials for sediment resuspension. For the present example, the first days of the period saw strong south-southeast (SSE) winds (perpendicular to GEL's main axis) while two major west-southwest (WSW) wind events (parallel to GEL's main axis)

occurred at the time of the second peak in organic detritus concentration (days 237 and 240, Fig. III-5a). Due to the lagoon's axis orientation and the northeastern position of the sampling stations, WSW winds may blow over a longer fetch and create stronger waves in the lagoon, potentially leading to more sediment resuspension. Hence, the model's parametrization only being sensitive to the wind intensity through the shear stress would probably lead to an overestimation/underestimation of resuspension during SSE/WSW wind events, as suggested by the comparison with observations (Fig. III-6i and III-7i) and the results of observed time series analysis by Pitre (2007) showing no direct relation between wind speed and water turbidity in GEL's deep basin.

Mussel growth observations consisted in the monitoring of two variables, shell length and dry meat weight. While shell length gives a quite stable measure of growth, dry meat weight not only reflects the somatic growth of mussels but also the gains and losses due to their reproductive cycle. Since the model equation predicting mussel individual weight only accounts for somatic growth, this part of the model was calibrated using a "composite" mussel weight obtained from the regression between the observed shell length and dry meat weight over the whole sampling period. The observed and composite mussel weights were converted to carbon biomass using a 40% carbon content for mussel dry meat (Grant et al., 1993) and then compared to the model predictions (Fig. III-6j). Very good agreement was reached between the composite weight and the model results and, as expected, the somatic growth equation failed to represent all the variability of the observed weight. This is particularly true for the first two observation dates (4 July and 5 August), for which the

model overestimates the mussel weight, and may be explained by mussel spawning, which occurs in late June – early July in GEL (Myrand et al., 2000) and lowers the weight of mussels for several weeks.

Fluxes

In order to ascertain that the model is a reliable tool to study the functioning of the lagoon ecosystem, it is necessary to check the accuracy of the results not only for state variables but for rate processes as well (Brush et al., 2002). Hence, fluxes such as primary production and sedimentation rates as well as inorganic nutrient exchange at the sediment–water interface, all measured in situ in summer 2003 or 2004, were also compared to the model predictions.

Primary production was measured during summer 2004 only using the ^{14}C fixation method (Trottet et al., 2007). Expressed as chlorophyll-specific production rates, these observations vary widely, ranging from 0.88 to 13.28 mgC.mgChl $a^{-1}.h^{-1}$ (Trottet et al., 2007). Model predictions fall well within this range, with values between 0.95 and 5.33 mgC.mgChl $a^{-1}.h^{-1}$, although they do not reach the maximum rates observed during diatom blooms. The comparison of measurements made inside and outside the mussel cultivation area showed that the primary productivity was between 0.11 and 61.3% higher inside the mussel farm (Trottet et al., 2008a). The model reproduces this characteristic as well, with a production rate higher by 0 to 48.4% at station 4.

Sedimentation rates were also measured both inside and outside the mussel farm on several occasions during summer 2003, and again higher rates were observed in the mussel

culture area (control: 0.32–0.92 $gC.m^{-2}.d^{-1}$; mussel farm: 0.43–1.96 $gC.m^{-2}.d^{-1}$; Callier et al., 2006). The model results fall in the range of observed values both in the mussel farm (0.15–0.60 $gC.m^{-2}.d^{-1}$) and outside (0.08–0.42 $gC.m^{-2}.d^{-1}$). The model also reproduces higher rates in the mussel farm due mainly to biodeposition. However, these rates tend to be underestimated, which may be in part explained by the absence in the model of some sources of suspended material, as mentioned earlier for the underestimation of organic detritus concentrations.

Dissolved oxygen and nutrient exchange through the sediment–water interface were measured using dark benthic chambers (Richard et al., 2007), which makes the comparison with the diffusive fluxes provided by the model difficult. As observed by Middelburg et al. (1995) chamber-measured fluxes may be 2 to 28 times higher than diffusive fluxes based on concentration gradients alone, since the former account for processes related to benthic flora and fauna as well. Using negative values for fluxes entering the sediment, dissolved oxygen fluxes observed during summer 2003 ranged from -43.2 to -677.3 $mgO_2.m^{-2}.h^{-1}$ and were not matched by the simulated diffusive fluxes, which ranged between -9.5 and -16.3 $mgO_2.m^{-2}.h^{-1}$ in the mussel cultivation area and between -8.7 and -14 $mgO_2.m^{-2}.h^{-1}$ outside. The diffusion coefficients used in the present model are among the highest values reported as they account for the bioturbation–irrigation activity of the benthic fauna (Chapelle, 1995). However, this was not enough to reproduce the magnitude of O2 fluxes, which may be considerably influenced by benthic flora and fauna respiration as well. Nevertheless, this allowed the model to reproduce NH4 and NO3 fluxes with more accuracy. Observed and simulated NH4 fluxes were always coming out of the sediment,

with observed and simulated values respectively in the range: 0.24 – 5.17 $mgN.m^{-2}.h^{-1}$ and 0.03 – 3.6 $mgN.m^{-2}.h^{-1}$ inside the mussel farm and 0.06 – 2.33 $mgN.m^{-2}.h^{-1}$ and 0 – 1.2 $mgN.m^{-2}.h^{-1}$ outside. Both observed and simulated NO3 fluxes were either entering into or coming out of the sediment, with observed and simulated values, respectively, in the range of -2×10^{-2} - 7×10^{-2} $mgN.m^{-2}.h^{-1}$ and -1.7×10^{-3} - 2.2×10^{-2} $mgN.m^{-2}.h^{-1}$ inside the farm and -5.10^{-2} - 4.10^{-2} $mgN.m^{-2}.h^{-1}$ and -7.6×10^{-4} - 1.4×10^{-2} $mgN.m^{-2}.h^{-1}$ outside.

Both observed (in the dark) and simulated NH4 and NO3 fluxes do not account for DIN uptake by benthic microalgae. Hence, the model may overestimate (underestimate) fluxes coming out of (entering into) the sediment during daytime. However, reduced light intensity at 6 m depth in GEL deep basin probably leads to slow primary production rates and slow DIN uptake rates at the surface of the sediment. On the other hand benthic microalgae biomass may be quite high, as 2% to 46% of diatoms sampled in the water column during summer 2003 were benthic species (Trottet et al., 2008a). The magnitude of the error associated with this model shortcoming is then difficult to predict without more precise information on benthic microalgae biomass and production.

Even if the model does not seem to reproduce all the high frequency variability observed during summer 2003, the calibration process overall led to a satisfactory quality of model results. In particular, good agreement was reached between observed and predicted mussel somatic growth. The model was also able to reproduce well the order of magnitude and seasonal trend for all the state variables and the order of magnitude of rate processes for which data were available. Consequently, this model would represent a

reliable tool to study the GEL ecosystem dynamics and its interactions with the mussel cultivation activity, provided that its predictive ability is ascertained by the results of the sensitivity analysis.

3.3.2 Sensitivity analysis

The results of the 168 simulation runs required to test the sensitivity of the model results for 70 parameters and 14 boundary conditions and meteorological forcing were compiled as mentioned in the METHODS section for pelagic variables only. Again, benthic variables were not included in this analysis because more data are needed to study in detail the behaviour of the benthic submodel. However, the influence of parameters related to benthic processes on pelagic variables was tested. The sensitivity index, representing the relative change of a state variable for a 1% change of a parameter or forcing, exceeded 3 only once (LP sensitivity to μ_0^{SP}, S = 5.3) and was >1 on 24 occurrences only. Overall, model results are very stable.

The system dynamics are revealed by the influence of the parameters on each state variable. Figure III-8 presents the sensitivity index values for each variable. Only parameters leading to an S>0.5 are shown, and O2, T and D are not presented as their S values were >0.5 for only one parameter or less. O2 does not present any S value >0.5 for any of the parameters, boundary conditions or forcing. T is only sensitive (S = 0.63) to one forcing, the air temperature. This shows that the water temperature inside GEL is more

influenced by exchange with the atmosphere than by exchange at the open boundaries, a logical result for a system with a water renewal time of several days and confirmed by the small influence of tides on observed water temperature variability (Pitre, 2007). D is also only sensitive (S = 0.54) to one parameter: its settling velocity.

LP is the most sensitive variable, showing both higher S values and higher numbers of parameters with S>0.5 (Fig. 8). LP is not only sensitive to its own parameters (μ_0^{LP}, K_{NH4}^{LP}) but also to several parameters related to SP and SZ, with an intensity even higher ($S(\mu_0^{SP})>S(\mu_0^{LP})$). The dynamics of LP are then more influenced by its competition with SP and by the top-down control of SZ than by its intrinsic processes. The concentrations of LP, SP and SZ at the open boundaries also slightly influence the LP biomass inside GEL as well as the light intensity (SolRad), one of the main forcings for photosynthesis.

Except for its own growth rate (μ_0^{SP}) and air temperature, which influences temperature-regulated processes through its control on water temperature, SP is only sensitive to SZ parameters. Like LP, the top-down control of SZ seems to be a major factor in the dynamics of SP more than light or nutrient limitation.

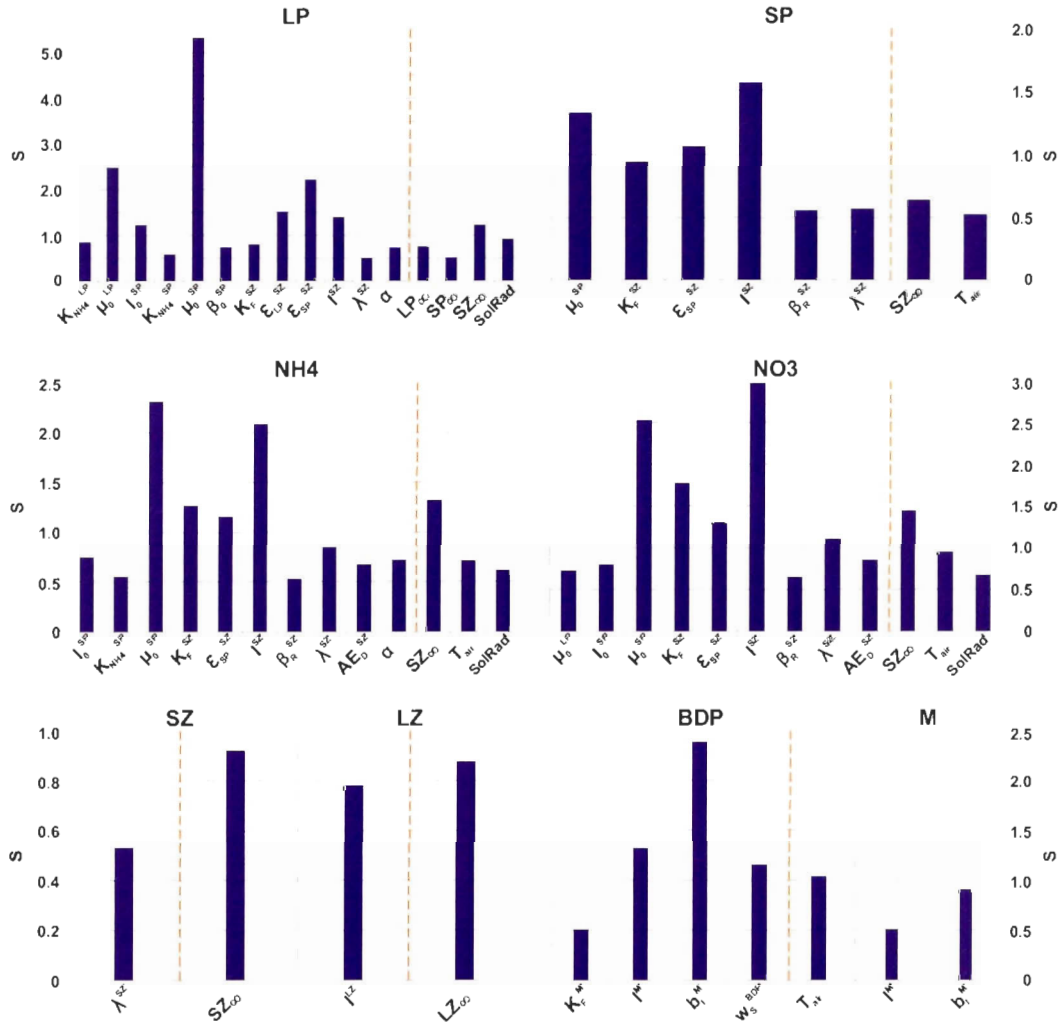

Figure III-8 Results of the model sensitivity analysis for pelagic variables (showing only parameters with a sensitivity index S>0.5; see Table III-3 for parameter definitions).

Both DIN forms (NH4 and NO3) show similar sensitivity patterns with both the influence of phytoplankton (both LP and SP for NO3 but only SP for NH4) as well as the influence of SZ, either directly (excretion of NH4, β_R^{SZ}) or indirectly through its control of LP and SP dynamics. Both nutrients also show a slight sensitivity to air temperature and light intensity, which may be explained by indirect effects of T_{air} on the water temperature and of SolRad on LP and SP photosynthesis. Moreover, except for K_{NH4}^{LP}, which very slightly influences LP dynamics, no other nutrient-related parameter appears to greatly affect either the nutrient concentrations or the dynamics of the primary producers. Therefore, DIN is not heavily limiting the primary production in the simulated ecosystem; this was also suspected from observations of low nutrient concentrations and rather high primary production rates (Roy et al., 1991; Souchu et al., 1991; Trottet et al., 2007).

Micro- and mesozooplankton are not very sensitive, being only slightly influenced by their respective boundary levels and either their mortality rate (SZ) or their ingestion rate (LZ). Their dynamics are thus controlled by exchanges at the open boundaries and intrinsic physiological processes. SZ may also be partly controlled by external processes not explicitly represented in the model but included in the mortality closure term.

Mussel variables (M and BDP) are only sensitive to mussel physiological parameters and air temperature (BDP only). Moreover, mussel parameters do not affect the sensitivity of any other variable. Hence, the mussel farm does not seem to greatly influence the ecosystem dynamics, at least at the scale of the entire lagoon given that the results of this sensitivity analysis were integrated over the whole model domain.

Among the five parameters showing the highest mean S over all variables, four are SZ parameters and the other is the maximum growth rate of SP. This again stresses the importance of small cells in the overall dynamics of the simulated ecosystem, which was also assumed in nature (Roy et al., 1991; Trottet et al., 2007; Trottet et al., 2008a).

3.4 DISCUSSION - CONCLUSION

The results of both the calibration process and the sensitivity analysis are strong indicators that the present model gives a reliable representation of GEL's ecosystem dynamics and allows a comprehensive study of the interactions between these dynamics and the cultured mussels. A final step in the model verification would be the validation of model results against a second independent dataset, which is not available at this time.

3.4.1 Nitrogen cycle in GEL

Since the present simulation covers only one summer period, the system cannot be considered in steady-state and an overall mass-balance showing whether the system is importing or exporting nitrogen (N) cannot be calculated. However, integrating all N fluxes over GEL and the whole simulation period gives a detailed picture of N pathways in the system (Fig. III-9). Figure III-9 shows the integrated N fluxes between the system variables (solid lines) as well as the input from precipitation and the net exchanges at GEL boundaries (dashed lines). The integration was done over 216 semi-diurnal tidal cycles

covering most of the simulation period to ensure that there was no net gain or loss of water by the system over the integration period. At first glance, a striking discrepancy appears to occur between the microbial food web (SP, SZ) and the herbivorous one (LP, LZ), with fluxes linking the microbial web variables at least one order of magnitude higher than their herbivorous web counterpart. This again highlights the dominance of small cells, which monopolize most of the nitrogen cycling in the system. A more detailed examination reveals the similarities and discrepancies of these two pathways, starting with common inorganic substrates. Considering the water column alone, external inputs of DIN come from precipitation as well as exchanges at the open boundaries and at the water–sediment interface while recycling mechanisms rely on excretion by heterotrophs and detritus mineralization for NH4 and nitrification for NO3. For both NH4 and NO3, fluxes are dominated by recycling over external inputs in a proportion of 4/1. While NO3 is considered as the form for new nutrient inputs in many coastal systems, nitrate, like ammonium, is mainly a product of recycling in GEL. Therefore, recycling processes provide most of the nutrients taken up by primary producers (93% for NH4 and 84% for NO3). This confirms the marginal dependence of primary production upon the external inputs of nutrients during summer. However, discriminating the different sources of external inputs reveals major discrepancies between the two forms of DIN. Almost three quarters of the external inputs of NH4 are due to the efflux from the sediment while 82% of external NO3 comes from the precipitation during the summer period. Even the external inputs of NH4 to the water column are mostly coming from recycling mechanisms occurring inside the ecosystem (benthic compartment).

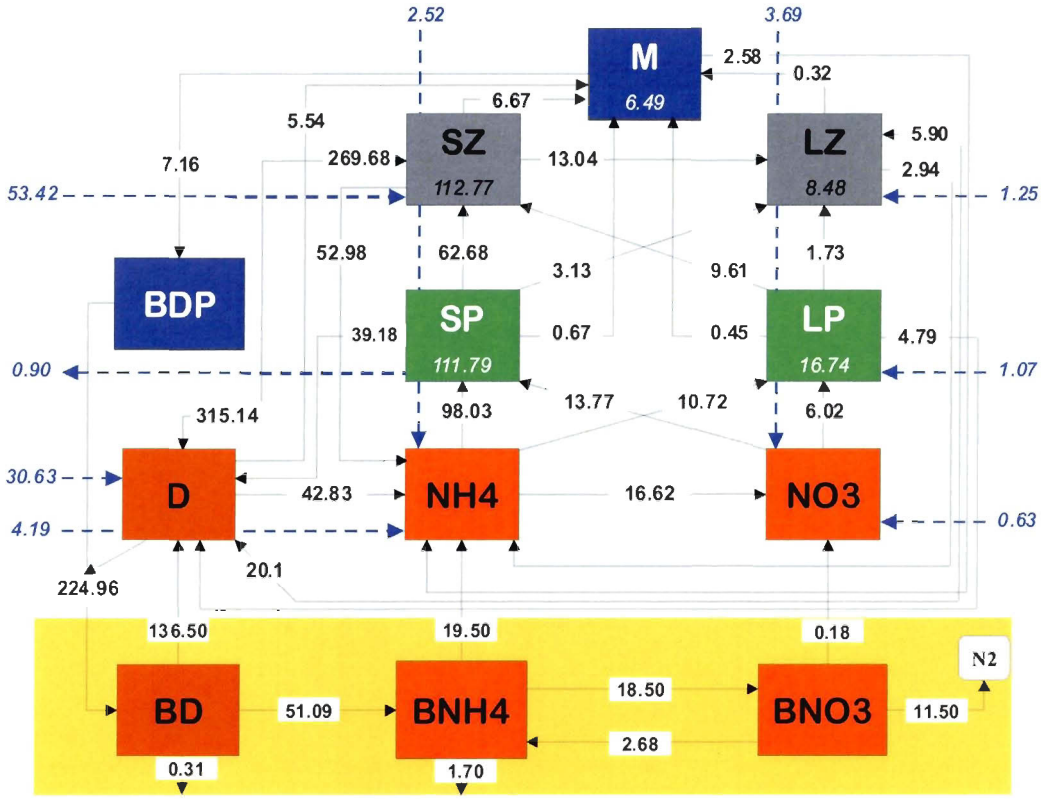

Figure III-9 Fluxes of nitrogen (tons N) obtained by integrating model results over the simulation period and the whole GEL to reveal the major pathways of the lagoonal ecosystem (dashed arrows represent fluxes between GEL and the outside either by precipitation or exchange at the open boundaries). Variable definitions same as in Fig.III-3.

If recycling provides most of the DIN, its sinks are dominated by SP uptake for primary production, which represents 70% and 90% of the total uptake of NO3 and NH4, respectively. These ratios correspond rather well with values observed in summer in the GSL, where phytoplankton < 5 μm is responsible for 71% of the NO3 uptake and 69% of the NH4 uptake (Tremblay et al., 2000). SP is also the only variable for which the model predicts a net export from GEL over the summer period. Conversely, LP plays a minor role, representing on average only 1.3% of the total nitrogen present in GEL waters over the summer period (7.5% for SP). Although NH4 is the preferred inorganic substrate for both LP and SP, SP is much more dependent on NH4 (almost 88%) than LP, which balances its uptake more evenly between NO3 (36%) and NH4 (64%).

Going further up in the trophic levels, the same hierarchy between small and large species of zooplankton persists, with SZ and LZ representing respectively 26.9% and 2.6% of the total N in the water column. Despite its low biomass, the role of LZ cannot be neglected. While its grazing on pelagic primary producers remains quite low, accounting only for 12% and 3.6% of the net production of LP and SP, respectively, it represents a stronger pressure on SZ, reaching nearly 22% of its net production. Nevertheless, SZ, with its important biomass and faster dynamics (see parameters in Table III-3), imposes a strong control over the whole system. Its grazing pressure amounts to 67% and 73% of the net production of LP and SP, respectively, values very close to the estimated microzooplankton grazing of 65% of total phytoplanktonic production based on dilution experiments in GEL (Trottet et al., 2008a). Excretion by SZ represents nearly 36% of all DIN inputs to the water

column, which may at least partly counterbalance the top-down effect of its grazing on phytoplankton.

Globally, the total net primary production could renew the total living pelagic biomass more than six times over the summer period but would only sustain one time the total water column respiration over the same period. Consequently, despite a rather high primary production, the overall dynamics of the system are dominated by the top-down pressure of heterotrophs (mainly SZ).

3.4.2 Role of cultured mussels

The study of the interactions between cultured mussels and the ecosystem will be detailed in a companion paper. Nevertheless, it can be noticed from Fig. III-9 that the mussel farming activity exerts only a limited influence on the pelagic ecosystem in its present state. Mussel grazing corresponds to only 3% and 0.8% of the net production of LP and SP, respectively. The pressure on zooplankton is slightly higher, with mussels grazing the equivalent of 5.8% and 11.2% of the net production of LZ and SZ, respectively. More than the actual results, the important point here is the ability of the present model to discriminate between the different prey the mussels can feed on. Table III-5 reviews a number of carrying-capacity studies for bivalve aquaculture, from the first production-oriented studies (Bacher, 1989) to the most recent studies using detailed physical–biological models (Grant et al., 2008). It should be noted that most of these studies do not discriminate more than two or three different types of food for the bivalves, the majority

only including one bulk variable representing phytoplankton (based on Chl *a*) and one variable representing organic detritus. Bivalves may not actively select between the different types of food within the range of particles they can filter, as has been observed for mussels in the Îles-de-la-Madeleine lagoons (Trottet et al., 2008b). Nevertheless, due to the limitations of their filtering apparatus in terms of retained particle size and the different function played by each type of prey, bivalve grazing is not neutral towards the ecosystem structure. In order to assess the ecological carrying capacity, i.e. how much the culture activity may be developed without significantly altering the energy fluxes in the ecosystem (Inglis et al., 2000), the tools employed should account for any functional alteration induced by the cultured bivalves. According to this requirement, the model presented here appears as an adequate tool to study the carrying capacity of GEL for mussel culture.

Table III-5 Review of bivalve aquaculture carrying-capacity studies comparing methods and types of food considered.

Reference	Method	Species	Types of food
Kaspar et al., 1985	Nitrogen mass balance	mussels (*Perna canaliculus*)	phyto
Rodhouse and Roden, 1987	Carbon mass balance	mussels (*Mytilus edulis*)	phyto
Bacher, 1989	Dynamic box model	oysters (*Crassostrea gigas*)	proteins, lipids, carbohydrates in seston
Carver and Mallet, 1990	POM mass balance	mussels (*Mytilus edulis*)	POM
Raillard and Ménesguen, 1994	Dynamic box model	oysters (*Crassostrea gigas*)	phyto, organic detritus
Dowd, 1997	Dynamic box model	mussels (*Mytilus edulis*)	phyto, organic detritus
Bacher et al., 1998	Dynamic box model	oysters (*Crassostrea gigas*)	phyto, organic detritus
Dame and Prins, 1998	Comparison of water renewal, primary production and bivalve clearance rates	several bivalve species	phyto
Ferreira et al., 1998	Dynamic box model	oysters (*Crassostrea gigas*)	phyto, organic detritus
Monteiro et al., 1998	Dynamic box model	mussels (*Mytilus galloprovincialis*)	phyto
van der Tol and Scholten, 1998	Dynamic box model	cockles (*Cerastoderma edule*) mussels (*Mytilus edulis*)	phyto, organic detritus
Inglis et al., 2000	Dynamic box model	mussels (*Perna canaliculus*)	phyto
Niquil et al., 2001	Inverse analysis	oysters (*Pinctada margaritifera*, *Pinctada maculata*)	phyto (3 classes), zoo (4 classes), organic detritus, bacteria

Table III-5 (end)

Reference	Method	Species	Types of food
Pastres et al., 2001	3D physical-biogeochemical model	clams (*Tapes philippinarum*)	phyto
Duarte et al., 2003	2D physical-biogeochemical model	oysters (*Crassostrea gigas*) scallops (*Chlamys farreri*)	phyto, organic detritus
Nunes et al., 2003	Dynamic box model	oysters (*Crassostrea gigas*) scallops (*Chlamys farreri*)	phyto, organic detritus
Guyondet et al., 2005	Comparison of water renewal, primary production and bivalve clearance rates	oysters (*Crassostrea virginica*)	phyto
Jiang and Gibbs, 2005	Steady-state food web model	mussels (*Perna canaliculus*) cockles, scallops	phyto, small zoo, organic detritus
Grant et al., 2007	Dynamic box model	mussels (*Mytilus edulis*)	phyto, organic detritus
Ferreira et al., 2008	Dynamic box model	mussels (*Mytilus edulis*) oysters (Crassostrea gigas)	phyto, POM (non-phyto)
Grant et al., 2008	2D physical-biogeochemical model	mussels (*Mytilus edulis*)	phyto, POM (non-phyto)
Spillman et al., 2008	3D physical-biogeochemical model	clams (*Tapes philippinarum*)	phyto, organic detritus
Marinov et al., 2009	3D physical-biogeochemical model	clams (*Tapes philippinarum*)	phyto (2 classes), zoo, bacteria, organic detritus
This study	2D physical-biogeochemical model	mussels (*Mytilus edulis*)	phyto (2 classes), zoo (2 classes), organic detritus

3.4.3 Limitations and possible improvements

The present study was successful as a first attempt to reproduce the main characteristics of the GEL ecosystem as well as mussel growth in this coastal environment. However, a few limitations may be identified both in terms of data available and model structure.

As for any model, more data to force and calibrate the model would probably lead to more reliability. Priorities should be put on the coverage of a longer period and on benthic parameters. A one-year dataset would give the opportunity to assess the relative importance of the high frequency fluctuations observed during summer 2003 and not always reproduced by the model. In addition to the cost of extensive field sampling, the present work was limited to the summer–fall period because of the technical difficulties raised by the ice cover during the winter months. The model would also benefit from additional information on variable concentrations in the sediment's interstitial water and benthic chemical processes since the calibration was only based on exchange rates at the sediment–water interface.

For improvements to the model structure, the benthic subsystem should be one of the priorities along with the representation of mussel ecophysiology. In such a shallow environment, the light intensity reaching the sediment may be sufficient to support primary production of benthic microalgae. The presence of such benthic species of microalgae observed in water-column samples (Trottet et al., 2007) confirms the existence of this production pathway in GEL and its participation in the pelagic food web via resuspension.

However, these primary producers were not included in the model due to the lack of data to estimate their biomass. Another improvement of the benthic subsystem would consist in accounting more precisely for the effects of the benthic fauna (bioturbation-irrigation, excretion-respiration) on the nutrient and dissolved oxygen fluxes at the sediment–water interface. This would confirm or cancel the role played by these effects in the discrepancy between the magnitudes of observed and simulated fluxes.

Although the present version of the model reproduced well the somatic growth of the cultured mussels, it does not account for all their energetic needs. Gametogenesis in particular requires much energy and may interfere with somatic growth (Lemaire et al., 2006). Thus, the simple ecophysiological representation used here could lead to an underestimation of the actual pressure of farmed mussels on ecosystem resources.

CHAPITRE 4

INTEGRATING MULTIPLE SPATIAL SCALES IN THE CARRYING CAPACITY ASSESSMENT OF A COASTAL ECOSYSTEM FOR BIVALVE AQUACULTURE

T. GUYONDET, J. GRANT,
S. ROY, V. G. KOUTITONSKY and G. TITA

RÉSUMÉ: Un modèle calibré physique-biogéochimique à fine résolution couplé avec un modèle écophysiologique de type budget d'énergie dynamique (DEB) est utilisé pour étudier les interactions entre une ferme mytilicole et l'écosystème côtier qui l'abrite, aussi bien à l'échelle locale qu'à celle du système au complet. En utilisant un jeu de paramètres de la littérature pour le DEB, le modèle couplé reproduit assez précisément la croissance locale des moules ainsi que sa répartition spatiale sur toute la ferme. Les flux métaboliques des moules sont également bien reproduits, ce qui autorise l'étude des relations moules/environnement.

Les résultats montrent l'importance des moules dans le cycle de l'azote à l'échelle locale dans la zone d'élevage. Malgré l'influence très réduite qu'exerce la ferme mytilicole à l'échelle du système complet, elle possède toutefois la capacité de modifier la structure de l'écosystème de la lagune de Grande-Entrée.

Selon les résultats du modèle couplé, le stock de moules en élevage pourrait être considérablement augmenté avant d'atteindre la capacité de production maximale de la GEL. Toutefois, si l'aspect écologique est pris en compte les résultats obtenus, utilisés conjointement avec des critères objectifs tels que les empreintes de déplétion, montrent que la capacité de support de la GEL est beaucoup plus restreinte.

L'outil numérique développé pour cette étude offre la possibilité d'estimer la capacité de support écologique d'une région côtière pour l'aquaculture de bivalves en incluant à la fois les processus à l'échelle locale et globale.

ABSTRACT: A calibrated fine resolution physical-biogeochemical model coupled with a dynamic energy budget (DEB) is used to investigate the local and system scale interactions between a mussel farm and the receiving coastal ecosystem. Using a set of published parameters for the DEB, the coupled model reproduces quite accurately both the local mussel growth and its spatial repartition over the farm area. Mussel related process rates are also well reproduced, allowing the study of mussel/environment interactions.

Results show the local importance of cultured mussels in the cycling of nitrogen within the cultivation area. Despite the strongly reduced influence exerted by the mussel farm at the scale of the entire system, the culture activity still has the ability to alter the structure of Grande-Entrée lagoon's ecosystem.

The coupled model results show that the mussel stock could be greatly increased before reaching the maximum production capacity of GEL. However, when the ecological aspect is accounted for, using model results along with objective criteria such as the depletion footprint curve, the overall carrying capacity of GEL must be significantly reduced.

The coupled fine scale numerical model developed for this study gives the opportunity to assess the ecological carrying capacity of a coastal region for shellfish culture accounting for both local and system scale processes.

4.1 INTRODUCTION

Shellfish aquaculture relies on natural resources to produce a valuable yield in the context of heavily exploited natural resources. By essence this yield is then constrained by the ability of the receiving ecosystem to provide the culture species with adequate food. The success of this type of culture is based on the capacity of sessile organisms, i.e. bivalve filter feeders, to collect their food from the surrounding waters. This success may be maximized through an appropriate site selection and culture density management. However, once established the culture production is dependent on three major aspects of the manipulated ecosystem. First the hydrodynamics drive the transport of food particles and wastes and may play a significant role in setting the productivity level of coastal areas (water renewal, exchange with open waters, inputs of nutrients through upwelling...). All biogeochemical processes that contribute to the production and consumption of the bivalve food represent the second aspect controlling the culture production. The third consists in the physiology of the cultured species which determines the rate of food consumption, waste production and biomass synthesis. The interactions of these three components define the level of culture a given system may support. This carrying capacity has been the subject of several studies in the past thirty years (Incze et al., 1981; Bacher et al., 1998; Nunes et al., 2003 among others). From the first production oriented studies to the recent ecologically oriented ones, the definition of the carrying capacity itself has evolved. It is now acknowledged that in the context of bivalve aquaculture this concept comprises several components. A physical, production, ecological or social carrying capacity may then be

defined (Inglis et al, 2000; McKindsey et al., 2006). So far, most of the studies have dealt with the production and ecological aspects as the physical capacity estimation is rather straightforward for a given system and cultivation technique and the social capacity is more subjective and depends on the three previous types (McKindsey et al., 2006). Gibbs (2007) noticed that neither the production nor the ecological carrying capacity is adequate in the context of bivalve aquaculture management. The strict ecological capacity is too strong a criterion, as it does not allow any significant alteration of the receiving ecosystem by human activities. Conversely, the production capacity is too loose as it does not include any environmental considerations. The ultimate goal being the development of the most productive farm without impairing its long term viability and the ecosystem stability, the carrying capacity for bivalve aquaculture should be a compromise between the ecological and production carrying capacities. A carrying capacity study has then to consider the effects of environmental conditions on the bivalves (temperature and salinity fluctuations, contaminant exposure, food supply) as well as the effects of bivalves on the ecosystem.

It was also soon acknowledged that a complete carrying capacity estimate should account for both local and system scales (Smaal et al., 1998). The local scale is particularly relevant for farm management considerations like cultivation structure orientation or bivalve density optimization in response to local hydrodynamics and the food depletion that may occur (Incze et al., 1981; Ferreira et al., 2007; Strohmeier et al., 2008). The propagation of local effects due to the hydrodynamics and the intense filtering of the bivalves has led to the concerns about system scale alterations (Officer et al., 1982). Hence, the carrying capacity of a system is bound to these local scale processes. However, until

recently few studies were able to combine both scales, as the modelling tools commonly used were limited by the computation power needed to represent the system at a fine scale and over a rather long period (> 1 year for most cultivation periods).

In the present contribution, a coupled hydrodynamic-biogeochemical model specifically designed and calibrated in a previous paper (Guyondet et al., Chap. III) is used to study the interactions (in either way) between cultured mussels and the receiving lagoon ecosystem. The fine spatial resolution combined with the integration of model results over the whole system give the opportunity to consider both the local and system scales in addressing the question of the lagoon's carrying capacity for suspended mussel aquaculture.

4.2 MATERIAL AND METHODS

4.2.1 Study area

The coupled hydrodynamic-biogeochemical model was successfully applied to reproduce the Grande-Entrée Lagoon (GEL) ecosystem, Iles-de-la-Madeleine, Québec, Canada (Guyondet et al., submitted). This shallow lagoon (mean depth 3 m) covers 58 km^2 in the southern Gulf of St. Lawrence (GSL; Fig. IV-1). It consists in a shallow western part and a deeper (5-6 m) eastern basin separated by an 8 m deep navigation channel running from a few kilometres off-shore through the main inlet and up to the north coast of the lagoon. The hydrodynamics of this system have been studied through a comprehensive analysis of water level and current time series (Koutitonsky et al., 2002) and successfully

reproduced with a finite element numerical model that serves as the hydrodynamic engine of the present coupled model (Guyondet and Koutitonsky, 2008). The 2.5 km^2 mussel culture lease covers most of the deep basin and is divided into 2 zones for the 2 successive mussel cohorts present at the same time in the lagoon during the winter months. During most of the growing season (May-November) only one cohort is present in the water after harvesting of the previous one in spring or early summer and before the seeding of the next one in October. The mussels are grown in suspension on long lines that hold continuous mussel socks at 2-4 m below the surface.

4.2.2 Model overview

A detailed description of the coupled model was given in Guyondet et al. (Chap. III). Here only an overview of the biogeochemical structure and a detailed description of the new mussel ecophysiological model will be presented.

Biogeochemical structure

The cycling of nitrogen (N), the limiting nutrient in this system (Souchu et al., 1991; Trottet et al., 2007), is reproduced through both a pelagic and benthic subdomain. In the water column, inorganic nutrients (ammonium: NH4 and nitrite-nitrate: NO3) fuel the primary production of two size classes of phytoplankton (LP>3 μm and SP< 3 μm). Two size classes of zooplankton are also considered (LZ: mesozooplankton and SZ:

microzooplankton) feeding on LP, SP and organic detritus (D) that complete the pelagic environment and may be either remineralized or deposited on the bottom. In the single layered benthic compartment, the particulate organic matter (BD) deriving from natural sedimentation and cultured mussel biodeposition is either resuspended into the water column or remineralized, increasing the sediment oxygen demand (SOD) and producing dissolved inorganic forms (ammonium: BNH4 and nitrite-nitrate: BNO3). The oxic mineralization (decreasing the SOD) and nitrification-denitrification processes are controlled by the concentration of dissolved oxygen (BO2) in interstitial water. All dissolved benthic variables are allowed to dynamically exchange with the water column through diffusive fluxes at the sediment-water interface. Water temperature, the main forcing for most of the biochemical processes is also simulated through a complete heat budget accounting for the exchange with the atmosphere.

All dissolved and particulate variables are transported by advection-dispersion in a 2D depth-averaged domain according to the current and water depth dynamics provided by the hydrodynamic model. The model domain presents two open boundaries where observed time series of the state variables are imposed, one off the main entrance in the GSL and one across the narrow south western passage leading to Havre-aux-Maisons Lagoon (HML, Fig. IV-1). The model also includes atmospheric forcing at the free surface in terms of atmospheric pressure fluctuations, wind stress and precipitation.

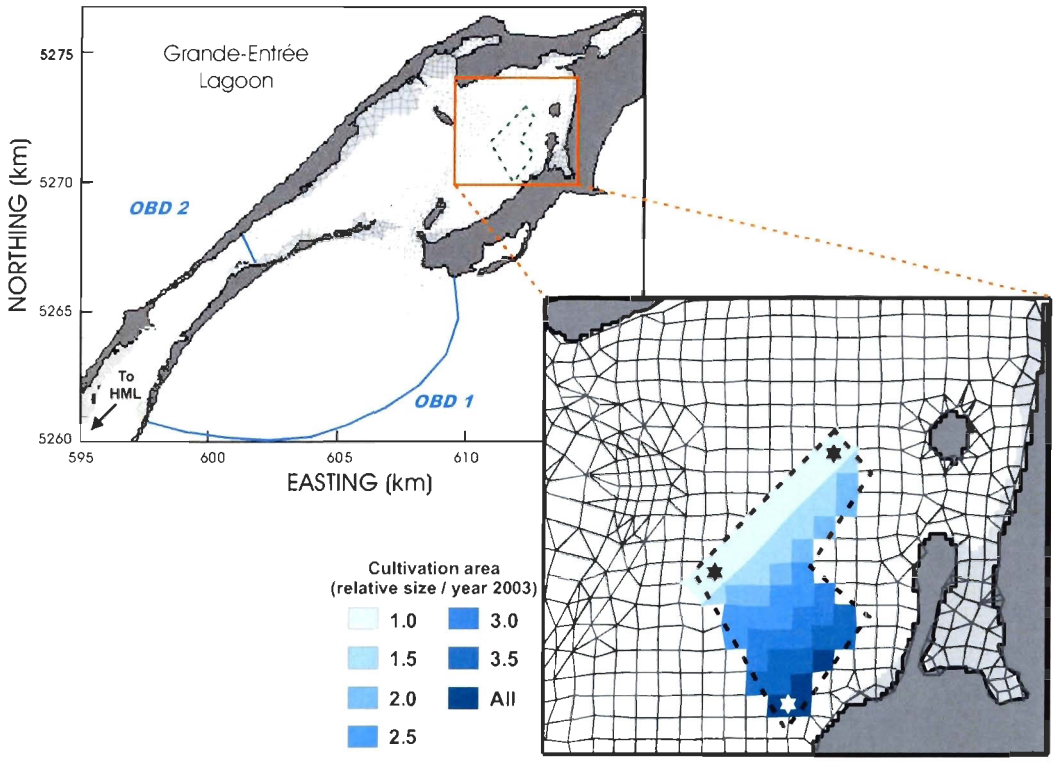

Figure IV-1 Map of Grande-Entrée lagoon (GEL) including the numerical model grid, the location of the mussel farm (dashed polygon in both views) and in the detailed view the 2003 cultivation area (marked with 1.0) and the increasing cultivation areas used in the "area" series of simulations (see Section 4.2.2 for details). The stars show the locations of the experimental long lines used to monitor in situ mussel growth in 2003-2004.

Mussel Dynamic Energy Budget (DEB)

One of the weaknesses of the model identified in the previous study (Guyondet et al., Chap. III) was the simple scope for growth representation of mussel physiology that did not account for all the energetic needs of the bivalves, especially in terms of their reproductive cycle. In order to avoid any bias in the representation of the interactions between the mussels and the surrounding ecosystem due to this simplification, the ecophysiological module was replaced here by a detailed dynamic energy budget based on the DEB theory (Kooijman, 2000). This theory has already been applied to several species of bivalve filter feeders and to *Mytilus edulis* in particular (van Haren and Kooijman, 1993; van der Veer et al., 2006; Maar et al., 2009; Rosland et al., 2009).

The DEB model comprises three state variables: storage, structure and reproduction. The storage (E_S) term represents the energy acquired from food assimilation and stored as reserves. A fixed fraction κ of the energy catabolized from the reserves supports the growth and maintenance of the body structure (E_V). The remainder ($1-\kappa$) is spent on reproduction (E_R), either maturation in juveniles or gametes production in adults and maintenance of the reproductive system. The model equations used here are the same as in Pouvreau et al. (2006) and the parameter set for *Mytilus edulis* is the same as in Rosland et al. (2009) who used most of the parameters evaluated by van der Veer et al. (2006) except for the maximum ingestion rate and κ.

The DEB model is linked to the biogeochemical model through the mussel food ingestion, their consumption of dissolved oxygen and waste production either in dissolved

(excretion of NH4) or particulate form (faeces that constitute the model biodeposit variable BDP). No pseudofaeces production is included in the model as total particulate matter concentrations stayed close to the threshold for pseudofaeces production by *Mytilus edulis* (4.5-5 $mg.L^{-1}$, Widdows et al. 1979) in summer 2003 and no pseudofaeces were observed during in situ biodeposition and sedimentation rate measurements carried out in GEL mussel farm (Callier et al., 2006). Mussel ingestion is limited by food availability following a type II Holling function: $f = X/(K_X+X)$ where X is the food concentration and K_X the half saturation coefficient. Mussels are allowed to feed on all particulate organic sources with a different preference for each type of prey. As in the previous version of the model (Guyondet et al., submitted), mussel preferences are mostky based on the range of particle sizes that mussels can feed on. The preferences and the half saturation coefficient are also given the same values as in the previous model. DEB variables being expressed in energy units, a conversion factor (J_mgC) is used for the mussel food to transform carbon equivalents ($mgC.m^{-3}$) into energy ($J.m^{-3}$). This conversion factor was determined during the calibration of the model using specifically the comparison of observed and predicted faeces production rates. Mussel respiration is considered proportional to the catabolic rate of reserve utilization with a conversion factor of 13.8 $J.mgO_2^{-1}$ (Bayne and Newell, 1983). All dissipative fluxes are converted to NH4 excretion using the energy-carbon and C/N ratios of the food. The same energy-carbon ratio was used to transform total mussel energy in mussel weight ($mgC.ind^{-1}$) that may be compared to observed mussel dry weight transformed to carbon equivalent assuming a 40% carbon content (Grant et al., 1993). Shell

length is also used for calibration. In the DEB model shell length relates to the energy invested in structure (E_V) as follows:

$L = (E_V / [E_G])^{1/3} / \delta$

where L is the shell length (cm), $[E_G]$ is the volume-specific costs for structure ($J.cm^{-3}$) and δ is a shape parameter.

Finally, in the DEB model spawning occurs only if two conditions are met: the water temperature is sufficiently high and enough energy has been fixed in the reproduction buffer E_R, i.e. the gonado-somatic index is above a given threshold. A spawning pattern observed in the Magdalen Islands (Myrand et al., 2000; Gauthier-Clerc et al., 2007) with a first partial event followed by a second one more complete was imposed to the model by emptying only 50% of E_R during the initial spawning and 100% during any potential subsequent one.

Model simulations

The period under study extends over summer 2003 from 27 June to 17 October, covering most of the growing season for mussels in GEL and for which all forcing data are available from a specifically designed field survey (Guyondet et al., Chap. III).

In order to observe the effects of the mussel culture activity, two basic simulations were performed. The comparison of the "standard" simulation including the mussel farm with its 2003 specifications (mussel density = 16.667 $ind.m^{-3}$ over the area shown on Fig. IV-1) and the "no mussel" simulation (everything left identical as the "standard" run except the

mussel farm has been removed) provides the basis for mussel impact investigations. The "standard" run was also used for calibration purposes (section 4.3.1).

A common way in numerical studies to estimate the production carrying capacity of a system is to increase the stock of farmed bivalves and observe the density effects on bivalve growth and total yield. Here the same approach was used but the number of farmed mussels was increased in two complementary ways leading to two series of simulations. First, in the "area" series of simulations the number of mussels was increased by increasing the cultivation area and keeping a constant mussel density equal to the 2003 value. Conversely, in the "density" series the cultivation area was fixed to its 2003 extent and the mussel density was increased such that the total number of mussels matches the number in the corresponding simulation of the "area" series. Hence, both series contain the standard run (relative mussel number = 1 corresponding to the 2003 value) and simulations that can be matched by pairs with the same number of mussels but either a modified cultivation density or area. The maximum increase in mussel number was set by the "area" series where the cultivation area was not allowed to go beyond the maximum farm area (Fig. IV-1). The relative mussel numbers used for each pair of simulations were then 1 ("standard" run), 1.5, 2, 2.5, 3, 3.5 and "All" (the whole mussel farm covered leading to a relative number of 3.8).

The combination of these two series of simulations and the comparison of the "standard" and "no mussel" runs was used to study both aspects of the carrying capacity estimation, the environmental conditions and mussel density effects on mussel growth on

one hand and the effects of the mussel farm on the lagoonal ecosystem on the other, and both at local and system scales.

In the following, time integration over the simulation period always refers to the integration over an exact number of 216 semi-diurnal tidal cycles covering most of the simulation period and used to ensure that there was no net gain or loss of water by the system.

4.3 RESULTS

4.3.1 Model calibration

For variables of the biogeochemical structure no significant difference in model results was introduced by the change in mussel ecophysiological model. These results being presented elsewhere (Guyondet et al., Chap. III) they will not be repeated here.

Concerning the DEB model the calibration process was based on the comparison of observed and predicted mussel meat weight ("standard" run) to account for both somatic growth and weight fluctuations related to the reproductive cycle (gametogenesis and spawning). The calibration concerned the following parameters: the mussel food energy content (J_mgC) and the thresholds for spawning (temperature and gonado-somatic index) as well as the initial values of the three state variables (E_S, E_V, E_R). The best fit (Fig. IV-2c) was obtained for J_mgC = 40 $J.mgC^{-1}$ and spawning thresholds of 10°C and 22% for the gonado-somatic index. The food energy content falls well in the range of values used in previous studies (J_mgC = 25 - 48 $J.mgC^{-1}$; Grangeré et al., 2009; Rosland et al., 2009) and gives a good agreement between observed (0.408–1.226 $mgC.ind^{-1}.d^{-1}$; Callier et al., 2006)

and predicted (0.41–1.82 $mgC.ind^{-1}.d^{-1}$) faeces production rates. The temperature threshold for spawning was actually set to 10°C, a commonly observed value for *Mytilus edulis* (Bayne, 1976; Hummel et al., 1989; Newell et al., 1991). It was not expected to play a significant role in the onset of spawning as mussels are known to start spawning at the end of June in GEL (Myrand et al., 2000; Gauthier-Clerc et al., 2007) when water was already in the 15 - 16°C range in 2003 (Fig. IV-2a). The spawning pattern imposed (first spawning event only partial) coupled with a minimum gonado-somatic index of 22% led to the mussel weight curve shown on Fig. IV-2c. The timing of the two spawning events (late June and early August) corresponds well to the timing already observed in GEL by Myrand et al. (2000). Once the model had been calibrated for mussel weight, the shape parameter δ was tuned to fit the predicted shell length with observations. A good agreement was reached for $\delta = 0.262$ (Fig. IV-2d). However, the model tends to underestimate both the mussel weight and shell length at the end of the simulation period. This probably follows from the underestimation by the model of both the mussel food concentration and water temperature (Fig. IV-2a and b) during the same period. To complete the calibration, the last mussel related processes interacting with the ecosystem were compared to observations. The mussel respiration rate predicted by the model averages 0.43 $mgO_2.ind^{-1}.h^{-1}$ (range 0.11–0.56) over the simulation period, close to the value of 0.52±0.03 $mgO_2.ind^{-1}.h^{-1}$ measured for GEL mussels in summer 2003 (Richard et al., 2006). Finally, mussel NH_4 excretion was only slightly underestimated by the model with predicted values ranging from 0.004 to 0.018 $mgN.ind^{-1}.h^{-1}$ compared to a measured rate of 0.0204±0.0014 $mgN.ind^{-1}.h^{-1}$ (Richard et al., 2006).

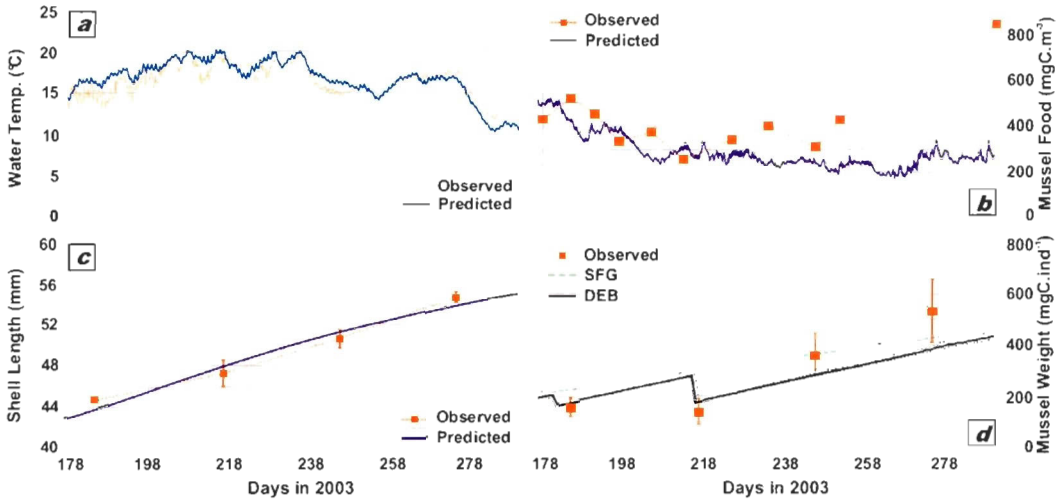

Figure IV-2 Results of the model calibration for mussel weight and shell length along with the two variables most influencing mussel growth: water temperature and mussel food (obtained by the aggregation of the model variables LP, SP, LZ, SZ and D weighted by the mussel preferences for each type of prey).

4.3.2 Production carrying capacity

First, the results of the simulation from the "area" series where the cultivation area extends over the whole farm (simulation "All") were used to map the spatial distribution of mussel growth. Figure IV-3 presents this distribution in terms of relative mussel weight gain over the simulation period. In addition to an approximate doubling of mass over this period, it shows that mussel growth presents a gradient along the east-north-east (ENE) – west-south-west (WSW) direction with a 15% difference between the two boundaries of the mussel farm. Data on the spatial distribution of mussel growth are relatively scarce;

however the mussel growth experiment providing the calibration data was conducted simultaneously in three different locations within the mussel farm, i.e. the southern most, western most and northern most corners of the farm (Fig. IV-1). Results of this experiment show no statistically significant spatial difference in the growth of mussels in terms of meat weight, but a tendency for mussels in the western corner to grow larger than in the southern one and even larger than in the northern one. In terms of shell length, the same tendency was observed but with a significant difference between the western location and the two others (Tita, 2005). The maximum difference in growth was observed between the northern and western corners and reaches up to 10% both in terms of meat dry weight and shell length. The spatial distribution obtained from the model (Fig. IV-3) shows a qualitative agreement with these observations and a slight overestimation of the growth gradient. Moreover, this spatial distribution agrees well with the spatial pattern of water renewal in GEL (Koutitonsky and Tita, 2006). Since the western part of the farm is closer to the lagoon's inlet and to the navigation channel which concentrates the tidal exchange with the GSL (Guyondet and Koutitonsky, 2008), it likely benefits from a better water renewal leading to better food availability for the mussels. Accordingly, the successive increases in cultivation area used in the "area" series of simulations were spread along the NE-SW direction (Fig. IV-1), i.e. approximately across the mussel growth gradient, in order to minimize the effects of this spatial distribution when averaging model results over the cultivation area.

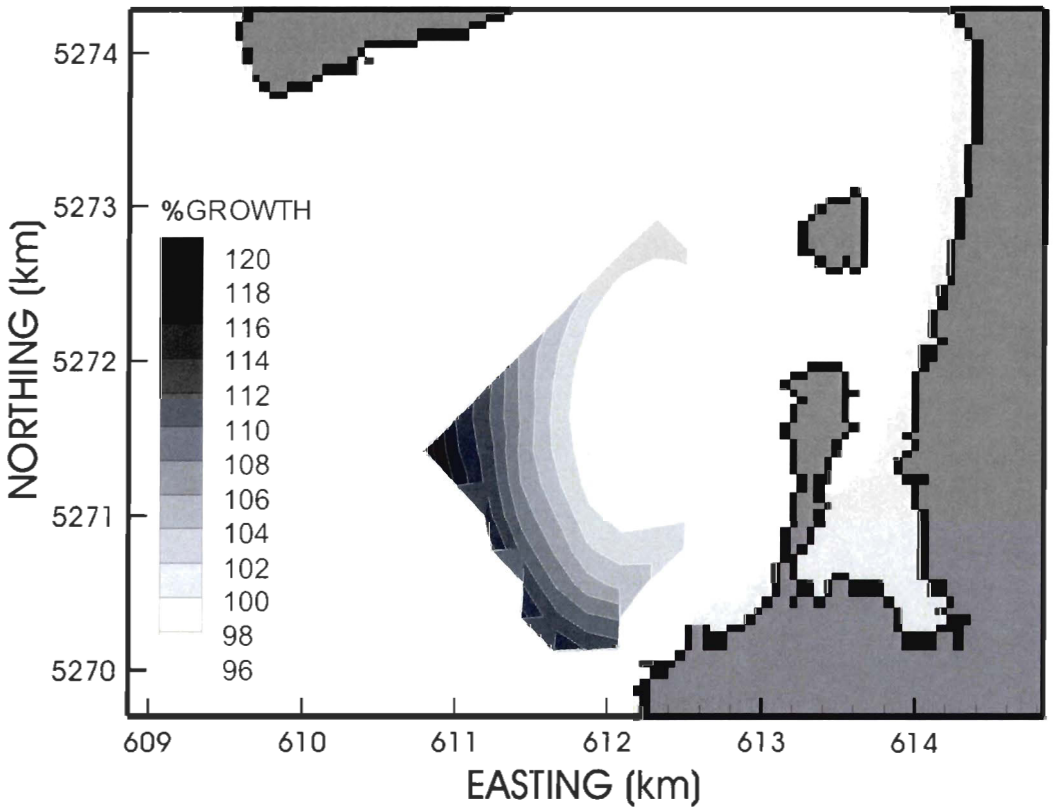

Figure IV-3 Map of the spatial distribution of mussel growth predicted by the model over the farm area and expressed as the relative mussel weight increase during the simulation period.

The production carrying capacity concerns arise from the ability of bivalves to filter large volumes of water leading to the food limitation of their growth. This food limitation may exist at both the local and system scales, locally if the filtration rate of the bivalves is strong compared to the food renewal by advection and mixing and at the scale of the system if the filtration capacity of the bivalve population is strong compared to food renewal through exchange with the outside and internal production (Heip et al., 1995). The "area" and "density" simulation series were designed to respectively minimize/maximize the local food limitation and maximize/minimize the system scale limitation. The comparison of mussel growth (relative mussel weight at the end of the simulation period, the reference being the mussel weight at the end of the "standard" run) from these two series is shown on Fig. IV-4. At low mussel stocks (relative mussel number < 2), increasing the cultivation area or the density has a similar effect on mussel growth. This indicates that at the local scale the food renewal (advection and mixing) is relatively intense as increasing the density does not affect the growth more strongly. Moreover at the scale of the system, the food renewal (exchange and internal production) must be slow as increasing the number of mussels without increasing their density also depresses their growth with the same magnitude. On the other hand, for higher mussel stocks, their growth starts to be more impaired in the case of an increasing density. At these higher densities the food demand by the mussels strongly exceeds the supply leading to a serious local depletion. In the case of an increasing cultivation area, the mussel growth continues to decrease at higher stocks as the bivalves more strongly deplete the resources of the whole system. However, this last result may be biased by the configuration of the mussel farm (new mussels added to the

East) in relation to the spatial repartition of mussel growth mentioned above (Fig. IV-3). When averaging over an increasing area, new mussels are placed in conditions intrinsically different introducing a difference in the averaged growth rate that may interfere with the effect of the increasing stock. In order to avoid this interference, results of the "area" series of simulations were also averaged on a fixed area corresponding to the 2003 cultivation area as for the "density" series. The relation with increasing stock obtained (curve "Area 2003" on Fig. IV-4) confirms the previous conclusion that adding new mussels in the remainder of the farm affects the growth of mussels in the initial cultivation area.

These results indicate that both the slow currents in the farm area and the slow water renewal at the lagoon scale affect the cultured mussels. A slightly less than four fold increase in mussel stock would lead at least to a 6-9% decrease in mussel growth depending on the expansion mode chosen (area or density). Moreover, if a further development of the culture activity is planned that would more than double the mussel stock, increasing the cultivation area rather than the culture density would be more beneficial from a production perspective.

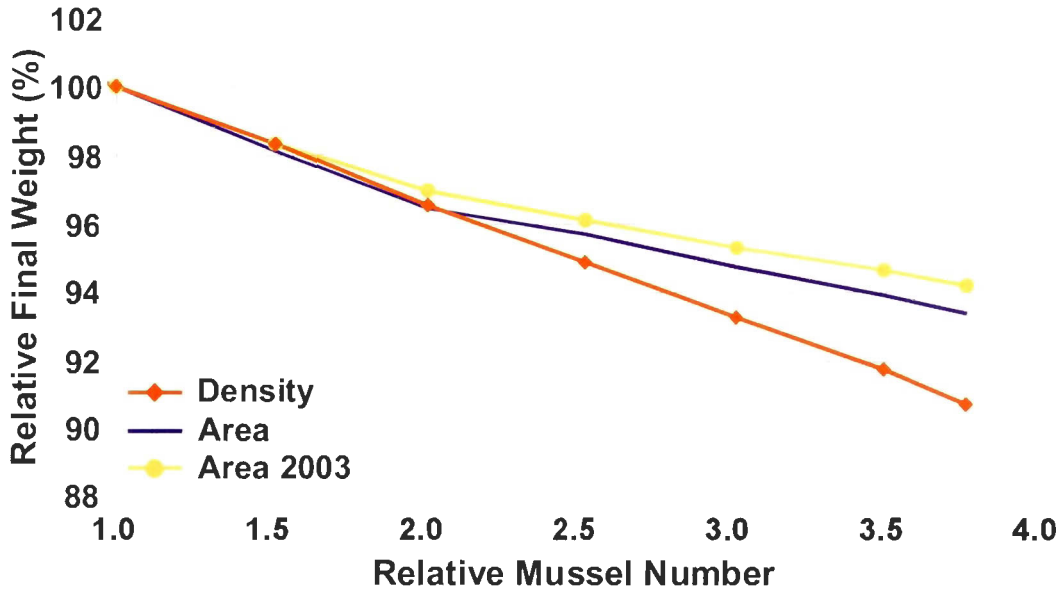

Figure IV-4 Comparison of the average response of mussel growth to increasing stocks in the case of increased cultivation density or area. The "Area 2003" curve derived from the integration of model results over the fixed 2003 cultivation area (as in the "density" series) to avoid any bias caused by the increasing integration area used in the "area" series.

4.3.3 Ecological carrying capacity

Here, the comparison of the results of the "no mussel" and "standard" simulations will be used to study in detail the effects of the cultured mussels on the N cycle both at the local scale inside the cultivation area and at the scale of the whole lagoon.

Local scale

The results of the "no mussel" and "standard" simulations, both N pools and fluxes, were integrated over a single grid element located in the centre of the 2003 cultivation area and over the simulation period. The comparison of this integration with and without cultured mussels is presented on Fig. IV-5a. Each numeric value refers to the percentage of change of the corresponding flux when the mussel farm is introduced in the system; for the living variables this value represents the percentage change in their production. Not surprisingly, all mussel living preys, except SP, are negatively affected by the introduction of this new grazer. The positive impact on SP has several explanations, a) the mussels only marginally feed on the small particles constituting SP, b) the top-down pressure of mussels on LZ and SZ reduces the grazing pressure on SP, c) competition with LP is reduced by the preferential grazing of mussels on LP and d) the SP production rate is increased thanks to the net increase in NH4 availability (its preferred substrate) due to mussel excretion and despite the reduced SZ excretion. For most of the water column processes the magnitude of the alteration related to the cultured mussel introduction is limited to around 10-20% (reaching 30-50% for the maximum mussel stock tested in this study, not shown).

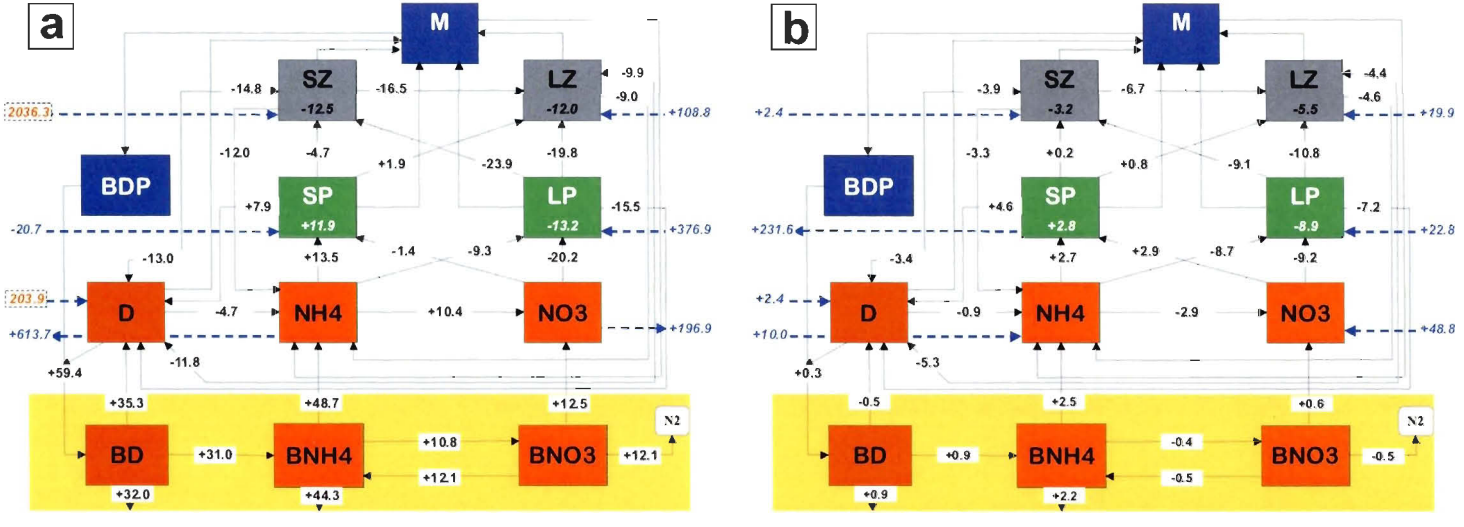

Figure IV-5 Modifications of the nitrogen (N) cycle predicted by the model when introducing the mussel culture activity in GEL (comparison of the "no mussel" and "standard" simulations), a) at the local scale (single grid element inside the cultivation area) and b) at the scale of the entire lagoon. Numerical values represent the percentage change averaged over the simulation period of each N flux (production rate for the living variables) between the two situations. Dashed arrows represent external exchange flows (import/export); if their value is shown in red in a dashed box it indicates that the corresponding exchange flow changed direction in the presence of mussels.

A 10-20% modification is close to the limit of model precision. However, these results give a qualitative overview of the alteration pattern introduced by mussel culture.

Water-sediment exchange is more strongly affected by the presence of the farm confirming that even if grown in suspension in the water column bivalve filter feeders enhance the pelagic-benthic coupling. This is mainly caused by the increase in organic matter sedimentation due to mussel biodeposition. The excess organic matter causes an increase in remineralization mainly by anaerobic processes (revealed by an SOD increase, not shown) which leads to a stronger efflux of inorganic nutrients (NH4 and NO3) to the water column. This also contributes to a stronger loss of N through BD and BNH4 burial and N2 gas production by denitrification processes.

Even stronger modifications are recorded for import/export fluxes of water column variables. Inorganic nutrients the only variables exported from this grid element are more strongly exported in the presence of mussels, following the increase in their availability in the water column through the mechanisms just mentioned. SP import is slightly reduced as its production is enhanced by the introduction of the cultured mussels while LP and LZ imports increase due to mussel consumption. Finally, SZ and D exchange fluxes are reversed; being exported in the absence of mussels they become imported when the farm is introduced. SZ exchange presents the strongest relative modification. These alterations do not represent major changes as the absolute values of these exchange fluxes are generally one order of magnitude weaker than other water column processes. However, they indicate that the mussel culture activity may involve system resources beyond its physical extent.

System scale

The question of the ecological carrying capacity is raised because, when introducing a large number of bivalves in a coastal system, the local effects just mentioned may induce consequences at the scale of the entire system. Understanding this translation of local effects to the scale of the system represents the main difficulty of the carrying capacity estimation as it follows from the interactions of hydrodynamics, biogeochemical processes and bivalve activity. The present coupled numerical model with its fine spatial resolution allows a direct observation of the distribution of the mussel farm effects over the lagoon. Representing the relative variation of the time average concentration of each variable at each node of the model grid between the "no mussel" and "standard" simulations provides 2D maps of depletion/accretion (Fig. IV-6). First, these maps show that the mussel effects are strongest directly over the cultivation area for all variables except NO3. Due to the calm hydrodynamic conditions prevailing in this area, these effects are mostly not exported elsewhere. However a slight spreading to the East and North-East can be observed. For all variables virtually no difference is observed west of the navigation channel. This spatial configuration may be explained by the particular hydrodynamics of the area which is covered by a clockwise tide-induced residual eddy that leads to the isolation of the eastern basin (Guyondet and Koutitonsky, 2008). This residual circulation combined with local mixing processes (most likely wind induced) are responsible for the confinement to the east of the navigation channel and the dispersion over the eastern basin of the mussel farm effects.

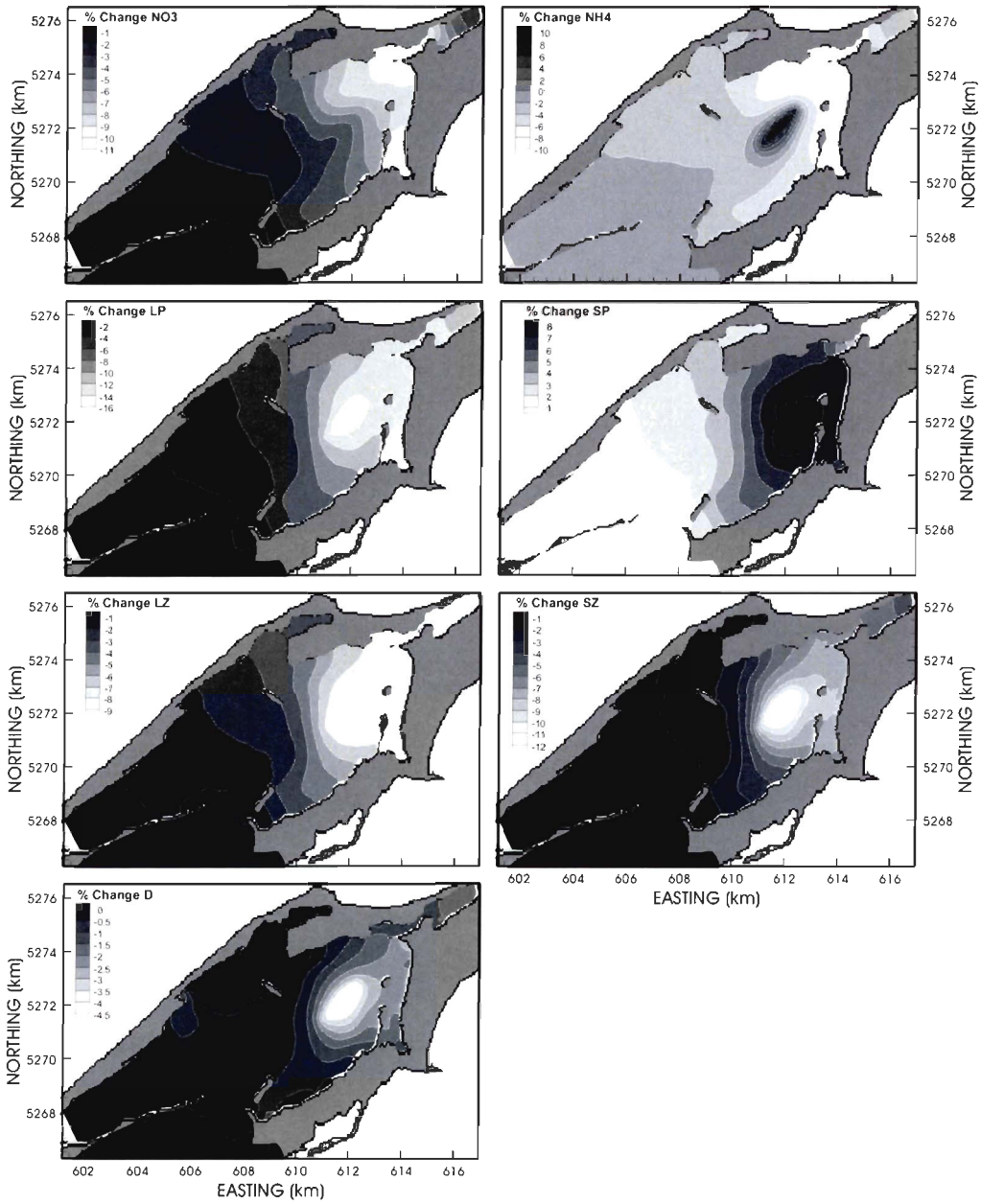

Figure IV-6 Map of the spatial distribution of depletion/excess predicted by the model when introducing the mussel culture activity in GEL (comparison of the "no mussel" and "standard" simulations) and expressed as the percentage change of each pelagic variable concentration averaged over the simulation period.

NO3 is not directly affected by any mussel process therefore it presents a different response to the presence of the mussel farm resulting from the combination of several indirect effects. Water column NO3 only presents one internal source, NH4 nitrification, and two sinks, uptakes by LP and SP. Inside the mussel cultivation area, mussel excretion provides an excess in NH4 leading to an increase in nitrification (Fig. IV-5a). This NH4 excess also induces an increase in the NH4/NO3 ratio. SP growing preferentially on NH4, its uptake of NH4 increases while NO3 uptake decreases (Fig. IV-5a). Part of the SP produced in excess in the cultivation area is exported in areas where the NH4/NO3 ratio is not affected by mussel excretion. Hence, outside the cultivation area the excess SP exported increases the demand of both NH4 and NO3 leading to the depletions observed on Fig. IV-6. These depletions may also result from the reduction of SZ biomass by mussel grazing that extends beyond the cultivation area and is followed by a decrease in SZ excretion of NH4 that would ultimately lead to a deficit in NO3 input by nitrification.

To conclude on the net effects of the mussel farm, the integration procedure reported in the previous section was repeated but over the entire lagoon instead of over a single grid element (Fig. IV-5b). Following Network Analysis procedures (Ulanowicz, 1986), the total internal throughflow of the system may be calculated as the sum of all N fluxes excluding imports/exports from/to the outside; this only amounts to around 7% of the total throughflow. Dividing this internal throughflow by the average total N stock in the system over the integration period provides an indication of N recycling within the lagoon. The introduction of the mussel farm tends to slow this recycling down by both increasing the N stock and slightly decreasing the internal throughflow. This overall decrease in recycling

originates mainly from the water column where the 70 cycles needed for the N stock to accommodate the internal throughflow are reduced to 60 cycles in the presence of the mussel farm while recycling in the sediment stays fairly unchanged. A particular attention must be paid to the inorganic nutrients that fuel the ecosystem production. Summing all internal inputs on one hand and all internal outputs on the other, for both NH4 and NO3 (Fig. IV-5b) reveals that the presence of the mussel farm speeds the dynamics of NH4 up (inputs: +1.4%, outputs: +0.8%) and slows the dynamics of NO3 down (inputs: -2.8%, outputs: -1.1%). Moreover, the relative difference between inputs and outputs reveals that the NH4 and NO3 availability are respectively increased and decreased at the scale of the lagoon. The increased NH4 availability being readily used up by SP, it does not translate into any change in the exchange fluxes or the overall NH4 stock, the imports of NH4 being even increased (Fig. IV-5b) and NH4 stock slightly reduced overall. Conversely, the decreased NO3 availability leads to a reduced NO3 stock and an increased import from the outside. Unlike other coastal systems where eutrophication is a concern, in GEL oligotrophic conditions prevail especially during summer (Trottet et al., 2007) and any reduction in inorganic nutrient availability has to be considered while estimating the ecological carrying capacity for mussel culture.

In this context the total nitrogen stock present in the system is also a critical factor considering that the mussel harvest removes an important fraction of this stock from the lagoon. Figure IV-7 was obtained by calculating the average over the simulation period of the N stock in the different compartments of the ecosystem (pelagic, benthic and total) for the increasing mussel stocks of the "density" series. The main result is that while the

mussels represent an increasing fraction of the total N stock, the N stock excluding the mussels (TotalN-M, Fig. IV-7) stays fairly constant when the mussel stock is increased. Moreover this constant stock results from the combination of a slightly decreasing pelagic stock (TotalNwc-M) and a comparably increasing benthic stock (TotalNbed). The net effect of the mussel farm then consists in redirecting a small fraction of the pelagic N stock to the benthic environment.

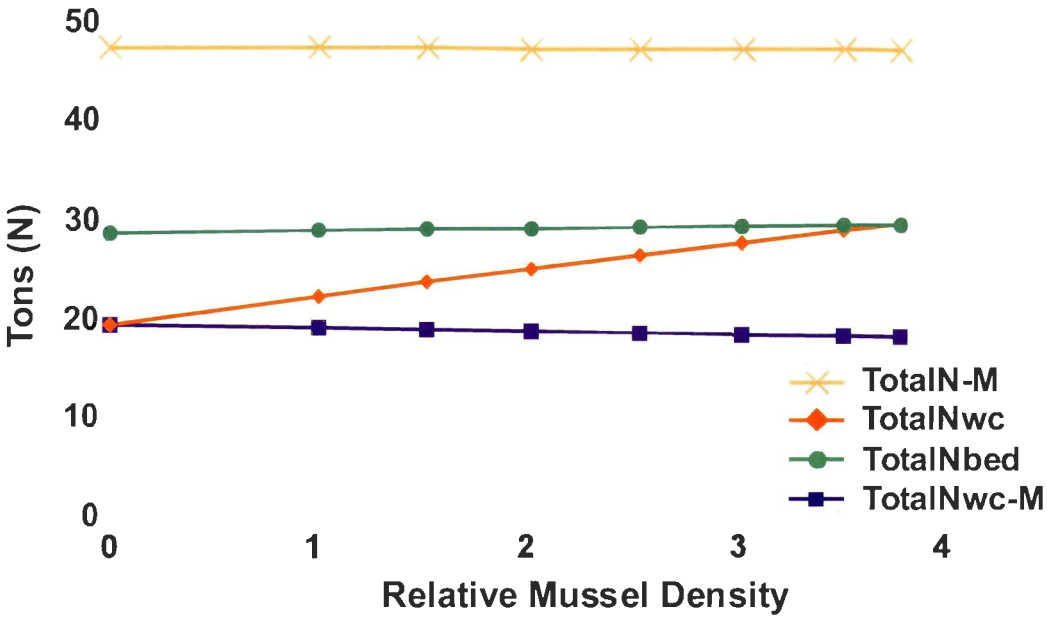

Figure IV-7 Model predicted evolution of the nitrogen inventory in the whole system (pelagic+benthic) excluding mussels ("TotalN-M"), in the water column only ("TotalNwc"), in the sediment only ("TotalNbed") and in the water column excluding mussels ("TotalNwc-M") for an increasing density of cultured mussels.

4.4 DISCUSSION

4.4.1 Production carrying capacity

Traditionally the production carrying capacity has been addressed with farm scale models using a fine spatial resolution to study the consequences on bivalve growth of cumulative food depletion as water flows through a farm or for site selection between different locations within the same system (Incze et al., 1981; Bacher et al., 2003; Ferreira et al., 2007). The main advantage of the present model is to directly include the feedbacks of the cultured bivalves on their growing environment while a farm scale model uses fixed boundary conditions that can not reflect the changes in environmental conditions caused by an increased bivalve stock.

Compared to ecosystem box models also commonly used in such studies to avoid the above mentioned approximation (Dowd, 1997; Grant et al., 2007; Ferreira et al., 2008), the fine scale of the present model allows a better representation of the hydrodynamics of the system and the inclusion of local food depletion, a potentially dominant factor in areas of calm hydrodynamic conditions such as GEL eastern basin. The ecosystem box model developed for GEL by Grant et al. (2007) for the same 2003 conditions predicted a mussel growth reduction of 11% and a phytoplankton depletion of 15% in response to a doubling in mussel stock from present levels. The present model predicts a mussel food depletion of only 8.4% over the cultivation area and 2.6% over GEL (when aggregating results of Fig. IV-6 for all mussel food variables) and an average reduction in mussel growth of 3.5% for the same doubling in stock. This is a priori in contradiction with the ability of the fine scale

model to account for local acute depletion. Several explanations for this contradiction may be found. First, considering non-phytoplankton organic seston, the second source of food for mussel that was virtually not affected by the increased mussel stock in the box model, would lead to a reduced depletion estimate for total mussel food with the box model. On the other hand, considering only LP, the preferred mussel prey in the fine scale model leads to a LP depletion of 15.2% over the cultivation area and 6.7% over GEL (by averaging results of Fig. IV-6 over the corresponding areas). This damps at least partly the contradiction between the two models. Another explanation resides directly in the different spatial resolution used by the two models. Although the box model distributes the mussel stock over a larger area, which should result in more diffuse food depletion, it also employs a water exchange rate averaged for the entire box. Yet, the 2003 cultivation area was located in the western most part of the mussel farm corresponding to the area of the mussel box (Box 3, Fig.1 in Grant et al., 2007) with the strongest water exchange rate leading to a not so strong depletion as revealed by the spatially detailed model. This shows the shortcomings introduced by box models but in the opposite direction compared to the commonly reported underestimation of bivalve food depletion and highlights the importance of the fine scale representation in accounting for the interactions between bivalve food limitation and local hydrodynamic conditions.

Along with the models developed by Duarte et al. (2003), Spillman et al. (2008) and Marinov et al. (2008), the present work is one of the rare attempts to include both local and system scale processes in the determination of the production carrying capacity of a coastal system for bivalve culture. The model succeeded in reproducing the mussel individual

growth as well as the spatial distribution of this growth inside the cultivation area. It allows the investigation of development scenari involving culture density and/or area manipulations not covered by either of the types of models previously used. The same model could also easily be employed for site selection purposes by simply indicating the new location of the farm in the model grid.

In the particular case of GEL, no major reduction in mussel growth was predicted for up to a 4 fold increase in cultivated stock. This represents a contrasting result with other systems such as Carlingford Lough or Marennes-Oléron Bay where a four fold increase in stock was expected to reduce oyster growth by a factor of 2 and 4, respectively (Bacher et al., 1998). However, as the mussels in GEL only reach the minimum size for harvest (55 mm) at the end of the simulation period in the present conditions, any increase in stock would delay the starting date of the harvesting period. This delay may be longer than the only slightly reduced growth suggests as mussel growth rate decreases rapidly with the onset of winter conditions. Further simulations extending beyond mid-October would then be necessary to give a more definitive estimate of the production capacity.

4.4.2 Ecological carrying capacity

Results of both the production and ecological carrying capacity sections show that even for the present stock, mussels exploit resources beyond the limits of the cultivation area, potentially affecting the whole ecosystem dynamics. However, the magnitude of these effects is limited to a 0 – 10% change compared to the "no mussel" case at the scale of the lagoon. It was also shown that despite a slight decrease in NH4 and NO3 concentrations,

the total N stock excluding mussels is not affected by an increase in mussel biomass. This last result agrees with previous studies concluding that mussel culture tends to enhance the retention of N in coastal systems (Cranford et al., 2007; Brigolin et al., 2009). Here, the nitrogen incorporated in mussel biomass is balanced by an increase in imports from outside GEL (Fig. IV-5b). Model results in this respect are reliable as long as the effects of the mussel culture activity on state variables do not reach the model open boundaries; otherwise the boundary conditions would not be appropriate anymore. For the present study such a situation did not occur as can be seen from the depletion maps obtained for the "standard" run (Fig. IV-6) and for the up to 4 fold increase in mussel biomass imposed (not shown). These increased imports reveal that the system increasingly depends on external resources which combined with the lesser stability following the reduced N recycling, accounts for an increased vulnerability of GEL's ecosystem. This conclusion for GEL is in contradiction with the stabilizing effect of bivalve populations reported for coastal systems with eutrophication concerns (Officer et al., 1982; Herman and Scholten, 1990). The increase in top-down control on phytoplankton usually introduced by the bivalves in such systems does not occur in GEL. In this lagoon the pelagic system is dominated by the microbial food web (Trottet et al., 2007), SP and SZ in the model, and as mussels cannot efficiently retain the small SP particles, they mainly feed on SZ, actually decreasing the overall top-down control on phytoplankton.

While the loss of N incorporated in mussel biomass is mitigated by imports, the culture activity also alters the distribution of the total N stock among the different components of the ecosystem. First, part of the pelagic stock is redirected to the sediment,

another process favouring the retention of N within the lagoonal system. Although the modifications of the benthic compartment dynamics due to biodeposition are significant inside the cultivation area (Fig. IV-5a), they do not translate into any major changes at the scale of GEL (Fig. IV-5b). This results from the limited area covered by the culture activity (1.2% of the lagoon area in 2003) and the weak dispersion of biodeposits due to the slow currents in GEL's eastern basin and the high settling velocity of these particles (Callier et al., 2006; Weise et al., 2009). The distribution of the N stock among pelagic variables is also slightly modified by the mussels. The most affected components are SP and SZ with an increase of 2% and decrease of 1.6% of their respective fraction of the total pelagic N stock (excluding mussel biomass) between the "no mussel" situation and the maximum mussel stock imposed in this study. Despite their apparent low magnitude, these modifications show the capacity of the mussels to alter the structure of the pelagic ecosystem. The phytoplankton composition would be particularly affected by such a mussel biomass increase as the abundance ratio SP/LP would increase from 5.2 in the 2003 conditions to 6.6 for an almost four fold increase in mussel stock. These alterations are induced at the local scale by the mussel excretion and grazing and have repercussions at the scale of the lagoon. Conversely, the local effects on NH4 and NO3 have virtually no net consequences on NH4 and NO3 shares in the water column N stock at the system scale. The enhanced primary production in the mussel cultivation area observed in GEL (Trottet et al., 2008a) and reproduced by the model (Guyondet et al., Chap. III) may be cited as a mitigation effect to the phytoplankton depletion caused by cultured bivalve grazing (Prins et al., 1998). However, it was shown here that a transfer of productivity from the

herbivorous food web (LP, LZ in the model) to the microbial food web (SP, SZ) goes along with this net mitigating effect. These last results show the importance of covering both scales and using a sufficiently detailed biogeochemical structure to obtain a complete description of the ecological implications of the shellfish farming activity.

The carrying capacity for bivalve culture is subjective by definition as it refers to the maximum level of stock not affecting the ecosystem functions in an unacceptable way (Inglis et al., 2000; Duarte et al., 2003). In a management perspective the results of detailed physical-biogeochemical models have to be compiled into meaningful indicators on which to base objective criteria. In the context of man manipulated ecosystems one has to accept relatively strong alterations over a restricted part of the system and make sure that these effects have a limited magnitude at larger scales. Based on this concept and the limit of acceptable change set to a maximum of 20% change over 10% of the system area by Zeldis et al. (2006), Gibbs (2007) defined a Depletion Footprint Curve that relates the magnitude of the effects of bivalve culture and their extent within the receiving system. Such a curve draws the limit of acceptable change at the different spatial scales and may be used as an objective criterion in combination with the present model results to get a clearer insight of GEL's carrying capacity for mussel culture. Figure IV-8 presents some of the depletion curves obtained for pelagic variables by comparing the "no mussel" simulation with each of the "density" simulations. First note that for the variable SP, Fig. IV-8 presents excess curves as the introduction of the mussel farm positively influences the small phytoplankton. For NH4, only the depletion curves are presented but excess curves can be drawn for each simulation, corresponding to the portion of the lagoon in the vicinity of the cultivation area

where NH4 concentrations are increased by mussel excretion (Fig. IV-6). However, while this excess reaches a slightly larger magnitude, it is restricted to a far smaller area (<4.5% of the lagoon) than the depletion that occurs elsewhere. All mussel preys present a similar pattern departing from the idealized curve in the range of 5 - 30% of affected area. After an initial decrease at the local scale (0 – 5%), the depletion (excess for SP) magnitude reaches a plateau showing that the same level of depletion (excess) spreads over an increasing fraction of the lagoon area. This corresponds to the situation of the eastern basin (covering approximately 35% of the lagoon area) mentioned in section 3.3.2, where the water renewal is slow and the water mass is homogenized by mixing processes. In the present conditions ("standard" run) all variables stay in the acceptable range with LP curve lying right on the edge. But as soon as the mussel stock is increased, the above mentioned plateau leads the curves for most of the pelagic variables to go across the acceptable limit marked by Gibbs curve. Despite the small extent of the cultivation area (1.2% of the lagoon area in 2003), the carrying capacity of GEL seems limited to 1.5 to 2 times the present level of stock, except for LP more sensitive to the presence of mussels and D less affected than all other pelagic variables. However, these results probably account for the strongest alterations by the mussels as simulations only cover the summer season and beginning of fall when the influence is more likely to be strongest due to close to maximum physiological rates allowed by high water temperatures. Spread over the course of one year, i.e. the minimum growing period in GEL (November to the following October), the effects of the cultured mussels would probably appear attenuated and the carrying capacity of GEL would be slightly increased.

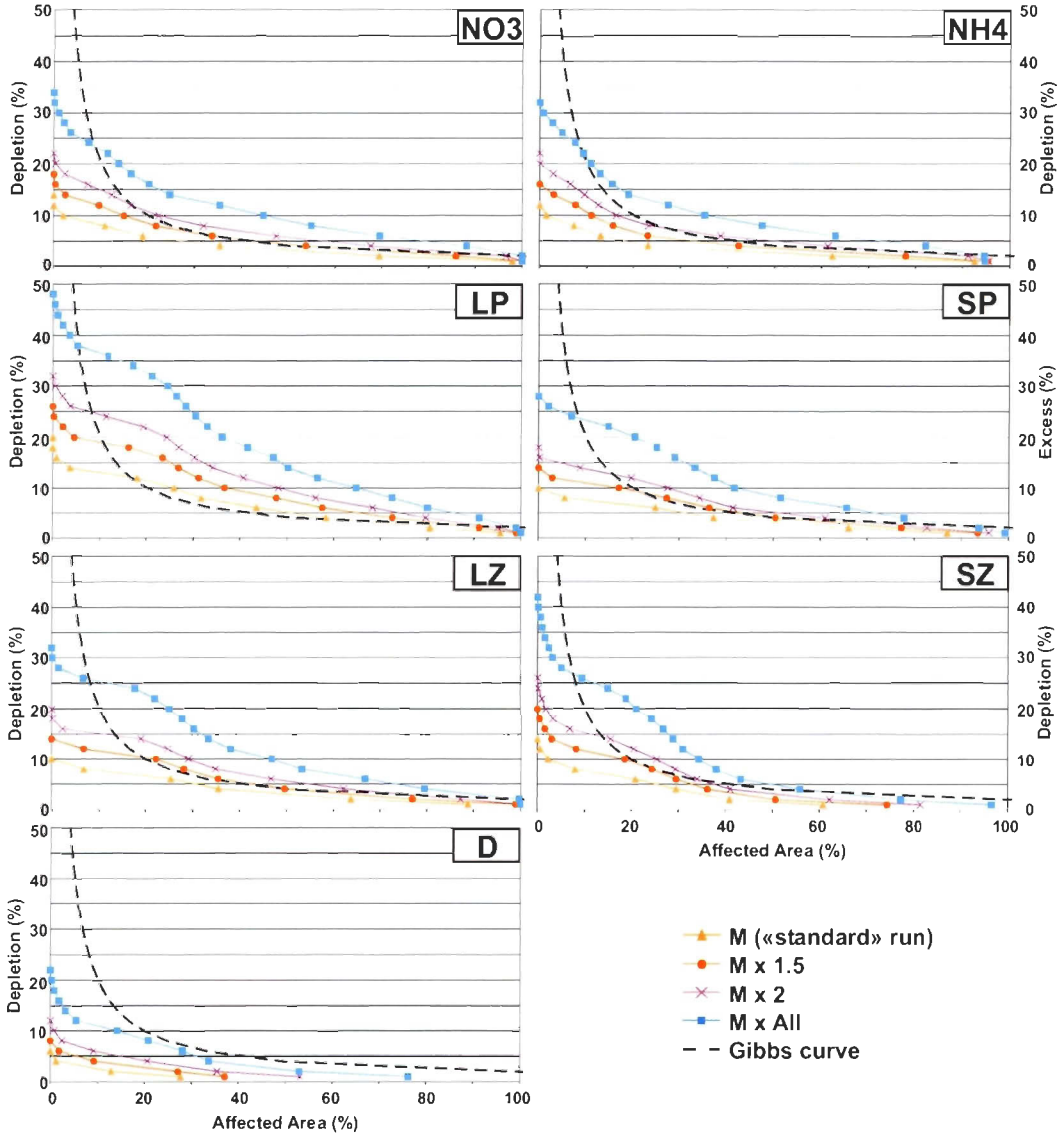

Figure IV-8 Depletion/Excess curves showing the relation between the magnitude of the mussel culture effects on pelagic variables and their spatial extent. As computed from the model results for the "standard" run (M) and for a 1.5, 2 and 3.8 fold increase in mussel stock (Mx1.5, Mx2 and MxAll). The theoretical curve defined by Gibbs (2007) as the limit between acceptable and unacceptable effects is also shown for comparison.

4.5 CONCLUSION

The present modelling study confirms the importance of considering both the local and system scales in the assessment of the carrying capacity for bivalve culture. This enables a better account of the effects of local food depletion and interactions of ecological processes with local hydrodynamic conditions on overall nitrogen cycling and stock alterations. From these results, GEL appears far from its maximum production capacity but considering the ecological impacts and a particular hydrodynamic context, it seems closer to its absolute carrying capacity for mussel culture.

Ecosystem modelling is bound to uncertainties related to the mathematical transcription of ecological processes (Jiang and Gibbs, 2005). Despite the good predictive ability expected from the sensitivity analysis (Guyondet et al., Chap. III), the model presented in this paper is no exception. The results reported here have to be used with caution as they reflect our present knowledge of the interactions between cultured bivalves and marine ecosystems. Nonetheless, numerical modelling stays the most appropriate tool to further our understanding of these processes as long as the validity of model results against observations is checked for the most diverse range of variables and processes, as attempted in the present study. Keeping in mind that the carrying capacity itself may change following modifications in biotic and abiotic conditions or as new interactions between aquaculture and the receiving ecosystem are revealed (Gibbs, 2009); the sustainable management of such systems does not ensue from a single decision at one point in time but from an ongoing assessment-reassessment process along which the modelling tools must evolve.

CHAPITRE 5

CONCLUSION GÉNÉRALE ET PERSPECTIVES

Dans le contexte de la surexploitation des stocks sauvages, l'aquaculture apparaît comme une alternative évidente pour subvenir aux besoins nutritionnels des populations humaines. La culture de bivalves filtreurs, qui nécessite généralement des investissements réduits, est amenée à poursuivre le fort développement qu'elle a connu dans les dernières décennies.

Ce type d'aquaculture se pratiquant principalement en zone côtière, son développement se heurte déjà, dans plusieurs régions, au manque d'espace, à d'autres activités humaines (pêche, tourisme...) et à la limitation des ressources naturelles dont elle dépend. La gestion et le développement durables de ces régions et l'importance croissante des apports nutritionnels de l'aquaculture nécessitent d'assurer la pérennité de l'ensemble des activités humaines ainsi que celle des services écologiques rendus par ces régions à l'interface entre les milieux terrestres et océaniques.

Pour ce faire, des outils permettant de mieux comprendre le fonctionnement des systèmes côtiers et leurs interactions avec les activités aquacoles ont été développés dans les trente dernières années. La diversité des interactions entre les bivalves filtreurs et leur environnement ainsi que la nécessité de prendre en compte des aspects hydrodynamique, biogéochimique et écophysiologique a conduit à l'utilisation de modèles numériques de plus en plus sophistiqués pour réaliser ces études. Toutefois, rares sont celles qui ont fait

intervenir de manière détaillée chacun de ces trois aspects et considéré simultanément les différentes échelles spatiales mises en jeu dans ces problèmes.

L'objectif principal de la présente thèse était donc de développer un outil numérique répondant à ces critères et de l'appliquer à l'étude de la capacité de support de la lagune de Grande-Entrée pour la mytiliculture. Les réalisations et principaux résultats obtenus seront récapitulés dans les prochaines sections avant de conclure sur les perspectives pour de futurs avancements dans ce champ de recherche.

5.1 VOLET HYDRODYNAMIQUE

Le développement de la partie hydrodynamique du modèle et l'analyse des données ont permis de préciser le fonctionnement du système lagunaire couplé Havre-aux-Maisons, Grande-Entrée (HML-GEL).

Concernant la circulation tidale, les embouchures des deux lagunes constituent les zones les plus dynamiques avec des courants atteignant 0.8 $m.s^{-1}$ et des flux tidaux maximum de 2500 $m^3.s^{-1}$ et 500 $m^3.s^{-1}$ à l'entrée de GEL et HML respectivement. Les bassins profonds situés dans la partie est de chacune des deux lagunes présentent des conditions beaucoup plus calmes avec des courants de marée de l'ordre de 0.05 $m.s^{-1}$. Les embouchures offrent par contre une résistance à la propagation de l'onde de marée différente d'une lagune à l'autre. La HML peut ainsi être qualifiée de «restreinte» car la marée est fortement atténuée et retardée à son embouchure contrairement à celle de la GEL

où une plus grande proportion de l'énergie tidale pénètre à l'intérieur de la lagune. Cette caractéristique morphologique crée un déséquilibre entre les conditions tidales des deux lagunes avec une marée en avance et de plus grande amplitude dans la GEL. Une autre disparité entre les deux embouchures concerne l'asymétrie tidale. Pour HML, on observe des courants de marée symétriques (même magnitude au flot et au jusant) alors que GEL présente une asymétrie favorisant les courants de jusant. Contrairement à d'autres systèmes dominés par les composantes semi-diurnes de la marée, où cette asymétrie résulte de la formation d'ondes secondaires (en particulier M4) par des processus non-linéaires, comme la friction; la dominance du jusant observée à l'embouchure de GEL découle de l'interaction directe de la composante semi-diurne M2 avec les composantes diurnes O1 et K1 qui sont ici d'amplitude comparable à M2.

Plus intéressante du point de vue du transport des matières dissoutes et en suspension, la circulation résiduelle, induite par le forçage tidal et les caractéristiques morphologiques du système, a également été décrite à l'aide du modèle. En dehors des embouchures qui présentent les plus forts courants résiduels (7 $cm.s^{-1}$ et 10 $cm.s^{-1}$ pour HML et GEL respectivement), la circulation résiduelle des deux lagunes ne présente aucune similitude. Aucun patron de circulation n'est observable dans la HML et les courants résiduels y sont très faibles (1 $cm.s^{-1}$ ou moins) en dehors de l'embouchure. La circulation résiduelle de la GEL est plus caractéristique des systèmes côtiers avec le développement d'un quadrupôle de tourbillons résiduels. Néanmoins, la morphologie particulière de l'embouchure de cette lagune avec le chenal de navigation et la présence d'un haut fond sableux à l'ouest et d'une île à l'est a pour effet de repousser le dipôle interne plus loin à l'intérieur de la lagune que

ce qui est généralement observé dans le cas de l'interaction des courants de marée avec les deux caps formant une embouchure. Le tourbillon résiduel à l'est du chenal couvre donc la majeure partie du bassin profond où se situe l'élevage mytilicole, limitant les échanges entre cette région et le reste de la lagune. D'autre part, l'un des tourbillons extérieurs n'est pas visible, soit parce qu'il n'existe pas du fait de la position excentrée du chenal de navigation, soit parce que sa présence est masquée par la proximité de la frontière ouverte du modèle. Enfin, l'opposition entre le déséquilibre tidal (mentionné au paragraphe précédent et induit par la nature «restreinte» et «coulante» des deux embouchures) et l'asymétrie interne du système (région longue et étroite à l'ouest de GEL s'opposant au bassin court et large à l'est de HML) se traduit par un flux résiduel d'environ 2 $m^3.s^{-1}$ dirigé de HML vers GEL, un mécanisme non négligeable pour le renouvellement des eaux de cette région éloignée des deux embouchures.

5.2 VOLET ÉCOSYSTÈME

Cette partie de l'étude a tout d'abord nécessité le développement du modèle numérique RMA-11, destiné initialement à des études de qualité des eaux, pour lui permettre de reproduire les grandes caractéristiques de l'écosystème de la GEL révélées par l'analyse des données de terrain (Chapitre 1, Site d'étude et Chapitre 3). Ainsi le phytoplancton a dû être réparti sur deux classes de taille et le zooplancton, initialement non reproduit, a également été inclus au moyen de deux variables, microzooplancton et mésozooplancton, pour tenir compte de la dominance des petites cellules et des

hétérotrophes observée au sein de l'écosystème pélagique. D'autre part l'importance des échanges benthos-pélagos en zone côtière peu profonde a forcé l'introduction d'un module benthique dans la structure biogéochimique du modèle. Ce module se contente de reproduire les mécanismes aérobies de minéralisation de la matière organique déposée sur le sédiment et les processus de nitrification-dénitrification pour compléter la chaîne de transformation de l'azote. Les processus anaérobies ne sont pas représentés explicitement mais regroupés sous une même variable décrivant la demande en oxygène du sédiment. Les compartiments pélagique et benthique sont liés dynamiquement par la représentation des processus de sédimentation-resuspension des matières particulaires et la diffusion des espèces dissoutes de l'azote. Enfin, la finalité du modèle étant l'étude des interactions entre l'élevage mytilicole et l'écosystème de la lagune, une variable représentant la masse individuelle d'une moule, représentative de l'ensemble de la population cultivée et une variable représentant les biodépôts produits par ces bivalves ont également été introduites dans la structure pélagique du modèle. À ce stade du développement l'équation qui décrit l'évolution de la masse individuelle de la moule témoin est de type «scope for growth», ne tenant compte que de la croissance somatique.

Le processus de calibration a permis une représentation correcte par le modèle de l'ordre de grandeur et des tendances saisonnières, lorsque existantes, pour toutes les variables pélagiques. La variabilité à plus courte échelle temporelle (due à la marée ou à des phénomènes météorologiques ponctuels) est en général moins bien représentée en raison, en partie au moins, d'un manque de séries temporelles détaillées pour plusieurs variables ce qui ne permet pas d'imposer toute la variabilité de ces composantes dans les

conditions frontières du modèle. La croissance somatique des moules, qui intègre au moins partiellement cette variabilité haute fréquence, est très bien simulée par le modèle. En plus de cette représentation satisfaisante des variables d'état, le modèle reproduit également correctement les flux entre les différents compartiments pour lesquels des données sont disponibles. Ceci constitue une première étape pour assurer que le modèle est un outil fiable pour étudier le fonctionnement dynamique de l'écosystème de la GEL.

La seconde étape est l'analyse de sensibilité qui est essentielle pour assurer la capacité prédictive du modèle. Dans le cas présent, aucune sensibilité majeure n'est observée, quels que soient les paramètres, forçages et variables considérés. De plus cette analyse montre que comme en nature, l'écosystème reproduit par le modèle est dominé par les cellules de petite taille, en particulier le microzooplancton qui exerce un influence importante sur le phytoplancton et les sels nutritifs. Au contraire, d'après ces résultats la ferme mytilicole ne semble jouer qu'un rôle mineur dans la dynamique de ce système, à l'échelle globale tout du moins.

L'intégration des résultats du modèle sur l'ensemble de la lagune et sur toute la période simulée met en évidence l'importance du réseau microbien qui mobilise la majeure partie de l'azote présent dans le système pélagique. Les processus de recyclage, notamment l'excrétion du microzooplancton, dominent quant à eux la dynamique des sels nutritifs fournissant quatre fois plus d'azote inorganique que les apports externes (précipitations et échanges aux frontières ouvertes et à l'interface eau-sédiment). Globalement, le niveau de productivité du système est principalement fixé par le contrôle exercé par les hétérotrophes (essentiellement le microzooplancton), plutôt que par la disponibilité en sels nutritifs.

5.3 VOLET INTERACTIONS MOULES/ENVIRONNEMENT

Afin de prendre en compte l'ensemble des besoins énergétiques des moules en culture et ainsi éviter au maximum les biais dans la représentation de leurs interactions avec le reste de l'écosystème, l'équation écophysiologique, qui était utilisée jusque là, a été remplacé par un bilan d'énergie dynamique (DEB) reproduisant aussi bien la croissance somatique que le cycle reproductif de ces bivalves.

La calibration du modèle DEB a permis de correctement simuler à la fois la croissance de la coquille des moules (indicateur de la croissance somatique) que les variations de leur masse sèche. En particulier, le modèle reproduit un patron de ponte dont le calendrier correspond précisément au patron déjà observé dans la GEL.

Le modèle couplé hydrodynamique-biogéochimique-DEB permet donc d'étudier l'aspect production (environnement/moules) ainsi que l'aspect écologique (moules/environnement) de la capacité de support en considérant à la fois l'échelle locale et l'échelle de la lagune.

Les résultats du modèle et les données de terrain montrent que la croissance des moules n'est pas homogène sur toute la ferme d'élevage. Un gradient de croissance selon la direction est-nord-est, ouest-sud-ouest est observé et reproduit par le modèle. D'après les observations, la croissance est accrue d'un maximum de 10% à l'extrémité sud-ouest de la ferme alors que le modèle surestime légèrement cette amplitude à 15%.

La comparaison des simulations où le stock de moules est augmenté soit par une augmentation de la surface d'élevage, soit par une augmentation de la densité, montre que

pour les faibles stocks (< deux fois le stock de 2003) la croissance des moules est contrôlée à la fois par la déplétion locale de nourriture et par la disponibilité de cette nourriture à l'échelle du système au complet. Lorsque le stock est encore accru (> deux fois le stock de 2003), la déplétion locale devient plus pénalisante. Néanmoins, aucune réduction majeure de la croissance des moules n'a été observée, même pour le stock maximal utilisé dans ces simulations (environ 4 fois le stock de 2003). La capacité de production pourrait toutefois s'avérer moins élevée en considérant le report de la période de récolte engendré par la diminution de croissance. Cette question ne pourra être tranchée qu'en prolongeant la durée des simulations au-delà de la mi-octobre, la limite fixée par les données disponibles pour la présente étude.

Localement, les effets de l'introduction de l'élevage mytilicole sur l'écosystème pélagique de la GEL se limitent à des changements de l'ordre de 10% des différents flux d'azote. Les flux dans les sédiments sont eux modifiés de façon plus importante (12 - 49%) et résultent en une augmentation de l'efflux de sels nutritifs (NH4 et NO3) suivant l'augmentation des apports en matière organique par la biodéposition et la minéralisation de cette matière par des processus principalement anaérobies. En valeur relative, les flux d'échange avec l'extérieur sont les plus affectés par la présence des moules à l'échelle locale. Bien que leur valeur absolue soit plus faible que celle des autres flux de la colonne d'eau, cela indique que l'activité mytilicole puise dans les ressources de la lagune à l'extérieur de la zone d'élevage.

Prévoir la répercussion des effets locaux à l'échelle du système complet est la principale difficulté dans l'estimation de la capacité de support écologique car elle fait

intervenir les interactions entre les trois composantes hydrodynamique, biogéochimique et physiologique. Le modèle développé lors de ce doctorat permet d'observer que les effets de la présence des moules sont maximum dans la zone d'élevage mais qu'ils sont également dispersés sur une région plus vaste correspondant approximativement à la totalité du bassin profond de la GEL. Ceci s'explique essentiellement par des considérations hydrodynamiques avec la présence du tourbillon résiduel qui isole cette zone du reste de la lagune et des processus de mélange (liés à l'action du vent principalement) qui tendent à disperser les effets de la ferme à l'intérieur de cette région.

Les sels nutritifs, à la base de la chaîne de production et présents en faible quantité dasn les eaux de la GEL, sont affectés différemment par la présence de l'élevage mytilicole. À l'échelle de la lagune, la dynamique de l'ammonium (NH4) est accélérée et sa disponibilité augmente, ce qui profite directement au phytoplancton de petite taille (SP). Au contraire, les nitrates (NO3) voient leur dynamique ralentir et leur disponibilité décroître, un effet pénalisant pour le phytoplancton de grande taille qui s'ajoute à la pression de broutage exercée par les moules. Lorsque le stock de moules en élevage est augmenté, la quantité totale d'azote (N) présente dans le système, en excluant les moules, reste pratiquement constante avec une légère diminution du stock pélagique de N et une augmentation équivalente du stock benthique. Ceci constitue un mécanisme de séquestration de l'azote déjà observé dans plusieurs systèmes côtiers abritant un élevage conchylicole. L'azote investit dans la biomasse croissante de moules est compensé par les apports extérieurs et n'entraîne donc pas un déficit majeur au moment de la récolte. Toutefois, cette dépendance accrue vis-à-vis des ressources externes et le ralentissement du

recyclage global de l'azote au sein de la GEL en présence de l'élevage ont pour conséquence une vulnérabilité accrue de cet écosystème.

Les changements importants observés dans les sédiments de la zone d'élevage ont des répercussions très limitées à l'échelle de la lagune du fait de la faible fraction de la superficie occupée par cet élevage (1.2% de la surface de GEL) et de la faible dispersion des biodépôts due à leur vitesse de sédimentation élevée et aux faibles courants dans cette région de la lagune.

L'utilisation de courbes de déplétion, qui mettent en relation l'intensité des effets et la surface affectée par la présence de l'élevage, conjointement avec les résultats du modèle numérique fournit un critère objectif d'estimation de la capacité de support considérant l'ensemble des échelles spatiales impliquées. Dans la situation présente (stock de moules de 2003), la lagune de Grande-Entrée peut être considérée comme en deçà de sa capacité de support. Toutefois, celle-ci est rapidement atteinte (une fois et demi à deux fois le stock de 2003) du fait de la situation hydrodynamique particulière qui concentre les effets dans le bassin profond. Il s'agit néanmoins d'une estimation pessimiste puisqu'elle ne s'appuie que sur la période estivale pendant laquelle les températures élevées maximisent le métabolisme des bivalves et leur influence sur l'écosystème.

5.4 PERSPECTIVES

Le modèle développé au cours de cette recherche doctorale représente un premier effort pour modéliser l'écosystème de la lagune de Grande-Entrée. Il devrait donc servir de

base à de futures améliorations, qui comme mentionné au long du texte, devraient porter en priorité sur le module benthique et le modèle écophysiologique DEB. L'inclusion d'une variable représentant le microphytobenthos et le raffinement du processus de remise en suspension des sédiments devraient permettre d'améliorer les résultats du modèle sans pour autant entraîner d'importants coûts de calcul supplémentaires. Le modèle DEB a été utilisé avec un jeu de paramètres issus de la littérature, qui a donné des résultats satisfaisants du point de vue de la croissance des moules. Toutefois, les détails du métabolisme serait probablement mieux décrits par l'utilisation d'un jeu de paramètres issus d'études physiologiques sur des moules du Golfe du Saint-Laurent, qui ont dû s'adapter aux conditions environnementales particulières à cette région.

Comme la plupart des modèles numériques, le présent modèle serait probablement amélioré par la confrontation avec de nouvelles données de terrain. Notamment, un jeu complet de données pour la GEL, indépendant de celui utilisé dans le présent travail, permettrait une validation plus approfondie. Quant à l'application de ce modèle à d'autres systèmes côtiers de la région, elle fournirait des renseignements intéressants sur sa portabilité et sa robustesse.

D'un point de vue plus général sur l'utilisation de la modélisation numérique comme outil dans la gestion et le développement durables des zones côtières, appliquer un même modèle à différents systèmes pourrait conduire à formuler des principes plus génériques pour l'estimation de la capacité de support des écosystèmes pour la culture de bivalves.

Ceci souligne l'importance de collaborations nationales et internationales dans ce secteur de recherche.

L'emploi d'un modèle tel que celui développé lors de cette thèse ne permet pas, néanmoins, de considérer l'ensemble des effets de l'introduction d'une activité conchylicole dans un écosystème côtier. Des effets tels que l'attrait suscité par les structures d'élevage qui peuvent agir comme des récifs artificiels, ne peuvent être pris en compte car ils font intervenir des niveaux trophiques plus élevés que ceux reproduits par le modèle. L'utilisation conjointe d'autres outils tels que les techniques d'analyse des réseaux trophiques s'avère toujours nécessaire pour compléter le diagnostique posé à l'aide de modèles dynamiques d'écosystèmes.

RÉFÉRENCES BIBLIOGRAPHIQUES

Ariathurai, R. and Krone, R.B. (1976) Finite element model for cohesive sediment transport. **Journal of the Hydraulics Division, ASCE** 102: 323-338.

Asmus, R.M. and Asmus, H. (1991) Mussel beds: limiting or promoting phytoplankton? **Journal of Experimental Marine Biology and Ecology** 148: 215-232.

Aubrey, D.G. and Speer, P.E. (1985) A Study of Non-linear Tidal Propagation in shallow Inlet/Estuarine Systems. Part I: Observations. **Estuarine, Coastal and Shelf Science** 21: 185-205.

Aubrey, D.G., McSherry, T.R. and Eliet, P.P. (1993) Effects of multiple inlet morphology on tidal exchange: Waquoit Bay, Massachusetts. In: D. G. Aubrey and G. S. Giese (Eds.), Formation and evolution of multiple tidal inlets. **Coastal and Estuarine Studies**. American Geophysical Union, Washington, Vol. 44, pp. 213-235.

Azam, F., Fenchel, T., Field, J.G., Gray, J.S., Meyer-Reil, L. and Thingstad, F. (1983) The ecological role of water-column microbes in the sea. **Marine Ecology Progress Series** 10: 257-263.

Bacher, C. (1989) Capacité trophique du bassin de Marennes-Oléron: couplage d'un modèle de transport particulaire et d'un modèle de croissance de l'huitre *Crassostrea gigas*. **Aquatic Living Resources** 2: 199-214.

Bacher, C., Millet, B. and Vaquer, A. (1997) Modelling the impact of cultivated filter-feeders on phytoplanktonic biomass of the Thau Lagoon (France). **Comptes Rendus de l'Academie des Sciences, Serie III. Sciences de la Vie/Life Sciences** 320: 73-81.

Bacher, C., Duarte, P., Ferreira, J.G., Héral, M. and Raillard, O. (1998) Assessment and comparison of the Marennes-Oléron Bay (France) and Carlingford Lough (Ireland) carrying capacity with ecosystem models. **Aquatic Ecology** 31: 379-394.

Bacher, C., Grant, J., Hawkins, A.J.S., Fang, J.G., Zhu, M. and Besnard, M. (2003) Modelling the effect of food depletion on scallop growth in Sungo Bay (China). **Aquatic Living Resources** 16: 10-24.

Baretta-Bekker, J.G., Baretta, J.W. and Rasmussen, E.K. (1995) The microbial food web in the European regional seas ecosystem model. **Netherlands Journal of Sea Research** 33: 363-379.

Barranguet, C., Alliot, E. and Plante-Cuny, M.-R. (1994) Benthic microphytic activity at two Mediterranean shellfish cultivation sites with reference to benthic fluxes. **Oceanologica Acta** 17: 211-221.

Bayne, B.L. (1976) The biology of mussel larvae. In: B. L. Bayne (Ed.), Marine mussels: their ecology and physiology. Cambridge University Press, Cambridge, pp. 81-120.

Bayne, B.L. and Widdows, J. (1978) The physiological ecology of two populations of *Mytilus edulis* L. **Oecologia** 37: 137-162.

Bayne, B.L. and Newell, R.C. (1983) Physiological energetics of marine molluscs. In: A. S. M. Saleudin and K. M. Wilber (Eds.), The Mollusca, Vol. 4, Physiology. Academic Press, New York, pp. 407-515.

Bayne, B.L., Hawkins, A.J.S. and Navarro, E. (1987) Feeding and digestion by the mussel *Mytilus edulis* L. (Bivalvia: Mollusca) in mixtures of silt and algal cells at low concentrations. **Journal of Experimental Marine Biology and Ecology** 111: 1-22.

Bayne, B.L., Hawkins, A.J.S., Navarro, E. and Iglesias, J.I.P. (1989) Effects of seston concentration on feeding, digestion and growth in the mussel *Mytilus edulis*. **Marine Ecology Progress Series** 55: 47-54.

Bayne, B.L., Iglesias, J.I.P., Hawkins, A.J.S., Navarro, E., Héral, M. and Deslous-Paoli, J.M. (1993) Feeding behaviour of the mussel *Mytilus edulis*: responses to variations in quantity and organic content of the seston. **Journal of the Marine Biological Association of UK** 73: 813-829.

Beaulieu, S.E. (2003) Resuspension of phytodetritus from the sea floor: A laboratory flume study. **Limnology and Oceanography** 48: 1235-1244.

Bergamasco, A. and Zago, C. (1999) Exploring the nitrogen cycle and macroalgae dynamics in the Lagoon of Venice using a multibox model. **Estuarine, Coastal and Shelf Science** 48: 155-175.

Blackburn, T.H. and Henriksen, K. (1983) Nitrogen cycling in different types of sediments from Danish waters. **Limnology and Oceanography** 28: 477-493.

Blackford, B.L. (1978) Wind-driven inertial currents in the Magdalen Shallows, Gulf of St. Lawrence. **Journal of Physical Oceanography** 8: 653-664.

Bompais, X. (1991) Les filières pour l'élevage des moules. IFREMER.

Booth, D. (1994) Tidal flushing of semi-enclosed bays. In: K. Beven, P. Chatwin and J. Millbank (Eds.), Mixing and transport in the environment. John Wiley & Sons, New York, pp. 203-219.

Boudreau, B.P. (1996) A method-of-lines code for carbon and nutrient diagenesis in aquatic sediments. **Computers & Geosciences** 22: 479-496.

Bougis, P. (1976) Marine plankton ecology, North-Holland, Amsterdam.

Brigolin, D., Dal Maschio, G., Rampazzo, F., Giani, M. and Pastres, R. (2009) An individual-based population dynamic model for estimating biomass yield and nutrient fluxes through an off-shore mussel (*Mytilus galloprovincialis*) farm. **Estuarine, Coastal and Shelf Science** 82: 365-376.

Brush, M.J., Brawley, J.W., Nixon, S.W. and Kremer, J.N. (2002) Modeling phytoplankton production: problems with the Eppley curve and an empirical alternative. **Marine Ecology Progress Series** 238: 31-45.

Caceres-Martinez, J. and Figueras, A. (1997) The mussel, oyster, clam and pectinid fisheries of Spain, NOAA Technical Report NMFS 129: 165-190.

Callender, E. and Hammond, D.E. (1982) Nutrient exchange across the sediment-water interface in the Potomac River Estuary. **Estuarine Coastal and Shelf Science** 15: 395-413.

Callier, M.D., Weise, A.M., McKindsey, C.W. and Desrosiers, G. (2006) Sedimentation rates in a suspended mussel farm (Great-Entry Lagoon, Canada): biodeposit production and dispersion. **Marine Ecology Progress Series** 322: 129-141.

Callier, M.D., McKindsey, C.W. and Desrosiers, G. (2007) Multi-scale spatial variations in benthic sediment geochemistry and macrofaunal communities under a suspended mussel culture. **Marine Ecology Progress Series** 348: 103-115.

Cameron, W.M. and Pritchard, D.W. (1963) Estuaries. In: M. N. Hill (Ed.), The Sea vol. 2. John Wiley and Sons, New York, pp. 306-324.

Carver, C.E.A. and Mallet, A.L. (1990) Estimating the carrying capacity of a coastal inlet for the mussel culture. **Aquaculture** 88: 39-53.

Cerco, C.F. and Cole, T.M. (1994) Three-dimensional model of Cheasapeake Bay. EL-94-4, US Army Corps of Engineers, Vicksburg, MS.

Chamberlain, J., Fernandes, T.F., Read, P., Nickell, T.D. and Davies, I.M. (2001) Impacts of deposits from suspended mussel (*Mytilus edulis* L.) culture on the surrounding surficial sediments. **ICES Journal of Marine Science** 58: 411-416.

Chapelle, A., Lazure, P. and Ménesguen, A. (1994) Modelling eutrophication events in a coastal ecosystem. Sensitivity analysis. **Estuarine, Coastal and Shelf Science** 39: 529-548.

Chapelle, A. (1995) A preliminary model of nutrient cycling in sediments of a Mediterranean lagoon. **Ecological Modelling** 80: 131-147.

Chapelle, A., Menesguen, A., Deslous-Paoli, J.-M., Souchu, P., Mazouni, N., Vaquer, A. and Millet, B. (2000) Modelling nitrogen, primary production and oxygen in a Mediterranean lagoon. Impact of oyster farming and inputs from the watershed. **Ecological Modelling** 127: 161-181.

Christensen, P.B., Glud, R.N., Dalsgaard, T. and Gillepsie, P. (2003) Impact of longline mussel farming on oxygen and nitrogen dynamics and biological communities of coastal sediments. **Aquaculture** 218: 567-588.

Claustre, H., Kerherve, P., Marty, J.-C., Prieur, L., Videau, C. and Hecq, J.-H. (1994) Phytoplankton dynamics associated with a geostrophic front: ecological and biogeochemical implications. **Journal of Marine Research** 52: 711-742.

Cloern, J.E. (1982) Does the benthos control phytoplankton biomass in South San Francisco Bay? **Marine Ecology Progress Series** 9: 191-202.

Conover, R.J. (1966) Assimilation of organic matter by zooplankton. **Limnology and Oceanography** 11: 338-345.

Cranford, P.J., Emerson, C.W., Hargrave, B.T. and Milligan, T.G. (1998) In situ feeding and absorption responses of sea scallops *Placopecten magellanicus* (Gmelin) to storm-induced changes in the quantity and composition of the seston. **Journal of Experimental Marine Biology and Ecology** 219: 45-70.

Cranford, P.J. and Hill, P.S. (1999) Seasonal variation in food utilization by the suspension-feeding bivalve molluscs *Mytilus edulis* and *Placopecten magellanicus*. **Marine Ecology Progress Series** 190: 223-239.

Cranford, P., Dowd, M., Grant, J., Hargrave, B. and McGladdery, S. (2003) Ecosystem level effects of marine bivalve aquaculture, In: A scientific review of the potential environmental effects of aquaculture in aquatic ecosystems. Volume 1. **Canadian Technical Report in Fisheries and Aquatic Sciences 2450**, pp. 64-95.

Cranford, P.J., Strain, P.M., Dowd, M., Hargrave, B.T., Grant, J. and Archambault, M.-C. (2007) Influence of mussel aquaculture on nitrogen dynamics in a nutrient enriched coastal embayment. **Marine Ecology Progress Series** 347: 61-78.

Cugier, P., Ménesguen, A. and Guillaud, J.-F. (2005) Three-dimensional (3D) ecological modelling of the Bay of Seine (English Channel, France). **Journal of Sea Research** 54: 104-124.

Dahlbäck, B. and Gunnarsson, L.A.H. (1981) Sedimentation and sulfate reduction under a mussel culture. **Marine Biology** 63: 269-275.

Dame, R.F., Dankers, N., Prins, T.C., Jongsma, H. and Smaal, A.C. (1991) The influence of mussel beds on nutrients in the Western Wadden Sea and Eastern Scheldt estuaries. **Estuaries** 14: 130-138.

Dame, R.F. (1993) The role of bivalve filter feeder material fluxes in estuarine ecosystems. In: R. F. Dame (Ed.), Bivalve filter feeders in estuarine and coastal ecosystem processes. NATO ASI Series, Vol. G33. Springer-Verlag, Heidelberg, pp. 371-420.

Dame, R.F. (1996) Ecology of marine bivalves: an ecosystem approach. CRC Press, Boca Raton.

Dame, R.F. and Prins, T.C. (1998) Bivalve carrying capacity in coastal ecosystems. **Aquatic Ecology** 31: 409-421.

Dame, R.F., Bushek, D., Allen, D., Lewitus, A., Edwards, D., Koepfler, E. and Gregory, L. (2002) Ecosystem response to bivalve density reduction: management implications. **Aquatic Ecology** 36: 51-65.

Darnell, P. (2000) Transfer of New Zealand mussel farming technology to Nova Scotia. **Bulletin of the Aquaculture Association of Canada** 100-2.

Deason, E.E. (1980) Grazing of *Acartia hudsonica* (*A. clausi*) on *Skeletonema costatum* in Narragansett Bay (USA): Influence of food concentration and temperature. **Marine Biology** 60: 101-113.

Deslous-Paoli, J.-M., Souchu, P., Mazouni, N., Juge, C. and Dagault, F. (1998) Relations milieu-ressources : impact de la conchyliculture sur un environnement lagunaire méditerranéen (Thau). **Oceanologica Acta** 21: 831-843.

DiLorenzo, J.L. (1988) The overtide and filtering response of small inlet/bay systems. In: D. G. Aubrey and L. Weishar (Eds.), Hydrodynamics and sediment dynamics of tidal inlets. **Lecture notes on Coastal and Estuarine Studies**. Springer-Verlag, New York, Vol. 29, pp. 24–53.

DiToro, D.M., Paquin, P.R., Subburamu, K. and Gruber, D.A. (1990) Sediment oxygen demand model: methane and ammonia oxidation. **Journal of Environmental Engineering** 116: 945-986.

Dowd, M. (1997) On predicting the growth of cultured bivalves. **Ecological Modelling** 104: 113-131.

Dowd, M. (2000) Oceanography and shellfish production: A bio-physical synthesis using a simple model. **Bulletin of the Aquaculture Association of Canada** 100-2: 3-9.

Dowd, M. (2003) Seston dynamics in a tidal inlet with shellfish aquaculture: a model study using tracer equations. **Estuarine, Coastal and Shelf Science** 57: 523-537.

Drapeau, G. (1988) Stability of tidal inlet navigation channels and adjacent dredge spoil islands. In: D. G. Aubrey and L. Weishar (Eds.), Hydrodynamics and sediment dynamics of tidal inlets. **Lecture Notes on Coastal and Estuarine Studies.** Springer-Verlag, New York, Vol. 29, pp. 226-244.

Dronkers, J. and Zimmerman, J.T.F. (1982) Some principles of mixing in tidal lagoons. **Oceanologica Acta** SP: 107-117.

Duarte, P., Meneses, R., Hawkins, A.J.S., Zhu, M., Fang, J. and Grant, J. (2003) Mathematical modelling to assess the carrying capacity for multi-species culture within coastal waters. **Ecological Modelling** 168: 109-143.

Dumbauld, B.R., Ruesink, J.L. and Rumrill, S.S. (2009) The ecological role of bivalve shellfish aquaculture in the estuarine environment: A review with application to oyster and clam culture in West Coast (USA) estuaries. **Aquaculture** 290: 196-223.

Dzierzbicka-Glowacka, L. (2005) A numerical investigation of phytoplankton and *Pseudocalanus elongatus* dynamics in the spring bloom time in the Gdansk Gulf. **Journal of Marine Systems** 53: 19-36.

Eppley, R.W. (1972) Temperature and phytoplankton growth in the sea. **Fishery Bulletin** 70: 1063-1085.

FAO (2009) The state of world fisheries and aquaculture 2008, FAO Fisheries and Aquaculture Department, Food and Agriculture Organization of the United Nations, Rome, 196p.

Feng, S., Cheng, R.T. and Xi, P. (1986a) On tide-induced lagrangian residual current and residual transport. 1. Lagrangian residual Current. **Water Resources Research** 22: 1623-1634.

Feng, S., Cheng, R.T. and Xi, P. (1986b) On tide-induced lagrangian residual current and residual transport. 2. Residual transport with application in South San Francisco Bay, California. **Water Resources Research** 22: 1635-1646.

Ferreira, J.G., Duarte, P. and Ball, B. (1998) Trophic capacity of Carlingford Lough for oyster culture - analysis by ecological modelling. **Aquatic Ecology** 31: 361-378.

Ferreira, J.G., Hawkins, A.J.S. and Bricker, S.B. (2007) Management of productivity, environmental effects and profitability of shellfish aquaculture — the Farm Aquaculture Resource Management (FARM) model. **Aquaculture** 264: 160–174.

Ferreira, J.G., Hawkins, A.J.S., Monteiro, P., Moore, H., Service, M., Pascoe, P.L., Ramos, L. and Sequeira, A. (2008) Integrated assessment of ecosystem-scale carrying capacity in shellfish growing areas. **Aquaculture** 275: 138-151.

Feuillet-Girard, M., Héral, M., Sornin, J.-M., Deslous-Paoli, J.-M., Robert, J.-M., Mornet, F. and Razet, D. (1988) Nitrogenous compounds in the water column and at the sediment-water interface in the estuarine bay Marennes-Oléron: influence of oyster farming. **Aquatic Living Resources** 1: 251-265.

Folke, C. and Kautsky, N. (1989) The role of ecosystems for a suitable development of aquaculture. **Ambio** 18: 234-243.

Folke, C. and Kautsky, N. (1992) Aquaculture with its environment: prospects for sustainability. **Ocean and Coastal Management** 17: 5- 24.

Foreman, M.G. (1977) Manual for tidal heights analysis and previsions. Pacific Marine Science Report 77-10.

Fortunato, A.B. and Oliveira, A. (2005) Influence of intertidal flats on tidal asymmetry. **Journal of Coastal Research** 21: 1062-1067.

Fréchette, M. and Bourget, E. (1985) Food-limited growth of *Mytilus edulis* L. in relation to the benthic boundary layer. **Canadian Journal of Fisheries and Aquatic Sciences** 42: 1166-1170.

Fry, V.A. and Aubrey, D.G. (1990) Tidal Velocity Asymmetries and Bedload Transport in Shallow Embayments. **Estuarine, Coastal and Shelf Science** 30: 453-473.

Garen, P., Robert, S. and Bougrier, S. (2004) Comparison of growth of mussel, *Mytilus edulis*, on longline, pole and bottom culture sites in the Pertuis Breton, France. **Aquaculture** 232: 511-524.

Gauthier-Clerc, S., Tita, T., Bourque, F., Tremblay, R., Pellerin, J., Fournier, M., St-Louis, R. and Pelletier, E. (2007) Comparaison de la gamétogenèse de la moule bleue (*Mytilus edulis*) en mer et en lagune aux Îles-de-la-Madeleine, Rapport scientifique, MAPAQ, Rimouski, 30p.

Gibbs, M.T. (2004) Interactions between bivalve shellfish farms and fishery resources. **Aquaculture** 240: 267-296.

Gibbs, M.T. (2007) Sustainability performance indicators for suspended bivalve aquaculture activities. **Ecological Indicators** 7: 94–107.

Gibbs, M.T. (2009) Implementation barriers to establishing a sustainable coastal aquaculture sector. **Marine Policy** 33: 83-89.

Gilbert, F., Souchu, P., Bianchi, P. and Bonin, M. (1997) Influence of shellfish farming activities on nitrification, nitrate reduction to ammonium and denitrification at the water-sediment interface of the Thau lagoon. **Marine Ecology Progress Series** 151: 143-153.

Giusti, E. and Marsili-Libelli, S. (2006) An integrated model for the Orbetello lagoon ecosystem. **Ecological Modelling** 196: 379-394.

Goloway, F. and Bender, M. (1982) Diagenetic models of interstitial nitrate profiles in deep sea sediments. **Limnology and Oceanography** 27: 624-638.

Grangeré, K., Ménesguen, A., Lefebvre, S., Bacher, C. and Pouvreau, S. (2009) Modelling the influence of environmental factors on the physiological status of the Pacific oyster *Crassostrea gigas* in an estuarine embayment; The Baie des Veys (France). **Journal of Sea Research** 62: 147-158.

Grant, J., Dowd, M., Thompson, K., Emerson, C. and Hatcher, A. (1993) Perspectives on field studies and related biological models of bivalve growth and carrying capacity. In: R. F. Dame (Editor), Bivalve Filter Feeders in Estuarine and Coastal Ecosystem Processes. Proceedings of the NATO Advanced Research Workshop on the role of Bivalve Filter Feeders in Marine Ecosystem Processes. Springer Verlag, pp. 370-420.

Grant, J., Hatcher, A., Scott, D.B., Pocklington, P., Schafer, C.T. and Honig, C. (1995) A multidisciplinary approach to evaluating benthic impacts of shellfish aquaculture. **Estuaries** 18: 124-144.

Grant, J., Curran, K.J., Guyondet, T.L., Tita, G., Bacher, C., Koutitonsky, V.G. and Dowd, M. (2007) A box model of carrying capacity for suspended mussel aquaculture in Lagune de la Grande-Entrée, Iles-de-la-Madeleine, Québec. **Ecological Modelling** 200: 193-206.

Grant, J., Bacher, C., Cranford, P.J., Guyondet, T. and Carreau, M. (2008) A spatially explicit ecosystem model of seston depletion in dense mussel culture. **Journal of Marine Systems** 73: 155-168.

Green, S., Visser, A.W., Titelman, J. and Kiørboe, T. (2003) Escape responses of copepod nauplii in the flow field of the blue mussel, *Mytilus edulis*. **Marine Biology** 142: 727-733.

Grenz, C., Hermin, M.-N., Baudinet, D. and Daumas, R. (1990) In situ biochemical and bacterial variation of sediments enriched with mussel biodeposits. **Hydrobiologia** 207: 153-160.

Grégoire, M., Beckers, J.M., Nihoul, J.C.J. and Stanev, E. (1998) Reconnaissance of the main Black Sea's ecohydrodynamics by means of a 3D interdisciplinary model. **Journal of Marine Systems** 16: 85-105.

Grégoire, M. and Lacroix, G. (2001) Study of the oxygen budget of the Black Sea waters using a 3D coupled hydrodynamical–biogeochemical model. **Journal of Marine Systems** 31: 175-202.

Grégoire, M., Raick, C. and Soetaert, K. (2008) Numerical modeling of the central Black Sea ecosystem functioning during the eutrophication phase. **Progress in Oceanography** 76: 286-333.

Griffin, S.L., Herzfeld, M. and Hamilton, D.P. (2001) Modelling the impact of zooplankton grazing on phytoplankton biomass during a dinoflagellate bloom in the Swan River Estuary, Western Australia. **Ecological Engineering** 16: 373-394.

Guillaud, J.-F., Andrieux, F. and Ménesguen, A. (2000) Biogeochemical modelling in the Bay of Seine (France): an improvement by introducing phosphorus in nutrient cycles. **Journal of Marine Systems** 25: 369-386.

Guyondet, T., Grant, J., Roy, S., Koutitonsky, V.G. and Tita, G. A coastal biogeochemical model to study the interactions between cultured bivalves and their environment - Model set-up and sensitivity analysis. **Submitted to Ecological Modelling**.

Guyondet, T., Koutitonsky, V.G. and Roy, S. (2005) Effects of water renewal estimates on the oyster aquaculture potential of an inshore area. **Journal of Marine Systems** 58: 35-51.

Guyondet, T. and Koutitonsky, V.G. (2008) Tidal and residual circulations in coupled restricted and leaky lagoons. **Estuarine, Coastal and Shelf Science** 77: 396-408.

Haag, I. (2006) A basic water quality model for the River Neckar: Part 1 – model development, parameter sensitivity and identifiability, calibration and validation. **Acta Hydrochimica et Hydrobiologica** 34: 533-548.

Heip, C.H.R., Goosen, N.K., Herman, P.M.J., Kromkamp, J., Middelburg, J. and Soetaert, K. (1995) Production and consumption of biological particles in temperate tidal estuaries. **Oceanography and Marine Biology: An Annual Review** 33: 1–149.

Herman, P.M.J. and Scholten, H. (1990) Can suspension feeders stabilize estuarine ecosystems? In: M. Barnes and R. Gibson (Eds.), Trophic relationships in the marine environment. Aberdeen University Press, Aberdeen, pp. 104–116.

Héral, M. (1991) Approche de la capacité trophique des écosystèmes conchylicoles: synthèse bibliographique. **ICES Marine Science Symposia** 192: 48-62.

Héral, M. (1993) Why carrying capacity models are useful tools for management of bivalve culture. In: R. F. Dame (Ed.), Bivalve Filter Feeders in Estuarine and Coastal Ecosystem Processes. Springer-Verlag,Heidelberg, pp. 455-477.

Hily, C. (1991) Is the activity of benthic suspension feeders a factor controlling water quality in the Bay of Brest? **Marine Ecology Progress Series** 69: 179-188.

Hofman, P.A.G., de Jong, S.A., Wagenvoort, E.J. and Sandee, A.J.J. (1991) Apparent sediment diffusion coefficients for oxygen and oxygen consumption rates measured with microelectrodes and bell jars: applications to oxygen budgets in estuarine intertidal sediments (Oosterschelde, SW Netherlands). **Marine Ecology Progress Series** 69: 261-272.

Hoitink, A.J.F., Hoekstra, P. and van Maren, D.S. (2003) Flow asymmetry associated with astronomical tides: Implications for the residual transport of sediment. **Journal of Geophysical Research** 108: 13:1-8.

Hummel, H., Fortuin, A.W., Bogaards, R.H., de Wolf, L. and Meyboom, A. (1989) Changes in *Mytilus edulis* in relation to short-term disturbances of the tide. In: R. Z. Klekowski, L. Falkowski and E. Stycynska-Jurewicz (Eds.), Proceedings 21st EMBS, Warsaw, Ossolineum, pp. 77–89.

Imasato, N. (1983) What is tide-induced residual current? **Journal of Physical Oceanography** 13: 1307-1317.

Incze, L.S., Lutz, R.A. and True, E. (1981) Modeling carrying capacities for bivalve molluscs in open, suspended-culture systems. **Journal of the World Mariculture Society** 12: 143-155.

Inglis, G.J., Hayden, B.J. and Ross, A.H. (2000) An overview of factors affecting the carrying capacity of coastal embayments for mussel culture. CHC00/69, NIWA, Christchurch, New Zealand.

Jahnke, R.A., Emerson, S.R. and Murray, J.W. (1982) A model of oxygen reduction, denitrification and organic matter mineralization in marine sediments. **Limnology and Oceanography** 27: 610-623.

Janzen, C.D. and Wong, K.-C. (1998) On the low-frequency transport processes in a shallow coastal lagoon. **Estuaries** 21: 754-766.

Jay, D.A. (1990) Residual circulation in shallow estuaries: shear, stratification and transport processes. In: R. T. Cheng (Ed.), Coastal and Estuarine studies Vol. 38. Springer-Verlag, New York, pp. 49-63.

Ji, R., Davis, C., Chen, C. and Beardsley, R. (2008) Influence of local and external processes on the annual nitrogen cycle and primary productivity on Georges Bank: A 3-D biological–physical modeling study. **Journal of Marine Systems** 73: 31-47.

Jiang, W. and Gibbs, M.T. (2005) Predicting the carrying capacity of bivalve shellfish culture using a steady, linear food web model. **Aquaculture** 244: 171-185.

Jimenez-Montealegre, R., Verdegem, M.C.J., van Dam, A. and Verreth, J.A.J. (2002) Conceptualization and validation of a dynamic model for the simulation of nitrogen transformations and fluxes in fish ponds. **Ecological Modelling** 147: 123-152.

Jones, J.E. and Davies, A.M. (2007) On the sensitivity of tidal residuals off the west coast of Britain to mesh resolution. **Continental Shelf Research** 27: 64-81.

Jørgenson, C.B. (1996) Bivalve filter feeding revisited. **Marine Ecology Progress Series** 142: 287-302.

Kaspar, H.F., Gillepsie, P.A., Boyer, I.C. and MacKenzie, A.L. (1985) Effects of mussel aquaculture on the nitrogen cycle and benthic communities in Kenepuru Sound. Marlborough Sound, New Zealand. **Marine Biology** 85: 127-136.

Keulegan, G.H. (1967) Tidal flow in entrances, water-level fluctuations of basins in communication with seas, Committee on Tidal Hydraulics, Corps of Engineers, U.S. Army, Vicksburg, Mississippi.

King, I.P. (1982) A finite element model for three dimensional flow, report prepared by Resource Management Associates, Lafayette California, for U.S. Army Corps of Engineers, Waterways Experiment Station, Vicksburg, Mississippi.

King, I.P. (1985) Strategies for finite element modeling of three dimensional hydrodynamic systems. **Advances in Water Resources** 8: 69-76.

King, I.P. (1988) A finite element model for three dimensional hydrodynamic systems, report prepared by Resource Management Associates, Lafayette California, for U.S. Army Corps of Engineers, Waterways Experiment Station, Vicksburg, Mississippi.

King, I. (1993) RMA-10. A finite element model for three-dimensional density stratified flow, Department of Civil and Environmental Engineering. University of California, Davis.

King, I.P. (2003) RMA-11 - A three dimensional finite element model for water quality in estuaries and streams, Resource Modelling Associates, Sydney, Australia. 84p.

Kjerfve, B. (1986) Comparative oceanography of coastal lagoons. In: D. A. Wolfe (Ed.), Estuarine variability. Academic Press, New York, pp. 63-81.

Kjerfve, B. and Knoppers, B.A. (1991) Tidal choking in a coastal lagoon. In: B. B. Parker (Ed.), Tidal Hydrodynamics. J.Wiley, New York, pp. 169-181.

Kjerfve, B. (1994) Coastal Lagoons. In: B. Kjerfve (Ed.), Coastal Lagoon Processes. **Elsevier Oceanography Series**. Elsevier, Amsterdam, The Netherlands, Vol. 60, pp. 1-8.

Kooijman, S.A.L.M. (2000) Dynamic energy and mass budgets in biological systems. Cambridge University Press, Cambridge, 419 pp.

Koutitonsky, V.G. and Bugden, G. (1991) The physical oceanography of the Gulf of St. Lawrence: a review with emphasis on the synoptic variability of the motion. In: J. C. Therriault (Ed.), The Gulf of St. Lawrence: small ocean or big estuary? Canadian Special Publication in Fisheries and Aquatic Science 113, pp. 57-90.

Koutitonsky, V.G., Navarro, N. and Booth, D. (2002) Descriptive physical oceanography of Great-Entry Lagoon, Gulf of St. Lawrence. **Estuarine, Coastal and Shelf Science** 54: 833-847.

Koutitonsky, V.G. (2005) Modélisation numérique intégrée des courants, des vagues et du transport des sédiments à l'entrée de la lagune de Havre-aux-Maisons, Rapport de recherche LHE-05-2. Laboratoire d'hydraulique environnementale. ISMER, Rimouski, Qc. 173p.

Koutitonsky, V.G. and Tita, G. (2006) Temps de renouvellement des eaux dans la lagune de Grande-Entrée aux Îles-de-la-Madeleine., Ministère de l'Agriculture, des Pêcheries et de l'Alimentation du Québec. Cahier d'information n°151. 73 p.

Koutitonsky, V.G. (2006) Three-dimensional structure of wind-driven currents in coastal lagoons. In: I. E. Gonenc and J. P. Wolfin (Eds.), Coastal Lagoons: Ecosystem Processes and Modeling for Sustainable Use and Development. CRC Press, pp. 376-391.

LeBlond, P.H. (1991) Tides and their interactions with other oceanographic phenomena in shallow water (Review). In: B. B. Parker (Ed.), Tidal Hydrodynamics. J. Wiley, New York, pp. 125-152.

Lee, J.C. and Davies, A.M. (1999) Open boundary and frictional influences in 3D tidal models. **Journal of Hydraulic Engineering** 125: 1084-1096.

Legrand, S., Deleersnijder, E., Hanert, E., Legat, V. and Wolanski, E. (2006) High-resolution, unstructured meshes for hydrodynamic models of the Great Barrier Reef, Australia. **Estuarine, Coastal and Shelf Science** 68: 36-46.

Lehane, C. and Davenport, J. (2002) Ingestion of mesozooplankton by three species of bivalve; *Mytilus edulis*, *Cerastoderma edule* and *Aequipecten opercularis*. **Journal of the Marine Biological Association of UK** 82: 615–619.

Lehane, C. and Davenport, J. (2006) A 15-month study of zooplankton ingestion by farmed mussels (*Mytilus edulis*) in Bantry Bay, Southwest Ireland. **Estuarine, Coastal and Shelf Science** 67: 645–652.

Lemaire, N., Pellerin, J., Fournier, M., Girault, L., Tamigneaux, E., Cartier, S. and Pelletier, E. (2006) Seasonal variations of physiological parameters in the blue mussel *Mytilus* spp. from farm sites of eastern Quebec. **Aquaculture** 261: 729-751.

Levin, S.A. (1992) The problem of pattern and scale in ecology (The Robert H. MacArthur award lecture). **Ecology** 73: 1943-1967.

Li, Y.-H. and Gregory, S. (1974) Diffusion of ions in sea water and in deep-sea sediments. **Geochimica et Cosmochimica Acta** 38: 703-714.

Li, M., Gargett, A. and Denman, K.L. (2000) What determines seasonal and interannual variability of phytoplankton and zooplankton in strongly estuarine systems? Application to the semi-enclosed estuary of Strait of Georgia and Juan de Fuca Strait. **Estuarine, Coastal and Shelf Science** 50: 467-488.

Liss, P.S. and Merlivat, L. (1986) Air-Sea gas exchange rates: Introduction and synthesis. In: P. Buat-Menard (Ed.), The Role of Air-Sea Exchange in Geochemical Cycling. Reidel, Hingham, MA, pp. 113-127.

Loder, J.W., Shen, Y. and Ridderinkhof, H. (1997) Characterization of three-dimensional Lagrangian circulation associated with tidal rectification over a submarine bank. **Journal of Physical Oceanography** 27: 1729-1742.

Lohrenz, S.E., Fahnenstiel, G.L., Redalje, D.G., Lang, G.A., Dagg, M.J., Whitledge, T.E. and Dortch, Q. (1999) Nutrients, irradiance, and mixing as factors regulating primary production in coastal waters impacted by the Mississippi River plume. **Continental Shelf Research** 19: 1113-1141.

Longuet-Higgins, M.S. (1969) On the transport of mass by time-varying ocean currents. **Deep-Sea Research** 16: 431-447.

Maa, J.P.-Y., Sanford, L. and Halka, J.P. (1998) Sediment resuspension characteristics in Baltimore Harbor, Maryland. **Marine Geology** 146: 137-145.

Maar, M., Bolding, K., Petersen, J.K., Hansen, J.L.S. and Timmermann, K. (2009) Local effects of blue mussels around turbine foundations in an ecosystem model of Nysted off-shore wind farm, Denmark. **Journal of Sea Research** 62: 159-174.

Maestrini, S.Y., Robert, J.-M., Lefley, J.W. and Collos, Y. (1986) Ammonium thresholds for simultaneous uptake of ammonium and nitrate by oyster-pond algae. **Journal of Experimental Marine Biology and Ecology** 102: 75-98.

MAPAQ (2001) L'aquaculture, un courant fort prometteur, Coordination ministérielle en aquaculture. Ministère de l'Agriculture, des Pêcheries et de l'Alimentation du Québec. 4p.

Marinov, D., Zaldivar, J.M., Norro, A., Giordani, G. and Viaroli, P. (2008) Integrated modelling in coastal lagoons: Sacca di Goro case study. **Hydrobiologia** 611: 147-165.

Mattson, J. and Linden, O. (1983) Benthic macrofauna succession under mussels *Mytilus edulis* L. cultured on hanging long-lines. **Sarsia** 68: 97-102.

Mayzaud, P., Koutitonsky, V.G., Souchu, P., Roy, S., Navarro, N. and Gomez-Reyez, E. (1992) L'impact de l'activité mytilicole sur la capacité de production du milieu lagunaire des Îles de la Madeleine. Rapport de recherche FP707-8-5140, de l'INRS-Océanologie pour Pêches et Océans Canada. 312p.

McKindsey, C.W., Thetmeyer, H., Landry, T. and Silvert, W. (2006) Review of recent carrying capacity models for bivalve culture and recommendations for research and management. **Aquaculture** 261: 451-462.

Meeuwig, J.J., Rasmussen, J. and Peters, R.H. (1998) Turbid waters and clarifying mussels: their moderation of chl:nutrient relations in estuaries in Prince Edward Island, Canada. **Marine Ecology Progress Series** 171: 139-150.

Mesnage, V. (1994) Contribution à l'étude de la mobilité des formes de phosphate à l'interface eau-sédiment dans les écosystèmes lagunaires, Thèse de Doctorat, Université Montpellier I, 252 pp.

Middelburg, J.J., Klaver, G., Nieuwenhuize, J. and Vlug, T. (1995) Carbon and nitrogen cycling in intertidal sediments near Doel, Scheldt Estuary. **Hydrobiologia** 311: 57-69.

Mirto, S., La Rosa, T., Danovaro, R. and Mazzola, A. (2000) Microbial and meiofaunal response to intensive mussel-farm biodeposition in coastal sediments of the Western Mediterranean. **Marine Pollution Bulletin** 40: 244-252.

Monteiro, P.M.S., Spolander, B., Brundit, G.B. and Nelson, G. (1998) Shellfish culture in the Benguela system: estimates of nitrogen-driven new production in Saldanha Bay using two physical models. **Journal of Shellfish Research** 17: 3-13.

Myrand, B., Guderley, H. and Himmelman, J.H. (2000) Reproduction and summer mortality of blue mussels *Mytilus edulis* in the Magdalen Islands, southern Gulf of St. Lawrence. **Marine Ecology Progress Series** 197: 193-207.

Nakamura, Y. and Kerciku, F. (2000) Effects of filter-feeding bivalves on the distribution of water quality and nutrient cycling in a eutrophic coastal lagoon. **Journal of Marine Systems** 26: 209-221.

Navarro, E., Iglesias, J.I.P., Perez-Camacho, A., Labarta, V. and Beiras, R. (1991) The physiological energetics of mussels (*Mytilus galloprovincialis* Lmk.) from different cultivation rafts in the Ria de Arosa (Galicia, N.W. Spain). **Aquaculture** 94: 197-212.

Newell, C.R., Shumway, S.E., Cucci, T.L. and Selvin, R. (1989) The effects of natural seston particle size and type on feeding rates, feeding selectivity and food resource availability for the mussel *Mytilus edulis* Linnaeus, 1758 at bottom culture sites in Maine. **Journal of Shellfish Research** 8: 187-196.

Newell, C.R., Hidu, H., McAlice, B.J., Podniesinski, G., Short, F. and Kindblom, L. (1991) Recruitment and commercial seed procurement of the blue mussel *Mytilus edulis* in Maine. **Journal of the World Aquaculture Society** 22: 134-152.

Nichols, F.H. (1985) Increased benthic grazing: an alternative explanation for low phytoplankton biomass in northern San Francisco Bay during the 1976-1977 drought. **Estuarine Coastal and Shelf Science** 21: 379-388.

Niquil, N., Pouvreau, S., Sakka, A., Legendre, L., Addessi, L., Le Borgne, R., Charpy, L. and Delesalle, B. (2001) Trophic web and carrying capacity in a pearl oyster farming lagoon (Takapoto, French Polynesia). **Aquatic Living Resources** 14: 165-175.

Nixon, S.W., Oviat, C.A., Garber, J. and Lee, V. (1976) Diel metabolism and nutrient dynamics in a salt marsh embayment. **Ecology** 57: 740-750.

Nixon, S.W., Kelly, J.R., Furnas, B.N., Oviatt, C.A. and Hale, S.S. (1980) Phosphorus regeneration and the metabolism of coastal marine bottom communities. In: K. R. Tenore and B. C. Coull (Eds.), Marine benthic dynamics. University of South Carolina Press, Columbia, pp. 219-242.

Nunes, J.P., Ferreira, J.G., Gazeau, F., Lencart-Silva, J., Zhang, X.L., Zhu, M.Y. and Fang, J.G. (2003) A model for sustainable management of shellfish polyculture in coastal bays. **Aquaculture** 219: 257-277.

Officer, C.B., Smayda, T.J. and Mann, R. (1982) Benthic filter feeding: a natural eutrophication control. **Marine Ecology Progress Series** 9: 203-210.

Oguz, T., Ducklow, H.W., Malanotte-Rizzoli, P., Murray, J.W., Shushkina, E.A., Vedernikov, V.I. and Unluata, U. (1999) A physical-biochemical model of plankton productivity and nitrogen cycling in the Black Sea. **Deep-Sea Research I** 46: 597-636.

Okunishi, T., Kishi, M.J., Shiomoto, A., Tanaka, H. and Yamashita, T. (2005) An ecosystem modeling study of spatio-temporal variations of phytoplankton distribution in the Okhotsk Sea. **Continental Shelf Research** 25: 1605-1628.

OSPAR, Villars, M., de Vries, I., Bokhorst, M., Ferreira, J., Gellers-Barkman, S., Kelly-Gerreyn, B., Lancelot, C., Menesguen, A., Moll, A., Patsch, J., Radach, G., Skogen, M., Soiland, H., Svendsen, E. and Vested, H.J. (1998) Report of the ASMO modelling workshop on eutrophication issues, 5–8 November 1996, OSPAR Commission Report, Netherlands Institute for Coastal and Marine Management, The Hague, The Netherlands.

Parker, B.B. (1991) The relative importance of the various nonlinear mechanisms in a wide range of tidal interactions (Review). In: B. B. Parker (Ed.), Tidal Hydrodynamics. J. Wiley, New York, pp. 237-268.

Pastres, R., Solidoro, C., Cossarini, G., Melaku Canu, D. and Dejak, C. (2001) Managing the rearing of Tapes philippinarum in the lagoon of Venice: a decision support system. **Ecological Modelling** 138: 231–245.

Percival, D.B. and Walden, A.T. (1993) Spectral Analysis for Physical Applications: Multitaper and Conventional Univariate Techniques. Cambridge University Press.

Pett, R.J. (1989) Kinetics of microbial mineralization of organic carbon from detrital *Skelatonema costatum* cells. **Marine Ecology Progress Series** 52: 123–128.

Pinazo, C., Marsaleix, P., Millet, B., Estournel, C. and Véhil, R. (1996) Spatial and temporal variability of phytoplankton biomass in upwelling areas of the northwestern Mediterranean: a coupled physical and biogeochemical modelling approach. **Journal of Marine Systems** 7: 161-191.

Pitre, O. (2007) Time series analysis of bio-physical variables in the water column of a mussel culture lagoon. MSc Thesis, Dalhousie University, Halifax, 125 p.

Pouvreau, S., Bourles, Y., Lefebvre, S., Gangnery, A. and Alunno-Bruscia, M. (2006) Application of a dynamic energy budget model to the Pacific oyster, *Crassostrea gigas*, reared under various environmental conditions. **Journal of Sea Research** 56: 156-167.

Prandle, D. (1991) Tides in estuaries and embayments (Review). In: B. B. Parker (Ed.), Tidal Hydrodynamics. J. Wiley, New York, pp. 125-152.

Prins, T.C., Smaal, A.C. and Dame, R.F. (1998) A review of feedbacks between bivalve grazing and ecosystem processes. **Aquatic Ecology** 31: 349-359.

Radach, G. and Moll, A. (2006) Review of three-dimensional ecological modelling related to the North Sea shelf system. Part II: model validation and data needs. **Oceanography and Marine Biology: An Annual Review** 44: 1–60.

Raillard, O. and Ménesguen, A. (1994) An ecosystem model for estimating the carrying capacity of a macrotidal shellfish system. **Marine Ecology Progress Series** 115: 117-130.

Ranasinghe, R. and Pattiaratchi, C. (2000) Tidal inlet velocity asymmetry in diurnal regimes. **Continental Shelf Research** 20: 2347-2366.

Richard, M., Archambault, P., Thouzeau, G. and Desrosiers, G. (2006) Influence of suspended mussel lines on the biogeochemical fluxes in adjacent water in the Îles-de-la-Madeleine (Quebec, Canada). **Canadian Journal of Fisheries and Aquatic Sciences** 63: 1198–1213.

Richard, M., Archambault, P., Thouzeau, G. and Desrosiers, G. (2007) Summer influence of 1 and 2 yr old mussel cultures on benthic fluxes in Grande-Entrée lagoon, Îles-de-la-Madeleine (Québec, Canada). **Marine Ecology Progress Series** 338: 131-143.

Ridderinkhof, H. (1988a) Tidal and residual flows in the western Dutch Wadden Sea. I: Numerical model results. **Netherlands Journal of Sea Research** 22: 1-21.

Ridderinkhof, H. (1988b) Tidal and residual flows in the western Dutch Wadden Sea. II: An analytical model to study the constant flow between connected tidal basins. **Netherlands Journal of Sea Research** 22: 185-198.

Ridderinkhof, H. and Zimmerman, J.T.F. (1990a) Residual Currents in the Western Dutch Wadden Sea. In: R. T. Cheng (Ed.), Residual Currents and Long-term Transport. **Costal and Estuarine Studies**. Springer-Verlag, New York, Vol. 38, pp. 93-104.

Ridderinkhof, H. and Zimmerman, J.T.F. (1990b) Mixing Processes in a Numerical Model of the Western Dutch Wadden Sea. In: R. T. Cheng (Ed.), Residual Currents and Long-term Transport. **Costal and Estuarine Studies**. Springer-Verlag, New York, Vol. 38, pp. 194-209.

Ridderinkhof, H. and Loder, J.W. (1994) Lagrangian characterization of circulation over submarine banks with application to the outer Gulf of Maine. **Journal of Physical Oceanography** 24: 1184-1200.

Robinson, I.S. (1981) Tidal vorticity and residual circulation. **Deep-Sea Research** 28A: 195-212.

Robinson, I.S. (1983) Tidally induced residual flows. In: B. Johns (Ed.), Physical oceanography of coastal and shelf seas. **Elsevier Oceanography Series**. Elsevier, Amsterdam.

Robson, B.J. and Hamilton, D.P. (2004) Three-dimensional modelling of a *Microcystis* bloom event in the Swan River estuary, Western Australia. **Ecological Modelling** 174: 203-222.

Rodhouse, P.G. and Roden, C.M. (1987) Carbon budget for a coastal inlet in relation to intensive cultivation of suspension-feeding bivalve molluscs. **Marine Ecology Progress Series** 36: 225-236.

Romero, J.R., Antenucci, J.P. and Imberger, J. (2004) One- and three-dimensional biogeochemical simulations of two differing reservoirs. **Ecological Modelling** 174: 143-160.

Rosland, R., Strand, Ø., Alunno-Bruscia, M., Bacher, C. and Strohmeier, T. (2009) Applying Dynamic Energy Budget (DEB) theory to simulate growth and bio-energetics of blue mussels under low seston conditions. **Journal of Sea Research** 62: 49-61.

Roy, S., Mayzaud, P. and Souchu, P. (1991) Environnement physico-chimique et trophique d'un site mytilicole aux Îles-de-laMadeleine (Québec) : II - Matière particulaire, composition biochimique et productivité primaire. In: J.-C. Therriault (Ed.), Le golfe du Saint-Laurent : petit océan ou grand estuaire? Publication spéciale canadienne des sciences halieutiques et aquatiques 113, pp. 219-230.

Ruardij, P. and van Raaphorst, W. (1995) Benthic nutrient regeneration in the ERSEM ecosystem model of the North Sea. **Netherlands Journal of Sea Research** 33: 453-483.

Ryther, J.H. and Dunstan, W.M. (1971) Nitrogen, phosphorus and eutrophication in the coastal marine environment. **Science** 171: 1008-1013.

Salles, P., Voulgaris, G. and Aubrey, D.G. (2005) Contribution of nonlinear mechanisms in the persistence of multiple tidal inlet systems. **Estuarine, Coastal and Shelf Science** 65: 475-491.

Schot, P.P. (1999) Wetlands. In: B. Narth., Hens, L., Compton, P. and Devuyst, D. (Ed.), Environment Management in Practice Vol. 3. Routledge, New York.

Sherman, K. (1994) Sustainability, biomass yields, and health of coastal ecosystems: an ecological perspective. **Marine Ecology Progress Series** 112: 277-301.

Shetye, S.R. and Gouveia, A.D. (1992) On the role of geometry of cross-section in generating flood-dominance in shallow estuaries. **Estuarine, Coastal and Shelf Science** 35: 113-126.

Skjelkvaale, B.L., Stoddard, J.L. and Andersen, T. (2001) Trends in surface water acidification in Europe and North America (1989-1998). **Water, Air & Soil Pollution** 130: 787-792.

Smaal, A.C. and van Stralen, M.R. (1990) Average annual growth and condition of mussels as a function of food source. **Hydrobiologia** 195: 179-188.

Smaal, A.C. and Prins, T.C. (1993) The uptake of organic matter and the release of inorganic nutrients by suspension feeding bivalve beds. In: R. F. Dame (Ed.), Bivalve filter feeders in estuarine and coastal ecosystem processes. **NATO ASI Series**. Springer-Verlag, Heidelberg, Vol. G33, pp. 273-298.

Smaal, A.C., Vonck, A.P.M.A. and Bakker, M. (1997) Seasonal variation in physiological energetics of *Mytilus edulis* and *Cerastoderma edule* of different size classes. **Journal of the Marine Biological Association of UK** 77: 817-838.

Smaal, A.C., Prins, T.C., Dankers, N. and Ball, B. (1998) Minimum requirements for modelling bivalve carrying capacity. **Aquatic Ecology** 31: 423–428.

Smaal, A.C., van Stralen, M. and Schuiling, E. (2001) The interaction between shellfish culture and ecosystem processes. **Canadian Journal of Fisheries and Aquatic Sciences** 58: 991-1002.

Smaal, A.C. (2002) European mussel cultivation along the Atlantic coast: production status, problems and perspectives. **Hydrobiologia** 484: 89-98.

Smagorinsky, J. (1963) General Circulation Experiment with the Primitive Equations. **Monthly Weather Review** 91: 99-164.

Smith, N.P. (1990) Wind domination of residual tidal transport in a coastal lagoon. In: R. T. Cheng (Ed.), Residual currents and long-term transport. **Coastal and Estuarine Studies**. Springer-Verlag, New York, Vol. 38, pp. 121-133.

SODIM (2002) L'état de la mariculture au Québec, Rapport annuel. 39 p.

Soto, D., Aguilar-Manjarrez, J., Brugère, C., Angel, D., Bailey, C., Black, K., Edwards, P., Costa-Pierce, B., Chopin, T., Deudero, S., Freeman, S., Hambrey, J., Hishamunda, N., Knowler, D., Silvert, W., Marba, N., Mathe, S., Norambuena, R., Simard, F., Tett, P., Troell, M. and Wainberg, A. (2008) Applying an ecosystem-based approach to aquaculture: principles, scales and some management measures. In: D. Soto, J. Aguilar-Manjarrez and N. Hishamunda (Eds.), Building an ecosystem approach to aquaculture. **FAO Fisheries and Aquaculture Proceedings**. No. 14, Rome, pp. 15-35.

Souchu, P., Mayzaud, P. and Roy, S. (1991) Environnement physico-chimique et trophique d'un site mytilicole aux Îles-de-laMadeleine (Québec) : I - Évolution estivale des composés de l'azote, du phosphore et du silicium. In: J.-C. Therriault (Ed.), Le golfe du Saint-Laurent : petit océan ou grand estuaire? Publication spéciale canadienne des sciences halieutiques et aquatiques 113, pp. 209-218.

Souchu, P. and Mayzaud, P. (1991) Inorganic nutrients in precipitation over the Magdalen Islands area (Quebec, Canada) and their impact on the primary productivity of the lagoons. **Atmospheric Research** 26: 543-554.

Speer, P.E. and Aubrey, D.G. (1985) A Study of Non-linear Tidal Propagation in shallow Inlet/Estuarine Systems. Part II: Theory. **Estuarine, Coastal and Shelf Science** 21: 207-224.

Spillman, C.M., Hamilton, D.P., Hipsey, M.R. and Imberger, J. (2008) A spatially resolved model of seasonal variations in phytoplankton and clam (*Tapes philippinarum*) biomass in Barbamarco Lagoon, Italy. **Estuarine, Coastal and Shelf Science** 79: 187-203.

Steele, J.H. (1962) Environmental control of photosynthesis in the sea. **Limnology and Oceanography** 7: 137– 150.

Stenton-Dozey, J.M.E., Jackson, L.F. and Busby, A.J. (1999) Impact of mussel culture on macrobenthic community structure in Saldanha Bay, South Africa. **Marine Pollution Bulletin** 39: 357-366.

Stenton-Dozey, J.M.E., Probyn, T. and Busby, A.J. (2001) Impact of mussel (*Mytilus galloprovincialis*) raftculture on benthic macrofauna, in situ oxygen uptake, and nutrient fluxes in Saldanha Bay, South Africa. **Canadian Journal of Fisheries and Aquatic Sciences** 58: 1-11.

Strain, P.M. (2002) Nutrient dynamics in Ship Harbour, Nova Scotia. **Atmosphere-Ocean** 40: 45-58.

Strohmeier, T., Duinker, A., Strand, Ø. and Aure, J. (2008) Temporal and spatial variation in food availability and meat ratio in a longline mussel farm (*Mytilus edulis*). **Aquaculture** 276: 83–90.

Taboada, J.J., Prego, R., Ruiz-Villarreal, M., Gomez-Gesteira, M., Montero, P., Santos, A.P. and Perez-Villar, V. (1998) Evaluation of the Seasonal Variations in the Residual Circulation in the Ria of Vigo (NW Spain) by Means of a 3D Baroclinic Model. **Estuarine Coastal and Shelf Science** 47: 661-670.

Tee, K.-T. and Lefaivre, D. (1990) Three-dimensional modeling of the tidally induced residual circulation off Southwest Nova Scotia. In: R. T. Cheng (Ed.), Residual currents and long-term transport. **Coastal and Estuarine Studies**. Spinger-Verlag, New York, Vol. 38, pp. 79-92.

Tenore, K.R., Boyer, L.F., Cal, R.M., Corral, J., Garcia-Fernandez, C., Gonzalez, N., Gonzalez-Gurriaran, E., Hanso, R.B., Oglesias, J., Krom, M., Lopez-Jamar, E., McClain, J., Pamarmat, M.M., Perez, A., Rhoads, D.C., De Santiago, G., Tiejen, J., Westrich, J. and Windom, H.L. (1982) Coastal upwelling in the Rias Bajas, NW Spain: contrasting the benthic regimes of the Rias de Arosa and de Muros. **Journal of Marine Research** 40: 701-772.

Tian, R.C., Vézina, A.F., Legendre, L., Ingram, R.G., Klein, B., Packard, T., Roy, S., Savenkoff, C., Silverberg, N., Therriault, J.-C. and Tremblay, J.-É. (2000) Effects of pelagic food-web interactions and nutrient remineralization on the biogeochemical cycling of carbon: a modeling approach. **Deep-Sea Research II** 47: 637-662.

Tita, G. (2005) Croissance des moules d'élevage de la lagune de Grande-Entrée (Îles-de-la-Madeleine) et comparaison de souches, Rapprt scientifique, MAPAQ, 10 p.

Tremblay, R., Myrand, B., Sévigny, J.-M., Blier, P. and Guderley, H. (1998) Bioenergetic and genetic parameters in relation to susceptibility of blue mussels, *Mytilus edulis* (L.) to summer mortality. **Jounal of Experimental Marine Biology and Ecology** 221: 27–58.

Tremblay, J.-É., Legendre, L., Klein, B. and Therriault, J.C. (2000) Size-differential uptake of nitrogen and carbon in a marginal sea (Gulf of St. Lawrence, Canada): significance of diel periodicity and urea uptake. **Deep-Sea Research II** 47: 489-518.

Trottet, A., Roy, S., Tamigneaux, E. and Lovejoy, C. (2007) Importance of heterotrophic planktonic communities in a mussel culture environment: the Grande-Entrée Lagoon, Magdalen Islands (Québec, Canada). **Marine Biology** 151: 377-392.

Trottet, A., Roy, S., Tamigneaux, E., Lovejoy, C. and Tremblay, R. (2008a) Influence of suspended mussel farming on planktonic communities in Grande-Entrée Lagoon, Magdalen Islands (Québec, Canada). **Aquaculture** 276: 91-102.

Trottet, A., Roy, S., Tamigneaux, E., Lovejoy, C. and Tremblay, R. (2008b) Impact of suspended mussels (*Mytilus edulis* L.) on plankton communities in a Magdalen Islands lagoon (Québec, Canada): A mesocosm approach. **Journal of Experimental Marine Biology and Ecology** 365: 103-115.

Ulanowicz, R.E. (1986) Growth and development: Ecosystems phenomenology. Springer-Verlag, New York, 185 p.

Uncles, R.J. (1982) Computed and observed residual currents in the Bristol Channel. **Oceanologica Acta** 5: 11-20.

Vadineanu, A. (2006) Identification of the lagoon ecosystems. In: E. Gönenç and J. P. Wolfin (Eds.), Coastal Lagoons: Ecosystem Processes and Modeling for Sustainable Use and Development. CRC Press, pp. 7-41.

van de Kreeke, J. (1976) Tide-induced mass transport: A flushing mechanism for shallow lagoons. **Journal of Hydraulic Research** 14: 61-67.

van de Kreeke, J. (1988) Hydrodynamics of tidal inlets. In: D. G. Aubrey and L. Weishar (Eds.), Hydrodynamics and sediment dynamics of tidal inlets. **Coastal and Estuarine Studies**. Springer-Verlag, New York, Vol. 29, pp. 1–23.

van der Tol, M.W.M. and Scholten, H. (1998) A model analysis on the effect of decreasing nutrient loads on the biomass of benthic suspension feeders in the Oosterschelde ecosystem (SW Netherlands). **Aquatic Ecology** 31: 395-408.

van der Veer, H.W., Cardoso, J.F.M.F. and van der Meer, J. (2006) The estimation of DEB parameters for various Northeast Atlantic bivalve species. **Journal of Sea Research** 56: 107-124.

van Haren, R.J.F. and Kooijman, S.A.L.M. (1993) Application of a dynamic energy budget model to *Mytilus edulis* (L.). **Netherlands Journal of Sea Research** 31: 119-133.

van Maren, D.S., Hoekstra, P. and Hoitink, A.J.F. (2004) Tidal flow asymmetry in the diurnal regime: bed-load transport and morphologic changes around the Red River Delta. **Ocean Dynamics** 54: 424-434.

van Stralen, M.R. and Dijkema, R.D. (1994) Mussel culture in a changing environment: the effects of a coastal engineering project on mussel culture (*Mytilus edulis*) in the Oosterschelde (SW Netherlands). **Hydrobiologia** 282/283: 359-379.

Wainright, S.C. and Hopkinson Jr., C.S. (1997) Effects of sediment resuspension on organic matter processing in coastal environments: a simulation model. **Journal of Marine Systems** 11: 353-368.

Walker, T.R. and Grant, J. (2009) Quantifying erosion rates and stability of bottom sediments at mussel aquaculture sites in Prince Edward Island, Canada. **Journal of Marine Systems** 75: 46-55.

Webster, I.T. and Harris, G.P. (2004) Anthropogenic impacts on the ecosystems of coastal lagoons: modelling fundamental biogeochemical processes and management implications. **Marine and Freshwater Research** 55: 67-78.

Wei, H., Hainbucher, D., Pohlmann, T., Feng, S. and Suendermann, J. (2004) Tidal-induced Lagrangian and Eulerian mean circulation in the Bohai Sea. **Journal of Marine Systems** 44: 141-151.

Weise, A.M., Cromey, C.J., Callier, M.D., Archambault, P., Chamberlain, J. and McKindsey, C.W. (2009) Shellfish-DEPOMOD: Modelling the biodeposition from suspended shellfish aquaculture and assessing benthic effects. **Aquaculture** 288: 239-253.

Widdows, J. and Bayne, B.L. (1971) Temperature acclimation of *Mytilus edulis* with reference to its energy budget. **Journal of the Marine Biological Association of UK** 51: 827-843.

Widdows, J., Fieth, P. and Worrall, C.M. (1979) Relationships between seston, available food and feeding activity in the common mussel *Mytilus edulis*. **Marine Biology** 50: 195-207.

Wildish, D.J. and Miyares, M.P. (1990) Filtration rate of blue mussels as a function of flow velocity: Preliminary experiments. **Journal of Experimental Marine Biology and Ecology** 142: 213-219.

Zeldis, J., Felsing, M. and Wilson, J. (2006) Limits of acceptable change: a framework for managing marine farming. **Water & atmosphere** 14: 16-17.

Zheng, W., Shia, H., Chen, S. and Zhu, M. (2009) Benefit and cost analysis of mariculture based on ecosystem services. **Ecological Economics** 68: 1626-1632.

Zimmerman, J.T.F. (1978) Topographic generation of residual circulation by oscillatory (tidal) currents. **Geophysical and Astrophysical Fluid Dynamics** 11: 35-47.

Zimmerman, J.T.F. (1979) On the Euler-Lagrange transformation and the Stokes' drift in the presence of oscillatory and residual currents. **Deep-Sea Research** 26A: 505-520.

Zimmerman, J.T.F. (1981) Dynamics, diffusion and geomorphological significance of tidal residual eddies. **Nature** 290: 549-555.